Halogenpiridinijevi kvarterni kationi kao donori halogenske veze

Fotović, Luka

Doctoral thesis / Disertacija

2022

Degree Grantor / Ustanova koja je dodijelila akademski / stručni stupanj: **University of Zagreb, Faculty of Science / Sveučilište u Zagrebu, Prirodoslovno-matematički fakultet**

Permanent link / Trajna poveznica: https://urn.nsk.hr/urn:nbn:hr:217:996672

Rights / Prava: In copyright / Zaštićeno autorskim pravom.

Download date / Datum preuzimanja: **2024-07-14**

Repository / Repozitorij:

Repository of the Faculty of Science - University of Zagreb

Sveučilište u Zagrebu
PRIRODOSLOVNO-MATEMATIČKI FAKULTET

Luka Fotović

HALOGENPIRIDINIJEVI KVATERNI KATIONI KAO DONORI HALOGENSKE VEZE

DOKTORSKI RAD

Mentor:
izv. prof. dr. sc. Vladimir Stilinović

Zagreb, 2022.

University of Zagreb
FACULTY OF SCIENCE

Luka Fotović

QUATERNARY HALOGENOPYRIDINIUM CATIONS AS HALOGEN BOND DONORS

DOCTORAL DISSERTATION

Supervisor:
Dr. Vladimir Stilinović, Associate Professor

Zagreb, 2022.

Ova doktorska disertacija izrađena je u Zavodu za opću i anorgansku kemiju Kemijskog odsjeka Prirodoslovno-matematičkog fakulteta Sveučilišta u Zagrebu pod mentorstvom izv. prof. dr. sc. Vladimira Stilinovića.

Doktorska disertacija izrađena je u okviru projekata Hrvatske zaklade za znanost pod nazivom „Projekt razvoja karijera mladih istraživača – izobrazba novih doktora znanosti" (HRZZ-DOK-2018-01-7325); „Kristalno inženjerstvo višekomponentnih metaloorganskih materijala povezanih halogenskom vezom: ususret supramolekulskom ugađanju strukture i svojstava" (HRZZ-IP-2014-09-7367) i "Nove građevne jedinke u supramolekulskom dizajnu složenih višekomponentnih molekulskih kristala temeljenih na halogenskim vezama" (HRZZ-IP-2019-04-1868).

Zahvale

Hvala mom mentoru i prijatelju, Vladimiru Stilinoviću, na vođenju pri izradi ove disertacije, svom prenesenom znanju, trudu, podršci i uvijek entuzijastičnim raspravama oko znanstvenih i manje znanstvenih tema.

Hvala Dominiku Cinčiću na pruženoj prilici da upoznam svijet znanosti.

Hvala Nikoli na rezultatima kvantno-kemijskih računa koji su upotpunili ovu disertaciju, a osobitno na svim diskusijama i podršci.

Hvala Josipu :)

Hvala mojim cimerima iz ureda i labosa (bivšim i sadašnjim), a posebno Nei, na druženjima i razgovorima u pauzama od napornog rada :)

Hvala i svim drugim kolegama i prijateljima na suradnji i/ili druženjima kako na poslu tako i u slobodno vrijeme.

Hvala mojoj Anamariji na podršci i razumijevanju tijekom izrade ove disertacije.

Na kraju, hvala mojoj obitelji na podršci.

Luka Fotović

Zagreb, 18. veljače 2022.

Sadržaj

Sveučilište u Zagrebu
Prirodoslovno-matematički fakultet
Kemijski odsjek

Doktorska disertacija

SAŽETAK

HALOGENPIRIDINIJEVI KVATERNI KATIONI KAO DONORI HALOGENSKE VEZE

Luka Fotović
Kemijski odsjek, Horvatovac 102a, 10000 Zagreb, Hrvatska

U ovome istraživanju, uvođenjem različitih (alifatskih) supstituenata na piridinski dušikov atom halogenpiridina (osobito *meta* izomera) pripravljeno je te strukturno, termički i spektroskopski okarakterizirano 49 novih soli protoniranih i *N*-alkiliranih halogenpiridina. Usporedbom halogenskih veza u strukturama *N*-alkil-3-jodpiridinijevih jodida utvđeno da postoji trend da što je duži ugljikovodični lanac supstituiran na dušikov atom jodpiridinskog prstena to su kraće halogenske veze C–I···I$^-$. Ustanovljeno je da afinitet prema halogenskoj vezi opada s veličinom halogenidnog aniona kao akceptora, odnosno slijedi isti trend kao i u slučaju vodikove veze. Analizom raspodjele naboja na halogenpiridinijevim kationima utvrđeno je da i protoniranje i *N*-metiliranje halogenpiridina dovode do značajnog povećanja elektrostatskog potencijala σ-šupljine halogena što uvelike povećava incidenciju ostvarivanja halogenskih veza u odnosu na neutralne halogenpiridine. To čini halogenpiridinijeve katione (jodpiridinijeve posebno) prilično pouzdanim donorima halogenskih veza, te na taj način opravdava njihovu upotrebu u dizajnu i sintezi supramolekulskih struktura povezanih halogenskom vezom.

(70 + XXIII stranica, 33 slike, 5 shema, 3 tablice, 176 literaturnih navoda, jezik izvornika: hrvatski)

Rad je pohranjen u Središnjoj kemijskoj knjižnici, Horvatovac 102a, Zagreb i Nacionalnoj i sveučilišnoj knjižnici, Hrvatske bratske zajednice 4, Zagreb.

Ključne riječi: halogenidni anioni/ halogenpiridinijevi kationi/ halogenska veza/ kristalno inženjerstvo/ soli/ vodikova veza

Mentor: izv. prof. dr. sc. Vladimir Stilinović

Rad prihvaćen: 2. veljače 2022.

Ocjenitelji:
1. prof. dr. sc. Biserka Prugovečki
2. dr. sc. Krešimir Molčanov, v. zn. sur.
3. izv. prof. dr. sc. Josip Požar

University of Zagreb
Faculty of Science
Department of Chemistry

Doctoral Thesis

ABSTRACT

QUATERNARY HALOGENPYRIDINIUM CATIONS AS HALOGEN BOND DONORS

Luka Fotović
Kemijski odsjek, Horvatovac 102a, 10000 Zagreb, Hrvatska

In this study, 49 novel salts of halogenopyridinium cations were prepared and characterized by single crystal X-ray diffraction, and by thermal and spectroscopic analysis methods. In the crystal structures of *N*-alkyl-3-iodopyridinium iodides it is observed trend that longer chains as *N*-substituents generally leading to shorter C–I···I$^-$ halogen bonds. Based on the trend observed in the relative shortenings of distances of the two interactions, both halogen and hydrogen bonds seem to be decreasing in strength with the size of the halogenide anion. Inspection of the distribution of the charge on the cations revealed that both protonation and *N*-methylation of halogenopyridines lead to a considerable increase in the electrostatic potential of the halogen σ-hole which increase incidence of the halogen bond in the structures comprising halogenopyridinium cations (as compared to neutral halogenopyridines). This makes halopyridiniom cations (iodopyridinium in particularly) fairly reliable halogen bond donors for deliberate synthesis of halogen bonded supramolecular structures.

(70 + XXIII pages, 33 figures, 5 schemes, 3 tables, 176 references, original in Croatian)

Thesis deposited in Central Chemical Library, Horvatovac 102A, Zagreb, Croatia and National and University Library, Hrvatske bratske zajednice 4, Zagreb, Croatia.

Keywords: crystal engineering/ halogen bond/ halogenide anions/ halogenpyridine cations/ hydrogen bond/ salts

Supervisor: Dr. Vladimir Stilinović, Associate Professor

Thesis accepted: February 2nd 2022

Reviewers:
Dr. Biserka Prugovečki, Professor
Dr. Krešimir Molčanov, Senior Research Associate
Dr. Josip Požar, Associate Professor

§ 1. UVOD

Početkom 19. stoljeća pripravljen je molekulski kompleks elementarnog joda i amonijaka koji je prvi sintetizirani kemijski spoj u kojem postoji privlačna interakcija između atoma halogena (joda) i Lewisove baze (atoma dušika).[1] Kemijski sastav tog kompleksa predložio je F. Guthrie pedesetak godina kasnije.[2] Prvi nepobitan dokaz postojanja kompleksa u kojima atomi halogena intereagiraju s Lewisovim bazama došao je s razvojem metoda rendgenske difrakcije što je omogućilo da pedesetih godina 20. stoljeća O. Hassel i suradnici strukturno okarakteriziraju supramolekulske komplekse molekula koje sadrže donorne atome joda i broma (molekule elementarnog joda i broma, jodov klorid, jodoform, itd.) i molekula koje sadrže akceptorske atome dušika, kisika i sumpora.[3–11] Daljnjim razvojem kristalografije i supramolekulske kemije čvrstog stanja, pokazano je da su *kompleksi prijenosa naboja* zapravo među najranijim primjerima povezivanja molekula halogenskom vezom kako u otopini tako i u čvrstom stanju. Unatoč tome što intenzivna istraživanja halogenske veze započinju tek krajem prošlog stoljeća,[12–18] halogenska veza nametnula se kao vrlo upotrebljiv alat za izradu supramolekulskih struktura te sintezu novih materijala čime je u području kristalnog inženjerstva novih materijala zauzela svoje zasluženo mjesto odmah do vodikove veze.[19,20]

Halogenska veza privlačna je interakcija koja se ostvaruje između donora halogenske veze, tj. elektrofilnog dijela atoma halogena i akceptora halogenske veze, odnosno nukleofilnog predjela druge (ili iste) molekule (atomi dušika, kisika, sumpora, delokalozirani π-sustavi, itd.).[17,21,22] Halogenske veze su uglavnom linearne (kutevi vrlo malo odstupaju od 180°) i usmjerenije u usporedbi s vodikovim vezama. Usmjerenost je posljedica lokaliziranosti pozitivnog elektrostatskog potencijala (V) na kovalentno vezanom atomu halogena u relativno uskom području koje se naziva σ-šupljina.[23–27] Jakost interakcije povećava se s polarizabilnošću atoma donora halogenske veze i raste u nizu I > Br > Cl.[28,29] Energije halogenskih veza kreću se u rasponu od 10 do 150 kJ mol^{-1},[28,30] a rastu s porastom elektrostatskog potencijala σ-šupljine donornog halogenog atoma (V_{max}(X), X = Cl, Br, I, Slika 1). Stoga su najbolji donori halogenske veze oni kod kojih je donorni halogeni atom vezan na molekulu koja ima elektron-izvlačeći učinak na taj atom halogena što za posljedicu ima smanjenje elektronske gustoće u području σ-šupljine (odnosno povećanje V_{max}(X)) donornog halogenog atoma i posljedično tome potencijala za ostvarivanje halogenske veze s Lewisovim bazama. [28,31–33]

Tijekom posljednjih desetljeća najviše se istražuju halogenske veze s neutralnim donorima. Do danas su najviše istraženi donori halogenske veze molekule elementarnih halogena[34] te neutralne halogenirane organske molekule od kojih su najzastupljeniji perfluorirani brom- i jodugljikovodici u kojima elektronegativni atomi fluora vezani na ugljikovodičnu okosnicu služe kao elektron-izvlačeći fragmenti.[16,18,35–42] Osim atoma fluora, u istu svrhu koriste se cijano i nitro funkcijske skupine.[43–47] Halogenalkini se također koriste kao donori halogenske veze u kojima se pozitivna vrijednost V_{max}(X) ostvaruje elektron-izvlačećim učinkom trostruke veze ugljik–ugljik.[48–51] Među najjače donore halogenske veze ubrajaju se *N*-halogenimidi kod kojih je halogeni atom direktno vezan na elektonegativni atom dušika.[52–60]

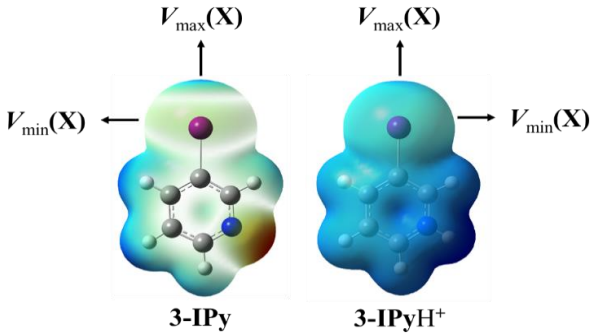

Slika 1. Elektrostatski potencijal (***V***) mapiran na 0.002 *e* Å^{-3} izoplohu elektornske gustoće za molekulu 3-jodpiridina (**3-IPy**) i 3-jodpiridinijev kation (**3IpyH**$^+$) s označenim mjestima na halogenu gdje je *V* maksimalan (V_{max}(X)) i minimalan (V_{min}(X)).

Do sada opisanim donorima halogenske veze zajedničko je da su neutralne molekule kod kojih se pozitivna vrijednost V_{max}(X) ostvaruje elekronegativnim supstituentima ili funkcijskim skupinama s elektron-izvlačećim učinkom. Drugi pristup dizajnu donora halogenske veze je vezati halogeni atom na pozitivno nabijenu kemijsku vrstu – kation. Za katione se očekuje da budu dobri donori halogenske veze upravo zbog njihovog ukupnog pozitivnog naboja, a samim time i izrazito pozitivne vrijednosti V_{max}(X).

Hipoteza ovog istraživanja bila je da će prevođenjem halogenpiridina u halogenpiridinijeve kvaterne katione (protoniranjem ili alkiliranjem dušikovog atoma) ukupan generirani pozitivni naboj pridonijeti povećanju pozitivnog naboja u području σ–šupljine halogenog atoma, što će učiniti priređene katione dobrim donorima halogenske veze. Stoga je glavni cilj bio istražiti (eksperimentalno i komputacijski) kakva će biti raspodjela ukupnog naboja na halogenpiridinijevim kationima te njezin utjecaj na ostvarivanje halogenskih veza i kompeticiju s ostalim nekovalentim interakcijama.

Kako bi se to istražilo, pripravljena je serija halogenidnih soli protoniranih i *N*-alkiliranih halogenpiridina. Halogenidni anioni izabrani su kao akceptori s obzirom da su zbog svog sferičnog oblika vrlo fleksibilne Lewisove baze koje mogu sudjelovati u raznim supramolekulskim interakcijama sa širokim spektrom Lewisovih kiselina zbog čega se kontinuirano proučavaju kao akceptori vodikove veze. Međutim, iako je već samo nekoliko godina nakon sinteze spomenutog kompleksa joda i amonijaka uočeno da elementarni halogeni reagiraju s halogenidnim anionima pri čemu nastaju polihalogenidni anioni,[61] intenzivnija istraživanja halogenidnih aniona kao akceptora halogenske veze krenula su tek u zadnje vrijeme. Osim s *jednostavnim* halogenidnim ionima priređene su soli halogenpiridinijevih kationa s većim anionima kao što su heksacijanoferati i polioksometalati što će dati uvid u mogućnost šire primjene halogenpiridinijevih kationa kao donora halogenske veze u kristalnom inženjerstvu. Dobivene soli okarakterizirane su difrakcijom rendgenskog zračenja na jediničnom kristalu, difrakcijom rendgenskog zračenja na polikristalnom uzorku, razlikovnom pretražnom kalorimetrijom (DSC) i termogravimetrijom (TG). Također su provedeni kvanto-kemijski izračuni molekulskih elektrostatskih potencijala priređenih kationa kako bi se ispitao utjecaj pozitivnog naboja na kationu na promjenu vrijednosti V_{max}(X).

Ova disertacija temelji se na 4 znanstvena rada koji čine jedinstvenu cjelinu. U radu **I** utvrđeno je da se u jodpiridinijevim halogenidima relativne duljine halogenskih veza povećavaju s veličinom halogenidnog aniona kao akceptora, ali da se preferira ostvarivanje halogenskih veza s većim halogenidima kao akceptorima što ukazuje na to da je jodidni anion najpouzdaniji građevni blok (od svih halogenidnih aniona) za sintezu struktura povezanih halogenskom vezom. Na temelju rezultata i zaključaka objavljenih u radu **I**, istraživanje je nastavljeno tako da je naglasak stavljen upravo na jodidne soli. Stoga su u radovima **II** i **III** sitetizirane jodidne soli *N*-alkiliranih halogenpiridina te je provedena analiza raspodjele naboja na halogenpiridinijevim kationima, odnosno utjecaj naravi halogena, duljine *N*-supstituiranog alkilnog lanca i naboja kationa na ostvarivanje halogenskih veza s jodidnim anionima. Studija *N*-protoniranih halogenpiridinijevih kationa, objavljena radu **I**, nastavljena je radu **IV** gdje je opisan primjer njihove primjene u kristalnom inženjerstu metaloorganskih sustava. Stoga ovi radovi čine cjelinu koja doprinosi boljem razumijevanju halogenpiridinijevih kationa kao donora halogenske veze te čini dobar temelj za daljnja istraživanja i njihovu primjenu u kristalnom inženjerstvu.

§ 2. POPIS RADOVA

Disertacija se temelji na sljedećim izvornim znanstvenim radovima koji su označeni rimskim brojevima:

I. L. Fotović, V. Stilinović, Halogenide anions as halogen and hydrogen bond acceptors in iodopyridinium halogenides, *CrystEngComm* **22** (2020) 4039-4046.

II. L. Fotović, N. Bedeković, V. Stilinović, Evaluation of halogenopyridinium cations as halogen bond donors, *Cryst. Growth Des.* **21** (2021) 6889–6901.

III. L. Fotović, V. Stilinović, Halogen Bonding in *N*-Alkyl-3-halogenopyridinium Salts, *Crystals* **11** (2021) 1240-1256.

IV. N. Jakupec, L. Fotović, V. Stilinović, The effect of halogen bonding on protonated hexacyanoferrate networks in hexacyanoferrates of halogenopyridines, *CrystEngComm* **22** (2020) 8142-8150.

I

Halogenide anions as halogen and hydrogen bond acceptors in iodopyridinium halogenides

L. Fotović i V. Stilinović,

CrystEngComm **22** (2020) 4039-4046. (objavljen)

Doprinos koautora:

L. Fotović – sinteza soli, kristalizacija, strukturna, termička i spektrokopska analiza, kristalografija, obrada rezultata i pisanje rada

V. Stilinović – savjetovanje i pisanje rada

Rad je reproduciran uz dozvolu Kraljevskog kremijskog društva.*

*Reproduced with permission from *CrystEngComm* **2020**, *22*, 4039-4046. Published by The Royal Society of Chemistry.

CrystEngComm

ROYAL SOCIETY OF CHEMISTRY

PAPER

View Article Online
View Journal | View Issue

Check for updates

Cite this: *CrystEngComm*, 2020, **22**, 4039

Halogenide anions as halogen and hydrogen bond acceptors in iodopyridinium halogenides†

Luka Fotović and Vladimir Stilinović *

In order to study halogenide anions simultaneously acting as hydrogen bond and halogen bond acceptors, we have prepared and crystallised halogenide salts (chlorides, bromides and iodides) of the three isomers of iodopyridine, 2-iodopyridine (**2-IPy**), 3-iodopyridine (**3-IPy**) and 4-iodopyridine (**4-IPy**). In all nine structures the pyridinium cations and the halogenide anions are interconnected through C–I···X$^-$ halogen and N–H···X$^-$ hydrogen bonds (X = Cl, Br, I). Based on the trend observed in the relative shortening of the two interactions, both halogen and hydrogen bonds seem to be decreasing in strength with the size of the halogenide anion, although the decrease is apparently more pronounced for hydrogen bonds. To study this further, we have performed a CSD study of structures comprising a halogenide and both hydrogen and halogen bond donors, which has indicated a tendency of chloride towards hydrogen and of iodide towards halogen bonds, in accord with our experimental results. Additionally, we have obtained crystals of ((**2-IPy**H)$_2$ Cl I), the first example of a double salt comprising both hydrogen and halogen bond donors and two different halogenides. In this structure, the halogen bonds were formed exclusively with the iodide anion, while the hydrogen bonds were formed only with the chloride anion.

Received 8th April 2020,
Accepted 8th May 2020

DOI: 10.1039/d0ce00534g

rsc.li/crystengcomm

Published on 12 May 2020. Downloaded by University of Zagreb on 10/21/2021 3:54:01 PM.

Introduction

Halogenide anions have a specific place in supramolecular chemistry and crystal engineering.[1] Being the only group of spherical anions available in aqueous solutions (as well as in most common organic solvents), they represent the archetypes of *flexible* Lewis bases, capable of participating in a variable number of supramolecular interactions with various Lewis acids in a wide array of configurations.[2] Classically, halogenides have been extensively studied as hydrogen bond acceptors, from the point of view of anion receptors,[3] sensors,[4] supramolecular assembly,[5] *etc.* More recently, in light of the widespread research of halogen bonds as an alternative to hydrogen bonds in crystal engineering and supramolecular chemistry in general,[6] halogenide anions have been attracting ever more attention as halogen bond acceptors as well.[7] Comparing the hydrogen and halogen bonding proclivities of the halogenide anions, it becomes apparent that, unlike in the case of hydrogen bonds which clearly become weaker with the diminishing basicity of the anion (*i.e.* $F^- > Cl^- > Br^- > I^-$), halogen bonded structures comprising iodide are often quite easily obtainable, while those with fluoride are extremely scarce.[8] This might indicate that the affinity of halogenides for halogen bonding changes in the opposite direction ($I^- > Br^- > Cl^- > F^-$), a proposition justifiable from the point of view of the HSAB principle[9] – the σ-hole[10] of the halogen atom (unlike hydrogen) is a *soft* Lewis acid, and therefore will preferentially bind to the *softest* Lewis base, *i.e.* iodide.[11]

However, solution measurements as well as computations have demonstrated that the halogen bond energies also diminish with the radius of the halogenide (*i.e.* $F^- > Cl^- > Br^- > I^-$). For example, Wei Jun Jin and co-workers have reported on halogen bonding with halogenide anions in ternary cocrystals of perfluorinated diiodoalkanes and tetrabuthylammonium halogenides, both in solution and the solid state. They found that halogen bond strength decreases with halogenide size.[12] Later, they confirmed the same trend in ternary cocrystals of tetrabuthylammonium tetraiodoethene halogenides, both by experiments and calculations.[13]

The possible reason for this apparent discrepancy is the relative strength of the two interactions and their competition. One of the approaches toward this question is through the study of simultaneous hydrogen and halogen bonding with the same halogenide anion. This was already addressed in several studies. Jones and co-workers thus reported on the simultaneous hydrogen and halogen bonds in the structures of 4-halopyridinium halogenides (4-chloropyridinium chloride, 4-bromopyridinium bromide and 4-iodopyridinium iodide). In

Department of Chemistry, Faculty of Science, University of Zagreb, Horvatovac 102a, HR-10002 Zagreb, Croatia. E-mail: vstilinovic@chem.pmf.hr

† Electronic supplementary information (ESI) available: Synthetic details and single crystal X-ray diffraction data. CCDC 1995437–1995447 contain crystallographic data for this paper. For ESI and crystallographic data in CIF or other electronic format see DOI: 10.1039/d0ce00534g

This journal is © The Royal Society of Chemistry 2020

Published on 12 May 2020. Downloaded by University of Zagreb on 10/21/2021 3:54:01 PM.

these structures hydrogen bonds became relatively longer, while halogen bonds became relatively shorter with increasing size of halogenides.[14] Solution measurement on the association constants of halogenides to isostructural halogen or hydrogen bond receptors published by Berryman *et al.* revealed that the halogen bond receptor preferred larger halogenides, while the hydrogen bond receptor preferred smaller halogenides.[15] Similarly, in their study of *N*,*N*-bis(4-iodobenzyl)-4,4-bipyridinium halogenide hydrates, García and co-workers found that halogen bonds were relatively shorter with bromide, while hydrogen bonds are shorter with the chloride anion.[16]

Recently, a combined crystallographic/solid-state NMR study was published by Bryce *et al.*, who have made a systematic study of hydrogen and halogen bonds in 2- and 3-iodoethynylpyridinium halogenides where the iodoethynylpyridinium cations act simultaneously as (N–H···X$^-$) hydrogen bond donors and (C–I···X$^-$) halogen bond donors. Using a pair of simple, conformationally rigid, pyridine derivatives as cations has enabled them to prepare (partially) isostructural series of compounds, making them ideal for the study of subtle interrelationships between the two supramolecular interactions in the solid state.[17]

Inspired by this, we have decided to perform a systematic study of interrelationship of halogen and hydrogen bonds with halogenide anions as acceptors using a series of even simpler – iodopyridinium – cations. As all three iodopyridines (**2-**, **3-** and **4-IPy**, Scheme 1) are readily obtainable, this has enabled us to prepare three (partially isostructural) series of halogenides and to observe systematic changes in the crystal structures due to the change of the halogenide anion.

Results and discussion

Through crystallisation of the three iodopyridines with hydrochloric, hydrobromic and hydroiodic acids, we have obtained all nine simple (1 : 1) salts (as well as a double salt and a hydrate). As expected, the general geometry of the structures of the simple salts formed through hydrogen and halogen bonds was found to depend primarily on the pyridine derivative used, *i.e.* the angle between the halogen bond donor (C–I) and the hydrogen bond donor (N–H) groups of the corresponding protonated cation.

In the case of **2-IPy**, all three halogenides comprise chains of alternating cations and anions connected by, again, alternating C–I···X$^-$ halogen and N–H···X$^-$ hydrogen bonds (Fig. 1). The bromide and the iodide are isostructural,

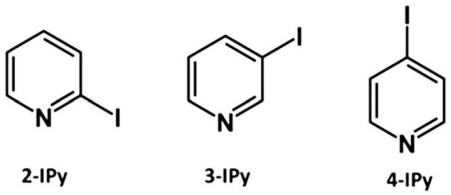

Scheme 1 Iodopyridines used in this study.

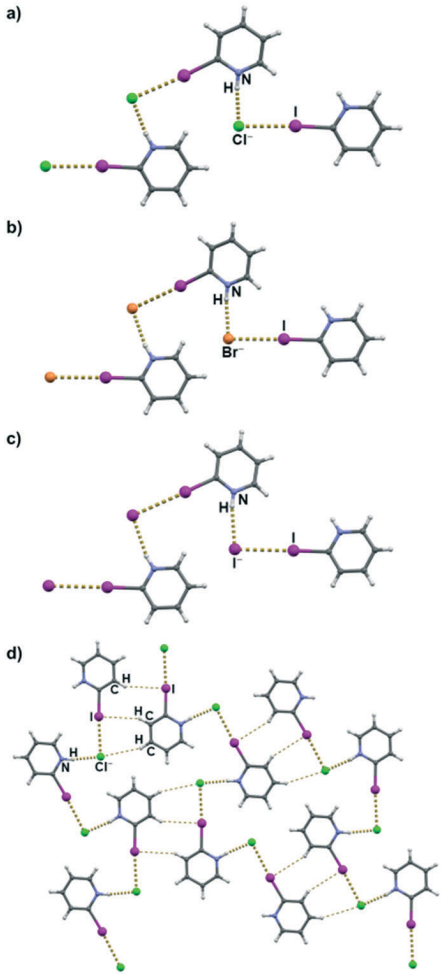

Fig. 1 a) Halogen and hydrogen bonded chains in **2-IPy**HCl; b) halogen and hydrogen bonded chains in **2-IPy**HBr; c) halogen and hydrogen bonded chains in **2-IPy**HI; d) layers formed by linking of chains through a combination of C–H···I and C–H···Cl$^-$ hydrogen bonds in the structure of **2-IPy**HCl. Only the shortest C–H···Cl$^-$ bonds are shown.

crystallising in the space group $Pca2_1$. The direction of the chains coincides with the polar axis of the space group (*c*), with all the cations oriented in the same direction. In spite of the almost identical basic motif of the interconnection of cations in the chain, the chloride crystallises in the centrosymmetric space group $P2_1/c$, with alternating directionality of the neighbouring chains. The change in the overall structure can be attributed to the formation of a pair of C–H···Cl$^-$ hydrogen bonds (with **2-IPy** hydrogen atoms in positions 5 and 6 of *ca.* 3.03 Å and 2.67 Å, respectively). These interconnect the chains into 2D networks (Fig. 1d) and make the pyridine rings of the interconnected chains almost coplanar, allowing for an additional, almost linear C–H···I contact involving the negative portion of the iodine atom orthogonal to the halogen bond (Fig. 1d) Analogous C–H···X$^-$ contacts do exist in the bromide and the iodide; however here they are considerably longer than the corresponding sums of van der Waals radii (3.21 Å and 3.23 Å in **2-IPy**HBr

 This journal is © The Royal Society of Chemistry 2020

Published on 12 May 2020. Downloaded by University of Zagreb on 10/21/2021 3:54:01 PM.

and 3.35 Å and 3.35 Å in **2-IPy**HI), and are complemented with a second pair of C–H···X^- contacts involving the **2-IPy** hydrogen atoms in the positions 3 and 4 (3.21 Å and 3.34 Å in **2-IPy**HBr and 3.28 Å and 3.44 Å in **2-IPy**HI). The resulting packing of the chains is markedly different than that in the chloride with a network of (weak) C–H···X^- contacts interconnecting the chains in a 3D structure.

In the structures of all **2-IPy** halogenides the C–I···X^- halogen bonds are *ca.* 17% shorter than the sum of van der Waals radii and almost linear with C–I···X^- angles of *ca.* 175°. Among hydrogen bonds however there is a slight decrease in the relative shortening of hydrogen bonds with the anion size; relative shortening for N–H···X^- hydrogen bonds range from *ca.* 11% for chloride to *ca.* 8% for iodide. As expected, the hydrogen bonds are less linear than the halogen bonds with the ∠(N–H···X^-) angle of *ca.* 173° in **2-IPy**HCl, while in the structures of bromide and iodide it is approximately 165°. The two bonds formed by the halogenide anions (C–I···X^- halogen bonds and N–H···X^- hydrogen bonds) in all three structures are almost perpendicular, with the I···X^-···H angles in the range from 93° to 95°, increasing from chloride to iodide.

When **3-IPy** was used, it also yielded isostructural bromide and iodide, although comprising not chains but rather centrosymmetric cyclical (**3-IPy**HX)$_2$ tetramers (Fig. 2). In both structures, the C–I···X^- halogen bonds are *ca.* 15.5% shorter than the sum of van der Waals radii and almost linear, ∠(C–I···X^-) angles of *ca.* 175°, while the relative shortening of the N–H···X^- hydrogen bonds in both structures is less than in the case of **2-IPy** analogues (*ca.* 6%), and the N–H···X^- angles are significantly lower (*ca.* 145°). This is a fine illustration of the difference between the geometrical flexibility of the hydrogen bonds, as opposed to much more rigidly linear halogen bonds. In the **2-IPy** halogenides the two bonds formed by the halogenide anions are approximately perpendicular with the I···X^-···H angle being 101° in **3-IPy**HBr and 97° in **3-IPy**HI.

Interestingly, **3-IPy**HCl could not be obtained using the same simple method of adding hydrochloric acid to a solution of **3-IPy** – this approach was found to yield a hemihydrate, in spite of the relatively small amount of water present in the system. In order to produce anhydrous **3-IPy**HCl, special care had to be taken to avoid introducing water into the system: **3-IPy** was dissolved in dry dichloromethane, and dried hydrogen chloride gas was passed through the solution. Thus, we have managed to prepare anhydrous **3-IPy**HCl as a microcrystalline precipitate. Fortunately, several obtained crystals were of sufficient size for X-ray diffraction measurements. The structure of **3-IPy**HCl was found to be markedly different than those of the bromide and the iodide. The geometries of the hydrogen and the halogen bonds formed with the chloride anion are quite similar to those with the bromide and the iodide in **3-IPy**HBr and **3-IPy**HI, although the C–I···Cl^- halogen bond is somewhat less linear (172°), and the N–H···Cl^- hydrogen bond is somewhat more linear (*ca.* 165°), with the angle between the two contacts being 106°. The resulting structure however does not comprise centrosymmetric tetramers, but rather helical chains – it is probable that a (**3-IPy**HCl)$_2$ tetrameric structure analogous to those with larger halogenides in the case of chloride would be too strained, which results in opening of the rings into chains.

The above mentioned **3-IPy**HCl hemihydrate ((**3-IPy**HCl)$_2$·H_2O), the only product obtained from **3-IPy** and HCl if particular care was not taken to eliminate water, presented an entirely different arrangement of halogen and hydrogen bonding. Unlike the simple salts, there are two distinct chloride anions independent of symmetry, of which one binds two **3-IPy**H^+ cations through a pair of C–I···Cl^- halogen bonds and the other through a pair of N–H···Cl^- hydrogen bonds, resulting in cyclic (**3-IPy**HCl)$_4$ octamers (Fig. 3). The water molecules (two per (**3-IPy**HCl)$_4$ unit) bridge between

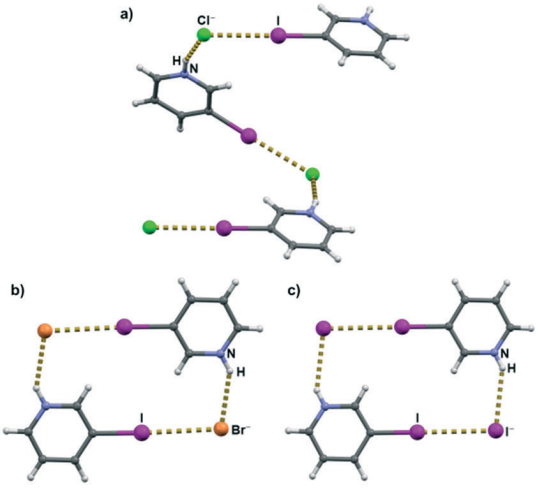

Fig. 2 a) Halogen and hydrogen bonded chains in **3-IPy**HCl; halogen and hydrogen bonded tetramers in b) **3-IPy**HBr and c) **3-IPy**HI.

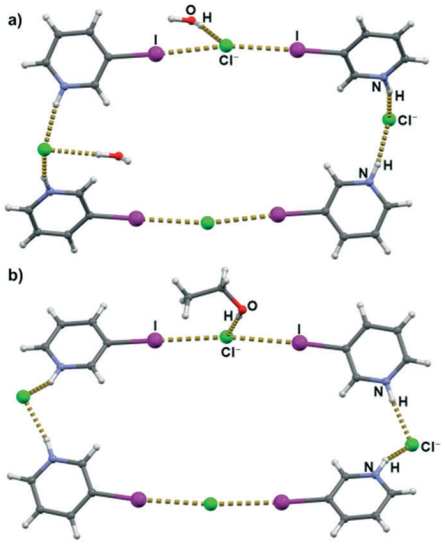

Fig. 3 Halogen and hydrogen bonded octamers in a) (**3-IPy**HCl)$_2$·H_2O and b) (**3-IPy**HCl)$_4$·EtOH.

Published on 12 May 2020. Downloaded by University of Zagreb on 10/21/2021 3:54:01 PM.

neighbouring octamers as hydrogen bond donors binding to chloride anions. Each chloride anion thus participates in three strong interactions – either three hydrogen bonds (two N–H···Cl^- bonds with cations and one O–H···Cl^- bond with a water molecule) or two C–I···Cl^- halogen bonds and an O–H···Cl^- hydrogen bond. The relative configurations of these interactions are such that the hydrogen bonds tend to be (approximately) orthogonal to other interactions (both halogen and hydrogen bonds), while the two C–I···Cl^- halogen bonds are almost collinear (Cl^-···I···Cl^- angle of 168°). This is in accordance with the fact that the hydrogen bond, being the stronger interaction, causes greater deformation of the electron density on the chloride anion, leading to depletion of electron density in the continuation of the hydrogen bond, which directs subsequent interactions. It is interesting to note that very similar assembly has also been found in the ethanol solvate ((**3-IPy**HCl)$_4$·EtOH),[18] albeit here only one (halogen bonded) chloride is an acceptor of the only O–H···Cl^- hydrogen bond.

The structures of the three halogenides derived from **4-IPy** again consist of chains with alternating cations and anions connected by hydrogen and halogen bonds (Fig. 4). Unlike the halogenides of **2-IPy** and **3-IPy**, here the bromide is isostructural with the chloride. Furthermore, in both structures the arrangement of the halogen and hydrogen bonds is much closer to linear – the I···X^-···H angle of *ca.* 160° – than to perpendicular as in all of the earlier cases. On the other hand, the C–I···X^- halogen bonds deviate more from linearity than in other structures: *ca.* 167° in **4-IPy**HCl and *ca.* 170° in **4-IPy**HBr. This is not the case in the structure of **4-IPy**HI – here the halogen bond is more linear (176°) and the angle between the bonds is significantly lower (126°). The change in the hydrogen/halogen bonded chains also reflects a change in the crystal packing. While in all three structures the halogenide anion along with the strong halogen and hydrogen bonds participates in two additional C–H···X^- contacts with cations from neighbouring chains, and in **4-IPy**HCl and **4-IPy**HBr, this interconnection of chains leads to layers, whereas in **4-IPy**HI this gives rise to a honeycomb-like 3D structure.

In addition to the deliberately synthesized iodopyridinium halogenides, a rather interesting and unexpected side product was also obtained. When the solution of **2-IPy** and hydrochloric acid was left to stand under ambient conditions for a prolonged period of time, a small amount of a double salt – 2-iodopyridinium chloride iodide ((**2-IPy**H)$_2$ Cl I) – was obtained, the iodide presumably having formed as a product of the decomposition of **2-IPy** over time. To the best of our knowledge, this is the first example of a double salt comprising both hydrogen and halogen bond donors and two different halogenide anions. In this most interesting structure, the C–I···X^- halogen bonds are formed exclusively with the iodide anion, while the N–H···X^- hydrogen bonds were formed only with the chloride anion (Fig. 5). Through these halogen and hydrogen bonds the 2-iodopyridinium cations and alternating chloride and iodide anions are connected into centrosymmetric [(**2-IPy**H)$_4$Cl$_2$I$_2$] octamers (Fig. 5). Besides the two N–H···Cl^- hydrogen bonds, each chloride anion is an acceptor of one additional C–H···Cl^- contact, while the iodide along with a pair of two C–I···I^- halogen bonds participates in two C–H···I^- contacts. These additional C–H···I^- and C–H···Cl^- contacts connect the [(**2-IPy**H)$_4$Cl$_2$I$_2$] units into layers.

When hydrogen and halogen bonds in all nine structures are compared, it can be noticed that the hydrogen bonds are in all nine cases more shortened (relative to the sum of the donor and acceptor van der Waals radii), with this shortening decreasing from chlorides (mean value of 71.9(1.2)%) over bromides (76(4)%) to iodides (80(3)%). The mean values for halogen bonds with the three halogenides on the other hand do not differ within even one standard deviation – 84.5(1.9)% for chloride, 84.7(1.4)% for bromide and 84.7(8) for iodide. In spite of this, there does seem to be a general trend for the structures exhibiting shorter hydrogen bonds to also have shorter halogen bonds (Fig. 6).

This trend is followed by six structures, while three structures – **3-IPy**HCl, **4-IPy**HCl, and **4-IPy**HBr – have some of the shortest hydrogen bonds, but longest halogen bonds. It is interesting to note that all three structures belong to space groups with non-translational symmetry elements ($P2/c$ in the first case and $P2_1/m$ in the latter two). Also, in all three structures the halogen bond angles are unusually low (*ca.* 171.8°, 166.8° and 170.8°, respectively). This would seem to

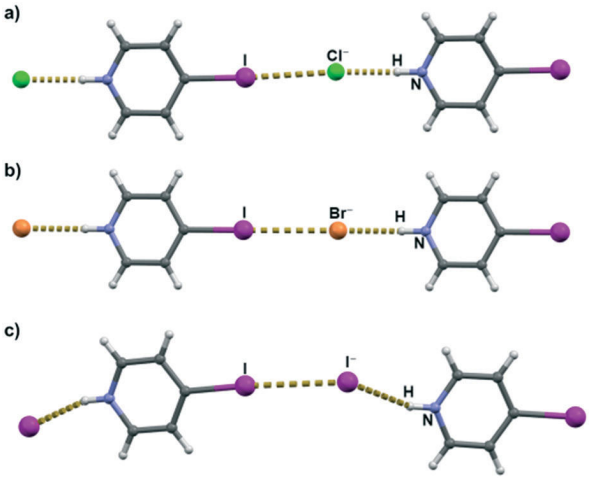

Fig. 4 Halogen and hydrogen bonded chains in a) **4-IPy**HCl; b) **4-IPy**HBr; c) **4-IPy**HI.

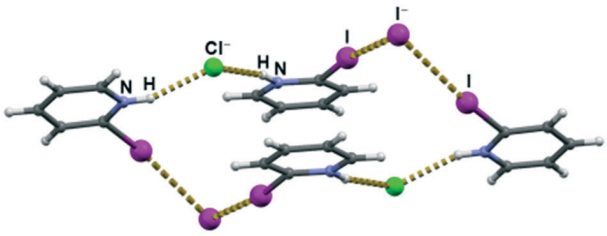

Fig. 5 Halogen and hydrogen bonded octamers in the double salt ((**2-IPy**H)$_2$ Cl I).

 This journal is © The Royal Society of Chemistry 2020

Published on 12 May 2020. Downloaded by University of Zagreb on 10/21/2021 3:54:01 PM.

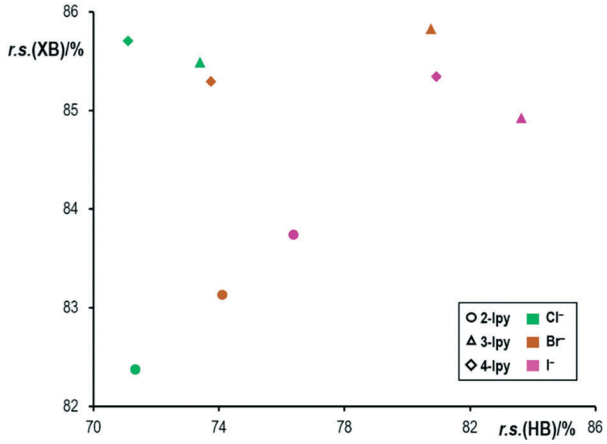

Fig. 6 The relative lengths of the halogen bonds (XB) and the hydrogen bonds (HB) in iodopyridinium halogenides (expressed as a percentage of the sum of the corresponding donor and acceptor van der Waals radii). Circles denote **2-IPy**, triangles **3-IPy** and rhombi **4-IPy**, while green symbols denote chlorides, brown bromides and purple iodides.

indicate that in these structures there are specific packing effects which allow for the higher symmetry of the packing, at the expense of bending the halogen bond and thus weakening it. Furthermore, the relationship between the halogen and the hydrogen bond relative lengths in the series of **2-IPy** halogenides is almost perfectly linear (Fig. 6, bottom left) both relative bond lengths increasing with the size of the halogenide (note that unlike the **3-IPy** and **4-IPy** series, the **2-IPy** halogenides all have almost identical motifs of halogen and hydrogen bonded chains; see Fig. 1). It therefore does seem that the halogen bond also follows the same general trend as the hydrogen bond: both diminish with the size of the halogenide anion acceptor. However, the hydrogen bond is more affected by the size of the halogenide acceptor than the halogen bond (in the **2-IPy** series the hydrogen bond relative length increases by *ca.* 5% from chloride to iodide, while the halogen bond increases by only *ca.* 1%). On the other hand, the halogen bond (being relatively weak in the studied series of compounds) is more affected by crystal packing sufficiently that the effect of changing the halogenide acceptor may be entirely concealed.

It is interesting to compare this result with the conclusions with a recent study of competition between halogen and hydrogen bonds in various solvents.[19] This has shown that halogen bonded products are more favourable in solvents of higher polarity because the hydrogen bond is more affected by the solvent, due to stronger solvation of the hydrogen bond donors, as compared to halogen bond donors. The effect of the smaller halogen (with larger charge density) is equivalent. A smaller halogenide (*e.g.* Cl^-) will form both stronger halogen and hydrogen bonds than a larger one (*e.g.* I^-); however, while the difference in hydrogen bond strengths will be considerable, the difference in halogen bond strengths will be small, or even negligible.

The difference in the sensitivity of the halogen bonds and the hydrogen bonds to the change of the halogenide is to be expected that in the case of possible competition between hydrogen and halogen donors and/or various halogenides as acceptors, the lighter halogenides (chloride, and in particularly fluoride) will preferentially form hydrogen bonds, and heavier halogenides (bromide, and in particularly iodide) will form halogen bonds. This expectation was indeed borne out by the structure of the (**2-IPy**H)$_2$ Cl I double salt with the chloride forming exclusively hydrogen bonds and iodide forming halogen bonds. We have therefore set out to test its validity on a wider base, and have thus performed a CSD survey of structures which comprise a halogenide anion (chloride, bromide or iodide) and both (at least one) strong hydrogen bond donor (O–H or N–H group) and a covalently bound iodine (specifically C–I or N–I) as a halogen bond donor. Our search has yielded a total of 68 structures satisfying the above conditions which contained chloride, 43 with bromide and 69 with iodide. A search was also made for structures containing fluoride but, as only three datasets were recovered, it was excluded from further analysis.

The first noticeable difference is in the fraction of structures in which one of the competing interactions is absent – while the halogen bond was found to be absent in *ca.* 20% of the cases for each halogenide (23% for chloride, 20% for bromide and 22% for iodide), the hydrogen bond was absent in only 17% of chlorides, 27% of bromides and as much as 58% of iodides. This trend is in agreement with the proposition of the halogen bond being less dependent on the halogenide than the hydrogen bond.

When the occurrence of structures with various numbers of halogen and hydrogen bonds are plotted for all three halogenides (Fig. 7), it can be seen that the general distribution of numbers of bonds for chloride and bromide is rather similar, with iodide showing a somewhat different distribution. In all three cases there is a large occurrence of structures where the halogenide is an acceptor of one halogen and one hydrogen bond.

The instances of multiple halogen and hydrogen bonds, however, again follow the above mentioned trend: there is little change in the frequency of occurrence of multiple (two or more) halogen bonds (29% for chloride, 33% for bromide, and only a slightly significant increase for iodide – 50%), while the frequency of multiple hydrogen bonds dramatically decreases from chloride (55%) over bromide (43%) to iodide (12%).

As can be seen from Fig. 7, all three halogenides preferentially form a small number of strong hydrogen and/or halogen bonds, with the total number of interactions rarely exceeding 4. As this would indicate very low coordination numbers, the halogenides must also participate in other interactions, primarily (weak) C–H$\cdots X^-$ hydrogen bonds. Therefore, a more detailed study of the interrelationship of the C–I$\cdots X^-$ halogen bond and the ubiquitous C–H$\cdots X^-$ hydrogen bonds was also performed.

When the C–H$\cdots X^-$ hydrogen bonds are also taken into account, the total coordination number (sum of halogen, strong hydrogen and weak hydrogen bonds) tends to be 6,

Published on 12 May 2020. Downloaded by University of Zagreb on 10/21/2021 3:54:01 PM.

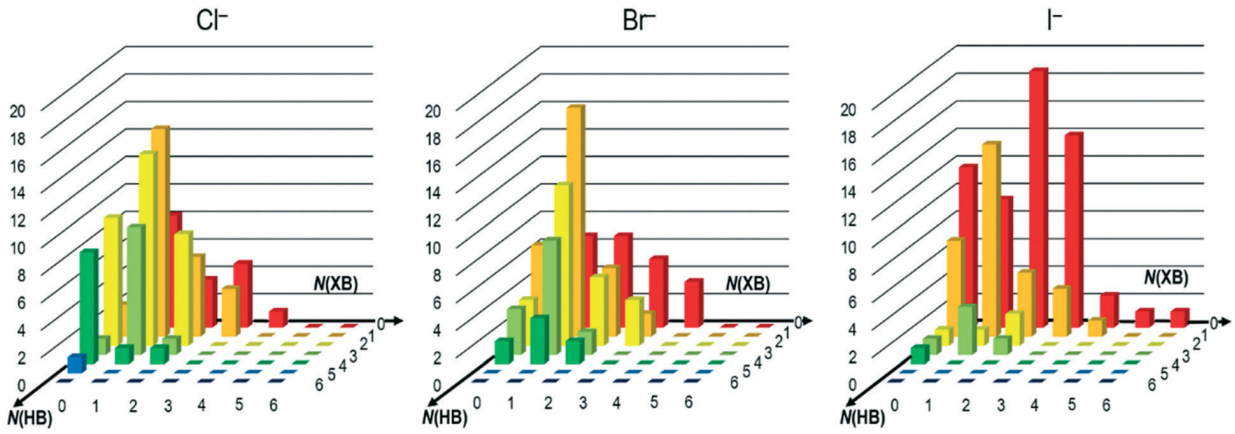

Fig. 7 The occurrence (in %) of combinations of numbers of hydrogen bonds (HB) and halogen bonds (XB) with a halogenide anion in structures where both hydrogen bond (O–H or N–H group) and halogen bond (C–I) donors are present.

with high frequencies of occurrence of coordination numbers 5–8 (with a surprisingly high occurrence of the 8-coordinate chloride, Fig. 8). The chloride anion mostly forms up to two halogen bonds, with the remainder of the contacts being strong and weak hydrogen bonds. There are also structures where the chloride anion acts as an acceptor of 3 or 4 halogen bonds. Except for two exceptions, in these structures strong N–H···Cl^- and O–H···Cl^- hydrogen bonds are absent. The bromide anion, as well as chloride, mostly forms up to two halogen bonds. In the structures in which the bromide anion is an acceptor of more than two C–I···Br^- halogen bonds, only C–H···Br^- hydrogen bonds are formed. The iodide anion mostly forms one C–I···I^- halogen bond with simultaneous hydrogen bonds. There are also a significant number of structures in which the iodide anion is an acceptor of two or three C–I···I^- halogen bonds, and a few examples of structures in which four, five or even six C–I···I^- halogen bonds with simultaneous C–H···I^- hydrogen bonds are formed.

Experimental

Synthesis

Iodopyridines (**2-**, **3-** and **4-IPy**) and solvents were purchased from Sigma-Aldrich Company and used as received. Iodopyridinium halogenides were obtained by dissolving the corresponding iodopyridine in hot ethanol, methanol (or a mixture thereof). To this solution, a stoichiometric amount of the corresponding concentrated (aqueous) acid (HCl, HBr and HI) was added, whereupon solutions were left to cool and evaporate. For synthesis of **3-IPy**HCl, dry hydrogen chloride was passed through a dry dichloromethane solution of **3-IPy**; solution was left to evaporate. Crystals suitable for single crystal X-ray diffraction experiment appeared in two to ten days.

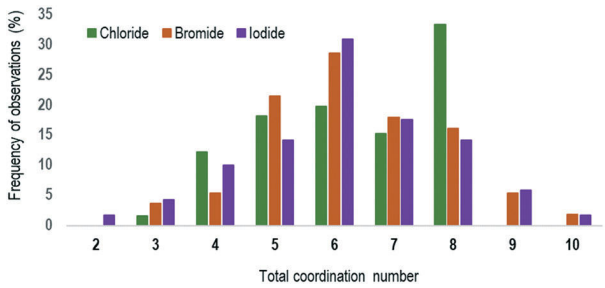

Fig. 8 Frequency of total coordination numbers (as acceptors of halogen, strong hydrogen and weak hydrogen bonds) of halogenide anions in crystal structures.

X-Ray diffraction measurements

All single crystal X-ray diffraction experiments were performed using an Oxford Diffraction Xcalibur Kappa CCD X-ray diffractometer with graphite-monochromated MoKα (λ = 0.71073 Å) radiation, except for the **3IPy**HCl crystal which was measured on an Oxford Diffraction Xcalibur Nova R (CCD detector, microfocus tube) with CuKα (λ = 1.54184 Å) radiation.[20] The data sets were collected using the ω-scan mode over the 2θ-range up to 54°. The structures were solved by SHELXT or by direct methods using the SHELXS and refined using SHELXL programs.[21] The structural refinement was performed on F^2 using all data. The hydrogen atoms were placed in calculated positions and treated as riding on their parent atoms [C–H = 0.93 Å and U_{iso}(H) = 1.2U_{eq}(C); C–H = 0.97 Å and U_{iso}(H) = 1.2U_{eq}(C)]. All calculations were performed using the WinGX crystallographic suite of programs.[22] A summary of data pertinent to X-ray crystallographic experiments is provided in Table S2 (see the ESI†). Further details are available from the Cambridge Crystallographic Centre. Molecular structures of compounds are presented using ORTEP-3 (ref. 23) and their packing diagrams were prepared using Mercury.[24]

Database survey

The CSD data survey has been performed with the ver. 5.41 update 2 (November 2019) CSD database using ConQuest version 2.0.5. When searching hydrogen- or halogen-bonded contacts, the contact angle was constrained to the range between 120° and 180°. For hydrogen and halogen bonded

 This journal is © The Royal Society of Chemistry 2020

Published on 12 May 2020. Downloaded by University of Zagreb on 10/21/2021 3:54:01 PM.

contacts, the upper limit for the distance between the donor atom (hydrogen or iodine) and acceptor ions (Cl^-, Br^-, I^-) was defined as the sum of their van der Waals radii + 0.4 Å. Halogenide ions were defined as halogens with no covalently bonded atoms. As 'strong' hydrogen bonds, only the O–H···X^- and N–H···X^- contacts have been taken into consideration.

Conclusions

Our results are in agreement with the expectations based on solution and computational studies and indicate that the affinity towards halogen bonds decreases with the size of the halogenide acceptor as does the affinity towards hydrogen bonds. On the other hand, the effect appears to be much more pronounced for hydrogen bonds than for halogen bonds, with the relative bond lengths of the latter increasing by only *ca.* 1% from chloride to iodide – the difference is so minor that other packing effects will have much greater effects. This difference between the halogen and hydrogen bonding with halogenides in the solid state is in agreement with the previously described effect of the solvent on the formation of hydrogen and halogen bonds. A smaller halogenide (*i.e.* one with larger charge density) will form both stronger halogen and hydrogen bonds than a larger one; however, while the difference in hydrogen bond strengths will be considerable, the difference in halogen bond strengths will be small, or even negligible. As a result, halogen bonds will occur more likely in the case of the larger halogenide, even though the halogen bond itself is weaker, as clearly seen from the results of our CSD study and vividly demonstrated by the structure of the (**2-IPy**H)$_2$ Cl I double salt.

From the synthetic point of view, lighter halogenides are better solvated in protic solvents (due to stronger hydrogen bonds) and are less likely to yield halogen bonded products (explaining the predominance of halogen bonded cocrystals with iodides over bromides and chlorides and the general absence of halogen bonded cocrystals with fluorides) as well as solvates (*e.g.* (**3-IPy**HCl)$_2$·H_2O and (**3-IPy**HCl)$_4$·EtOH). The latter can be avoided using non-protic solvents (in our case CH_2Cl_2 for **3-IPy**HCl).

In conclusion, iodide, in spite of it being the weakest halogen bond acceptor among the (non-radioactive) halogenides and due to it being an even weaker hydrogen bond donor, is the most reliable halogenide building block for halogen bonded structures.

Conflicts of interest

There are no conflicts to declare.

Acknowledgements

This research was supported by the Croatian Science Foundation under the project IP-2019-04-1868. We are grateful to Dr. Krešimir Molčanov from the Ruđer Bošković Institute, Zagreb, for collecting the diffraction data for the **3-IPy**HCl crystal.

Notes and references

1 (*a*) L. Brammer, E. A. Bruton and P. Sherwood, *Cryst. Growth Des.*, 2001, **1**, 277; (*b*) G. Aullón, D. Bellamy, L. Brammer, E. A. Bruton and A. G. Orpen, *Chem. Commun.*, 1998, 653; (*c*) M. Mascal, *J. Chem. Soc., Perkin Trans. 2*, 1997, **10**, 1999; (*d*) T. Steiner, *Acta Crystallogr., Sect. B: Struct. Sci.*, 1998, **54**, 456; (*e*) P. K. Thallapallya and A. Nangia, *CrystEngComm*, 2001, **3**, 114–119.

2 (*a*) C. I. Ilioudis, K. S. B. Hancock, D. G. Georganopoulou and J. W. Steed, *New J. Chem.*, 2000, **24**, 787; (*b*) A. G. Avent, P. A. Chaloner, M. P. Day, K. R. Seddon and T. Welton, *J. Chem. Soc., Dalton Trans.*, 1994, 3405; (*c*) G. Gil-Ramírez, E. Escudero-Adán, J. Benet-Buchholz and P. Ballester, *Angew. Chem., Int. Ed.*, 2008, **47**, 4114; (*d*) S. Chowdhuri and A. Chandra, *J. Phys. Chem. B*, 2006, **110**, 9674.

3 (*a*) P. D. Beer and P. A. Gale, *Angew. Chem., Int. Ed.*, 2001, **40**, 486; (*b*) J. M. Llinares, D. Powell and K. Bowman-James, *Coord. Chem. Rev.*, 2003, **240**, 57; (*c*) Y. Wang, J. Xiang and H. Jiang, *Chem. – Eur. J.*, 2011, **17**, 613; (*d*) K. Choi and A. D. Hamilton, *J. Am. Chem. Soc.*, 2001, **123**, 2456.

4 (*a*) S. Muhammad, C. Liu, L. Zhao, S. Wu and Z. Su, *Theor. Chem. Acc.*, 2009, **122**, 77; (*b*) F. Zapata, A. Caballero, N. G. White, T. D. W. Claridge, P. J. Costa, V. Félix and P. D. Beer, *J. Am. Chem. Soc.*, 2012, **134**, 11533.

5 (*a*) R. Vilar, D. M. P. Mingos, A. J. P. White and D. J. Williams, *Angew. Chem., Int. Ed.*, 1998, **37**, 1258; (*b*) J. S. Fleming, K. L. V. Mann, C.-A. Carraz, E. Psillakis, J. C. Jeffrey, J. A. McCleverty and M. D. Ward, *Angew. Chem., Int. Ed.*, 1998, **37**, 1279; (*c*) J. C. Mareque Rivas and L. Brammer, *New J. Chem.*, 1998, **22**, 1315.

6 (*a*) G. Cavallo, P. Metrangolo, R. Milani, T. Pilati, A. Priimagi, G. Resnati and G. Terraneo, *Chem. Rev.*, 2016, **116**, 2478; (*b*) R. W. Troff, T. Mäkelä, F. Topić, A. Valkonen, K. Raatikainen and K. Rissanen, *Eur. J. Org. Chem.*, 2013, 1617; (*c*) K. Lisac, F. Topić, M. Arhangelskis, S. Cepić, P. A. Julien, C. W. Nickels, A. J. Morris, T. Friščić and D. Cinčić, *Nat. Commun.*, 2019, **10**, 61; (*d*) M. Saccone, G. Cavallo, P. Metrangolo, A. Pace, I. Pibiri, T. Pilati, G. Resnati and G. Terraneo, *CrystEngComm*, 2013, **15**, 3102; (*e*) C. B. Aakeroy, M. Baldrighi, J. Desper, P. Metrangolo and G. Resnati, *Chem. – Eur. J.*, 2013, **19**, 16240; (*f*) C. B. Aakeröy, T. K. Wijethunga, M. A. Haj, J. Desper and C. Moore, *CrystEngComm*, 2014, **16**, 7218; (*g*) K. Lisac and D. Cinčić, *CrystEngComm*, 2018, **20**, 5955; (*h*) V. Nemec, L. Fotović, T. Vitasović and D. Cinčić, *CrystEngComm*, 2019, **21**, 3251; (*i*) M. Eraković, D. Cinčić, K. Molčanov and V. Stilinović, *Angew. Chem., Int. Ed.*, 2019, **58**, 15702.

7 (*a*) T. A. Logothetis, F. Meyer, P. Metrangolo, T. Pilati and G. Resnati, *New J. Chem.*, 2004, **28**, 760; (*b*) A. Caballero, F. Zapata, N. G. White, P. J. Costa, V. Félix and P. D. Beer, *Angew. Chem., Int. Ed.*, 2012, **51**, 1876; (*c*) J. Grebe, G. Geiseler, K. Harms, B. Neumüller and K. Dehnicke, *Angew. Chem., Int. Ed.*, 1999, **38**, 222; (*d*) J. Grebe, G. Geiseler, K. Harms and K. Dehnicke, *Z. Naturforsch., B: J. Chem. Sci.*, 1999, **54**, 77.

Published on 12 May 2020. Downloaded by University of Zagreb on 10/21/2021 3:54:01 PM.

8 A CSD search of the cocrystals of halogenide salts with perfluorinated iodobenzenes yields 50 crystal structures with iodide, 30 with bromide, 27 with cloride and 0 with fluoride.
9 (*a*) A. M. S. Riel, M. J. Jessop, D. A. Decato, C. J. Massena, V. R. Nascimento and O. B. Berryman, *Acta Crystallogr., Sect. B: Struct. Sci., Cryst. Eng. Mater.*, 2017, **73**, 203; (*b*) P. K. Chattaraj, H. Lee and R. G. Parr, *J. Am. Chem. Soc.*, 1991, **113**, 1855.
10 (*a*) J. S. Murray, P. Lane, T. Clark and P. Politzer, *J. Mol. Model.*, 2007, **13**, 1033; (*b*) P. Politzer, J. S. Murray and T. Clark, *Phys. Chem. Chem. Phys.*, 2010, **12**, 7748; (*c*) V. Stilinović, G. Horvat, T. Hrenar, V. Nemec and D. Cinčić, *Chem. – Eur. J.*, 2017, **23**, 5244.
11 (*a*) M. Freytag and P. G. Jones, *Z. Naturforsch., B: J. Chem. Sci.*, 2001, **56**, 889; (*b*) P. G. Jones and V. Lozano, *Acta Crystallogr., Sect. E: Struct. Rep. Online*, 2003, **59**, 632; (*c*) N. Bedeković, V. Stilinović, T. Friščić and D. Cinčić, *New J. Chem.*, 2018, **42**, 10584; (*d*) V. Nemec, L. Fotović, T. Friščić and D. Cinčić, *Cryst. Growth Des.*, 2017, **17**, 6169.
12 Q. Jin Shen and W. J. Jin, *Phys. Chem. Chem. Phys.*, 2011, **13**, 13721.
13 H. Wang, X. Ran Zhao and W. J. Jin, *Phys. Chem. Chem. Phys.*, 2013, **15**, 4320.
14 M. Freytag, P. G. Jones, B. Ahrens and A. K. Fischer, *New J. Chem.*, 1999, **23**, 1137.
15 A. M. S. Riel, D. A. Decato, J. Sun, C. J. Massena, M. J. Jessop and O. B. Berryman, *Chem. Sci.*, 2018, **9**, 5828.
16 M. D. García, V. Blanco, C. Platas-Iglesias, C. Peinador and J. M. Quintela, *Cryst. Growth Des.*, 2009, **9**, 5009.
17 P. M. J. Szell, G. Cavallo, G. Terraneo, P. Metrangolo, B. Gabidullin and D. L. Bryce, *Chem. – Eur. J.*, 2018, **24**, 11364.
18 K. Raatikainen, M. Cametti and K. Rissanen, *Beilstein J. Org. Chem.*, 2010, **6**, 4.
19 C. C. Robertson, J. S. Wright, E. J. Carrington, R. N. Perutz, C. A. Hunter and L. Brammer, *Chem. Sci.*, 2017, **8**, 5392.
20 Oxford Diffraction, CrysAlis CCD and CrysAlis RED. Version 1.170, Oxford Diffraction Ltd., Wroclaw, Poland, 2003.
21 G. M. Sheldrick, *Acta Crystallogr., Sect. A: Found. Crystallogr.*, 2008, **64**, 112.
22 L. J. Farrugia, *J. Appl. Crystallogr.*, 1999, **32**, 837.
23 L. J. Farrugia, *J. Appl. Crystallogr.*, 1997, **30**, 565.
24 C. F. Macrae, I. J. Bruno, J. A. Chisholm, P. R. Edgington, P. McCabe, E. Pidcock, L. Rodriguez-Monge, R. Taylor, J. van de Streek and P. A. Wood, *J. Appl. Crystallogr.*, 2008, **41**, 466.

 This journal is © The Royal Society of Chemistry 2020

II

Evaluation of halogenopyridinium cations as halogen bond donors

L. Fotović, N. Bedeković i V. Stilinović,

Cryst. Growth Des. **21** (2021) 6889–6901. (objavljen)

Doprinos koautora:

L. Fotović – sinteza soli, kristalizacija, strukturna, termička i spektrokopska analiza, kristalografija, obrada rezultata i pisanje rada

N. Bedeković – kvantno-kemijski računi

V. Stilinović – savjetovanje i pisanje rada

Rad je reproduciran uz dozvolu Američkog kemijskog društva.*

*Reprinted with permission from *Cryst. Growth Des.* **2021**, *21*(12), 6889–6901. Copyright 2021 American Chemical Society.

CRYSTAL GROWTH & DESIGN

pubs.acs.org/crystal

Article

Evaluation of Halogenopyridinium Cations as Halogen Bond Donors

Luka Fotović, Nikola Bedeković, and Vladimir Stilinović*

Cite This: *Cryst. Growth Des.* 2021, 21, 6889−6901

Read Online

ACCESS | Metrics & More | Article Recommendations | Supporting Information

ABSTRACT: We have performed a database survey and a structural and computational study of the potential and the limitations of halogenopyridinium cations as halogen bond donors. The database survey demonstrated that adding a positive charge on a halogenopyridine ring increases the probability that the halogen atom will participate in a halogen bond, although for chloropyridines it remains below 60%. Crystal structures of both protonated and *N*-methylated monohalogenated pyridinium cations revealed that the iodo- and bromopyridinium cations always form halogen-bonding contacts with the iodide anions shorter than the sum of the vdW radii, while chloropyridinium cations mostly participate in longer contacts or fail to form halogen bonds. Although a DFT study of the electrostatic potential has shown that both protonation and *N*-methylation of halogenopyridines leads to a considerable increase in the ESP of the halogen σ-hole, it is generally not the most positive site on the cation, allowing for alternate binding sites.

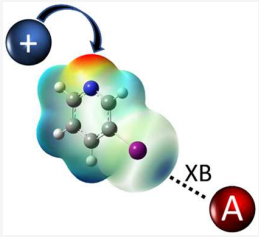

Downloaded via UNIV OF ZAGREB on February 8, 2022 at 09:07:10 (UTC).
See https://pubs.acs.org/sharingguidelines for options on how to legitimately share published articles.

INTRODUCTION

The crucial feature that enables halogen atoms to act as Lewis acids in order to form halogen bonds[1−6] is the presence of an area of depleted electron density (σ-hole)[7,8] in the continuation of the covalent bond. The energy of a halogen bond formed between donors with a given acceptor increases with the electrostatic potential of the σ-hole on the donor halogen atom. Therefore, the best halogen-bond donors are those that comprise polarizable halogen atoms (iodine and bromine) bonded to a molecule that can exhibit an electron-withdrawing effect on the halogen atom—thus increasing the electrostatic potential of the σ-hole on the halogen atom and consequently the potential of the halogen atom to form a halogen bond with a Lewis base.[9−12]

To date, most commonly used halogen bond donors have been perfluorinated iodo- or/and bromohydrocarbons,[13−22] where the electronegative fluorine substituents on the hydrocarbon skeleton act as electron-withdrawing fragments. Other electron-withdrawing substituents, such as cyano and nitro groups, can also be employed.[23−27] Halogenoethyne derivatives were also successfully used as halogen bond donors, as there the large positive potential of the σ-hole is ensured by the electron-withdrawing properties of the C−C triple bond.[28−31] Alternatively, halogen atoms can be directly bonded to a (more electronegative) heteroatom, such as nitrogen in (*N*-halogeno)imides—a strategy that has yielded some of the strongest organic halogen bond donors studied to date.[32−39] Another approach is using hypervalent halogens such as in iodine(I) and iodine(III) compounds. This can lead to much higher positive charges on the halogen atoms, making them very strong halogen bond donors.[40,41]

The aforementioned principles have mainly been employed for the design of neutral halogen bond donors. There is, however, another approach for ensuring a large positive electrostatic potential on a halogen atom: making the halogen atom a part of a positively charged species. The most widely studied group of compounds has been based on halogenated aromatic (primary) amines,[42−45] as well as halogenated N-heterocycles (such as halogenopyridines and halogenoimidazoles) and their derivatives.[46−77] These compounds are a logical starting point for the synthesis of cationic halogen-bond donors: on the one hand, their structural rigidity allows for simple control of the geometry of the formed bonds, and on the other hand, they can easily be transformed into cations, either by protonation or by alkylation of the nitrogen atom.

Over the last 20 years both protonated and methylated halogenopyridines have been extensively studied as halogen-bond donors. They have been found to form halogen bonds with organic (such as saccharinate,[46] bromanilate[47]) and inorganic anions (such as halogenides,[48−53] halogenometalates,[54−64] cyanometalates,[65−67] etc.) Molecules containing iodopyridinium groups have also been designed to act as anion receptors[68−72] and even as halogen-bond donors in catalysts of halogenide abstraction.[73]

N-Alkylated halogenopyridinium cations have also found their place as counterions in Ni(dmit)$_2$ (dmit = 1,3-dithiol-2-thione-4,5-dithiolate) salts, which have been synthesized and investigated as supramolecular conductors—because of the possibility of participating in multiple hydrogen and halogen bonds, cations of this type were used to control the conductivity and magnetic properties of these materials.[74−77]

Received: July 15, 2021
Revised: October 26, 2021
Published: November 8, 2021

ACS Publications

© 2021 The Authors. Published by American Chemical Society

https://doi.org/10.1021/acs.cgd.1c00805
Cryst. Growth Des. 2021, 21, 6889−6901

Table 1. Overview of Halogen Bonding in Iodides of Protonated and Methylated Halogenopyridinium Cations (X- Ray Data Measured at Room Temperature)

protonated halogenopyridinium iodide	d(XB)/Å	RS[a]/%	*N*-methylated halogenopyridinium iodide	d(XB)/Å	RS/%
[**2-ClPy**H]I	3.768	−0.1	[**2-ClPy**Me]I[b]	3.496	6.3
				3.509	5.9
				3.511	5.9
[**2-BrPy**H]I	3.575	5.9			
[**2-IPy**H]I	3.467	12.4	[**2-IPy**Me]I	3.459	12.7
[**3-ClPy**H]I	3.739	−0.2	[**3-ClPy**Me]I	3.774	−1.2
[**3-BrPy**H]I	3.589	6.3	[**3-BrPy**Me]I	3.637	5.0
[**3-IPy**H]I	3.516	11.2	[**3-IPy**Me]I	3.538	10.7
[**4-ClPy**H]I	3.733	−0.1	[**4-ClPy**Me]I	3.587	3.8
[**4-BrPy**H]I	3.648	4.8			
[**4-IPy**H]I	3.532	10.8	[**4-IPy**Me]I	3.552	10.3

[a]RS(XB) = 100[1 − (d(X···I$^-$)/(r(X) + r(I$^-$))],where r(X) and r(I$^-$) are the van der Waals radii of the corresponding atoms. [b]Measured at 170 K.

Similarly to neutral halogen-bond donors, cationic halogen-bond donors decrease in strength from iodo to chloro derivatives.[50,52,70,78,79] Indeed, while iodopyridinium cations form halogen bonds rather predictably, chloropyridinium cations often fail to form halogen bonds, even though accessible acceptors are present in the crystal structure. Willett and co-workers have shown that in the structures of halogenopiridinium tetrahalocuprate(II) salts the C−Br···X$^-$ halogen bonds are relatively shorter than the analogous C−Cl···X$^-$ halogen bonds, which sometimes are even not present.[55] Likewise, our previous work on halogenopyridinium hexacyanoferrates has shown that in structures containing a chloropyridinium cation a halogen bond with chlorine as the donor was not present, despite the presence of multiple potential acceptor sites.[67]

In this paper we have endeavored to investigate more closely both the potential and the limitations of halogenopyridinium cations as halogen-bond donors. For this purpose, we have selected monohalogenated pyridine derivatives (*ortho*, *meta*, and *para*; chloro, bromo, and iodo), as both protonated and *N*-methylated pyridinium cations. For the study of their halogen-bonding potential in the solid state, we have opted for the iodide salts—the iodide anion has been shown to be the most reliable halogen bond acceptor among halogenides.[50] The structures of (protonated) halogenopyridinium iodides have been previously reported[50,51] and were included in the analysis as such, while the *N*-methylated halogenopyridinium iodides were synthesized and structurally characterized. Along with the comparative study of halogen bond geometries in the crystals of the two series of crystalline solids, we have performed DFT calculations in order to better understand the fundamental reasons for the observed behavior of halogenopyridinium cations.

RESULTS AND DISCUSSION

To ascertain whether there is a statistical trend toward an increase in the halogen-bond probability with addition of a positive charge on a halogenopyridine ring, we have performed a Cambridge Structural Database[80] (version 5.42 Update 3 (May 2021) CSD database using ConQuest Version 2020.3.0) survey of structures that comprise a halogen substituent on an aromatic nitrogen heterocycle. This has yielded a total of 3112 data sets, the majority of which corresponded to neutral molecules, and 655 to cations derived from them. Of these, 524 were structures containing *N*-protonated cations and only 131 structures with *N*-alkylated cations. For neutral halogen-oheterocycles it has been found that in ca. 33% of the structures the halogen atom is in close contact (less than the sum of van der Waals radii) with a potential halogen-bond acceptor (either a nitrogen or oxygen atom or a halogenide anion), indicating the presence of a halogen bond. Halogen-bonding contacts were expectedly found to be the least frequent in chloroheterocycles (27%) followed by bromoheterocycles (39%) and finally iodoheterocycles, where they were found with the greatest frequency (70%). Adding a positive charge (either by protonation or by alkylation of the heterocyclic nitrogen atom) led to a definite increase in the frequencies of halogen bonding, which increased to 56% for cations derived from chloroheterocycles, 82% for bromobromoheterocycles, and 89% for iodoheterocycles. In order to obtain a more detailed picture, we have also performed a series of searches limited to monohalogenopyridines. This has also shown a clear and drastic increase of incidence of halogen bonding upon addition of a positive charge to the pyridine ring—from ca. 7% to ca. 51% for chloropyridines, from ca. 8% to ca. 87% for bromopyridines, and from ca. 40% to ca. 90% for iodopyridines. The increase appears to be somewhat larger for *o*-halogenopyridines (from ca. 8% to ca. 79%) than for *m*-halogenopyridines (from ca. 4% to ca. 70%), as one might expect on the basis of both the proximity of the halogen to the protonated/alkylated nitrogen atom and the resonance effect. The influence of the resonance should also be significant when the halogen is in the *para* position. Unfortunately, this could not be confirmed on the basis of the CSD data—while the incidence of halogen bonds in cations derived from *p*-halogenopyridines is close to that in *o*-halogenopyridinium cations (81%), the number of structures with neutral *p*-halogenopyridines (only four structures with *p*-iodopyridine) in the CSD was too low to allow for a reasonable estimate of the incidence of halogen bonds.

Overall, the CSD data indicate that halogen atoms on a neutral pyridine ring are quite poor halogen-bond donors (except for iodine), but when the pyridine ring is charged, the incidence of the halogen atom acting as a halogen-bond donor dramatically increases. However, this increase does not necessarily make the halogen atoms on charged pyridine rings optimal halogen bond donors—while iodine atoms on either protonated or *N*-alkylated pyridinium cations act as halogen bond donors in ca. 90% of the cases, chlorine does so in only ca. 40−50% of the structures. For comparison, neutral molecules used as "classical" halogen bond donors generally form halogen bonds with reliability similar to that of

https://doi.org/10.1021/acs.cgd.1c00805
Cryst. Growth Des. 2021, 21, 6889−6901

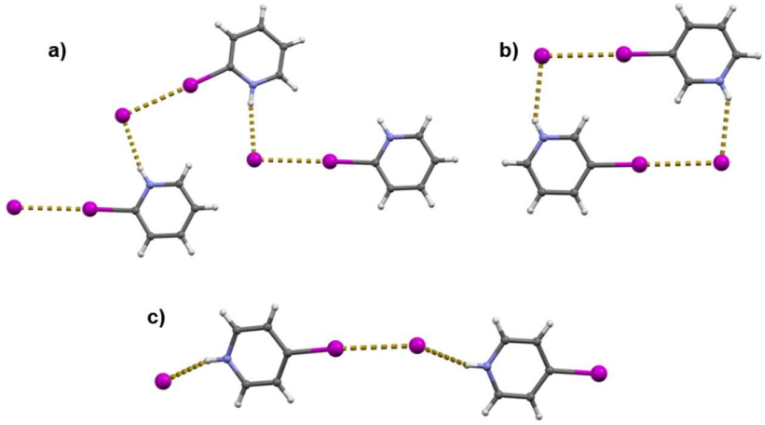

Figure 1. (a) Halogen- and hydrogen-bonded chains in *o*-iodopyridinium iodide. (b) Halogen- and hydrogen-bonded tetramers in *m*-iodopyridinium iodide. (c) Halogen- and hydrogen-bonded chains in *p*-iodopyridinium iodide.[51] Halogen bond lengths are given in Table 1.

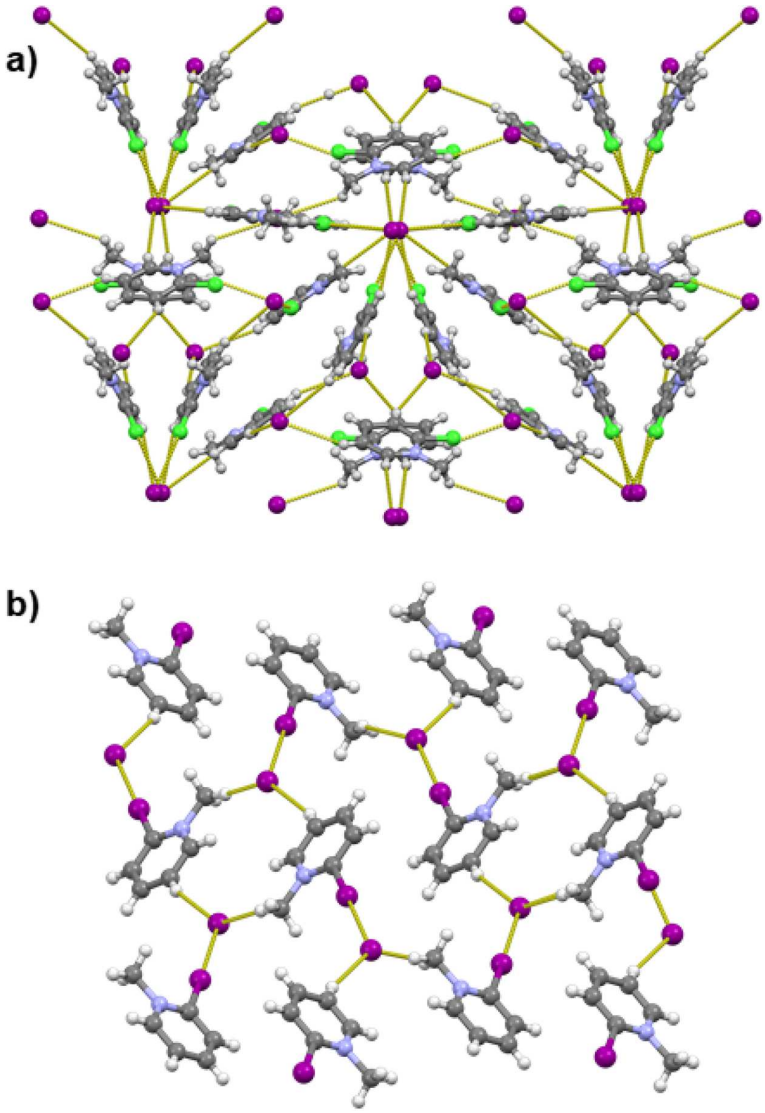

Figure 2. Halogen bonds and short C−H···I$^-$ contacts in crystal structures of *N*-methyl-2-halogenopyridinium iodides: (a) the 3D network in [**2-ClPy**Me]I (view along the *c* axis); (b) the 2D network in [**2-IPy**Me]I (view along the *a* axis). Halogen bond lengths are given in Table 1.

https://doi.org/10.1021/acs.cgd.1c00805
Cryst. Growth Des. 2021, 21, 6889−6901

iodopyridinium cations: fluorinated iodobenzenes form a halogen bond with a potential halogen-bond acceptor (a nitrogen or oxygen atom or a halogenide anion) in 85% (447 out of 524) of the structures where such acceptors are present, fluorinated bromobenzenes in 87% (45 out of 52) of structures, iodoalkynes in 85% (289 out of 339), bromoalkynes in 69% (34 out of 49), and in virtually all structures of *N*-halogenoimides (37 out of 38 *N*-bromoimides and 32 out of 32 *N*-iodoimides).

As the CSD search provided us with the average behavior of halogenopyridines and corresponding cations with a varied collection of (potential) halogen bond acceptors, we decided to take a closer look at the halogen bonding of protonated and *N*-methylated pyridinium cations with the iodide anion. The iodide was a logical choice, as it is on the one hand a halogenide, a simple spherical anion without steric or other issues that might complicate the overall picture of the supramolecular interactions in the crystal, and also as it was found to form halogen bonds most reliably among the halogenides.[50] The crystal structures of chloropyridinium and bromopyridinium iodides have been investigated by Awwadi, Willett and co-workers,[51] while iodopyridinium iodides were reported recently by our group.[50] All of the crystal structures featured in both studies have been determined at room temperature, allowing for meaningful comparisons among the halogen bond geometries. The bond lengths and angles are given in Table 1.

In the structures of all three *o*-halogenopyridinium ([**2-XPy**H]) iodides, halogenopyridinium cations and iodide anions are interconnected in chains trough N−H···I$^-$ hydrogen and C−X···I$^-$ halogen bonds (Figure 1a). In [**2-ClPy**H]I the C−X···I$^-$ halogen bonds are longer than in the bromo and iodo analogues and longer than the sum of van der Waals radii (Table 1). The crystal structures of *m*-halogenopyridinium ([**2-XPy**H]) iodides comprise centrosymmetric cyclical (**3-XPy**H)$_2$I$_2$ tetramers in which **3-XPy**H$^+$ cations and iodide anions are interconnected trough N−H···I$^-$ hydrogen and C−X···I$^-$ halogen bonds (Figure 1b). The relative shortening of the C−X···I$^-$ halogen bonds decreases from ca. 11.2% in the **3-IPy** derivative over ca. 6.3% in the **3-BrPy** derivative to ca. 0.2% in the **3-ClPy** derivative, again with the C−Cl···I$^-$ contact being longer than the sum of the van der Waals radii. Also, the halogen bonds in [**3-IPy**H]I and [**3-BrPy**H]I are almost linear (C−X···I$^-$ angles above 176°), while in [**3-ClPy**H]I the analogous C−Cl···I$^-$ angle is ca. 165°. In the case of *p*-halogenopyridinium (**4-XPy**) iodides, chains are again formed by alternating hydrogen and halogen bonds between alternating **4-XPy**H$^+$ cations and iodide anions (Figure 1c). The C−X···I$^-$ halogen bonds in the iodide salts of the *para* isomers are somewhat longer than in the *ortho* and *meta* isomers but also follow the same trend in decreasing from ca. 10.8% in [**4-IPy**H]I to ca. 4.8% in [**4-BrPy**H]I. The C−Cl···I$^-$ contact in [**4-ClPy**H]I is again longer than the sum of the van der Waals radii by ca. 0.1%. The halogen bond angle is approximately linear only in [**4-IPy**H]I, whereas in both [**4-ClPy**H]I and [**4-BrPy**H]I the angles considerably deviate from linearity (C−X···I$^-$ angles of ca. 164°).

In order to observe the halogen-bonding behavior of positively charged halogenopyridines in the absence of a strong N−H···I$^-$ hydrogen bond, we decided to synthesize and crystallize an equivalent series of *N*-methylated halogenopyridinium iodides. Although we were unfortunately unable to produce two members of the series (derived from **2-BrPy** and **4-BrPy**; see the Experimental Section for details), the crystal structures of the seven compounds we have obtained were sufficient to accentuate significant differences in the observed trends in protonated halogenopyridinium iodides.

Among the salts of *N*-methylated halogenopyridines there is considerably less structural similarity within the *o*-, *m*-, and *p*-substituted groups. This is to be expected, as in the absence of the directing influence of the hydrogen bond that can combine with the halogen bond, the only interaction of significance is the halogen bond, and the crystal structure will be predominantly determined by assembly of (halogen-bonded) ion pairs by weak interactions.

The most dissimilar are the structures of the *o*-substituted [**2-ClPy**Me]I and [**2-IPy**Me]I. The structure of [**2-IPy**Me]I consists of the expected assembly of halogen-bonded ion pairs of *o*-iodopyridinium cations and iodide anions trough C−I···I$^-$ halogen bonds, which further interconnect via C−H···I$^-$ hydrogen bonds into helical chains (Figure 2a). Conversely, the structure of [**2-ClPy**Me]I is a complex 3D network assembled through C−Cl···I$^-$ and C−H···I$^-$ contacts with four *o*-chloropyridinium cations and four iodide anions in the asymmetric unit (Figure 2a). These do not form clear halogen-bonded ion pairs as was the case in [**2-IPy**Me]I—only two iodide anions and three cations form halogen bonds (two cations bind to the same iodide), while the remaining cation and anions participate only in C−H···I$^-$ hydrogen bonds. Of the four cations, one is disordered over a crystallographic inversion center; the disordered cations form C−Cl···I$^-$ halogen bonds along the crystallographic *b* axis and C−H···I$^-$ hydrogen bonds along the crystallographic *c* axis with independent iodide anions (both somewhat disordered over inversion centers), thus forming disordered layers perpendicular to the crystallographic *a* axis.

In the structures of iodides derived from *meta*-substituted pyridines ([**3-IPy**Me]I, [**3-BrPy**Me], and [**3-ClPy**Me]I) the halogenopyridinium cations and iodide anions are connected into chains via C−X···I$^-$ halogen and C−H···I$^-$ hydrogen bonds. [**3-BrPy**Me]I and [**3-IPy**Me]I are quite similar in structural arrangement, although they are not isostructural, as they differ in the space group symmetry. In both structures, the hydrogen- and halogen-bonded chains are interconnected into planar layers trough additional C−H···I$^-$ hydrogen-bonding contacts (Figure 3b,c). The C−I···I$^-$ and C−Br···I$^-$ halogen bonds are shorter than the corresponding sum of van der Waals radii by ca. 11% and 5%, respectively. In [**3-ClPy**Me]I the chains of ion pairs are also interconnected into layers through C−H···I$^-$ hydrogen bonds (Figure 3a); however, the layers formed here are not planar but corrugated. Although it is longer (ca. 1%) than the sum of the corresponding van der Waals radii, the C−Cl···X$^-$ contact can still have a significant effect on the structural arrangement,[81] as appears to be the case in the structure of [**3-ClPy**Me]I.

In the case of the structures derived from *para*-substituted pyridines, [**4-IPy**Me]I and [**4-ClPy**Me]I, the cations and the anions are connected via C−X···I$^-$ halogen and C−H···I$^-$ hydrogen bonds into centrosymmetric cyclical ([**4-XPy**Me]I)$_2$ tetramers (Figure 4). In both structures the C−I···X$^-$ contacts are shorter than the sum of van der Waals radii and are quite linear (ca. 10% and 4% with a ∠(C−I···I$^-$) angle of ca. 172° and a ∠(C−Cl···I$^-$) angle of ca. 170°, respectively). The C−H···I$^-$ hydrogen bond is achieved in both cases through equivalent hydrogen atoms (*ortho* relative to the methylated nitrogen), but the geometry of the C−H···I$^-$ hydrogen-bonded

https://doi.org/10.1021/acs.cgd.1c00805
Cryst. Growth Des. 2021, 21, 6889−6901

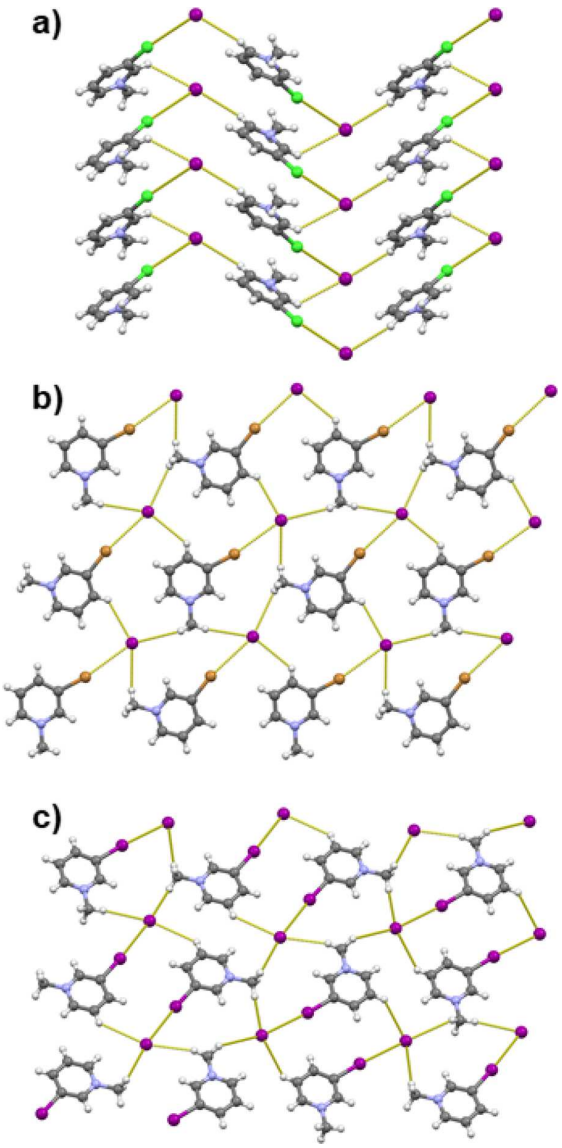

Figure 3. Halogen- and hydrogen (C−H···I⁻)-bonded 2D networks in crystal structures of *N*-methyl-3-halogenopyridinium iodides: (a) [**3-ClPy**Me]I (view along the *a* axis); (b) [**3-BrPy**Me]I (view along the *c* axis); (c) [**3-IPy**Me]I (view along the *a* axis). Halogen bond lengths are given in Table 1.

tetramers is quite different. In the case of [**4-IPy**Me]I the hydrogen bond is almost linear (∠(C−H···I⁻) angle of ca. 178°) and the two pyridinium rings within the tetramer are almost perfectly coplanar (the mean planes of the cations are offset by a mere 0.12 Å). Conversely, in [**4-ClPy**Me]I the ∠(C−H···I⁻) angle is significantly lower (ca. 152°) and the mean planes of the pyridinium cations are offset by ca. 2.18 Å.

The lengths of halogen bonds formed by the *N*-methylated iodopyridinium cations are in most structures comparable to those formed by their respective protonated analogues, the differences between the relative shortenings of any two analogues generally being less than 0.5% (Table 1). However, there is a considerable difference between protonated and methylated chloropyridinium iodides, the C−Cl···I⁻ contact in [**4-ClPy**Me]I being 3.8% shorter and in [**4-ClPy**H]I 0.1% longer than the sum of the van der Waals radii. This implies that the presence of a strong N−H···I⁻ hydrogen bond has a greater effect on the elongation of the (weaker) C−Cl···I⁻ halogen bond, while its effect on the (stronger) C−I···I⁻ halogen bond is negligible. The comparison of halogen bond lengths in [**2-ClPy**Me]I and [**2-ClPy**H]I would also seem to support this conclusion on first glance. However, as the two data sets have not been measured at the same temperature ([**2-ClPy**Me]I could not be measured at room temperature due to the instability of the crystals), the even shorter C−Cl···I⁻ contacts (5.9−6.3% shorter than the sum of the van der Waals radii) in [**2-ClPy**Me]I are at least partially due to the lower temperature (170 K) at which the crystal was measured and therefore cannot be compared to the rest of the halogen bonds in this study, which were all measured at room temperature.

On comparison of halogen bonds between the "classical" (neutral) halogen bond donors and the iodide anion as an acceptor, it can be seen that there is only a slight difference in halogen bond length between halogen bonds formed with iodopyridinium cations and neutral perfluorinated iodobenzenes as halogen bond donors. The former form halogen bonds which are on average 11.4% shorter than the sum of the van der Waals radii, while the latter form halogen bonds which are on average 9.9% shorter than the sum of the van der Waals radii (based on 19 crystal structures of cocrystals of iodides with neutral perflorinated iodobenzenes measured at room temperature deposited in the CSD). On comparison to an even stronger neutral halogen bond donor such as *N*-iodosuccinimide, the iodopyridinium cations are clearly poorer halogen-bond donors, as in the only crystal structure reported to date of a cocrystal of *N*-iodosuccinimide and an iodide[82] the halogen bond is ca. 21% shorter than the corresponding sum of the van der Waals radii. Comparing the lengths of halogen bonds with N and O acceptors where the donors are cations derived from halogenoheterocycles with those formed by different types of neutral donors (Table 2) shows that with nitrogen acceptors all three groups of cationic halogen-bond donors tend to form longer bonds in comparison to some of the most commonly used neutral donors (fluorinated halogenobenzenes, halogenoalkynes, and halogenoimides). Only in the case of halogen bonds with oxygen acceptors do the lengths of halogen bonds formed by bromo- and iodo-heterocyclic cations approach the mean values for halogen bonds formed by their fluorinated halogenobenzene counterparts.

As was mentioned earlier, the C−I···I⁻ halogen bonds in both protonated and *N*-methylated iodopyridinium iodides display the largest relative shortening (RS) in comparison to the corresponding van der Waals radii (generally double that for C−Br···I⁻ halogen bonds). In comparison to the hydrogen bonds present in all three structures with protonated cations, C−I···I⁻ halogen bonds have somewhat smaller RS values than the hydrogen bonds (19.3% for N−H···I⁻ in [**2-IPyH**]**I**, 11.5% in [**3-IPyH**]**I**, and 14.5% in [**4-IPyH**]**I**), except in [**3-IPy**H]I, where they are practically equivalent. As expected, aromatic hydrogen atoms in [**3-IPy**Me]I and [**4-IPy**Me]I are again involved in C−H···I⁻ hydrogen-bonding contacts shorter than the sum of the van der Waals radii (with **3-IPy** hydrogen atoms in the *ortho* and *para* positions to the nitrogen atom by 1% and 3%, respectively, and with **4-IPy** hydrogen atoms in both *ortho* positions by 3% and 1%). In the methylated series additional hydrogen bonds have been formed between methyl hydrogen atoms and the iodide (with **3-IPy** methyl hydrogen atoms by 5% and with **4-IPy** methyl hydrogen and aromatic hydrogen

https://doi.org/10.1021/acs.cgd.1c00805
Cryst. Growth Des. 2021, 21, 6889−6901

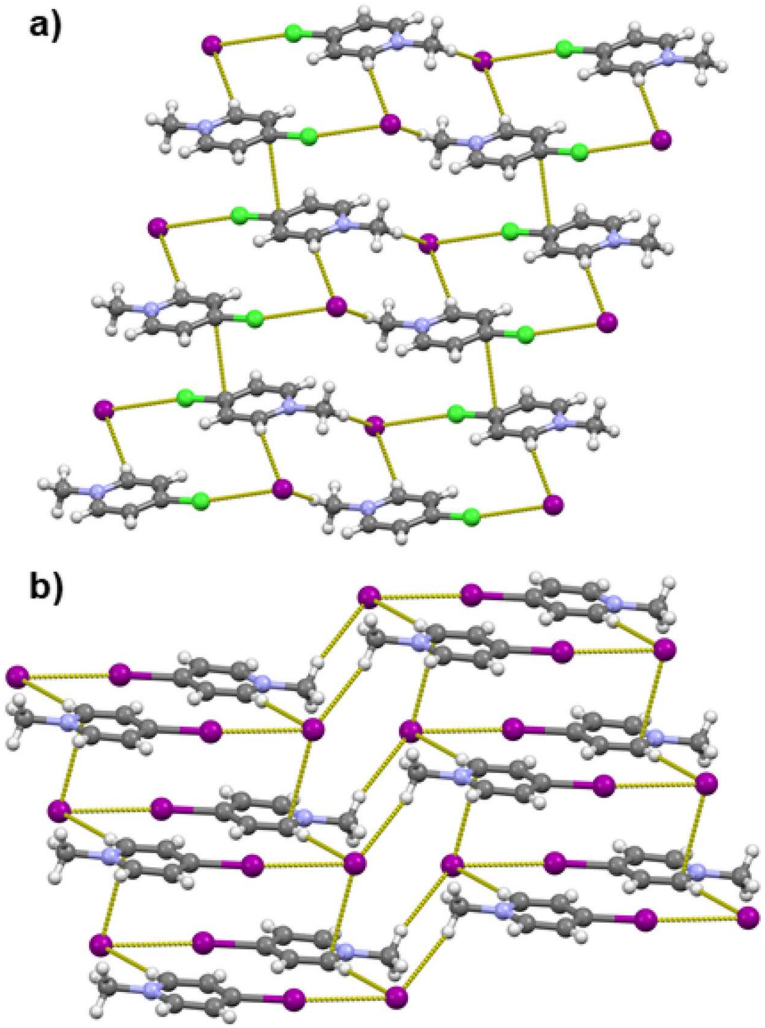

Figure 4. Halogen- and hydrogen (C−H···I$^-$)-bonded tetramers of *N*-methyl-4-halogenopyridinium iodides interconnected by (a) π-stacking in [4-**Cl**Py**Me**]I and (b) anion−π contacts in [**4-IPyMe**]I. Halogen bond lengths are given in Table 1.

Table 2. Relative Shortenings (Mean Values in Percent Based on the CSD Data for Structures Measured at Room Temperature) for Halogen Bonds with N and O Acceptors

	halogen bond acceptor	
halogen bond donor	N	O
chloro-heterocyclic cation	1.2	5.5
bromo-heterocyclic cation	6.5	6.2
iodo-heterocyclic cation	7.3	10.9
fluorinated iodobenzenes	15.3	13.3
fluorinated bromobenzenes	12.0	5.8
iodoalkynes	23.0	16.5
bromoalkynes	16.5	9.6
N-bromoimides	31.4	19.2
N-iodoimides	29.9	26.3

atom in a *para* position longer than sum of the van der Waals radii by 1%). Interestingly, in [**4-IPyMe**]I the iodide anion also participates in a short contact with an aryl carbon atom of a [**4-IPyMe**]$^+$ cation. The carbon atom is in the *ortho* position relative to the methylated nitrogen, and the iodide approaches it orthogonally to the plane of the ring. This anion···π contact (with a corresponding RS value of ca. 1%)[83,84] can therefore be classified as a tetrel π-hole interaction between the iodide and a positive region on the carbon atom perpendicular to the ring plane. Similar anion···π contacts have also been found in crystal structures of several *N*-alkyl-3-halogenopyridinium halogenides.[85]

It can be seen that, although in all of the studied structures the C−X···I$^-$ halogen bonding contacts are present, only among the *N*-methyl-3-bromopyridinium and *N*-methyl-iodopyridinium iodides is this halogen bond clearly the dominant interaction in the crystal structures. The cations interact with the iodides not only through the halogen atom (and the N−H group in the protonated pyridine series) but also through fairly short C−H···I$^-$ hydrogen-bonding contacts and even C···I$^-$ π-hole tetrel bonding contacts. Indeed, in chloropyridinium iodides these "weak" interactions seem to be dominant. The reasons for this phenomenon can be made clear by a detailed study of the electrostatic potential of the potential donor and acceptor sites on both protonated and *N*-methylated pyridinium cations.

As expected, both protonation and *N*-methylation of halogenopyridines lead to an increase in the ESP of the

https://doi.org/10.1021/acs.cgd.1c00805
Cryst. Growth Des. 2021, 21, 6889−6901

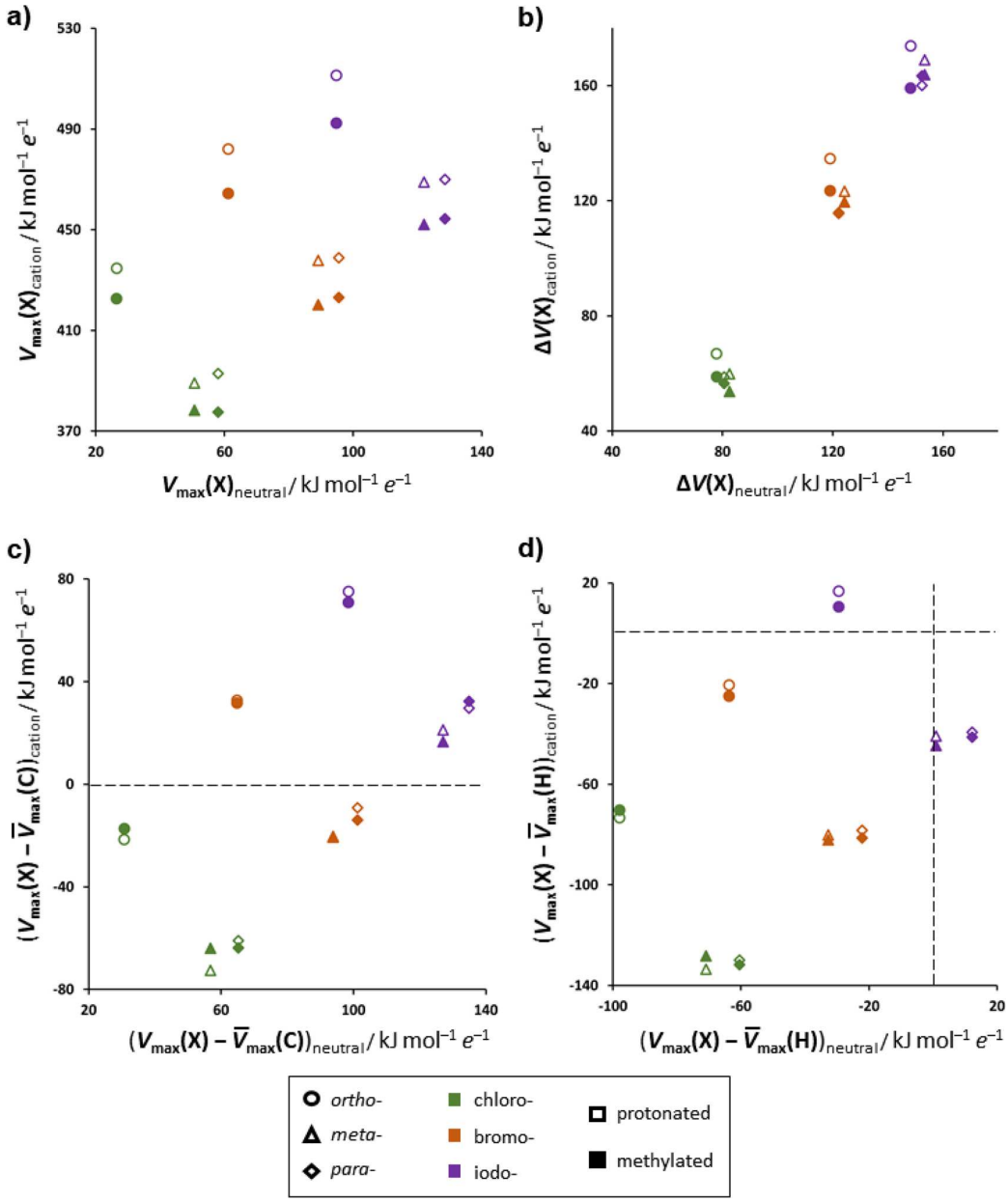

Figure 5. Changes in molecular ESP on halogenopyridines upon protonation and *N*-methylation: (a) plot of the halogen σ-hole ESP ($V_{max}(X)$) on cations vs neutral halogenopyridines; (b) plot of the difference between the $V_{max}(X)$ value and the ESP of the halogen atom perpendicular to it ($(\Delta V(X))$) on cations vs neutral halogenopyridines; (c) plot of the difference between the $V_{max}(X)$ value and the mean ESP on non-hydrogen atoms of the pyridine ring (ESP perpendicular to the plane of the ring) on cations vs neutral halogenopyridines; (d) plot of the difference between the $V_{max}(X)$ value and the mean ESP on the pyridine ring C−H hydrogen atoms on cations vs neutral halogenopyridines. In (c) and (d) the dashed lines denote where the corresponding values equal zero.

halogen atom σ-hole ($V_{max}(X)$). This is most pronounced in *o*-halogenopyridines where the $V_{max}(X)$ value increases by ca. 400−420 kJ mol^{-1} e^{-1}, while in *m*- and *p*-halogenopyridines it increases by ca. 320−350 kJ mol^{-1} e^{-1}. Protonation leads to somewhat larger increase of $V_{max}(X)$ (10−20 kJ mol^{-1} e^{-1}) on the halogen atom in comparison to *N*-methylation, as can be expected since in the protonated pyridinium cation there are fewer atoms on which the positive charge is distributed.

Along with the increase in the $V_{max}(X)$ value, adding a positive charge on the halogenopyridine ring also leads to a change in the polarization of the halogen atom. A convenient measure for the polarization of the halogen atom is the difference between the $V_{max}(X)$ value and the ESP of the halogen atom perpendicular to it ($V_{min}(X)$) (see Tables S4−S9 in the Supporting Information). The $V_{max}(X) - V_{min}(X)$ difference ($\Delta V(X)$) was generally found to not be considerably affected by the position of the halogen atom and was found in neutral halogenopyridines to be on the average 80 ± 2 kJ mol^{-1} e^{-1} for chlorine, 122 ± 2 kJ mol^{-1} e^{-1}, for bromine and 151 ± 3 kJ mol^{-1} e^{-1} for iodine. In the cations, both $V_{max}(X)$ and $V_{min}(X)$ are considerably more positive. The $\Delta V(X)$ value is again barely affected by the position of the halogen atom as

https://doi.org/10.1021/acs.cgd.1c00805
Cryst. Growth Des. 2021, 21, 6889−6901

well as whether the cation is protonated or *N*-methylated and depends primarily on the halogen atom. If one is to compare the $\Delta V(X)$ in neutral halogenopyridines to those in the cations, one can see that in the case of all three chloropyridines the $\Delta V(X)$ value in the cations is reduced on average to 59 ± 4 kJ mol^{-1} e^{-1} and for bromopyridines it remains almost unchanged (122 ± 7 kJ mol^{-1} e^{-1}), while for iodopyridines the $\Delta V(X)$ value in the cations increases to 164 ± 6 kJ mol^{-1} e^{-1}. It therefore follows that the polarization of chlorine is reduced by the presence of the positive charge of the pyridine ring and the polarization of bromine is not affected, while the iodine becomes more polarized when pyridine is protonated or methylated (note that in all cases the $V_{min}(X)$ value changes sign—it is negative in all neutral halogenopyridines and positive in the corresponding cations).

One would expect that the dramatic increase in the $V_{max}(X)$ value should also lead to an equally dramatic increase in the potential of the halogenopyridinium cations as halogen-bond donors. However, as evidenced by CSD data, although there is a definite increase in the incidence of a halogen bond in structures comprising halogenopyridinium cations (in comparison to neutral halogenopyridines), it does not appear as dramatic, particularly in the case of chloropyridinium cations. This discrepancy seems particularly surprising if one takes into account that, even in the case of choropyridinium cations, the $V_{max}(X)$ value on the halogen atom is considerably larger (390−435 kJ mol^{-1} e^{-1}) than that on neutral donors (e.g., 175 kJ mol^{-1} e^{-1} in 1,4-diodotetrafluorobenzene), which form halogen bonds with potential donors present in the crystal structures much more reliably in comparison to cations derived from chloroheterocycles (see above).

As a probable reason for this, we propose the distribution of the positive charge throughout the halogenopyridinium cation. Adding a proton or a methyl group on the pyridine nitrogen does not affect just the halogen atom—the positive charge is distributed on the entire molecule. To test how this would affect the halogen-bonding proclivity of the halogenopyridinium cation, we set out to see how the $V_{max}(X)$ value compares to the ESP of the remainder of the molecule in the case of the neutral halogenopyridines as well as halogenopyridinium cations (Figure 5).

If one is to compare the $V_{max}(X)$ value with the ESP on the other non-hydrogen atoms on the neutral halogenopyridine molecules (i.e., their corresponding π-holes, perpendicular to the plane of the ring), one can see that a σ-hole on the halogen is in all cases the most positive feature. This dramatically changes upon adding a positive charge on a pyridine ring. The added charge is distributed over the entire pyridine ring, leading to an increase in the ESP of all atoms of the molecule (most prominently that of the nitrogen atom and the neighboring carbon atoms). As a result, the σ-hole of the halogen atom does not necessarily correspond to the most positive region on the cation. Indeed, only in the case of iodopyridines and *o*-bromopyridine does the $V_{max}(X)$ value remain larger than the mean ESP of the nitrogen and carbon atoms of the pyridine ring. However, even in these structures the ESP on the π-holes of the nitrogen and carbon atoms remains significant and in the structure of [**4-IPy**Me]I leads to the appearance of a short iodide···carbon contact corresponding to an anion···π interaction; with the ESP carbon atom π-hole the $V_{max}(C)$ value of 436 kJ mol^{-1} e^{-1} is only slightly lower than that of the iodine atom σ-hole (456 kJ mol^{-1} e^{-1}).

The most ubiquitous contacts in all of the crystal structures have been the C−H···I$^-$ hydrogen bonds. If one is to compare the $V_{max}(X)$ value with the ESP of hydrogen atoms of the pyridine ring ($V_{max}(H)$), in neutral halogenopyridines, the mean $V_{max}(H)$ value is more positive than the σ-hole of the halogen in all cases except for *m*- and *p*-iodopyridines. In the cations the $V_{max}(H)$ values of all the hydrogen atoms increase dramatically so that almost all hydrogen atoms of the aromatic ring in the *m*- and *p*-iodopyridinium cations become more positive than the $V_{max}(X)$ value of the iodine. However, in both *o*-iodopyridinium cations the $V_{max}(X)$ value is sufficiently increased so that it becomes more positive than the aromatic hydrogen atoms, with the exception of the hydrogen atom in the position *ortho* to the pyridinium nitrogen. Of course, in the case of all protonated halogenopyridinium cations the hydrogen located on the nitrogen atom is by far the most positive feature of the molecule (the $V_{max}(H)$ value being in the range ca. 665−690 kJ mol^{-1} e^{-1}, exceeding the $V_{max}(X)$ value by ca. 150−310 kJ mol^{-1} e^{-1}, depending on the cation). It is therefore evident that, in the case of protonated halogenopyridinium cations, the hydrogen bond formed by the N−H group will always be the dominant interaction, while in the *N*-methylated cations a competition between the C−H hydrogen-bond donors and C−X halogen-bond donors can always be expected, even in the case of iodopyridinium cations.

In order to correlate the $V_{max}(X)$ values with halogen-bonding energies, we have computed the binding energies of a pyridine molecule (a neutral halogen bond acceptor) to *N*-methylated halogenopyridines (Figure 6). The bond energies

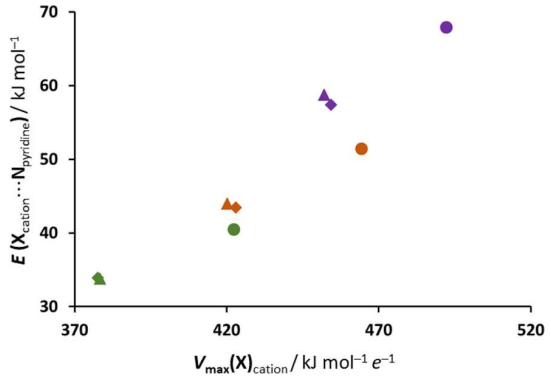

Figure 6. Correlation of $V_{max}(X)$ values of *N*-methylated halogenopyridines with energies of halogen bonds between a (neutral) pyridine molecule and *N*-methylated halogenopyridines.

obtained were quite considerable: ca. 34−40 kJ mol^{-1} for chloropyridinium, 43−51 kJ mol^{-1} for bromopyridinium, and 57−68 kJ mol^{-1} for iodopyridinium cations. Although the absolute values of the obtained energies may be somewhat untrustworthy, they do seem to indicate that the binding energies follow the same general trend as do the $V_{max}(X)$ values within each series of isomers—the *meta* and *para* isomers form bonds with energies very similar to one another, and the *ortho* isomer forms a bond which is ca. 6−10 kJ mol^{-1} stronger. Indeed, the bond energies for chloropyridines and bromopyridines are very closely linearly dependent on the $V_{max}(X)$ values for the free cations (R^2 = 0.96), while the bond energies for iodopyridinium cations are somewhat higher: although $V_{max}(Br)$ on the **2-BrPy**Me$^+$ cation is ca. 40 kJ mol^{-1} e^{-1} larger than $V_{max}(I)$ on **3-IPy**Me$^+$ and **4-IPy**Me$^+$ cations,

https://doi.org/10.1021/acs.cgd.1c00805
Cryst. Growth Des. 2021, 21, 6889−6901

the energy of the Br···N halogen bond it forms with a pyridine molecule is ca. 6−7 kJ mol^{-1} less than those of the I···N halogen bonds formed by **3-IPy**Me$^+$ and **4-IPy**Me$^+$. This implies that the Cl···N and the Br···N halogen bonds formed by the halogenopyridinium cations are primarily electrostatic, while the I···N halogen bonds have a more significant charge-transfer component.

The rather high bond energies for all of the studied cases show that all halogenopyridinium cations form rather strong halogen bonds. This would seem to be in contradiction with the fact that chloropyridinium cations participate only rarely in halogen bonding. However, as the positive charge is distributed over the entire molecule, leading to numerous local maxima of the ESP, the halogen bond formed through the chloropyridinium chlorine σ-hole is not necessarily the most favorable interaction between the cation and the pyridine molecule. On the other hand, the fact that chloropyridinium cations do participate in halogen-bonding contacts in almost 50% of the crystal structures clearly shows that the behavior of chlorine as a donor atom cannot be accounted for solely by the ESP of the σ-hole—a significant role must also be played by other contributions such as the size of the halogen atom (making the approach of the Lewis base easier) and possibly dispersion.[86]

CONCLUSION

Although both protonation and *N*-methylation of halogenopyridines lead to a considerable increase in the ESP of the halogen σ-hole, a closer inspection of the distribution of the charge on the resulting cations clearly demonstrates that the halogen σ-hole is generally not the most positive site on the surface of the cation. This is most pronounced in the case of chloropyridinium cations, where the electrostatic potential maxima on almost all hydrogen and carbon atoms of the cation are more positive than the chlorine σ-hole. Such a charge distribution leads to the observed relatively low percentage of occurrence of halogen bonds with chloropyridinium chlorine donors in the CSD and the long C−Cl···I$^-$ contacts encountered in the structures of chloropyridinium iodides. Even among iodopyridinium cations, only in those derived from **2-IPy** (with the iodine atom on the first neighbor of the "charged" nitrogen) is the iodine σ-hole ESP more positive than that of the majority of hydrogen atoms. Consequently, they form the shortest C−I···I$^-$ halogen bonds both among protonated and methylated halogenopyridinium iodides. In spite of this, cations derived from not only all iodopyridines but also those derived from bromopyridines form halogen bonds with remarkable consistency—they have formed halogen-bonding contacts shorter than the sum of the van der Waals radii in all of the iodide salts and have been found to act as halogen bond donors in a formidable 90% of structures deposited in the CSD which comprise an iodo- or bromopyridinium cation and an appropriate acceptor. It is therefore probable that the lower ESP on the halogen σ-hole is compensated by the size of the halogen atom: enabling on the one hand a closer approach of a Lewis base (with less steric hindrance to the halogen σ-hole as opposed to the hydrogen atoms of the pyridine ring) and on the other hand a larger potential contact surface between the contact atoms. This, however, does not exclude the formation of competing interactions, as evidenced in the structures of iodides by numerous short C−H···I$^-$ and even π···I$^-$ contacts between the cations and the iodide. Therefore, the halogenopyridinium cations, in spite of much larger V_{max}(X) values, have not been shown to be superior in comparison to "classical" neutral halogen bond donors.

This having been said, although adding a positive charge on the halogenopyridine ring forms numerous potential binding sites for Lewis bases in bromopyridinium and particularly in iodopyridinium cations, binding of the base to the halogen atom is likely to occur. This makes halopyridinium cations (particularly iodopyridinium) fairly reliable halogen-bond donors and thus justifies their use in the development of design strategies for the deliberate synthesis of halogen-bonded supramolecular structures.

EXPERIMENTAL SECTION

Synthesis. Halogenopyridines (**2-ClPy**, **2-BrPy**, **2-IPy**, **3-ClPy**, **3-BrPy**, **3-IPy** and **4-IPy**), methyl iodide, and solvents were purchased from Sigma-Aldrich and used as received. **4-ClPy** was prepared by dissolving 4-hydroxypyridine (700 mg, 6 mmol) in thionyl chloride (5 mL) and heating the mixture until the evolution of HCl gas ceased, after which the excess thionyl chloride was removed by distillation. To the remaining solid was added diethyl ether, and the mixture was treated with aqueous sodium hydrogencarbonate. The ether layer was separated and dried over sodium sulfate. The resulting solution was directly used in further synthesis.

N-Methylhalogenopyridinium iodides (except for [**4-ClPy**Me]I) were obtained by dissolving the halogenopyridine (1 mmol) in hot acetone and adding methyl iodide in excess (ca. 20% above the stoichiometric amount), whereupon the solutions were left to cool and evaporate. [**4-ClPy**Me]I was prepared in a similar fashion by adding methyl iodide to an ether solution obtained as described above. Solid products appeared in 1−3 days. Single crystals (suitable for single-crystal X-ray diffraction experiments) of [**2-IPy**Me]I, [**3-ClPy**Me]I, [**3-BrPy**Me]I, [**3-IPy**Me]I, [**4-ClPy**Me]I and [**4-IPy**Me]I were prepared by the synthesis procedure or by recrystallizing the obtained salt from a mixture of ethanol and water.

Single crystals (suitable for a single-crystal X-ray diffraction experiment) of [**2-ClPy**Me]I were prepared by recrystallizing the obtained salt from a mixture of ethanol, acetone, and water.

In the case of [**2-BrPy**Me]I, all attempts at crystallization led to partial or complete replacement of covalently bonded bromine with iodine and subsequent crystallization of mixed crystals containing both [**2-BrPy**Me]$^+$ and [**2-IPy**Me]$^+$ cations on equivalent crystallographic positions. This has precluded us from obtaining single crystals of [**2-BrPy**Me]I suitable for study.

FT-IR spectra (see the Supporting Information) of all prepared salts were recorded on a PerkinElmer Spectrum Two FTIR spectrometer using the attenuated total reflectance (ATR) technique.

[**2-ClPy**Me]I: selected IR data (cm^{-1}) 1617 (C=N)$_{py}$, 1567 (C=C)$_{ring}$, 1439 (N−C)$_{methyl}$, 2950−3050 (C−H); yield 116 mg (45.4%).

[**2-IPy**Me]I: selected IR data (cm^{-1}) 1616 (C=N)$_{py}$, 1500 (C=C)$_{ring}$, 1436 (N−C)$_{methyl}$, 2900−3050 (C−H); yield 91 mg (26.2%).

[**3-ClPy**Me]I: selected IR data (cm^{-1}) 1620 (C=N)$_{py}$, 1560 (C=C)$_{ring}$, 1484 (N−C)$_{methyl}$, 2950−3050 (C−H); yield 183 mg (71.6%).

[**3-BrPy**Me]I: selected IR data (cm^{-1}) 1622 (C=N)$_{py}$, 1486 (C=C)$_{ring}$, 1460 (N−C)$_{methyl}$, 2950−3100 (C−H); yield 231 mg (77%).

[**3-IPy**Me]I: selected IR data (cm^{-1}) 1622 (C=N)$_{py}$, 1489 (C=C)$_{ring}$, 1453 (N−C)$_{methyl}$, 2940−3070 (C−H); yield 276 mg (79.6%).

[**4-ClPy**Me]I: selected IR data (cm^{-1}) 1627 (C=N)$_{py}$, 1495 (C=C)$_{ring}$, 1465 (N−C)$_{methyl}$, 2850−3070 (C−H); yield 93 mg (6.1%).

[**4-IPy**Me]I: only a few crystals were isolated, which were used for X-ray and thermal analysis.

X-ray Diffraction Measurements. All single-crystal X-ray diffraction experiments were performed using an Oxford Diffraction XtaLAB Synergy, Dualflex, HyPix Xray four-circle diffractometer with mirror-monochromated Mo Kα (λ = 0.71073 Å) radiation. The data sets were collected using the ω-scan mode over a 2θ range up to 60°. The programs CrysAlis PRO CCD and CrysAlis PRO RED were employed for data collection, cell refinement, and data reduction.[87,88] The structures were solved by SHELXT or by direct methods using

https://doi.org/10.1021/acs.cgd.1c00805
Cryst. Growth Des. 2021, 21, 6889−6901

SHELXS and refined using SHELXL programs.[89,90] The structural refinement was performed on F^2 using all data. The hydrogen atoms were placed in calculated positions and treated as riding on their parent atoms (C−H = 0.93 Å and U_{iso}(H) = 1.2[U_{eq}(C)] for aromatic hydrogen atoms; C−H = 0.97 Å and U_{iso}(H) = 1.5[U_{eq}(C)] for methyl hydrogen atoms). All calculations were performed using the WinGX or Olex2 1.3-ac4 crystallographic suite of programs.[91] A summary of data pertinent to X-ray crystallographic experiments is provided in Table S1 in the Supporting Information. Further details are available from the Cambridge Crystallographic Centre (CCDC 2089226−2089232 contain crystallographic data for this paper). The molecular structures of compounds and their packing diagrams were prepared using Mercury.[92]

Thermal Analysis. Differential scanning calorimetry (DSC) and thermogravimetric (TG) measurements were performed simultaneously on a Mettler-Toledo TGA/DSC 3+ module (Mettler Toledo, Greifensee, Switzerland). Samples were placed in alumina crucibles (40 μL) and heated from 25 to 300 °C, at a heating rate of 10 °C min^{-1} under a nitrogen flow of 150 mL min^{-1}.

Data collection and analysis were performed using the program package STARe (Version 15.00, Mettler Toledo, Greifensee, Switzerland).[93] TG and DSC thermograms of the prepared compounds are shown in Figures S11−S15 in the Supporting Information.

Database Survey. A data survey has been performed on the CSD database, version 5.42 (May 2021) with three updates using ConQuest Version 2020.3.0. For hydrogen- and halogen-bonded contacts, the upper limit of the distance between the donor atom (hydrogen or iodine) and acceptor ions (Cl^-, Br^-, I^-) was defined as the sum of their van der Waals radii. Nitrogen halogenoheterocycles were defined as containing a six-membered aromatic ring with one nitrogen atom and a halogen substituent on the *ortho*, *meta*, or *para* position. Perfluorinated iodobenzenes were searched as the aromatic ring of six carbon atoms with iodo and fluoro substituents in *ortho* positions. The resulting hits were checked manually.

In order to ascertain the frequency of halogen bonding, for each donor a pair of searches were made. One was for structures with a close contact of a donor halogen and nitrogen, oxygen, chloride, bromide, or iodide (fluoride was excluded because of the extremely small number of structures). The other search was for structures containing both the donor and the potential acceptor (defined as above) without the two necessarily being in short contact. From these the structures that contained only quaternary nitrogen (which cannot act as halogen bond acceptor) were removed manually. The incidence of each donor type was than calculated as the ratio of the number of hits obtained by the two searches.

Computational Details. All calculations were performed using the Gaussian 09 software package.[94] Geometry optimizations were performed using the M062X/dgdzvp level of theory,[95−97] with an ultrafine integration grid (99 radial shells and 590 points per shell). This method has been shown to reproduce experimental halogen-bond energies in the gas phase with good accuracy, which are comparable to energies obtained by using larger and more time consuming triple-ζ basis sets.[98] Harmonic frequency calculations were performed on the optimized geometries to ensure the success of each geometry optimization. The figures were prepared using GaussView.[99]

■ ASSOCIATED CONTENT

Supporting Information

The Supporting Information is available free of charge at https://pubs.acs.org/doi/10.1021/acs.cgd.1c00805.

Crystallographic data for all compounds, ORTEP representations of the formula units of the prepared compounds, overview of supramolecular interactions in iodides of *N*-methylated and protonated halogenopyridinium cations, TG and DSC curves, total electron energies and Cartesian coordinates for optimized structures of *N*-methylated, protonated, and neutral halogenopyridines, molecular electrostatic potentials (MEPs) on halogen, nitrogen, carbon, and hydrogen atoms in *N*-methylated, protonated, and neutral halogenated pyridines, and bonding energies and Cartesian coordinates for optimized complexes of *N*-methylated halogenopyridinium cations and a neutral pyridine molecule (PDF)

Accession Codes

CCDC 2089226−2089232 contain the supplementary crystallographic data for this paper. These data can be obtained free of charge via www.ccdc.cam.ac.uk/data_request/cif, or by emailing data_request@ccdc.cam.ac.uk, or by contacting The Cambridge Crystallographic Data Centre, 12 Union Road, Cambridge CB2 1EZ, UK; fax: +44 1223 336033.

■ AUTHOR INFORMATION

Corresponding Author

Vladimir Stilinović − *Department of Chemistry, Faculty of Science, University of Zagreb, 10000 Zagreb, Croatia;* orcid.org/0000-0002-4383-5898; Email: vstilinovic@chem.pmf.hr

Authors

Luka Fotović − *Department of Chemistry, Faculty of Science, University of Zagreb, 10000 Zagreb, Croatia*

Nikola Bedeković − *Department of Chemistry, Faculty of Science, University of Zagreb, 10000 Zagreb, Croatia*

Complete contact information is available at: https://pubs.acs.org/10.1021/acs.cgd.1c00805

Author Contributions

The manuscript was written through contributions of all authors. All authors have given approval to the final version of the manuscript.

Funding

Croatian Science Foundation, project IP-2019−04−1868.

Notes

The authors declare no competing financial interest.

■ ACKNOWLEDGMENTS

This research was supported by the Croatian Science Foundation under the project IP-2019-04-1868. We also acknowledge the support of the project CIuK cofinanced by the Croatian Government and the European Union through the European Regional Development Fund-Competitiveness and Cohesion Operational Programme (Grant KK.01.1.1.02.0016).

■ ABBREVIATIONS

2-ClPy, 2-chloropyridine; **2-BrPy**, 2-bromopyridine; **2-IPy**, 2-iodopyridine; **3-ClPy**, 3-chloropyridine; **3-BrPy**, 3-bromopyridine; **3-IPy**, 3-iodopyridine; **4-ClPy**, 4-chloropyridine; **4-BrPy**, 4-bromopyridine; **4-IPy**, 4-iodopyridine; Me, methyl group; CSD, Cambridge Structural Database; X, halogen; V_{min}, minimum electrostatic potential of the corresponding atom; V_{max}, maximum electrostatic potential of the corresponding atom; DSC, differential scanning calorimetry; TG, thermogravimetric

■ REFERENCES

(1) Cavallo, G.; Metrangolo, P.; Milani, R.; Pilati, T.; Priimagi, A.; Resnati, G.; Terraneo, G. The Halogen Bond. *Chem. Rev.* **2016**, *116*, 2478−2601.

(2) Metrangolo, P.; Resnati, G. *Halogen Bonding*; Metrangolo, P., Resnati, G., Eds.; Springer Berlin Heidelberg: 2008; Vol. *126*. DOI: 10.1007/978-3-540-74330-9.
(3) Metrangolo, P.; Resnati, G. Halogen Bonding: A Paradigm in Supramolecular Chemistry. *Chem. - Eur. J.* **2001**, *7* (12), 2511−2519.
(4) Erdélyi, M. Halogen Bonding in Solution. *Chem. Soc. Rev.* **2012**, *41* (9), 3547−3557.
(5) Gilday, L. C.; Robinson, S. W.; Barendt, T. A.; Langton, M. J.; Mullaney, B. R.; Beer, P. D. Halogen Bonding in Supramolecular Chemistry. *Chem. Rev.* **2015**, *115* (15), 7118−7195.
(6) Cinčić, D.; Friščić, T.; Jones, W. Structural Equivalence of Br and i Halogen Bonds: A Route to Isostructural Materials with Controllable Properties. *Chem. Mater.* **2008**, *20* (21), 6623−6626.
(7) Politzer, P.; Murray, J. S.; Clark, T. Halogen Bonding: An Electrostatically-Driven Highly Directional Noncovalent Interaction. *Phys. Chem. Chem. Phys.* **2010**, *12* (28), 7748−7757.
(8) Legon, A. C. The Halogen Bond: An Interim Perspective. *Phys. Chem. Chem. Phys.* **2010**, *12* (28), 7736−7747.
(9) Aakeröy, C. B.; Wijethunga, T. K.; Desper, J. Practical Crystal Engineering Using Halogen Bonding: A Hierarchy Based on Calculated Molecular Electrostatic Potential Surfaces. *J. Mol. Struct.* **2014**, *1072* (1), 20−27.
(10) Stilinović, V.; Horvat, G.; Hrenar, T.; Nemec, V.; Cinčić, D. Halogen and Hydrogen Bonding between (*N*-Halogeno)-Succinimides and Pyridine Derivatives in Solution, the Solid State and In Silico. *Chem. - Eur. J.* **2017**, *23* (22), 5244−5257.
(11) Kolář, M.; Hostaš, J.; Hobza, P. The Strength and Directionality of a Halogen Bond Are Co-Determined by the Magnitude and Size of the σ-Hole. *Phys. Chem. Chem. Phys.* **2014**, *16* (21), 9987−9996.
(12) Oliveira, V.; Kraka, E.; Cremer, D. The Intrinsic Strength of the Halogen Bond: Electrostatic and Covalent Contributions Described by Coupled Cluster Theory. *Phys. Chem. Chem. Phys.* **2016**, *18* (48), 33031−33046.
(13) Roper, L. C.; Präsang, C.; Kozhevnikov, V. N.; Whitwood, A. C.; Karadakov, P. B.; Bruce, D. W. Experimental and Theoretical Study of Halogen-Bonded Complexes of DMAP with Di- and Triiodofluorobenzenes. A Complex with a Very Short N···I Halogen Bond. *Cryst. Growth Des.* **2010**, *10* (8), 3710−3720.
(14) Bedeković, N.; Stilinović, V.; Friščić, T.; Cinčić, D. Comparison of Isomeric *meta*- and *para*-Diiodotetrafluorobenzene as Halogen Bond Donors in Crystal Engineering. *New J. Chem.* **2018**, *42* (13), 10584−10591.
(15) Nemec, V.; Lisac, K.; Bedeković, N.; Fotović, L.; Stilinović, V.; Cinčić, D. Crystal Engineering Strategies towards Halogen-Bonded Metal-Organic Multi-Component Solids: Salts, Cocrystals and Salt Cocrystals. *CrystEngComm* **2021**, *23* (17), 3063−3083.
(16) Uran, E.; Fotović, L.; Bedeković, N.; Stilinović, V.; Cinčić, D. The Amine Group as Halogen Bond Acceptor in Cocrystals of Aromatic Diamines and Perfluorinated Iodobenzenes. *Crystals* **2021**, *11* (5), 529.
(17) Ding, X. H.; Chang, Y. Z.; Ou, C. J.; Lin, J. Y.; Xie, L. H.; Huang, W. Halogen Bonding in the Co-Crystallization of Potentially Ditopic Diiodotetrafluorobenzene: A Powerful Tool for Constructing Multicomponent Supramolecular Assemblies. *Natl. Sci. Rev.* **2020**, *7* (12), 1906−1932.
(18) Nemec, V.; Fotović, L.; Vitasović, T.; Cinčić, D. Halogen Bonding of the Aldehyde Oxygen Atom in Cocrystals of Aromatic Aldehydes and 1,4-Diiodotetrafluorobenzene. *CrystEngComm* **2019**, *21* (21), 3251−3255.
(19) Lunghi, A.; Cardillo, P.; Messina, T.; Metrangolo, P.; Panzeri, W.; Resnati, G. Perfluorocarbon-Hydrocarbon Self Assembling. Thermal and Vibrational Analyses of One-Dimensional Networks Formed by α,ω-Diiodoperfluoroalkanes with K.2.2. And K.2.2.2. *J. Fluorine Chem.* **1998**, *91* (2), 191−194.
(20) Messina, M. T.; Metrangolo, P.; Panzeri, W.; Ragg, E.; Resnati, G. Perfluorocarbon-Hydrocarbon Self-Assembly. Part 3. Liquid Phase Interactions between Perfluoroalkylhalides and Heteroactom Containing Hydrocarbons. *Tetrahedron Lett.* **1998**, *39* (49), 9069−9072.
(21) Farina, A.; Meille, S. V.; Messina, M. T.; Metrangolo, P.; Resnati, G.; Vecchio, G. Resolution of Racemic 1,2-Dibromohexafluoropropane through Halogen- Bonded Supramolecular Helices. *Angew. Chem., Int. Ed.* **1999**, *38* (16), 2433−2436.
(22) Metrangolo, P.; Meyer, F.; Pilati, T.; Resnati, G.; Terraneo, G. Halogen Bonding in Supramolecular Chemistry. *Angew. Chem., Int. Ed.* **2008**, *47* (33), 6114−6127.
(23) Raatikainen, K.; Rissanen, K. Hierarchical Halogen Bonding Induces Polymorphism. *CrystEngComm* **2009**, *11* (5), 750−752.
(24) Nguyen, S. T.; Ellington, T. L.; Allen, K. E.; Gorden, J. D.; Rheingold, A. L.; Tschumper, G. S.; Hammer, N. I.; Watkins, D. L. Systematic Experimental and Computational Studies of Substitution and Hybridization Effects in Solid-State Halogen Bonded Assemblies. *Cryst. Growth Des.* **2018**, *18* (5), 3244−3254.
(25) Rosokha, S. V.; Loboda, E. A. Interplay of Halogen and π-π Charge-Transfer Bondings in Intermolecular Associates of Bromo- or Iododinitrobenzene with Tetramethyl-*p*-Phenylenediamine. *J. Phys. Chem. A* **2015**, *119* (16), 3833−3842.
(26) Nwachukwu, C. I.; Kehoe, Z. R.; Bowling, N. P.; Speetzen, E. D.; Bosch, E. Cooperative Halogen Bonding and Polarized π-Stacking in the Formation of Coloured Charge-Transfer Co-Crystals. *New J. Chem.* **2018**, *42* (13), 10615−10622.
(27) Baykov, S. V.; Filimonov, S. I.; Rozhkov, A. V.; Novikov, A. S.; Ananyev, I. V.; Ivanov, D. M.; Kukushkin, V. Y. Reverse Sandwich Structures from Interplay between Lone Pair-π-Hole Atom-Directed C···dz^2[M] and Halogen Bond Interactions. *Cryst. Growth Des.* **2020**, *20* (2), 995−1008.
(28) Aakeröy, C. B.; Baldrighi, M.; Desper, J.; Metrangolo, P.; Resnati, G. Supramolecular Hierarchy among Halogen-Bond Donors. *Chem. - Eur. J.* **2013**, *19* (48), 16240−16247.
(29) Barry, D. E.; Hawes, C. S.; Blasco, S.; Gunnlaugsson, T. Structure Direction, Solvent Effects, and Anion Influences in Halogen-Bonded Adducts of 2,6-bis(Iodoethynyl)Pyridine. *Cryst. Growth Des.* **2016**, *16* (9), 5194−5205.
(30) Nguyen, S. T.; Rheingold, A. L.; Tschumper, G. S.; Watkins, D. L. Elucidating the Effects of Fluoro and Nitro Substituents on Halogen Bond Driven Assemblies of Pyridyl-Capped π-Conjugated Molecules. *Cryst. Growth Des.* **2016**, *16* (11), 6648−6653.
(31) Baldrighi, M.; Bartesaghi, D.; Cavallo, G.; Chierotti, M. R.; Gobetto, R.; Metrangolo, P.; Pilati, T.; Resnati, G.; Terraneo, G. Polymorphs and Co-Crystals of Haloprogin: An Antifungal Agent. *CrystEngComm* **2014**, *16* (26), 5897−5904.
(32) Raatikainen, K.; Rissanen, K. Interaction between Amines and *N*-Haloimides: A New Motif for Unprecedentedly Short Br···N and I···N Halogen Bonds. *CrystEngComm* **2011**, *13* (23), 6972−6977.
(33) Raatikainen, K.; Rissanen, K. Breathing Molecular Crystals: Halogen- and Hydrogen-Bonded Porous Molecular Crystals with Solvent Induced Adaptation of the Nanosized Channels. *Chem. Sci.* **2012**, *3* (4), 1235−1239.
(34) Makhotkina, O.; Lieffrig, J.; Jeannin, O.; Fourmigué, M.; Aubert, E.; Espinosa, E. Cocrystal or Salt: Solid State-Controlled Iodine Shift in Crystalline Halogen-Bonded Systems. *Cryst. Growth Des.* **2015**, *15* (7), 3464−3473.
(35) Puttreddy, R.; Jurček, O.; Bhowmik, S.; Mäkelä, T.; Rissanen, K. Very Strong $^{-}$N-X^{+}···$^{-}$O-N^{+} Halogen Bonds. *Chem. Commun.* **2016**, *52* (11), 2338−2341.
(36) Puttreddy, R.; Rautiainen, J. M.; Mäkelä, T.; Rissanen, K. Strong N−X···O−N Halogen Bonds: A Comprehensive Study on *N*-Halosaccharin Pyridine *N*-Oxide Complexes. *Angew. Chem., Int. Ed.* **2019**, *58* (51), 18610−18618.
(37) Mavračić, J.; Cinčić, D.; Kaitner, B. Halogen Bonding of: *N*-Bromosuccinimide by Grinding. *CrystEngComm* **2016**, *18* (19), 3343−3346.
(38) Dolenc, D.; Modec, B. EDA Complexes of *N*-Halosaccharins with N- and O-Donor Ligands. *New J. Chem.* **2009**, *33* (11), 2344−2349.
(39) Eraković, M.; Cinčić, D.; Molčanov, K.; Stilinović, V. A Crystallographic Charge Density Study of the Partial Covalent Nature

of Strong N···Br Halogen Bonds. *Angew. Chem., Int. Ed.* **2019**, *58* (44), 15702−15706.
(40) Turunen, L.; Erdélyi, M. Halogen Bonds of Halonium Ions. *Chem. Soc. Rev.* **2020**, *49* (9), 2688−2700.
(41) Robidas, R.; Reinhard, D. L.; Legault, C. Y.; Huber, S. M. Iodine(III)-Based Halogen Bond Donors: Properties and Applications. *Chem. Rec.* **2021**, *21* (8), 1912−1927.
(42) Oszajca, M.; Smrčok, L.; Pálková, H.; Łasocha, W. Synthesis and Structure Determination of Tetrakis(4-Iodoanilinum) *β*-Octamolybdate Dihydrate. *J. Mol. Struct.* **2012**, *1021*, 70−75.
(43) Attrell, R. J.; Widdifield, C. M.; Korobkov, I.; Bryce, D. L. Weak Halogen Bonding in Solid Haloanilinium Halides Probed Directly via Chlorine-35, Bromine-81, and Iodine-127 NMR Spectroscopy. *Cryst. Growth Des.* **2012**, *12* (3), 1641−1653.
(44) Raatikainen, K.; Cametti, M.; Rissanen, K. The Subtle Balance of Weak Supramolecular Interactions: The Hierarchy of Halogen and Hydrogen Bonds in Haloanilinium and Halopyridinium Salts. *Beilstein J. Org. Chem.* **2010**, *6*, 1.
(45) Kubo, K.; Takahashi, K.; Nakagawa, S.; Sakai, K. I.; Noro, S. I.; Akutagawa, T.; Nakamura, T. Substituent Effect on Molecular Motions of *m*-Halogenated Anilinium/Dibenzo[18]Crown-6 Supramolecular Cations in $[Ni(Dmit)_2]$- Crystals. *Cryst. Growth Des.* **2021**, *21* (4), 2340−2347.
(46) Aubert, E.; Espinosa, E.; Nicolas, I.; Jeannin, O.; Fourmigué, M. Toward a Reverse Hierarchy of Halogen Bonding between Bromine and Iodine. *Faraday Discuss.* **2017**, *203*, 389−406.
(47) Thomas, L. H.; Adam, M. S.; O'Neill, A.; Wilson, C. C. Utilizing Proton Transfer to Produce Molecular Salts in Bromanilic Acid Substituted-Pyridine Molecular Complexes-Predictable Synthons? *Acta Crystallogr., Sect. C: Cryst. Struct. Commun.* **2013**, *69* (11), 1279−1288.
(48) Decato, D. A.; Riel, A. M. S.; May, J. H.; Bryantsev, V. S.; Berryman, O. B. Theoretical, Solid-State, and Solution Quantification of the Hydrogen Bond-Enhanced Halogen Bond. *Angew. Chem.* **2021**, *133* (7), 3729−3736.
(49) Logothetis, T. A.; Meyer, F.; Metrangolo, P.; Pilati, T.; Resnati, G. Crystal Engineering of Brominated Tectons: *N*-Methyl-3,5-Dibromopyridinium Iodide Gives Particularly Short C-Br···I Halogen Bonding. *New J. Chem.* **2004**, *28* (6), 760−763.
(50) Fotović, L.; Stilinović, V. Halogenide Anions as Halogen and Hydrogen Bond Acceptors in Iodopyridinium Halogenides. *CrystEngComm* **2020**, *22* (23), 4039−4046.
(51) Awwadi, F. F.; Willett, R. D.; Peterson, K. A.; Twamley, B. The Nature of Halogen···Halide Synthons: Theoretical and Crystallographic Studies. *J. Phys. Chem. A* **2007**, *111* (12), 2319−2328.
(52) Freytag, M.; Jones, P. G.; Ahrens, B.; Fischer, A. K. Hydrogen Bonding and Halogen-Halogen Interactions in 4-Halopyridinium Halides. *New J. Chem.* **1999**, *23* (12), 1137−1139.
(53) Minguez Espallargas, G.; Zordan, F.; Arroyo Marin, L.; Adams, H.; Shankland, K.; van de Streek, J.; Brammer, L. Rational Modification of the Hierarchy of Intermolecular Interactions in Molecular Crystal Structures by Using Tunable Halogen Bonds. *Chem. - A Eur. J.* **2009**, *15* (31), 7554−7568.
(54) Awwadi, F. F.; Willett, R. D.; Twamley, B. The Aryl Chlorine - Halide Ion Synthon and Its Role in the Control of the Crystal Structures of Tetrahalocuprate(II) Ions. *Cryst. Growth Des.* **2007**, *7* (4), 624−632.
(55) Willett, R. D.; Awwadi, F.; Butcher, R.; Haddad, S.; Twamley, B. The Aryl Bromine-Halide Ion Synthon and Its Role in the Control of the Crystal Structures of Tetrahalocuprate(II) Ions. *Cryst. Growth Des.* **2003**, *3* (3), 301−311.
(56) Brammer, L.; Minguez Espallargas, G.; Adams, H. Involving Metals in Halogen-Halogen Interactions: Second-Sphere Lewis Acid Ligands for Perhalometallate Ions (M-X···X'-C). *CrystEngComm* **2003**, *5* (60), 343−345.
(57) Mínguez Espallargas, G.; Brammer, L.; Sherwood, P. Designing Intermolecular Interactions between Halogenated Peripheries of Inorganic and Organic Molecules: Electrostatically Directed M-X··· X'-C Halogen Bonds. *Angew. Chem., Int. Ed.* **2006**, *45* (3), 435−440.
(58) Zordan, F.; Brammer, L. Water Molecules Insert into N-H···Cl-M Hydrogen Bonds While M-Cl···X-C Halogen Bonds Remain Intact in Dihydrates of Halopyridinium Hexachloroplatinates. *Acta Crystallogr., Sect. B: Struct. Sci.* **2004**, *60* (5), 512−519.
(59) Zordan, F.; Purver, S. L.; Adams, H.; Brammer, L. Halometallate and Halide Ions: Nucleophiles in Competition for Hydrogen Bond and Halogen Bond Formation in Halopyridinium Salts of Mixed Halide-Halometallate Anions. *CrystEngComm* **2005**, *7* (57), 350−354.
(60) Vitorica-Yrezabal, I. J.; Sullivan, R. A.; Purver, S. L.; Curfs, C.; Tang, C. C.; Brammer, L. Synthesis and Polymorphism of $(4\text{-ClpyH})_2[CuCl_4]$: Solid-Gas and Solid-Solid Reactions. *CrystEngComm* **2011**, *13* (9), 3189−3196.
(61) Zordan, F.; Brammer, L.; Sherwood, P. Supramolecular Chemistry of Halogens: Complementary Features of Inorganic (M-X) and Organic (C-X′) Halogens Applied to M-X···X′-C Halogen Bond Formation. *J. Am. Chem. Soc.* **2005**, *127* (16), 5979−5989.
(62) Wolf, J.; Huber, F.; Erochok, N.; Heinen, F.; Guérin, V.; Legault, C. Y.; Kirsch, S. F.; Huber, S. M. Activation of a Metal-Halogen Bond by Halogen Bonding. *Angew. Chem., Int. Ed.* **2020**, *59* (38), 16496−16500.
(63) Sutar, R. L.; Engelage, E.; Stoll, R.; Huber, S. M. Bidentate Chiral Bis(Imidazolium)-Based Halogen-Bond Donors: Synthesis and Applications in Enantioselective Recognition and Catalysis. *Angew. Chem., Int. Ed.* **2020**, *59* (17), 6806−6810.
(64) Bulfield, D.; Huber, S. M. Halogen Bonding in Organic Synthesis and Organocatalysis. *Chem. - Eur. J.* **2016**, *22* (41), 14434−14450.
(65) Derossi, S.; Brammer, L.; Hunter, C. A.; Ward, M. D. Halogen Bonded Supramolecular Assemblies of $[Ru(Bipy)(CN)_4]^{2-}$ Anions and *N*-Methyl-Halopyridinium Cations in the Solid State and in Solution. *Inorg. Chem.* **2009**, *48* (4), 1666−1677.
(66) Ormond-Prout, J. E.; Smart, P.; Brammer, L. Cyanometallates as Halogen Bond Acceptors. *Cryst. Growth Des.* **2012**, *12* (1), 205−216.
(67) Jakupec, N.; Fotović, L.; Stilinović, V. The Effect of Halogen Bonding on Protonated Hexacyanoferrate Networks in Hexacyanoferrates of Halogenopyridines. *CrystEngComm* **2020**, *22* (46), 8142−8150.
(68) Amendola, V.; Bergamaschi, G.; Boiocchi, M.; Fusco, N.; La Rocca, M. V.; Linati, L.; Lo Presti, E.; Mella, M.; Metrangolo, P.; Miljkovic, A. Novel Hydrogen- and Halogen-Bonding Anion Receptors Based on 3-Iodopyridinium Units. *RSC Adv.* **2016**, *6* (72), 67540−67549.
(69) Riel, A. M. S.; Jessop, M. J.; Decato, D. A.; Massena, C. J.; Nascimento, V. R.; Berryman, O. B. Experimental Investigation of Halogen-Bond Hard-Soft Acid-Base Complementarity. *Acta Crystallogr., Sect. B: Struct. Sci., Cryst. Eng. Mater.* **2017**, *73* (2), 203−209.
(70) Riel, A. M. S.; Decato, D. A.; Sun, J.; Massena, C. J.; Jessop, M. J.; Berryman, O. B. The Intramolecular Hydrogen Bonded-Halogen Bond: A New Strategy for Preorganization and Enhanced Binding. *Chem. Sci.* **2018**, *9* (26), 5828−5836.
(71) Foyle, E. M.; White, N. G. Anion Templated Crystal Engineering of Halogen Bonding Tripodal Tris(Halopyridinium) Compounds. *CrystEngComm* **2020**, *22* (14), 2526−2536.
(72) Lohrman, J. A.; Deng, C. L.; Shear, T. A.; Zakharov, L. N.; Haley, M. M.; Johnson, D. W. Methanesulfonyl-Polarized Halogen Bonding Enables Strong Halide Recognition in an Arylethynyl Anion Receptor. *Chem. Commun.* **2019**, *55* (13), 1919−1922.
(73) Jungbauer, S. H.; Huber, S. M. Cationic Multidentate Halogen-Bond Donors in Halide Abstraction Organocatalysis: Catalyst Optimization by Preorganization. *J. Am. Chem. Soc.* **2015**, *137* (37), 12110−12120.
(74) Kosaka, Y.; Yamamoto, H. M.; Nakao, A.; Tamura, M.; Kato, R. Coexistence of Conducting and Magnetic Electrons Based on Molecular *π*-Electrons in the Supramolecular Conductor (Me-3,5-DIP)$[Ni(Dmit)_2]_2$. *J. Am. Chem. Soc.* **2007**, *129* (11), 3054−3055.
(75) Kusamoto, T.; Yamamoto, H. M.; Tajima, N.; Oshima, Y.; Yamashita, S.; Kato, R. Bilayer Mott System Based on $Ni(Dmit)_2$

https://doi.org/10.1021/acs.cgd.1c00805
Cryst. Growth Des. 2021, 21, 6889−6901

(Dmit = 1,3-Dithiole-2-Thione-4,5-Dithiolate) Anion Radicals: Two Isostructural Salts Exhibit Contrasting Magnetic Behavior. *Inorg. Chem.* **2012**, *51* (21), 11645−11654.
(76) Kosaka, Y.; Yamamoto, H. M.; Tajima, A.; Nakao, A.; Cui, H.; Kato, R. Supramolecular Ni(Dmit)$_2$ Salts with Halopyridinium Cations - Development of Multifunctional Molecular Conductors with the Use of Competing Supramolecular Interactions. *CrystEngComm* **2013**, *15* (16), 3200−3211.
(77) Ren, X.; Meng, Q.; Song, Y.; Lu, C.; Hu, C.; Chen, X. Unusual Magnetic Properties of One-Dimensional Molecule-Based Magnets Associated with a Structural Phase Transition. *Inorg. Chem.* **2002**, *41* (22), 5686−5692.
(78) Garcia, M. D.; Blanco, V.; Platas-Iglesias, C.; Peinador, C.; Quintela, J. M. Interplay between Halogen/Hydrogen Bonding and Electrostatic Interactions in 1,1′-Bis(4-Iodobenzyl)-4,4′-Bipyridine-1,1′-Diium Salts. *Cryst. Growth Des.* **2009**, *9* (12), 5009−5013.
(79) Jones, P. G.; Lozano, V. A Second Polymorph of 3,5-Dibromopyridinium Bromide. *Acta Crystallogr., Sect. E: Struct. Rep. Online* **2003**, *59* (5), o632−o634.
(80) Groom, C. R.; Bruno, I. J.; Lightfoot, M. P.; Ward, S. C. The Cambridge Structural Database. *Acta Crystallogr., Sect. B: Struct. Sci., Cryst. Eng. Mater.* **2016**, *72* (2), 171−179.
(81) Posavec, L.; Nemec, V.; Stilinović, V.; Cinčić, D. Halogen and Hydrogen Bond Motifs in Ionic Cocrystals Derived from 3-Halopyridinium Halogenides and Perfluorinated Iodobenzenes. *Cryst. Growth Des.* **2021**, DOI: 10.1021/acs.cgd.1c00755.
(82) Ghassemzadeh, M.; Dehnicke, K.; Goesmann, H.; Fenske, D. μ_2-Halogenokomplexe von *N*-Iodsuccinimid. Die Kristallstrukturen von $PPh_4[X(N\text{-Iodsuccinimid})_2] \cdot CH_3CN$ mit X = Cl, Br, I. *Z. Naturforsch., B: J. Chem. Sci.* **1994**, *49* (5), 602−608.
(83) Quiñonero, D.; Garau, C.; Rotger, C.; Frontera, A.; Ballester, P.; Costa, A.; Deyà, P. M. Anion−π Interactions: Do They Exist? *Angew. Chem.* **2002**, *114* (18), 3539−3542.
(84) Mascal, M.; Armstrong, A.; Bartberger, M. D. Anion-Aromatic Bonding: A Case for Anion Recognition by π-Acidic Rings. *J. Am. Chem. Soc.* **2002**, *124* (22), 6274−6276.
(85) Fotović, L.; Stilinović, V. Halogen Bonding in *N*-Alkyl-3-halogenopyridinium Salts. *Crystals* **2021**, *11*, 1240−1256.
(86) Riley, K. E.; Murray, J. S.; Fanfrlík, J.; Řezáč, J.; Solá, R. J.; Concha, M. C.; Ramos, F. M.; Politzer, P. Halogen bond tunability II: the varying roles of electrostatic and dispersion contributions to attraction in halogen bonds. *J. Mol. Model.* **2013**, *19*, 4651−4659.
(87) *CrysAlis Pro*; Agilent Technologies Ltd: 2010.
(88) *CrysAlis PRO CCD*; Agilent Technologies Ltd: 2014.
(89) Sheldrick, G. M. SHELXT - Integrated Space-Group and Crystal-Structure Determination. *Acta Crystallogr., Sect. A: Found. Adv.* **2015**, *71* (1), 3−8.
(90) Sheldrick, G. M. Crystal Structure Refinement with SHELXL. *Acta Crystallogr., Sect. C: Struct. Chem.* **2015**, *71* (1), 3−8.
(91) Farrugia, L. J. WinGX Suite for Small-Molecule Single-Crystal Crystallography. *J. Appl. Crystallogr.* **1999**, *32* (4), 837−838.
(92) Macrae, C. F.; Bruno, I. J.; Chisholm, J. A.; Edgington, P. R.; McCabe, P.; Pidcock, E.; Rodriguez-Monge, L.; Taylor, R.; Van De Streek, J.; Wood, P. A. Mercury CSD 2.0 - New Features for the Visualization and Investigation of Crystal Structures. *J. Appl. Crystallogr.* **2008**, *41* (2), 466−470.
(93) *STARe Software v.15.00*; Mettler Toledo: 2016.
(94) Frish, M. J.; Trucks, G. W.; Schlegel, H. B.; Scuseria, G. E.; Robb, M. A.; Cheseman, J. R.; Scalmani, G.; Barone, V.; Petersson, G. A.; Nakatsuji, H.; Li, X.; Caricato, H.; Marenich, A. V.; Bloino, J.; Janesko, B. G.; Gomperts, R.; Mennucci, B.; Hratchian, H. P.; Ortiz, J. V.; Izmaylov, A. F.; Sonnerberg, J. L.; Williams-Young, D.; Ding, F.; Lipparini, F.; Egidi, F.; Goings, J.; Peng, B.; Petrone, A.; Henderson, T.; Ranasinghe, D.; Zakrzewski, V. G.; Gao, J.; Rega, N.; Zheng, G.; Liang, W.; Hada, M.; Ehara, M.; Toyota, K.; Fukuda, R.; Hasegawa, J.; Ishida, M.; Nakajima, T.; Honda, Y.; Kitao, O.; Nakai, H.; Vreven, T.; Throssell, K.; Montgomery, J. A.; Peralta, J. E.; Ogliaro, F.; Bearpark, M.; Heyd, J. J.; Brothers, E.; Kudin, K. N.; Staroverov, V. N.; Keith, T. A.; Kobayashi, R.; Normand, J.; Raghavachari, K.; Rendell, A.; Burant, J. C.; Iyengar, S. S.; Tomasi, J.; Cossi, M.; Millam, J. M.; Klene, M.; Adamo, C.; Cammi, R.; Ochterski, J. W.; Martin, R. L.; Morokuma, K.; Farkas, O.; Foresman, J. B.; Fox, D. J. *Gaussian 09, Rev. A.02*; Gaussian, Inc.: 2009.
(95) Zhao, Y.; Truhlar, D. G. The M06 Suite of Density Functionals for Main Group Thermochemistry, Thermochemical Kinetics, Noncovalent Interactions, Excited States, and Transition Elements: Two New Functionals and Systematic Testing of Four M06-Class Functionals and 12 Other Functionals. *Theor. Chem. Acc.* **2008**, *120* (1−3), 215−241.
(96) Godbout, N.; Salahub, D. R.; Andzelm, J.; Wimmer, E. Optimization of Gaussian-Type Basis Sets for Local Spin Density Functional Calculations. Part I. Boron through Neon, Optimization Technique and Validation. *Can. J. Chem.* **1992**, *70* (2), 560−571.
(97) Sosa, C.; Andzelm, J.; Elkin, B. C.; Wimmer, E.; Dobbs, K. D.; Dixon, D. A. A Local Density Functional Study of the Structure and Vibrational Frequencies of Molecular Transition-Metal Compounds. *J. Phys. Chem.* **1992**, *96* (16), 6630−6636.
(98) Siiskonen, A.; Priimagi, A. Benchmarking DFT Methods with Small Basis Sets for the Calculation of Halogen-Bond Strengths. *J. Mol. Model.* **2017**, *23* (2), 50.
(99) Keith, T. A.; Millam, J. M. *GaussView, Ver. 5.1*; Semichem Inc.: 2008.

III

Halogen Bonding in *N*-Alkyl-3-halogenopyridinium Salts

L. Fotović, V. Stilinović,

Crystals **11** (2021) 1240-1256. (objavljen)

Doprinos koautora:

L. Fotović – sinteza soli, kristalizacija, strukturna, termička i spektrokopska analiza, kristalografija, obrada rezultata i pisanje rada

V. Stilinović – savjetovanje i pisanje rada

Rad je objavljen u otvorenom pristupu i reproduciran uz dozvolu MDPI-a.*

*Reprinted with permission from *Crystals* **2021**, *11*(10), 1240-1256. Published by MDPI.

crystals

MDPI

Article

Halogen Bonding in *N*-Alkyl-3-halogenopyridinium Salts

Luka Fotović and Vladimir Stilinović *

Department of Chemistry, Faculty of Science, University of Zagreb, Horvatovac 102a, HR-10002 Zagreb, Croatia; lfotovic@chem.pmf.hr

* Correspondence: vstilinovic@chem.pmf.hr; Tel.: +385-1-4606-371

Abstract: We performed a structural study of *N*-alkylated halogenopyridinium cations to examine whether choice of the *N*-substituent has any considerable effect on the halogen bonding capability of the cations. For that purpose, we prepared a series of *N*-ethyl-3-halopyridinium iodides and compared them with their *N*-methyl-3-halopyridinium analogues. Structural analysis revealed that *N*-ethylated halogenopyridinium cations form slightly shorter C−X···I$^-$ halogen bonds with iodide anion. We have also attempted synthesis of ditopic symmetric bis-(3-iodopyridinium) dications. Although successful in only one case, the syntheses have afforded two novel ditopic asymmetric monocations with an iodine atom bonded to the pyridine ring and another on the aliphatic *N*-substituent. Here, the C−I···I$^-$ halogen bond lengths involving pyridine iodine atom were notably shorter than those involving an aliphatic iodine atom as a halogen bond donor. This trend in halogen bond lengths is in line with the charge distribution on the Hirshfeld surfaces of the cations—the positive charge is predominantly located in the pyridine ring making the pyridine iodine atom σ-hole more positive than the one on the alkyl chan.

Keywords: pyridinium cations; halogen bond; halogenide anions

check for updates

Citation: Fotović, L.; Stilinović, V. Halogen Bonding in *N*-Alkyl-3-halogenopyridinium Salts. *Crystals* **2021**, *11*, 1240. https://doi.org/10.3390/cryst11101240

Academic Editors: Sergiy Rosokha and Atash V. Gurbanov

Received: 29 September 2021
Accepted: 12 October 2021
Published: 14 October 2021

Publisher's Note: MDPI stays neutral with regard to jurisdictional claims in published maps and institutional affiliations.

Copyright: © 2021 by the authors. Licensee MDPI, Basel, Switzerland. This article is an open access article distributed under the terms and conditions of the Creative Commons Attribution (CC BY) license (https://creativecommons.org/licenses/by/4.0/).

1. Introduction

A halogen bond [1–5], an attractive σ-hole [6–8] interaction between a halogen atom (Lewis acid) and a Lewis base, is a well-established tool of crystal engineering and supramolecular chemistry [9–12]. To date, various Lewis bases (neutral molecules or charged species) have been employed as halogen bond acceptors in constructing halogen-bonded supramolecular assemblies. These have most commonly been organic [13,14] and metal-organic [15] molecules containing electron-rich nitrogen [16–26] and oxygen atoms [27–41], as well as inorganic anions such as halogenides [42–54]. The most commonly used halogen bond donors have traditionally been neutral organic molecules where a halogen atom is bonded to electron-withdrawing molecular residues. Fluorine atoms [55–60], nitro and cyano groups [61–65], or C–C triple bond [16,66–68], exhibit an electron withdrawing effect on the halogen atom and consequently increase the positive electrostatic potential (ESP) of the σ-hole of the halogen atom. The same effect can be archived if the halogen atom is bonded to a more electronegative heteroatom such as nitrogen in *N*-halogenoimides [69–76] or oxygen in organic hypoiodites [77].

There is an alternative approach to making a reliable halogen bond donor by placing a halogen atom on a positively charged species. To date, a number of halogenoimidazolium and halogenopyridinum cations employed as halogen bond donors in salts with organic [78,79] and inorganic [13,25,44–54,80–91] counterions have been published. Halogenopyridinium cations have been studied as anion receptors [92–96], catalysts in halogenide abstraction [97], colour tuning [98,99] and as counterions for tuning conductivity and magnetic properties in supramolecular conductors [100–103].

Generally, *N*-methylation of halogenopyridines (iodopyridines in particular) greatly increases the ESP of the σ-hole of the halogen atom, rendering them formidable halogen bond donors. This is also evident from the structural data, which show that iodopyridinium

cations tend to form quite short halogen bonds with both neutral and anionic halogen bond acceptors, such as halogenide anions [104].

Herein, we report a structural study of a series of halogenides of *N*-alkylated 3-halogenopyridinium cations with *N*-substituents other than methyl group. In the first place, we prepared a series of s of *N*-ethyl-3-halopyridinium (chloro, bromo and iodo) iodides, in order to compare them with the *N*-methyl-3-halopyridinium analogues to examine whether the increased *N*-substituent has any observable effect on the halogen bonding capability of the cations. In addition, we have attempted preparation of dications comprising a pair of 3-iodopyridinium rings separated by an aliphatic linker, which might act as ditopic cationic halogen bond donors (Scheme 1).

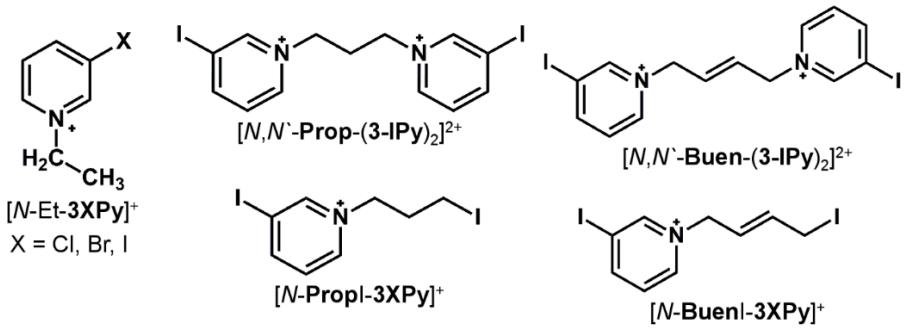

Scheme 1. Cationic halogen bond donors examined in this study.

2. Materials and Methods

All the solvents used (ethanol, acetone, dichloromethane) were procured from Sigma-Aldrich Chemie GmbH, Taufkirchen, Germany. Ethyl iodide (EtI) and 3-chloropyridine (**3-ClPy**) were procured from Acros Organics, Fisher Scientific UK Ltd., Leicestershire, United Kingdom. 3-bromopyridine (**3-BrPy**), 3-iodopyridine (**3-IPy**), 4-iodopyridine (**4-IPy**), 1,3-diiodopropane (**Prop**I_2) and 1,4-dibromobuta-2-ene (**Buen**Br_2) were procured from Apollo Scientific Ltd., Cheshire, United Kingdom. All reagents, as well as the organic solvents, were used without additional purification.

2.1. Solution and Single Crystal Synthesis of Cocrystals

N-ethyl-3-chloropyridinium iodide [*N*-Et-**3-ClPy**]I and was obtained by dissolving halogenopyridine (1 mmol) in hot acetone and adding ethyl iodide in excess (ca 1.2 mmol) whereupon the solutions were left to cool and evaporate. Yellow crystals suitable for single-crystal X-ray diffraction experiments appeared in one day. Yield: 213 mg (79%).

N-ethyl-3-bromopyridinium iodide [*N*-Et-**3-BrPy**]I was obtained by dissolving halogenopyridine (1 mmol) in hot dichloromethane and adding ethyl iodide in excess (ca 1.2 mmol) whereupon the solution was left to cool and evaporate. Brown crystals suitable for single-crystal X-ray diffraction experiments appeared in three days. Yield: 183 mg (58%).

N-ethyl-3-iodopyridinium iodide [*N*-Et-**3-IPy**]I was obtained by dissolving halogenopyridine (1 mmol) in hot dichloromethane and adding ethyl iodide in excess (ca 1.2 mmol) whereupon the solution was left to cool and evaporate. Yellow crystals suitable for single-crystal X-ray diffraction experiments appeared in three days. Yield: 297 mg (82%).

N-(2-oxopropyl)-3-bromopyridinium iodide ([*N*-**Ace-3-BrPy**]I) was obtained by dissolving 3-bromopyridine (1 mmol) in hot acetone and adding ethyl iodide in excess (ca 1.2 mmol) whereupon the solution was left to cool and evaporate. Mixture of brown crystals ([*N*-Et-**3-BrPy**]I and [*N*-**Ace-3-BrPy**]I) appeared in 12 h.

4-iodopyridinium hemihydroiodide ([**4-Ipy**]$_2$HI) was obtained by dissolving 4- iodopyridine (1 mmol) in mixture of hot acetone and dichloromethane (1:1; volume ratio) and adding ethyl iodide in excess (ca 1.2 mmol) whereupon the solution was left to cool and evaporate. Blue crystals suitable for single-crystal X-ray diffraction experiments appeared in one day.

N-(3-iodopropanyl)-3-iodopyridinium iodide ([*N*-I**Prop-3-IPy**]I) was obtained by dissolving 3-iodopyridine (2 mmol) in hot acetone and adding 1,3-diiodopropane (1 mmol) whereupon the solution was left to cool and evaporate. Yellow powder appeared in three days, while yellow crystals suitable for single-crystal X-ray diffraction experiments appeared in ten days. Yield: 144 mg (29%).

(2*E*)-1,4-bis(pyridin-1-ium-1-yl)but-2-en dibromide ([*N*,*N*′-**Buen**-(**3-IPy**)$_2$]Br$_2$) was obtained by dissolving 3-iodopyridine (2 mmol) in mixture of hot acetone and ethanol (1:1; volume ratio) and adding (*E*)-1,4-dibromobuta-2-ene (1 mmol) whereupon the solution was left to cool and evaporate. White microcrystalline product appeared in one day. Yield: 494 mg (79%).

N-((2*E*)-4-iodobuta-2-enyl)-3-iodopyridinium iodide ([*N*-I**Buen-3-IPy**]I) was obtained by dissolving [*N*,*N*′-**Buen**-(**3-IPy**)$_2$]Br$_2$ (1mmol) in deionized water (20 mL) and passing the solution through an anion exchange column. The ion-exchange resin (Dowex 21K chloride form, 16-30 mesh, Sigma-Aldrich Chemie GmbH, Taufkirchen, Germany) was regenerated with 50 mL aqueous solution of sodium hydroxide (c = 1 mol L^{-1}). Hydroiodic acid (c = 1 mol L^{-1}) was added dropwise in the obtained solution until neutralization. Yellow crystals suitable for single-crystal X-ray diffraction experiments appeared in three days. Yield: 57 mg (9%).

Single crystals (suitable for single crystal X-ray diffraction experiment) of [3-**ClPy**Me]I, [**3-BrPy**Me]I, [**3-IPy**Me]I, ([*N*-**Ace-3-BrPy**]I, [**4Ipy**]$_2$HI, [*N*-I**Prop-3-IPy**]I and [*N*-I**Buen-3-IPy**]I were obtained from the synthetic procedure, while single crystals of ([*N*,*N*′-**Buen**-(**3-IPy**)$_2$]Br$_2$) were prepared by crystalizing the initially obtained microcrystalline salt from mixture of ethanol and water (3:1; volume ratio).

FT-IR (ATR) spectra of prepared compounds are shown in Figures S21–S26 in Supplementary Materials.

2.2. Powder X-ray Diffraction Measurements

Powder X-ray diffraction experiments on the samples were performed on an Aeris X-ray diffractometer (Malvern Panalytical, Malvern Worcestershire, UK) with Cu$K\alpha$1 (λ = 1.54056 Å) radiation. The scattered intensities were measured with a PIXcel-1D-Medipix3 detector. The angular range was from 5° to 40° (2θ) with a continuous step size of 0.02° and measuring a time of 0.5 s per step.

Data collection methods were created using the program package START XRDMP CREATOR (Malvern Panalytical, Malvern Worcestershire, UK) while the data were analysed using X'Pert HighScore Plus (Version 2.2, Malvern Panalytical, Malvern Worcestershire, UK) [105]. Comparison of measured and calculated PXRD patterns of the prepared compounds are shown in Figures S9–S14 in Supplementary Materials.

2.3. Single Crystal X-ray Diffraction Measurements

Single crystal X-ray diffraction experiments were performed using an Oxford Diffraction Xcalibur Kappa CCD X-ray diffractometer (Oxford Diffraction Ltd., Abingdon, UK) with graphite-monochromated Mo$K\alpha$ (λ = 0.71073 Å) radiation. The data sets were collected using the ω-scan mode over the 2θ—range up to 54°. Programs CrysAlis PRO CCD and CrysAlis PRO RED were employed for data collection, cell refinement, and data reduction [106,107]. The structures were solved and refined using SHELXS (Version 2013, Göttingen, Germany), SHELXL programs (Version 2013, Göttingen, Germany), SHELXT programs (Version 2013, Göttingen, Germany), respectively [108,109]. The structural refinement was performed on F^2 using all data. The hydrogen atoms were placed in calculated positions and treated as riding on their parent atoms (C–H = 0.93 Å and U_{iso}(H) = 1.2 U_{eq}(C) for aromatic and methine hydrogen atoms; C–H = 0.96 Å and U_{iso}(H) = 1.5 U_{eq}(C) for methyl hydrogen atoms, C–H = 0.97 Å and U_{iso}(H) = 1.2 U_{eq}(C) for methylene hydrogen atoms). The position of the proton in [**4-IPy**···H···**4-IPy**]$^+$ cation could not be reliably located from the electron difference map, and it was modelled as disordered over two positions on the nitrogen atoms of both **4-IPy** molecules with

0.5 occupancy. All calculations were performed using the WinGX or Olex2 1.3-ac4 crystallographic suite of programs [110,111]. The figures were prepared using Mercury 2020.2.0 (CCDC, Cambridge, UK) [112]. Crystallographic data of the prepared compounds are shown in Table S2 in Supplementary Materials. ORTEP plots of the obtained compounds are shown in Figures S1–S8 in Supplementary Materials. CCDC No. 2109490-2109497, contain crystallographic data for this paper.

2.4. Thermal Analysis

Differential scanning calorimetry (DSC) and thermogravimetric (TG) measurements were performed simultaneously on a Mettler-Toledo TGA/DSC 3+ module (Mettler Toledo, Greifensee, Switzerland). Samples were placed in alumina crucibles (40 µL) and heated 25 to 300 °C, at a heating rate of 10 °C min^{-1} under nitrogen flow of 150 mL min^{-1}.

Data collection and analysis were performed using the program package STARe Software (Version 15.00, Mettler Toledo, Greifensee, Switzerland) [113]. TG and DSC thermograms of the prepared compounds are shown in Figures S15–S20 in the Supplementary Materials.

2.5. Calculations

All calculations were performed using CrystalExplorer software package [114]. Hirshfeld surfaces were generated with high resolution. Molecular electrostatic potentials were calculated at B3LYP-DGDZVP level of theory [115–118].

3. Results and Discussion

All three *meta*-halogenopyridines (chloro, bromo and iodo) were successfully *N*-ethylated using EtI, producing corresponding iodide salts. The crystal structure of [*N*-Et-**3-ClPy**]I comprises centrosymmetric cyclical [*N*-Et-**3-ClPy**]$_2$I$_2$ tetramers in which [*N*-Et-**3-ClPy**]$^+$ cations and iodide anions are interconnected through C−H···I$^-$ hydrogen bonds (d(C3···I1) = 3.901(6) Å, d(C4···I1) = 3.876(6) Å) (Figure 1a). C−H···I$^-$ hydrogen bonds and anion-π interactions, d(C5···I1) = 3.729(7) Å). The tetramers are connected into a layer via C−H···I$^-$ hydrogen bonds (d(C1···I1) = 3.866(6) Å), and the layers are then stacked on top of each other. Chlorine atoms do not participate in any significant supramolecular interactions. Analysing the electrostatic potential plotted on the Hirshfeld surface (Figure 1b), it has been found that ESP on the Hirshfeld surface in the σ-hole area (0.112 a.u.) is less positive than the mean ESP of chloropyridinium cation (0.148 a.u.). On the other hand, ESP on Hirshfeld surface near hydrogen atoms, which participate in supramolecular interactions, corresponds to the most positive regions of the [*N*-Et-**3-ClPy**]$^+$ cation (0.229 au).

Substitution of chlorine on the pyridine ring with bromine leads to a significant difference in the structural arrangement of the cations and anions. The main difference is the presence of a C−Br···I$^-$ halogen bond shorter by ca. 6% than the sum of the corresponding van der Waals radii (d(Br1···I1) = 3.611(7) Å, ∠ (C2–Br1··· I1) = 169.2(2)°). A methylene hydrogen atom of the ethyl group participates in a C−H···I$^-$ hydrogen bond with the iodide anion (d(C6···I1) = 4.013(6) Å). This combination of halogen and hydrogen bonds connects bromopyridinium cations and iodide anions in helical chains extending along the crystallographic *b* axis. The iodide anions also participate in anion-π contacts (d(C1···I1) = 3.575(5) Å) with cations from the neighbouring chains, which leads to formation of layers perpendicular to the *c* axis in the structure of [*N*-Et-**3-BrPy**]I (Figure 2).

In the structure of [*N*-Et-**3-Ipy**]I the cations and the anions are also connected in chains (along the crystallographic *b* axis) with combinations of C−I···I$^-$ halogen bonds (d(I1···I2) = 3.473(3) Å, ∠ (C2–I1··· I2) = 178.25(7)°) shorter by ca. 12% than the sum of the corresponding van der Waals radii, and C−H···I$^-$ hydrogen bonds (d(C1···I2) = 3.778(3) Å), but here the hydrogen bond is formed by an aromatic hydrogen atom in ortho position to the pyridine nitrogen. The chains are connected into layers via C−H···I$^-$ hydrogen bonds (d(C7···I2) = 4.094(3) Å) with a methyl hydrogen atom (Figure 3).

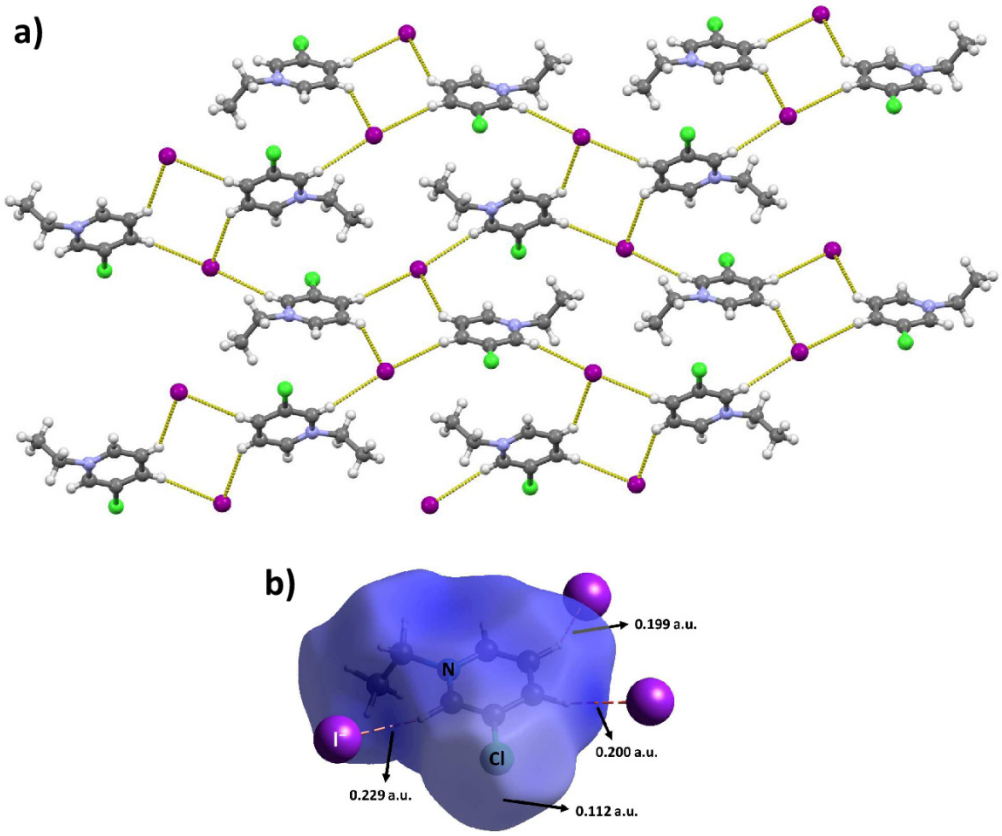

Figure 1. (**a**) Layers of [*N*-Et-**3-ClPy**]$^+$ cations and iodide anions connected through C−H···I$^-$ hydrogen bonds in the structure of [*N*-Et-**3-ClPy**]I; (**b**) Hirshfeld surface with mapped ESP (computed on B3LYP-DGDZVP level of theory) of the [*N*-Et-**3-ClPy**]$^+$ cation and the contact iodide anions in [*N*-Et-**3-ClPy**]I.

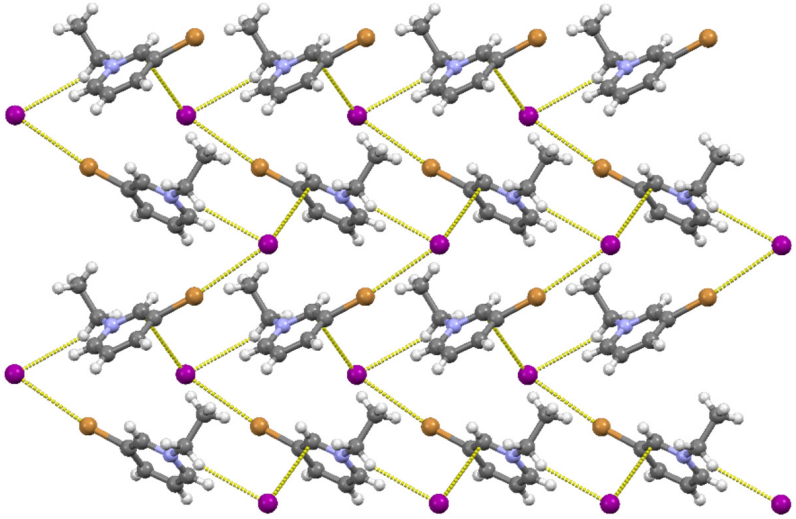

Figure 2. [*N*-Et-**3-BrPy**]$^+$ cations and iodide anions connected into layers through C−Br···I$^-$ halogen bonds, C−H···I$^-$ hydrogen bonds and anion-π contacts in the structure of [*N*-Et-**3-BrPy**]I.

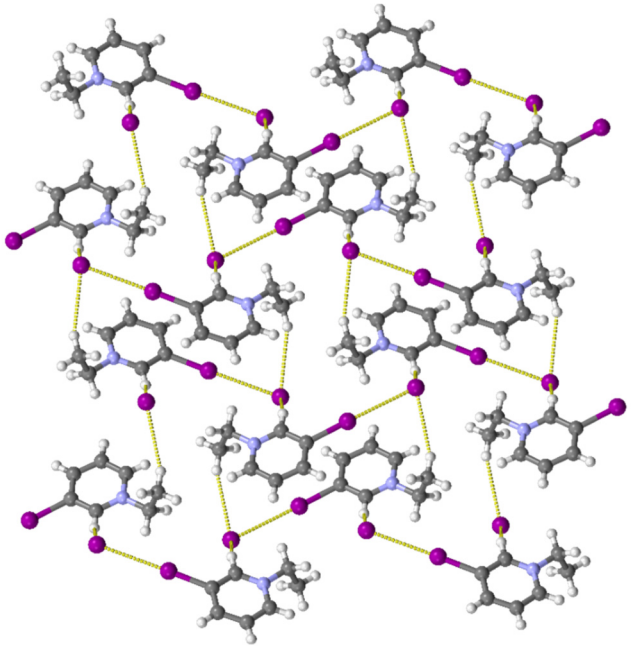

Figure 3. [*N*-Et-**3-IPy**]$^+$ cations and iodide anions connected into layers through C−I···I$^-$ halogen bonds and C−H···I$^-$ hydrogen bonds in the structure of [*N*-Et-**3-IPy**]I.

The halogen bond strengths also reflect the thermal stability of the iodide salts of the *N*-ethylated 3-halogenopyridines. The inspection of the results of the thermal analysis (see DSC and TG thermograms in the ESI) revealed that all three compounds exhibit well-defined melting points, which are then followed by simultaneous decomposition and evaporation. Melting point temperatures increase from 110 °C for [*N*-Et-**3-ClPy**]I to 116 °C for [*N*-Et-**3-BrPy**]I and finally 127 °C for [*N*-Et-**3-IPy**]I showing a clear increase in the melting point temperature with the size of halogen bond donor atom and, therefore, the strength of the C−X···I$^-$ halogen bond.

If one is to compare halogen bonding in *N*-ethylated 3-halogenopyridinium iodides to those in *N*-methylated 3-halogenopyridinium iodides, one can see that in both series cations derived from 3-bromopyridine and 3-iodopyridine participate in C−X···I$^-$ halogen bonds. Conversely, in *N*-ethyl-3-chloropyridinium iodide, cations do not participate in halogen bonding, while in *N*-methyl-3-chloropyridinium iodide some of symmetrically independent cations participate in the C−Cl···I$^-$ halogen bonds with iodide anion, but these halogen bonds are longer than the sum of the corresponding van der Waals radii. When comparing the lengths of the halogen bonds in the two series of iodides, both the C−Br···I$^-$ and the C−I···I$^-$ halogen bonds are shorter in the *N*-ethylated salts than in the *N*-methylated salts (Table 1). The ESP values plotted on the Hirshfeld surface of cations are similar in 3-bromopyridinium cations while in case of 3-iodopyridinium cations *N*-methylated one have somewhat smaller ESP value than the *N*-ethylated one. All in all, there is no significant difference in halogen bonding between the *N*-ethylated and the *N*-methylated halogenopyridinium cations with iodide anions.

Table 1. An overview of the C−X···I$^-$ halogen bonds and ESP values in σ-hole area in the *N*-ethylated and *N*-methylated 3-halogenopyridines [104].

	***N*-ethylated**			***N*-methylated**		
	***d*(XB)/Å**	***R.S.* (XB)/%**	**ESP (X)/kJ mol^{-1} e^{-1}**	***d*(XB)/Å**	***R.S.* (XB)**	**ESP (X)/kJ mol^{-1} e^{-1}**
3ClPy	/	/	294	3.776	–1.2	381
3BrPy	3.611	5.7	449	3.637	5.0	452
3IPy	3.473	12.3	570	3.538	10.7	554

Interestingly, while the reaction of iodoethane with 3-chloropyridine and 3-iodopyridine in acetone yielded only the expected *N*-ethyl-3-pyridinium iodides, 3-bromopyridine yielded a mixture of the expected [*N*-Et-**3-Brpy**]I and *N*-(2-oxopropyl)-3-bromopyridinium iodide ([*N*-**Ace-3Brpy**]I, Figure 4a). This by-product was formed by reaction of an acetone molecule with 3-bromopyridine, presumably through the formation of an intermediate iodoacetone in situ. When dichloromethane was used as the solvent, only pure [*N*-Et-**3-Brpy**]I was obtained.

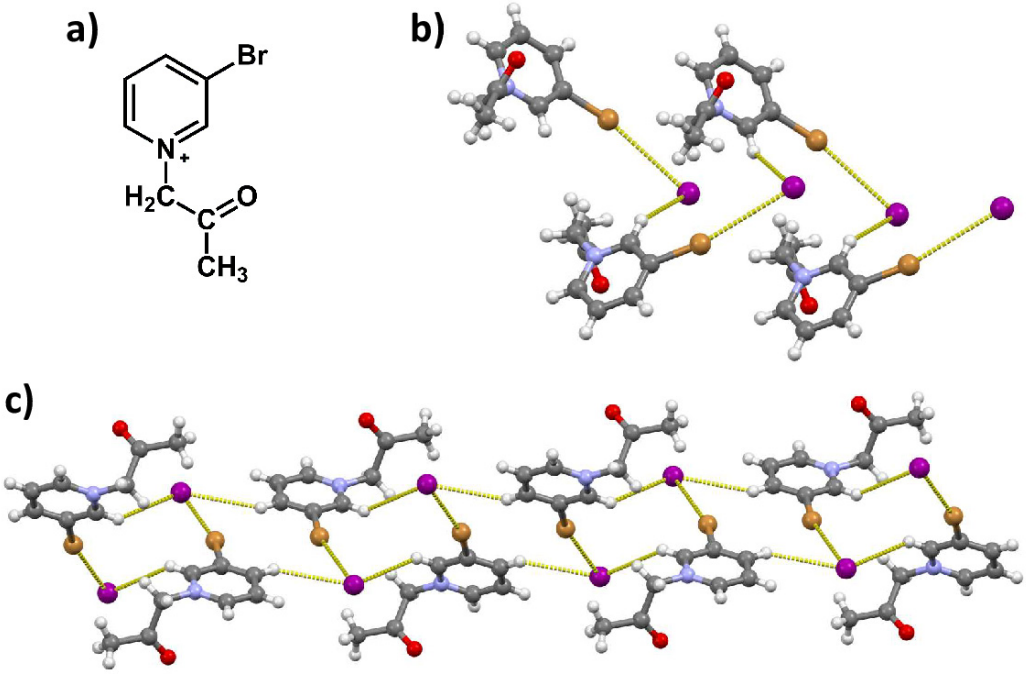

Figure 4. (**a**) [*N*-**Ace-3-BrPy**]$^+$ cation; (**b**) [*N*-**Ace-3-BrPy**]$^+$ cations and iodide anions connected through C−Br···I$^-$ halogen bonds and C−H···I$^-$ hydrogen bonds into chains in the structure of [*N*-**Ace-3-BrPy**]I; (**c**) View along crystallographic *b* axis—chains connected into layer through C−H···I$^-$ hydrogen bonds.

In the structure of [*N*-**Ace-3-Brpy**]I, the bromine atom again forms a halogen bond with the iodide anion (d(Br1···I1) = 3.694(7) Å, ∠ (C2–Br1··· I1) = 166.4(1)°). Iodide anion also binds [*N*-**Ace-3-Brpy**]$^+$ cation through C−H···I$^-$ hydrogen bonds (d(C1···I1) = 3.754(4) Å) with an aromatic hydrogen atom in *ortho* position to the pyridine nitrogen which lead to the formation of helical chains extending along the crystallographic *b* axis (Figure 4b). A different set of C−H···I$^-$ hydrogen bonds (d(C3···I1) = 3.847(5) Å) leads to the formation of the 2D structure (Figure 4c).

In order to expand the series of *N*-ethylated iodopyridinium salts, we have attempted to synthesize *N*-ethyl-4-iodopyridinium iodide from 4-iodopyridine and ethyl iodide. However, despite numerous attempts of synthesis, we were not able to isolate the desired product. Instead, when the reaction was performed in a mixture of hot acetone and dichloromethane, a minute amount (two single crystals) of solid product was obtained, which was identified as 4-iodopyridinium hemihydroiodide ((**4-IPy**)$_2$HI). It was presumably formed by a reaction of **4-IPy** and the traces of hydroiodic acid produced by hydrolysis of ethyl iodide with water absorbed from the atmosphere over time. Although in the structure of (**4-IPy**)$_2$HI the position of the HI hydrogen atom could not be ascertained from the electron difference map, it is evident that it is placed between the nitrogen atoms of a pair of molecules, interconnecting them by a charge assisted [119] (probably symmetrical) N···H···N hydrogen bond (d(N···N) = 3.202(8) Å) into a [(**4-IPy**)$_2$H]$^+$ complex. The iodide anion participates in two C−I···I$^-$ halogen bonds (d(I1···I3) = 3.502(7) Å, ∠ (C3–I1···I3) = 173.8(2)°; d(I2···I3) = 3.533(7) Å, ∠ (C8–I2···I3) = 172.7(2)°), with two neighbouring [(**4-IPy**)$_2$H]$^+$ hydrogen-bonded complexes. This combination of hydrogen

and halogen bonds forms supramolecular chains which are further connected into double chains through C−H···I$^-$ hydrogen bonds (d(C6···I1) = 4.028(7) Å) (Figure 5). It is interesting to note that this structure presents an excellent illustration of the HSAB principle in supramolecular chemistry[120,121]—the iodine atom of the [(**4-IPy**)$_2$H]$^+$ complex is the *softer* Lewis acid and therefore preferentially binds to the *softer* Lewis base, i.e., iodide. In contrast, the proton is the *hardest* Lewis acid and preferentially bind to the *harder* Lewis base, i.e., pyridine nitrogen.

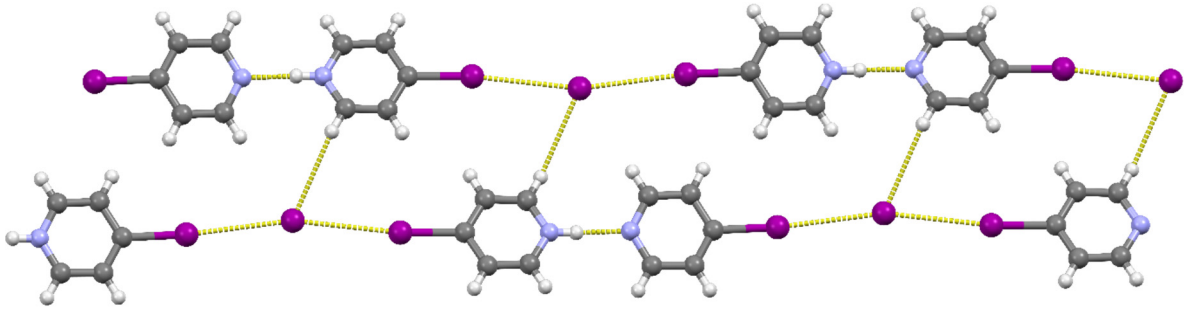

Figure 5. [(**4-IPy**)$_2$H]$^+$ hydrogen bonded complexes and iodide anions connected through C−I···I$^-$ halogen bonds and C−H···I$^-$ hydrogen bonds into double chains in the structure of [(**4-IPy**)$_2$H]I.

As shown above, the hydrogen bonded [(**4-IPy**)$_2$H]$^+$ complex acts in the crystal structure of (**4-IPy**)$_2$HI as a linear ditopic cationic halogen bond donor. This observation inspired us to attempt deliberate synthesis of ditopic cationic halogen bond donors by linking a pair of iodinated pyridine rings with different hydrocarbon linkers. For this purpose, we selected **3-IPy** (which has shown to be a more reliable substrate for *N*-alkylation) as the iodopyridine, and propylene and (*E*)-buta-2-enylene chains as linkers. These linkers were selected as the latter was expected to result in a linear ditopic donor (due to the constricted rotation about the double bond), while the former would result in a bent molecule (the linker being an odd-numbered hydrocarbon chain).

The reaction of **3-IPy** with 1,3-diiodopropane in 2:1 ratio, which was expected to produce the bent dication did not yield the desired product. Instead, we obtained *N*-(3-iodopropane)-3-iodopyridinium iodide ([*N*-I**Prop-3-IPy**]I). [*N*-I**Prop-3-IPy**]I crystalized in centrosymmetric $P2_1/c$ space group with two crystallographically independent ion pairs in the asymmetric unit. This structure comprised chains of alternating cations and anions connected by C−I···I$^-$ halogen bonds (Figure 6). In spite of the fact that only one iodine atom of the reactant 1,3-diiodopropane was substituted by **3-IPy**, the cations acted as ditopic halogen bond donors. Both cations bind two iodide anions, one through C−I···I$^-$ halogen bonds (d(I1···I5) = 3.487(7) Å, ∠ (C2–I1···I5) = 174.3(2)°; d(I3···I6) = 3.558(7) Å, ∠ (C10–I3···I6) = 174.4(2)°) with the iodine bonded to pyridine ring, and the other through C−I···I$^-$ halogen bonds (d(I4···I5) = 3.870(8) Å, ∠ (C8–I4···I5) = 176.0(2)°; d(I2···I6) = 4.044(8) Å, ∠ (C16–I2···I6) = 152.4(2)°) with the iodine atom bonded to alkyl chain. Halogen bonds involving the pyridine iodine atom as halogen bond donor are ca. 10% and 12% shorter than the sum of the corresponding van der Waals radii. On the other hand, one of the two halogen bonds involving an alkyl iodine atom as a halogen bond donor is ca. 2% shorter, while the other one is ca. 2% longer than the sum of the corresponding van der Waals radii. The neighbouring chains are further interconnected by a network of C−H···I$^-$ and C−H···I contacts in a 3D structure (Figure 6).

Unlike 1,3-diiodopropane, (*E*)-1,4-dibromobuta-2-ene reacted with **3-IPy** in the expected 1:2 ratio, yielding a bromide salt of a [*N*,*N*'-**Buen**-(**3-IPy**)$_2$]$^{2+}$ cation (Figure 7a). This salt crystalized in the centrosymmetric space group $P\ 2_1/c$ with the cation placed on an inversion centre. The cation binds two bromide anions via C−I···Br$^-$ halogen bonds (d(I1···Br1) = 3.240(6) Å, ∠ (C2–I1···Br1) = 174.5(1)°). In addition to this halogen bond, the bromide anion participates only in C−H···Br$^-$ hydrogen bonds with aromatic and

methine hydrogen atoms of four neighbouring cations (Figure 7b) leading to formation of a 3D structure.

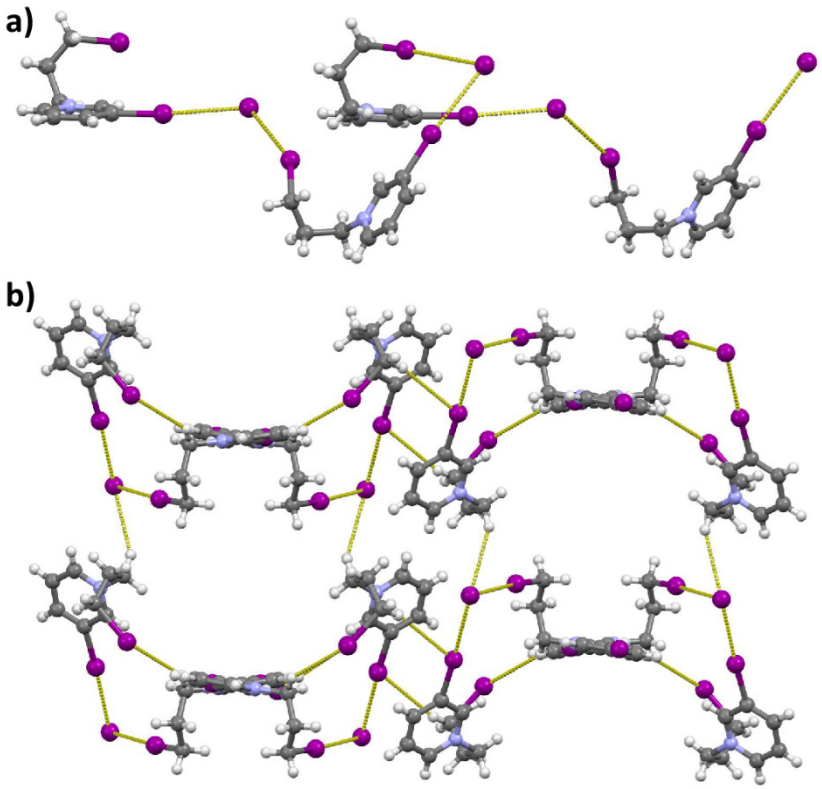

Figure 6. (**a**) [*N*-I**Prop-3-IPy**]$^{+}$ cations and iodide anions connected through C—I···I^{-} halogen bonds in chains in the structure of [*N*-Et-**3-IPy**]I; (**b**) Neighbouring chains are further interconnected by a network of C—H···I^{-} and C—H···I contacts into a 3D structure.

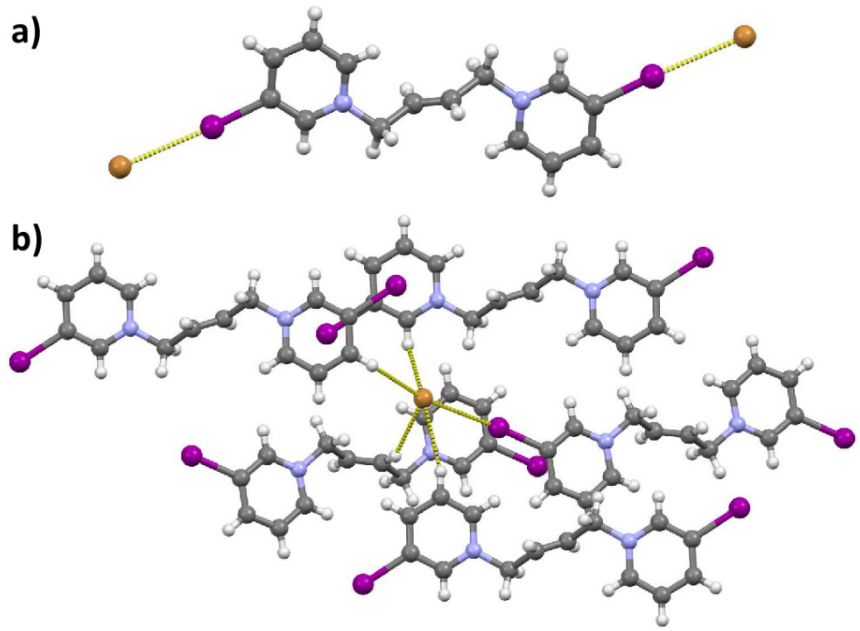

Figure 7. (**a**) One [*N*,*N*′-**Buen**-(**3-IPy**)$_2$]$^{2+}$ cation binds two bromide anions by C—I···Br^{-} halogen bonds in the structure of [*N*,*N*′-**Buen**-(**3-IPy**)$_2$]Br$_2$; (**b**) Bromide anion binds four neighbouring cations through C—H···Br^{-} and one cation through C—I···Br^{-} halogen bonds leading to formation of a 3D structure.

In order to be able to better compare the [*N*,*N*′-**Buen**-(**3-IPy**)$_2$]$^{2+}$ cation to other halogen bond donors covered by this study (all obtained as iodide salts), we attempted to obtain its iodide salt by ion exchange. Unfortunately, the cation was decomposed by the process: instead of the expected product, we obtained [*N*-I**Buen**-(**3-IPy**)]I, an iodide salt of a monocation equivalent to the [*N*-I**Prop**-**3-IPy**]$^+$ cation described above. In contrast to [*N*-I**Prop**-**3-IPy**]I, in [*N*-I**Buen**-(**3-IPy**)]I, the cation does not act as a ditopic donor. Only the pyridyl iodine atoms participate in halogen bonding with iodide anions. The C−I···I$^-$ halogen bonds are ca. 14% and 10% shorter than the sum of the corresponding van der Waals radii (d(I1···I3) = 3.395(1) Å, ∠ (C2–I1···I5) = 176.1(4)°; d(I4···I6) = 3.569(1) Å, ∠ (C11–I4···I6) = 177.2(4)°). Those two halogen-bonded ion pairs (independent by symmetry) are connected in tetramers through C−H···I$^-$ hydrogen bonds with methylene and aromatic hydrogen atoms (*orhto* to the pyridine nitrogen) (d(C1···I6) = 3.841(1) Å, d(C6···I6) = 3.874(2) Å; d(C10···I3) = 3.852(1) Å, d(C15···I3) = 3.987(1) Å). Tetramers are linked into chains through C−H···I$^-$ hydrogen bonds with hydrogen atoms in *meta* position to the pyridine nitrogen atom (d(C4···I6) = 3.961(2) Å, d(C13···I3) = 3.918(2) Å) (Figure 8).

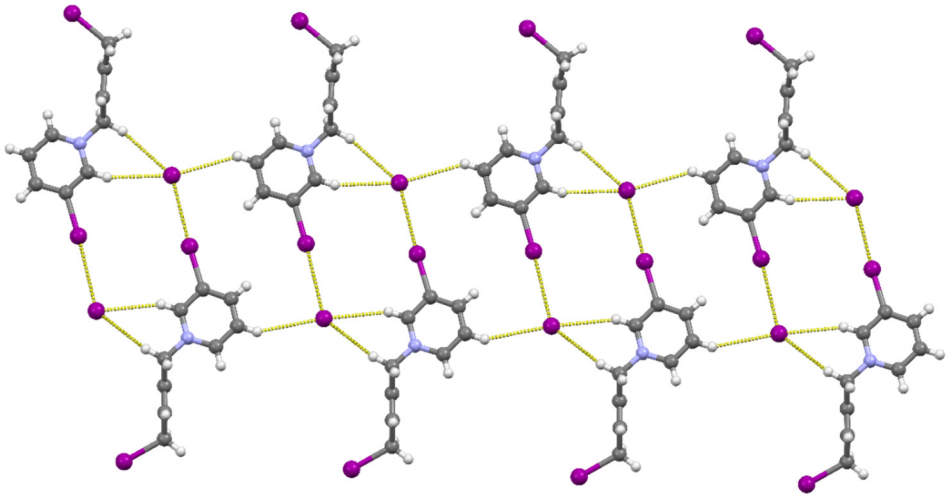

Figure 8. [*N*-I**Buen**-(**3-IPy**)]$^+$ cations and iodide anions connected through C−I···I$^-$ halogen and C−H···I$^-$ hydrogen bonds in cyclical [*N*-I**Buen**-(**3-IPy**)]$_2$I$_2$ tetramers linked via C−H···I$^-$ hydrogen bonds into chains the structure of [*N*-I**Buen**-(**3-IPy**)]I.

The failure of the alkyl iodine atom of [*N*-I**Buen**-(**3-IPy**)]$^+$ to act as a donor of a halogen bond can be rationalised by an examination of the ESP values plotted on the Hirshfeld surfaces of the cations (Figure 9a). Generally, it can be seen that the positive charge is mainly located around pyridine nitrogen atom and neighbouring atoms (carbon and hydrogen) and spread on the pyridine ring rather than on the alkyl chain. As a result, the ESP in the region of the σ-hole of the aliphatic iodine atom on the aliphatic chain is considerably lower than that of the iodine on the pyridine ring. Consequently, the aliphatic iodine atom is a weaker halogen bond donor. This can also be seen from the comparison of the lengths of the C−I···I$^-$ halogen bond involving pyridine iodine atom and aliphatic iodine atom as halogen bond donor in [*N*-I**Prop**-**3-IPy**]I. Halogen bonds involving iodine atoms bonded to pyridine ring (ESP of 0.227 a.u. and 0.203 a.u.) are ca. 10–14% shorter than the sum of the corresponding van der Waals radii, while those involving iodine bonded to the aliphatic chain are in one case (ESP of 0.118 a.u.) slightly shorter, and in the other (ESP of 0.100 a.u.) even longer, than the sum of the corresponding van der Waals radii (Figure 9a).

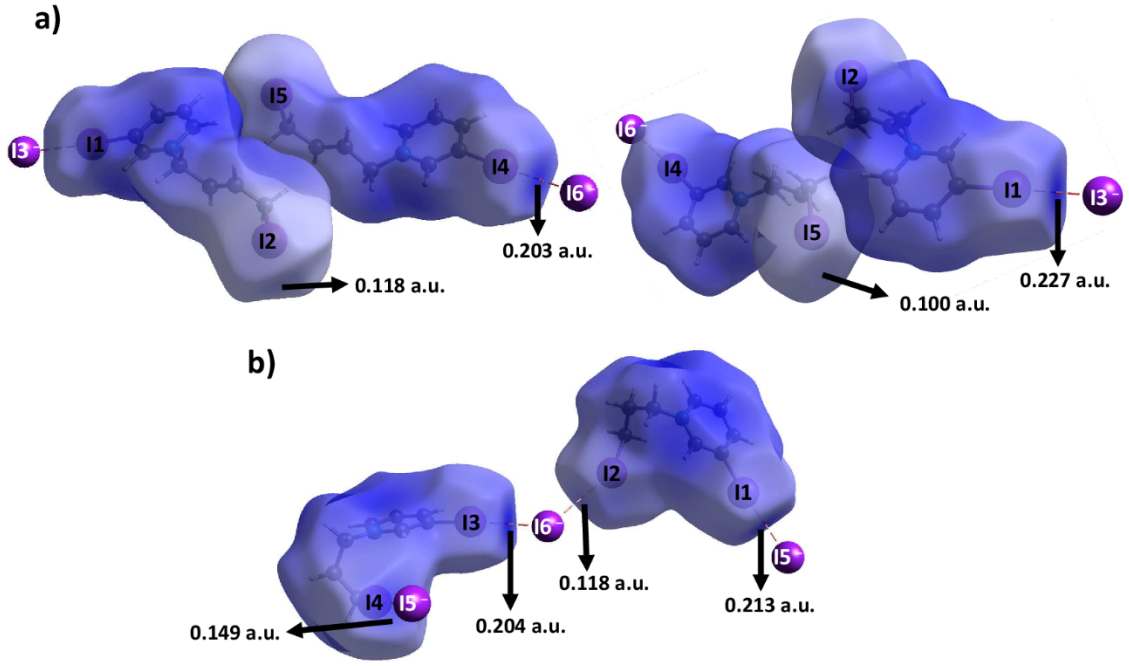

Figure 9. Hirshfeld surface with mapped ESP (computed on B3LYP-DGDZVP level of theory) for: (**a**) [*N*-I**Buen**-(**3-IPy**)]$^+$ cation and (**b**) [*N*-I**Prop**-(**3-IPy**)]$^+$ cation.

If we compare the $C_{py}-I\cdots I^-$ halogen bonds in [*N*-I**Prop-3-IPy**]I and [*N*-I**Buen**-(**3-IPy**)]I, we can see that [*N*-I**Buen**-(**3-IPy**)]$^+$ forms somewhat shorter halogen bond with iodide anion than [*N*-I**Prop**-(**3-IPy**)]$^+$ cation. Furthermore although the $C_{py}-I\cdots I^-$ halogen bonds in [*N*-I**Prop-3-IPy**]I are somewhat longer than the one in [*N*-Et-**3-Ipy**]I, there appears to be a trend of longer chains as *N*-substituents generally leading to shorter $C_{py}-I\cdots I^-$ halogen bonds in *N*-alkyl-3-iodopyridinium iodides (Figure 10a). The values of ESP corresponding to the σ-hole of the iodine on the pyridinium ring (plotted on the Hirshfeld surfaces of these four cations in the crystal structures of the corresponding iodides) also follow the same trend, with the σ-hole of the iodine being the most positive in [*N*-I**Buen**-(**3-IPy**)]$^+$, and least positive in [*N*-Me-**3-Ipy**]$^+$ (Figure 10b).

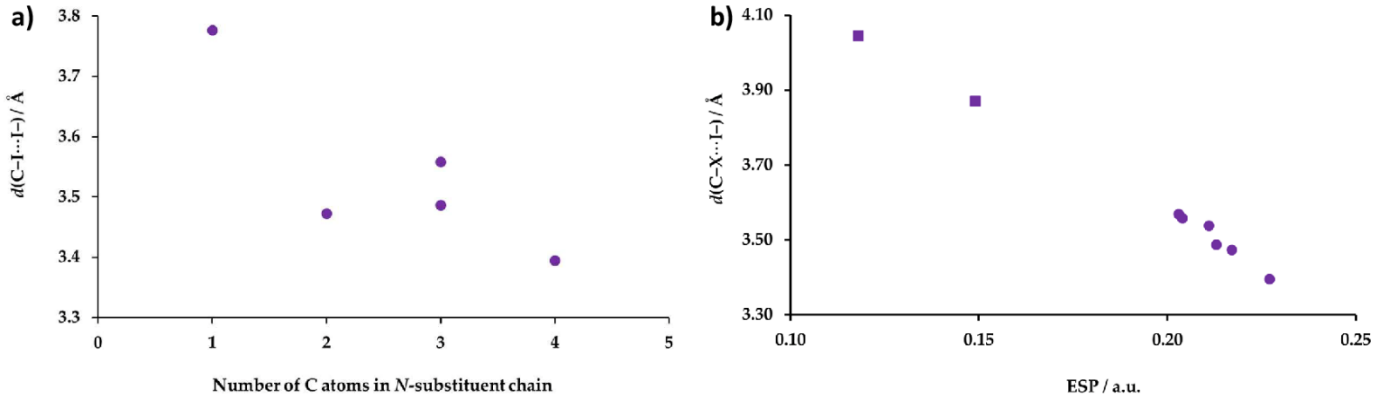

Figure 10. (**a**) Correlation of the number of carbon atoms in *N*-substituent chain of *N*-alkyl-3-iodipyridinium cations with $C-I\cdots I^-$ halogen bonds lengths; (**b**) plot of the values of ESP corresponding to the σ-hole of the halogen atom. vs. $C-X\cdots I^-$ halogen bonds lengths.

4. Conclusions

Introducing various (aliphatic) *N*-substituents on the pyridine ring of 3-bromo- and 3-iodopyridine appears to be a viable method for preparation of an entire class of cationic halogen bond donors. Using aliphatic dihalogenides to produce bis-(halogenopyridinium) dications capable of acting as ditopic halogen bond donors has proven to be somewhat less successful—of the two attempted target cations, only one was isolated, and it decomposed during an attempted ion exchange. However, this opened the possibility of the synthesis of potentially ditopic asymmetric aliphatic–aromatic monocationic halogen bond donors, with two halogens which greatly differ in ESP values corresponding to the halogen σ-hole, and therefore in halogen bonding potential.

Supplementary Materials: The following are available online at https://www.mdpi.com/article/10.3390/cryst11101240/s1, Figure S1. Molecular structure of [*N*-Et-**3-ClPy**]I showing the atom-labelling scheme. Displacement ellipsoids are drawn at the 50% probability level, and H atoms are shown as small spheres of arbitrary radius; Figure S2. Molecular structure of [*N*-Et-**3-BrPy**]I showing the atom-labelling scheme. Displacement ellipsoids are drawn at the 50% probability level, and H atoms are shown as small spheres of arbitrary radius; Figure S3. Molecular structure of [*N*-Et-**3-IPy**]I showing the atom-labelling scheme. Displacement ellipsoids are drawn at the 50% probability level, and H atoms are shown as small spheres of arbitrary radius; Figure S4. Molecular structure of [*N*-**Ace**-**3-ClPy**]I showing the atom-labelling scheme. Displacement ellipsoids are drawn at the 50% probability level, and H atoms are shown as small spheres of arbitrary radius; Figure S5. Molecular structure of [**4-IPy**]$_2$HI showing the atom-labelling scheme. Displacement ellipsoids are drawn at the 50% probability level, and H atoms are shown as small spheres of arbitrary radius; Figure S6. Molecular structure of [*N*-**Prop**I-**3-IPy**]I showing the atom-labelling scheme. Displacement ellipsoids are drawn at the 50% probability level, and H atoms are shown as small spheres of arbitrary radius; Figure S7. Molecular structure of [***N,N'*-Buen**-(**3-IPy**)$_2$]Br$_2$ showing the atom-labelling scheme. Displacement ellipsoids are drawn at the 50% probability level, and H atoms are shown as small spheres of arbitrary radius; Figure S8. Molecular structure of [*N*-**Buen**I-**3-IPy**]I showing the atom-labelling scheme. Displacement ellipsoids are drawn at the 50% probability level, and H atoms are shown as small spheres of arbitrary radius; Figure S9. Measured (black) and calculated (blue) PXRD patterns of [*N*-Et-**3-ClPy**]I; Figure S10. Measured (black) and calculated (blue) PXRD patterns of [*N*-Et-**3-BrPy**]I; Figure S11. Measured (black) and calculated (blue) PXRD patterns of [*N*-Et-**3-IPy**]I; Figure S12. Measured (black) and calculated (blue) PXRD patterns of [*N*-**Prop**I-**3-IPy**]Br; Figure S13. Measured (black) and calculated (blue) PXRD patterns of [*N,N'*-**Buen**-(**3-IPy**)$_2$]Br$_2$; Figure S14. Measured (black) and calculated (blue) PXRD patterns of [*N*-**Buen**I-**3-IPy**]I; Figure S15. TG (black) and DSC (red) thermograms of [*N*-Et-**3-ClPy**]I; Figure S16. TG (black) and DSC (red) thermograms of [*N*-Et-**3-BrPy**]I; Figure S17. TG (black) and DSC (red) thermograms of [*N*-Et-**3-IPy**]I; Figure S18. TG (black) and DSC (red) thermograms of [*N*-**Prop**I-**3-IPy**]I; Figure S19. TG (black) and DSC (red) thermograms of [***N,N'*-Buen**-(**3-IPy**)$_2$]Br$_2$; Figure S20. TG (black) and DSC (red) thermograms of [*N*-**Buen**I-**3-IPy**]I; Figure S21. IR spectrum (ATR) of [*N*-Et-**3-ClPy**]I; Figure S22. IR spectrum (ATR) of [*N*-Et-**3-BrPy**]I; Figure S23. IR spectrum (ATR) of [*N*-Et-**3-IPy**]I; Figure S24. IR spectrum (ATR) of [*N*-**Prop**I-**3-IPy**]I; Figure S25. IR spectrum (ATR) of [*N,N'*-**Buen**-(**3-IPy**)$_2$]Br$_2$; Figure S26. IR spectrum (ATR) of [*N*-**Buen**I-**3-IPy**]I; Table S1. An overview and crystallographic data of the prepared compounds. CCDC 2109490-2109497 contain crystallographic data for this paper. These data can be obtained free of charge from the Director, CCDC, 12 Union Road, Cambridge, CBZ 1EZ, UK (Fax: +44-1223-336033; email: deposit@ccdc.cam.ac.uk or www: http://www.ccdc.cam.ac.uk accessed on 25 August 2021).

Author Contributions: Conceptualization, L.F. and V.S.; methodology, L.F. and V.S.; formal analysis, L.F.; investigation, L.F.; data curation, L.F.; writing—original draft preparation, L.F.; writing—review and editing, L.F. and V.S.; visualization, L.F. and V.S.; supervision, V.S. All authors have read and agreed to the published version of the manuscript.

Funding: This research was funded by the Croatian Science Foundation under the project IP-2019-04-1868.

Institutional Review Board Statement: Not applicable.

Informed Consent Statement: Not applicable.

Data Availability Statement: Not applicable.

Acknowledgments: We acknowledge the support of project CIuK co-financed by the Croatian Government and the European Union through the European Regional Development Fund-Competitiveness and Cohesion Operational Programme (Grant KK.01.1.1.02.0016.).

Conflicts of Interest: The authors declare no conflict of interest. The funders had no role in the design of the study; in the collection, analyses, or interpretation of data; in the writing of the manuscript, or in the decision to publish the results.

References

1. Cavallo, G.; Metrangolo, P.; Milani, R.; Pilati, T.; Priimagi, A.; Resnati, G.; Terraneo, G. The halogen bond. *Chem. Rev.* **2016**, *116*, 2478–2601. [CrossRef]
2. Metrangolo, P.; Resnati, G. *Halogen Bonding*; Metrangolo, P., Resnati, G., Eds.; Springer: Berlin/Heidelberg, Germany, 2008; Volume 126.
3. Metrangolo, P.; Resnati, G. Halogen bonding: A paradigm in supramolecular chemistry. *Chem. Eur. J.* **2001**, *7*, 2511–2519. [CrossRef]
4. Erdélyi, M. Halogen bonding in solution. *Chem. Soc. Rev.* **2012**, *41*, 3547–3557. [CrossRef]
5. Gilday, L.C.; Robinson, S.W.; Barendt, T.A.; Langton, M.J.; Mullaney, B.R.; Beer, P.D. Halogen bonding in supramolecular chemistry. *Chem. Rev.* **2015**, *115*, 7118–7195. [CrossRef] [PubMed]
6. Politzer, P.; Murray, J.S.; Clark, T. Halogen bonding: An electrostatically-driven highly directional noncovalent interaction. *Phys. Chem. Chem. Phys.* **2010**, *12*, 7748–7757. [CrossRef] [PubMed]
7. Politzer, P.; Murray, J.S.; Clark, T.; Resnati, G. The σ-hole revisited. *Phys. Chem. Chem. Phys.* **2017**, *19*, 32166–32178. [CrossRef] [PubMed]
8. Legon, A.C. The halogen bond: An interim perspective. *Phys. Chem. Chem. Phys.* **2010**, *12*, 7736–7747. [CrossRef] [PubMed]
9. Cinčić, D.; Friščić, T.; Jones, W. Structural equivalence of Br and I halogen bonds: A route to isostructural materials with controllable properties. *Chem. Mater.* **2008**, *20*, 6623–6626. [CrossRef]
10. Ding, X.; Tuikka, M.; Haukk, M. Halogen Bonding in Crystal Engineering. In *Recent Advances in Crystallography*; InTech: London, UK, 2012; Volume 262, pp. 143–168.
11. Mukherjee, A.; Tothadi, S.; Desiraju, G.R. Halogen Bonds in Crystal Engineering: Like Hydrogen Bonds yet Different. *Acc. Chem. Res.* **2014**, *47*, 2514–2524. [CrossRef] [PubMed]
12. Aakeröy, C.B.; Wijethunga, T.K.; Desper, J. Practical crystal engineering using halogen bonding: A hierarchy based on calculated molecular electrostatic potential surfaces. *J. Mol. Struct.* **2014**, *1072*, 20–27. [CrossRef]
13. Bulfield, D.; Huber, S.M. Halogen Bonding in Organic Synthesis and Organocatalysis. *Chem. Eur. J.* **2016**, *22*, 14434–14450. [CrossRef]
14. Lisac, K.; Topić, F.; Arhangelskis, M.; Cepić, S.; Julien, P.A.; Nickels, C.W.; Morris, A.J.; Friščić, T.; Cinčić, D. Halogen-bonded cocrystallization with phosphorus, arsenic and antimony acceptors. *Nat. Commun.* **2019**, *10*, 61. [CrossRef]
15. Nemec, V.; Lisac, K.; Bedeković, N.; Fotović, L.; Stilinović, V.; Cinčić, D. Crystal engineering strategies towards halogen-bonded metal-organic multi-component solids: Salts, cocrystals and salt cocrystals. *CrystEngComm* **2021**, *23*, 3063–3083. [CrossRef]
16. Aakeröy, C.B.; Baldrighi, M.; Desper, J.; Metrangolo, P.; Resnati, G. Supramolecular hierarchy among halogen-bond donors. *Chem. Eur. J.* **2013**, *19*, 16240–16247. [CrossRef] [PubMed]
17. Aakeröy, C.B.; Wijethunga, T.K.; Haj, M.A.; Desper, J.; Moore, C. The structural landscape of heteroaryl-2-imidazoles: Competing halogen-and hydrogen-bond interactions. *CrystEngComm* **2014**, *16*, 7218. [CrossRef]
18. Eraković, M.; Cinčić, D.; Molčanov, K.; Stilinović, V. A Crystallographic Charge Density Study of the Partial Covalent Nature of Strong N···Br Halogen Bonds. *Angew. Chem. Int. Ed.* **2019**, *58*, 15702–15706. [CrossRef]
19. Aakeröy, C.B.; Wijethunga, T.K.; Desper, J.; Đaković, M. Electrostatic Potential Differences and Halogen-Bond Selectivity. *Cryst. Growth Des.* **2016**, *16*, 2662–2670. [CrossRef]
20. Turunen, L.; Warzok, U.; Puttreddy, R.; Beyeh, N.K.; Schalley, C.A.; Rissanen, K. [N···I^+···N] Halogen-Bonded Dimeric Capsules from Tetrakis(3-pyridyl)ethylene Cavitands. *Angew. Chem. Int. Ed.* **2016**, *55*, 14033–14036. [CrossRef] [PubMed]
21. Turunen, L.; Pan, F.; Beyeh, N.K.; Trant, J.F.; Ras, R.H.A.; Rissanen, K. Bamboo-like Chained Cavities and Other Halogen-Bonded Complexes from Tetrahaloethynyl Cavitands with Simple Ditopic Halogen Bond Acceptors. *Cryst. Growth Des.* **2018**, *18*, 513–520. [CrossRef]
22. Saccone, M.; Siiskonen, A.; Fernandez-Palacio, F.; Priimagi, A.; Terraneo, G.; Resnati, G.; Metrangolo, P. Halogen bonding stabilizes a *cis*-azobenzene derivative in the solid state: A crystallographic study. *Acta Crystallogr. Sect. B Struct. Sci. Cryst. Eng. Mater.* **2017**, *73*, 227–233. [CrossRef]
23. Meazza, L.; Foster, J.A.; Fucke, K.; Metrangolo, P.; Resnati, G.; Steed, J.W. Halogen-bonding-triggered supramolecular gel formation. *Nat. Chem.* **2013**, *5*, 42–47. [CrossRef] [PubMed]
24. Saccone, M.; Cavallo, G.; Metrangolo, P.; Pace, A.; Pibiri, I.; Pilati, T.; Resnati, G.; Terraneo, G. Halogen bond directionality translates tecton geometry into self-assembled architecture geometry. *CrystEngComm* **2013**, *15*, 3102–3105. [CrossRef]

25. Jakupec, N.; Fotović, L.; Stilinović, V. The effect of halogen bonding on protonated hexacyanoferrate networks in hexacyanoferrates of halogenopyridines. *CrystEngComm* **2020**, *22*, 8142–8150. [CrossRef]
26. Uran, E.; Fotović, L.; Bedeković, N.; Stilinović, V.; Cinčić, D. The amine group as halogen bond acceptor in cocrystals of aromatic diamines and perfluorinated iodobenzenes. *Crystals* **2021**, *11*, 529. [CrossRef]
27. Aakeröy, C.B.; Wijethunga, T.K.; Benton, J.; Desper, J. Stabilizing volatile liquid chemicals using co-crystallization. *Chem. Commun.* **2015**, *51*, 2425–2428. [CrossRef]
28. Aakeröy, C.B.; Wijethunga, T.K.; Desper, J. Constructing molecular polygons using halogen bonding and bifurcated *N*-oxides. *CrystEngComm* **2014**, *16*, 28–31. [CrossRef]
29. Carletta, A.; Zbačnik, M.; Vitković, M.; Tumanov, N.; Stilinović, V.; Wouters, J.; Cinčić, D. Halogen-bonded cocrystals of *N*-salicylidene Schiff bases and iodoperfluorinated benzenes: Hydroxyl oxygen as a halogen bond acceptor. *CrystEngComm* **2018**, *20*, 5332–5339. [CrossRef]
30. Topić, F.; Lisac, K.; Arhangelskis, M.; Rissanen, K.; Cinčić, D.; Friščić, T. Cocrystal trimorphism as a consequence of the orthogonality of halogen- and hydrogen-bonds synthons. *Chem. Commun.* **2019**, *55*, 14066–14069. [CrossRef]
31. Martinez, V.; Bedeković, N.; Stilinović, V.; Cinčić, D. Tautomeric Equilibrium of an asymmetric β-diketone in halogen-bonded cocrystals with perfluorinated iodobenzenes. *Crystals* **2021**, *11*, 699. [CrossRef]
32. Stilinović, V.; Grgurić, T.; Piteša, T.; Nemec, V.; Cinčić, D. Bifurcated and monocentric halogen bonds in cocrystals of metal(ii) acetylacetonates with *p*-dihalotetrafluorobenzenes. *Cryst. Growth Des.* **2019**, *19*, 1245–1256. [CrossRef]
33. Nemec, V.; Piteša, T.; Friščić, T.; Cinčić, D. The morpholinyl oxygen atom as an acceptor site for halogen-bonded cocrystallization of organic and metal–organic units. *Cryst. Growth Des.* **2020**, *20*, 3617–3624. [CrossRef]
34. Syssa-Magalé, J.-L.; Boubekeur, K.; Schöllhorn, B. First molecular self-assembly of 1,4-diiodo-tetrafluoro-benzene and a ketone via (O···I) non-covalent halogen bonds. *J. Mol. Struct.* **2005**, *737*, 103–107. [CrossRef]
35. Goodwin, M.J.; Steed, B.W.; Yufit, D.S.; Musa, O.M.; Berry, D.J.; Steed, J.W. Halogen and Hydrogen Bonding in Povidone-Iodine and Related Co-Phases. *Cryst. Growth Des.* **2017**, *17*, 5552–5558. [CrossRef]
36. Tothadi, S.; Sanphui, P.; Desiraju, G.R. Obtaining synthon modularity in ternary cocrystals with hydrogen bonds and halogen bonds. *Cryst. Growth Des.* **2014**, *14*, 5293–5302. [CrossRef]
37. Saha, B.K.; Nangia, A.; Jaskólski, M. Crystal engineering with hydrogen bonds and halogen bonds. *CrystEngComm* **2005**, *7*, 355. [CrossRef]
38. Cinčić, D.; Friščić, T. Synthesis of an extended halogen-bonded metal–organic structure in a one-pot mechanochemical reaction that combines covalent bonding, coordination chemistry and supramolecular synthesis. *CrystEngComm* **2014**, *16*, 10169–10172. [CrossRef]
39. Nemec, V.; Fotović, L.; Vitasović, T.; Cinčić, D. Halogen bonding of the aldehyde oxygen atom in cocrystals of aromatic aldehydes and 1,4-diiodotetrafluorobenzene. *CrystEngComm* **2019**, *21*, 3251–3255. [CrossRef]
40. Nemec, V.; Fotović, L.; Friščić, T.; Cinčić, D. A large family of halogen-bonded cocrystals involving metal-organic building blocks with open coordination sites. *Cryst. Growth Des.* **2017**, *17*, 6169–6173. [CrossRef]
41. Zbačnik, M.; Pajski, M.; Stilinović, V.; Vitković, M.; Cinčić, D. The halogen bonding proclivity of the: *Ortho*-methoxy-hydroxy group in cocrystals of *o*-vanillin imines and diiodotetrafluorobenzenes. *CrystEngComm* **2017**, *19*, 5576–5582. [CrossRef]
42. Lisac, K.; Cinčić, D. The Influence of Liquid on the Outcome of Halogen-Bonded Metal–Organic Materials Synthesis by Liquid Assisted Grinding. *Crystals* **2017**, *7*, 363. [CrossRef]
43. Lisac, K.; Cinčić, D. Simple design for metal-based halogen-bonded cocrystals utilizing the M–Cl···I motif. *CrystEngComm* **2018**, *20*, 5955–5963. [CrossRef]
44. Zordan, F.; Brammer, L. Water molecules insert into N–H···Cl–M hydrogen bonds while M–Cl···X–C halogen bonds remain intact in dihydrates of halopyridinium hexachloroplatinates. *Acta Crystallogr. Sect. B Struct. Sci.* **2004**, *60*, 512–519. [CrossRef] [PubMed]
45. Zordan, F.; Purver, S.L.; Adams, H.; Brammer, L. Halometallate and halide ions: Nucleophiles in competition for hydrogen bond and halogen bond formation in halopyridinium salts of mixed halide-halometallate anions. *CrystEngComm* **2005**, *7*, 350–354. [CrossRef]
46. Zordan, F.; Brammer, L.; Sherwood, P. Supramolecular chemistry of halogens: Complementary features of inorganic (M-X) and organic (C-X′) halogens applied to M-X···X′-C halogen bond formation. *J. Am. Chem. Soc.* **2005**, *127*, 5979–5989. [CrossRef] [PubMed]
47. Decato, D.A.; Riel, A.M.S.; May, J.H.; Bryantsev, V.S.; Berryman, O.B. Theoretical, solid-state, and solution quantification of the hydrogen bond-enhanced halogen bond. *Angew. Chem.* **2021**, *133*, 3729–3736. [CrossRef]
48. Logothetis, T.A.; Meyer, F.; Metrangolo, P.; Pilati, T.; Resnati, G. Crystal engineering of brominated tectons: *N*-methyl-3,5-dibromopyridinium iodide gives particularly short C-Br···I halogen bonding. *New J. Chem.* **2004**, *28*, 760–763. [CrossRef]
49. Fotović, L.; Stilinović, V. Halogenide anions as halogen and hydrogen bond acceptors in iodopyridinium halogenides. *CrystEngComm* **2020**, *22*, 4039–4046. [CrossRef]
50. Awwadi, F.F.; Willett, R.D.; Peterson, K.A.; Twamley, B. The nature of halogen···halide synthons: Theoretical and crystallographic studies. *J. Phys. Chem. A.* **2007**, *111*, 2319–2328. [CrossRef]
51. Freytag, M.; Jones, P.G.; Ahrens, B.; Fischer, A.K. Hydrogen bonding and halogen-halogen interactions in 4-halopyridinium halides. *New J. Chem.* **1999**, *23*, 1137–1139. [CrossRef]

52. Willett, R.D.; Awwadi, F.; Butcher, R.; Haddad, S.; Twamley, B. The aryl bromine-halide ion synthon and its role in the control of the crystal structures of tetrahalocuprate (II) ions. *Cryst. Growth Des.* **2003**, *3*, 301–311. [CrossRef]
53. Brammer, L.; Mínguez Espallargas, G.; Adams, H. Involving metals in halogen-halogen interactions: Second-sphere Lewis acid ligands for perhalometallate ions (M-X···X′-C). *CrystEngComm* **2003**, *5*, 343–345. [CrossRef]
54. Mínguez Espallargas, G.; Brammer, L.; Sherwood, P. Designing intermolecular interactions between halogenated peripheries of inorganic and organic molecules: Electrostatically directed M-X···X′- C halogen bonds. *Angew. Chem. Int. Ed.* **2006**, *45*, 435–440. [CrossRef] [PubMed]
55. Roper, L.C.; Präsang, C.; Kozhevnikov, V.N.; Whitwood, A.C.; Karadakov, P.B.; Bruce, D.W. Experimental and theoretical study of halogen-bonded complexes of DMAP with di-and triiodofluorobenzenes. A complex with a very short N···I halogen bond. *Cryst. Growth Des.* **2010**, *10*, 3710–3720. [CrossRef]
56. Ding, X.H.; Chang, Y.Z.; Ou, C.J.; Lin, J.Y.; Xie, L.H.; Huang, W. Halogen bonding in the co-crystallization of potentially ditopic diiodotetrafluorobenzene: A powerful tool for constructing multicomponent supramolecular assemblies. *Natl. Sci. Rev.* **2020**, *7*, 1906–1932. [CrossRef]
57. Lunghi, A.; Cardillo, P.; Messina, T.; Metrangolo, P.; Panzeri, W.; Resnati, G. Perfluorocarbon-hydrocarbon self assembling. Thermal and vibrational analyses of one-dimensional networks formed by α,ω-diiodoperfluoroalkanes with K.2.2. and K.2.2.2. *J. Fluor. Chem.* **1998**, *91*, 191–194. [CrossRef]
58. Messina, M.T.; Metrangolo, P.; Panzeri, W.; Ragg, E.; Resnati, G. Perfluorocarbon-hydrocarbon self-assembly. Part 3. Liquid phase interactions between perfluoroalkylhalides and heteroactom containing hydrocarbons. *Tetrahedron Lett.* **1998**, *39*, 9069–9072. [CrossRef]
59. Farina, A.; Meille, S.V.; Messina, M.T.; Metrangolo, P.; Resnati, G.; Vecchio, G. Resolution of racemic 1,2-dibromohexafluoropropane through halogen- bonded supramolecular helices. *Angew. Chem. Int. Ed.* **1999**, *38*, 2433–2436. [CrossRef]
60. Metrangolo, P.; Meyer, F.; Pilati, T.; Resnati, G.; Terraneo, G. Halogen bonding in supramolecular chemistry. *Angew. Chem. —Int. Ed.* **2008**, *47*, 6114–6127. [CrossRef]
61. Raatikainen, K.; Rissanen, K. Hierarchical halogen bonding induces polymorphism. *CrystEngComm* **2009**, *11*, 750–752. [CrossRef]
62. Nguyen, S.T.; Ellington, T.L.; Allen, K.E.; Gorden, J.D.; Rheingold, A.L.; Tschumper, G.S.; Hammer, N.I.; Watkins, D.L. Systematic experimental and computational studies of substitution and hybridization effects in solid-state halogen bonded assemblies. *Cryst. Growth Des.* **2018**, *18*, 3244–3254. [CrossRef]
63. Rosokha, S.V.; Loboda, E.A. Interplay of halogen and π-π charge-transfer bondings in intermolecular associates of bromo- or iododinitrobenzene with tetramethyl-*p*-phenylenediamine. *J. Phys. Chem. A.* **2015**, *119*, 3833–3842. [CrossRef]
64. Nwachukwu, C.I.; Kehoe, Z.R.; Bowling, N.P.; Speetzen, E.D.; Bosch, E. Cooperative halogen bonding and polarized π-stacking in the formation of coloured charge-transfer co-crystals. *New J. Chem.* **2018**, *42*, 10615–10622. [CrossRef]
65. Baykov, S.V.; Filimonov, S.I.; Rozhkov, A.V.; Novikov, A.S.; Ananyev, I.V.; Ivanov, D.M.; Kukushkin, V.Y. Reverse Sandwich structures from interplay between lone pair-π-hole atom-directed C···dz^2[M] and halogen bond interactions. *Cryst. Growth Des.* **2020**, *20*, 995–1008. [CrossRef]
66. Barry, D.E.; Hawes, C.S.; Blasco, S.; Gunnlaugsson, T. Structure Direction, solvent effects, and anion influences in halogen-bonded adducts of 2,6-bis(iodoethynyl)pyridine. *Cryst. Growth Des.* **2016**, *16*, 5194–5205. [CrossRef]
67. Nguyen, S.T.; Rheingold, A.L.; Tschumper, G.S.; Watkins, D.L. Elucidating the effects of fluoro and nitro substituents on halogen bond driven assemblies of pyridyl-capped π-conjugated molecules. *Cryst. Growth Des.* **2016**, *16*, 6648–6653. [CrossRef]
68. Baldrighi, M.; Bartesaghi, D.; Cavallo, G.; Chierotti, M.R.; Gobetto, R.; Metrangolo, P.; Pilati, T.; Resnati, G.; Terraneo, G. Polymorphs and co-crystals of haloprogin: An antifungal agent. *CrystEngComm* **2014**, *16*, 5897–5904. [CrossRef]
69. Stilinović, V.; Horvat, G.; Hrenar, T.; Nemec, V.; Cinčić, D. Halogen and hydrogen bonding between (*N*-halogeno)-succinimides and pyridine derivatives in solution, the solid state and in silico. *Chem. Eur. J.* **2017**, *23*, 5244–5257. [CrossRef]
70. Raatikainen, K.; Rissanen, K. Interaction between amines and *N*-haloimides: A new motif for unprecedentedly short Br···N and I···N halogen bonds. *CrystEngComm* **2011**, *13*, 6972–6977. [CrossRef]
71. Raatikainen, K.; Rissanen, K. Breathing molecular crystals: Halogen-and hydrogen-bonded porous molecular crystals with solvent induced adaptation of the nanosized channels. *Chem. Sci.* **2012**, *3*, 1235–1239. [CrossRef]
72. Makhotkina, O.; Lieffrig, J.; Jeannin, O.; Fourmigué, M.; Aubert, E.; Espinosa, E. Cocrystal or salt: Solid state-controlled iodine shift in crystalline halogen-bonded systems. *Cryst. Growth Des.* **2015**, *15*, 3464–3473. [CrossRef]
73. Puttreddy, R.; Jurček, O.; Bhowmik, S.; Mäkelä, T.; Rissanen, K. Very strong $^{-}$N–X^{+}···$^{-}$O–N^{+} halogen bonds. *Chem. Commun.* **2016**, *52*, 2338–2341. [CrossRef]
74. Puttreddy, R.; Rautiainen, J.M.; Mäkelä, T.; Rissanen, K. Strong N−X···O−N halogen bonds: A comprehensive study on *N*-halosaccharin pyridine *N*-oxide complexes. *Angew. Chem. Int. Ed.* **2019**, *58*, 18610–18618. [CrossRef]
75. Mavračić, J.; Cinčić, D.; Kaitner, B. Halogen bonding of: *N*-bromosuccinimide by grinding. *CrystEngComm* **2016**, *18*, 3343–3346. [CrossRef]
76. Dolenc, D.; Modec, B. EDA Complexes of *N*-halosaccharins with *N*- and *O*-donor ligands. *New J. Chem.* **2009**, *33*, 2344–2349. [CrossRef]
77. Yu, S.; Ward, J.S.; Truong, K.; Rissanen, K. Carbonyl hypoiodites as extremely strong halogen bond donors. *Angew. Chem. Int. Ed.* **2021**, *60*, 20739–20743. [CrossRef]

78. Aubert, E.; Espinosa, E.; Nicolas, I.; Jeannin, O.; Fourmigué, M. Toward a reverse hierarchy of halogen bonding between bromine and iodine. *Faraday Discuss.* **2017**, *203*, 389–406. [CrossRef]
79. Thomas, L.H.; Adam, M.S.; O'Neill, A.; Wilson, C.C. Utilizing proton transfer to produce molecular salts in bromanilic acid substituted-pyridine molecular complexes-predictable synthons? *Acta Crystallogr. Sect. C Cryst. Struct. Commun.* **2013**, *69*, 1279–1288. [CrossRef]
80. Espallargas, G.M.; Zordan, F.; Marín, L.A.; Adams, H.; Shankland, K.; van de Streek, J.; Brammer, L. Rational modification of the hierarchy of intermolecular interactions in molecular crystal structures by using tunable halogen Bonds. *Chem. Eur. J.* **2009**, *15*, 7554–7568. [CrossRef] [PubMed]
81. Awwadi, F.F.; Willett, R.D.; Twamley, B. The aryl chlorine-halide ion synthon and its role in the control of the crystal structures of tetrahalocuprate(II) ions. *Cryst. Growth Des.* **2007**, *7*, 624–632. [CrossRef]
82. Vitorica-Yrezabal, I.J.; Sullivan, R.A.; Purver, S.L.; Curfs, C.; Tang, C.C.; Brammer, L. Synthesis and polymorphism of (4-ClpyH)$_2$[CuCl$_4$]: Solid-gas and solid-solid reactions. *CrystEngComm* **2011**, *13*, 3189–3196. [CrossRef]
83. Wolf, J.; Huber, F.; Erochok, N.; Heinen, F.; Guérin, V.; Legault, C.Y.; Kirsch, S.F.; Huber, S.M. Activation of a metal-halogen bond by halogen bonding. *Angew. Chem. Int. Ed.* **2020**, *59*, 16496–16500. [CrossRef]
84. Sutar, R.L.; Engelage, E.; Stoll, R.; Huber, S.M. Bidentate chiral bis(imidazolium)-based halogen-bond donors: Synthesis and applications in enantioselective recognition and catalysis. *Angew. Chem. Int. Ed.* **2020**, *59*, 6806–6810. [CrossRef]
85. Derossi, S.; Brammer, L.; Hunter, C.A.; Ward, M.D. Halogen bonded supramolecular assemblies of [Ru(bipy)(CN)$_4$]$^{2-}$ anions and *N*-methyl-halopyridinium cations in the solid state and in solution. *Inorg. Chem.* **2009**, *48*, 1666–1677. [CrossRef] [PubMed]
86. Ormond-Prout, J.E.; Smart, P.; Brammer, L. Cyanometallates as halogen bond acceptors. *Cryst. Growth Des.* **2012**, *12*, 205–216. [CrossRef]
87. Awwadi, F.F.; Willett, R.D.; Twamley, B. The Role of Charge Assisted Arylhalogen-Halide Ion Interactions in the Structures of the Dibromopyridinium Halide Salts. *J. Mol. Struct.* **2009**, *918*, 116–122. [CrossRef]
88. Awwadi, F.F.; Taher, D.; Kailani, M.H.; Alwahsh, M.I.; Odeh, F.; Rüffer, T.; Schaarschmidt, D.; Lang, H. Halogen Bonding Interactions in Halopyridine–Iodine Monochloride Complexes. *Cryst. Growth Des.* **2020**, *20*, 543–551. [CrossRef]
89. Awwadi, F.F.; Taher, D.; Maabreh, A.; Alwedian, F.Z.; Al-Ebaisat, H.; Rüffer, T.; Lang, H. The Role of Fe–X···X–Fe Contacts in the Crystal Structures of [(2-Iodopyridinium)$_2$FeX$_4$]X (X = Cl, Br). *Struct. Chem.* **2013**, *24*, 401–408. [CrossRef]
90. Bondarenko, M.A.; Adonin, S.A.; Novikov, A.S.; Sokolov, M.N.; Fedin, V.P. Supramolecular Bromoantimonate(V) Polybromide (2,6-BrPyH)$_3$[SbBr$_6$]{(Br$_2$)Br} · 2H$_2$O: Specific Features of Halogen···Halogen Contacts in the Crystal Structure. *Russ. J. Coord. Chem.* **2020**, *46*, 302–307. [CrossRef]
91. Anagnostis, J.; Cipi, J.; Landee, C.P.; Tremelling, G.W.; Turnbull, M.M.; Twamley, B.; Wikaira, J.L. Transition Metal Salts of 2-Amino-3,5-Dihalopyridine—Dimers: Syntheses, Structures and Magnetic Properties of (3,5-DiCAPH)$_2$Cu$_2$Br$_6$ and (3,5-DiBAPH)$_2$Cu$_{2\times6}$. *J. Coord. Chem.* **2017**, *70*, 3892–3906. [CrossRef]
92. Amendola, V.; Bergamaschi, G.; Boiocchi, M.; Fusco, N.; La Rocca, M.V.; Linati, L.; Lo Presti, E.; Mella, M.; Metrangolo, P.; Miljkovic, A. Novel hydrogen- and halogen-bonding anion receptors based on 3-iodopyridinium units. *RSC Adv.* **2016**, *6*, 67540–67549. [CrossRef]
93. Riel, A.M.S.; Jessop, M.J.; Decato, D.A.; Massena, C.J.; Nascimento, V.R.; Berryman, O.B. Experimental investigation of halogen-bond hard-soft acid-base complementarity. *Acta Crystallogr. Sect. B Struct. Sci. Cryst. Eng. Mater.* **2017**, *73*, 203–209. [CrossRef] [PubMed]
94. Riel, A.M.S.; Decato, D.A.; Sun, J.; Massena, C.J.; Jessop, M.J.; Berryman, O.B. The intramolecular hydrogen bonded-halogen bond: A new strategy for preorganization and enhanced binding. *Chem. Sci.* **2018**, *9*, 5828–5836. [CrossRef] [PubMed]
95. Foyle, É.M.; White, N.G. Anion templated crystal engineering of halogen bonding tripodal tris(halopyridinium) compounds. *CrystEngComm* **2020**, *22*, 2526–2536. [CrossRef]
96. Lohrman, J.A.; Deng, C.L.; Shear, T.A.; Zakharov, L.N.; Haley, M.M.; Johnson, D.W. Methanesulfonyl-polarized halogen bonding enables strong halide recognition in an arylethynyl anion receptor. *Chem. Commun.* **2019**, *55*, 1919–1922. [CrossRef]
97. Jungbauer, S.H.; Huber, S.M. Cationic multidentate halogen-bond donors in halide abstraction organocatalysis: Catalyst optimization by preorganization. *J. Am. Chem. Soc.* **2015**, *137*, 12110–12120. [CrossRef]
98. Adonin, S.A.; Gorokh, I.D.; Novikov, A.S.; Samsonenko, D.G.; Yushina, I.V.; Sokolov, M.N.; Fedin, V.P. Halobismuthates with Halopyridinium Cations: Appearance or Non-Appearance of Unusual Colouring. *CrystEngComm* **2018**, *20*, 7766–7772. [CrossRef]
99. Adonin, S.A.; Gorokh, I.D.; Novikov, A.S.; Abramov, P.A.; Sokolov, M.N.; Fedin, V.P. Halogen Contacts-Induced Unusual Coloring in Bi III Bromide Complex: Anion-to-Cation Charge Transfer via Br···Br Interactions. *Chem. A Eur. J.* **2017**, *23*, 15612–15616. [CrossRef]
100. Kosaka, Y.; Yamamoto, H.M.; Nakao, A.; Tamura, M.; Kato, R. Coexistence of conducting and magnetic electrons based on molecular π-electrons in the supramolecular conductor (Me-3,5-DIP)[Ni(dmit)$_2$]$_2$. *J. Am. Chem. Soc.* **2007**, *129*, 3054–3055. [CrossRef]
101. Kusamoto, T.; Yamamoto, H.M.; Tajima, N.; Oshima, Y.; Yamashita, S.; Kato, R. Bilayer mott system based on Ni(dmit)2 (dmit = 1,3-dithiole-2-thione-4,5-dithiolate) anion radicals: Two isostructural salts exhibit contrasting magnetic behavior. *Inorg. Chem.* **2012**, *51*, 11645–11654. [CrossRef]

102. Kosaka, Y.; Yamamoto, H.M.; Tajima, A.; Nakao, A.; Cui, H.; Kato, R. Supramolecular Ni(dmit)$_2$ salts with halopyridinium cations-development of multifunctional molecular conductors with the use of competing supramolecular interactions. *CrystEngComm* **2013**, *15*, 3200–3211. [CrossRef]
103. Ren, X.; Meng, Q.; Song, Y.; Lu, C.; Hu, C.; Chen, X. Unusual magnetic properties of one-dimensional molecule-based magnets associated with a structural phase transition. *Inorg. Chem.* **2002**, *41*, 5686–5692. [CrossRef] [PubMed]
104. Fotović, L.; Stilinović, V. Evaluation of halogenopyridinium cations as halogen bond donors. *Cryst. Growth Des.* Unpublished work.
105. Degen, T.; Sadki, M.; Bron, E.; König, U.; Nénert, G. The HighScore suite. *Powder Diffr.* **2014**, *29*, S13–S18. [CrossRef]
106. CrysAlis PRO CCD. *User Inspired Software for Single Crystal X-ray Diffractometers*; Rigaku Corporation: Tokyo, Japan, 2014.
107. Manual, U. CrysAlis Pro. Power. 2010. Available online: https://www.agilent.com/cs/library/usermanuals/Public/CrysAlis_Pro_User_Manual.pdf (accessed on 17 July 2021).
108. Sheldrick, G.M. SHELXT—Integrated space-group and crystal-structure determination. *Acta Crystallogr. Sect. A Found. Crystallogr.* **2015**, *71*, 3–8. [CrossRef] [PubMed]
109. Sheldrick, G.M. Crystal structure refinement with SHELXL. *Acta Crystallogr. Sect. C Struct. Chem.* **2015**, *71*, 3–8. [CrossRef]
110. Farrugia, L.J. WinGX suite for small-molecule single-crystal crystallography. *J. Appl. Crystallogr.* **1999**, *32*, 837–838. [CrossRef]
111. Dolomanov, O.V.; Bourhis, L.J.; Gildea, R.J.; Howard, J.A.K.; Puschmann, H. OLEX2: A complete structure solution, refinement and analysis program. *J. Appl. Crystallogr.* **2009**, *42*, 339–341. [CrossRef]
112. Macrae, C.F.; Bruno, I.J.; Chisholm, J.A.; Edgington, P.R.; McCabe, P.; Pidcock, E.; Rodriguez-Monge, L.; Taylor, R.; van De Streek, J.; Wood, P.A. Mercury CSD 2.0—New features for the visualization and investigation of crystal structures. *J. Appl. Crystallogr.* **2008**, *41*, 466–470. [CrossRef]
113. STARe Software, v.15.00. *Thermal Analysis Software*; Mettler Toledo: Greifensee, Switzerland, 2016.
114. Spackman, P.R.; Turner, M.J.; McKinnon, J.J.; Wolff, S.K.; Grimwood, D.J.; Jayatilaka, D.; Spackman, M.A. CrystalExplorer: A program for Hirshfeld surface analysis, visualization and quantitative analysis of molecular crystals. *J. Appl. Crystallogr.* **2021**, *54*, 1006–1011. [CrossRef]
115. Lee, C.; Yang, W.; Parr, R.G. Development of the Colle-Salvetti correlation-energy formula into a functional of the electron density. *Phys. Rev. B.* **1988**, *37*, 785–789. [CrossRef]
116. Peverati, R.; Truhlar, D.G. An improved and broadly accurate local approximation to the exchange–correlation density functional: The MN12-L functional for electronic structure calculations in chemistry and physics. *Phys. Chem. Chem. Phys.* **2012**, *14*, 13171. [CrossRef] [PubMed]
117. Yurieva, A.G.; Poleshchuk, O.K.; Filimonov, V.D. Comparative analysis of a full-electron basis set and pseudopotential for the iodine atom in DFT quantum-chemical calculations of iodine-containing compounds. *J. Struct. Chem.* **2008**, *49*, 548–552. [CrossRef]
118. Feller, D. The role of databases in support of computational chemistry calculations. *J. Comput. Chem.* **1996**, *17*, 1571–1586. [CrossRef]
119. Gilli, G.; Gilli, P. Towards an unified hydrogen-bond theory. *J. Mol. Struct.* **2000**, *552*, S0022–S2860. [CrossRef]
120. Parr, R.G.; Chattaraj, P.K. Principle of maximum hardness. *J. Am. Chem. Soc.* **1991**, *113*, 1854–1855. [CrossRef]
121. Chattaraj, P.K.; Lee, H.; Parr, R.G. HSAB principle. *J. Am. Chem. Soc.* **1991**, *113*, 1855–1856. [CrossRef]

IV

The effect of halogen bonding on protonated hexacyanoferrate networks in hexacyanoferrates of halogenopyridines

N. Jakupec, L. Fotović i V. Stilinović,

CrystEngComm **2020**, *22*, 8142-8150. (objavljen)

Doprinos koautora:

L. Fotović – strukturna, termička i spektrokopska analiza, kristalografija, obrada rezultata i pisanje rada

N. Jakupec – sinteza i kristalizacija soli

V. Stilinović – savjetovanje i pisanje rada

Rad je reproduciran uz dozvolu Kraljevskog kremijskog društva.*

*Reproduced with permission from *CrystEngComm* **2020**, *22*, 8142-8150. Published by The Royal Society of Chemistry.

CrystEngComm

ROYAL SOCIETY OF CHEMISTRY

PAPER

View Article Online
View Journal | View Issue

Check for updates

Cite this: *CrystEngComm*, 2020, **22**, 8142

The effect of halogen bonding on protonated hexacyanoferrate networks in hexacyanoferrates of halogenopyridines†

Nikola Jakupec, Luka Fotović and Vladimir Stilinović *

In order to examine the possibility of controlling formation of hydrogen bonded hexacyanoferrous networks through combination of hydrogen and halogen bonding, seven new crystalline compounds were obtained by reacting hexacyanoferrous acid ($H_4[Fe(CN)_6]$) with seven halogenopyridines. The (protonated) halogenopyridines were present in all seven obtained solids, and the extent in which they participate in halogen bonding varied with the halogen atom (Cl, Br and I) and the geometry of the halogenopyridines (*o*-, *m*- or *p*-). Iodopyridines have been found to always form halogen bonds with the cyano groups of the anions, while neither chloropyridine used in this study was found to act as a halogen bond donor. Of the prepared solids, four comprise hydrogen bonded hexacyanoferrate networks achieved by direct binding of $H_2[Fe(CN)_6]^{2-}$ and $H_3[Fe(CN)_6]^-$ anions through [Fe–CN···H···NC–Fe] hydrogen bonds into 2D and 3D networks respectively, two are formed from $H_2[Fe(CN)_6]^{2-}$ anions bridged by water molecules, and one from $[Fe(CN)_6]^{4-}$ anions bridged by H_3O^+ cations. This variability in hydrogen bonding patterns can be brought into connection with different halogen bonding proclivities of the halopyridinium cations.

Received 18th September 2020,
Accepted 6th November 2020

DOI: 10.1039/d0ce01359e

rsc.li/crystengcomm

Published on 09 November 2020. Downloaded by University of Zagreb on 10/21/2021 3:52:05 PM.

Introduction

Prussian blue analogues have been widely studied over the past decades, as they have been shown to have numerous potential applications ranging from electrode materials,[1–7] molecular magnets,[8–15] or photoswitchable magnetic solids,[16–20] to molecular sieves,[21–23] decontaminants and antidotes for radioactive metals,[24–26] and as gas storage materials.[27–30] The majority of design strategies for such materials have been based on Lewis basicity of the polycyanometalate (such as hexacyanoferrate anions), employing them as bridging ligands to form coordination networks,[31–45] but also as hydrogen bond acceptors with organic hydrogen donors interposed between the polycyanometalate anions.[46–56]

Recently, however, we have demonstrated that a widely versatile design strategy for Prussian blue analogues (hexacyanoferrate(II) derivatives in particular) can be based on partially protonated hexacyanoferrate(II) anions acting as hydrogen bond donors.[57] This in principle leads to hydrogen bonded chains or networks (2D and 3D) of anions interconnected by symmetric [Fe–CN···H···NC–Fe] hydrogen bonds.[58–60] Of these, the most common structural motif was found to be an approximately planar 2D network of $H_2[Fe(CN)_6]^{2-}$ anions in which each anion acts as a donor and an acceptor of two [Fe–CN···H···NC–Fe] hydrogen bonds, which leaves two cyanide ligands orthogonal to the network free to form hydrogen bonds with the cations and solvent molecules on each side of the hydrogen bonded anionic layer. The crystal packing in such structures is primarily determined not only by the strength of the base used, but also by hydrogen bonding abilities and close packing of the cations and solvent molecules. Because of this, exact control of the structure, or even protonation state of the hexacyanoferrates, has proven elusive, as closely related base molecules have shown to lead to compounds of significantly different structures and stoichiometries.

A possible method for achieving a higher degree of control could be by using halogenopyridines as bases. Within each series of halogenopyridines (*o*-, *m*-, *p*-), there is very little variability of either pK_a values (Table 1), molar volumes or molecular geometries, the only significant variable which changes within a series being halogen bonding potential. In the Cambridge Structural Database,[61] there are almost three hundred datasets corresponding to salts and cocrystals comprising halogenopyridines. The majority of these (184) are salts of protonated halogenopyridinium cations, mostly involved in halogen bonding, the incidence of halogen bonding increasing from chloropyridines to iodopyridines

Department of Chemistry, Faculty of Science, University of Zagreb, Horvatovac 102a, HR-10002 Zagreb, Croatia. E-mail: vstilinovic@chem.pmf.hr

† Electronic supplementary information (ESI) available: Crystal structure determination and refinement details, ORTEP plots with atom numbering schemes, database search results, PXRD patterns, IR and thermal analyses. Single crystal X-ray diffraction data. CCDC 2031799–2031805, contain crystallographic data for this paper. For ESI and crystallographic data in CIF or other electronic format see DOI: 10.1039/d0ce01359e

This journal is © The Royal Society of Chemistry 2020

Published on 09 November 2020. Downloaded by University of Zagreb on 10/21/2021 3:52:05 PM.

Table 2 Overview of the prepared compounds

Product	Formula	HB-network type[a]
I	(**2-Clpy**)$_2$(PyH)$_2$(H$_3$O)$_2$([Fe(CN)$_6$]$^{2-}$)	**d**
II	(**2-Brpy**)$_5$(**2-BrpyH**)$_3$(H$_3$[Fe(CN)$_6$]$^{2-}$)$_3$	**b**
III	(**2-IpyH**)$_2$(H$_2$[Fe(CN)$_6$]$^{2-}$)	**a**
IV	(**3-ClpyH**)$_2$(MeOH)(H$_2$[Fe(CN)$_6$]$^{2-}$)	**a**
V	(**3-BrpyH**)$_2$(H$_2$O)$_2$(H$_2$[Fe(CN)$_6$]$^{2-}$)	**c**
VI	(**3-IpyH**)$_2$(H$_2$O)$_2$(H$_2$[Fe(CN)$_6$]$^{2-}$)	**c**
VII	(**4-IpyH**)$_2$(MeOH)(H$_2$[Fe(CN)$_6$]$^{2-}$)	**a**

[a] For definition of the hydrogen bonded network types, see Fig. 6.

(47 of total 71 structures (62%) with chloropyridines show halogen bonding, 75 out of 83 (90%) with bromopyridines, as do all (30) the structures with iodopyridines), in accord with the general trend of halogen bond potential in of the donor halogens.[62–69]

Being Lewis bases (with non-bonding electron pairs on the cyanide groups), polycyanometalates can also act as halogen bond acceptors. This has indeed been shown for hexacyanoferrates of *N*-alkylated halogenopyridine derivatives as both counterions and halogen bond donors.[70,71] Therefore, protonated halogenopyridines should also be able to form halogen bonds with hexacyanoferrate anions. As halogenopyridines are relatively weak bases (Table 1), they should yield structures comprising partially protonated hexacyanoferrate anions upon reaction with hexacyanoferric acid. Such anions will be capable of forming hydrogen bonded networks either through [Fe–CN···H···NC–Fe] hydrogen bonds or with bridging solvent molecules. Protonated halogenopyridines will be present as counterions, capable of both hydrogen and halogen bonding with the anions, similarly to their behaviour in previously studied halogenopyridinium halometallates.[72–78]

In this study, we have thus set out to investigate whether using (protonated) halogenopyridines as counterions, can indeed lead to a higher degree of control of structures of corresponding hexacyanoferrates through halogen bonding between the constituents (or absence thereof). The study involved *o*- and *m*-halogenopyridines (Cl, Br and I), as well as *p*-iodopyridine, in order to ascertain both the effect of the position and of the nature of the halogen atom.

Results and discussion

For our study seven halogenopyridines (three *o*- and *m*-halogenopyridines, and *p*-iodopyridine); (Table 1) were reacted with hexacyanoferric(II) acid (H$_4$[Fe(CN)$_6$]) (Scheme 1) in a water/methanol/ethanol solution (the halogenopyridine being in stoichiometric excess), and have yielded seven crystalline materials (Table 2).

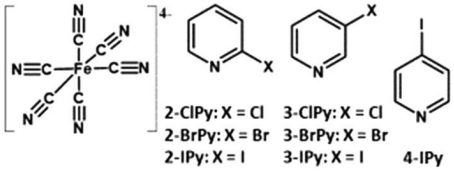

Scheme 1 Hexacyanoferrate(II) anion and halogenopyridines used in this study.

Crystal structures

The three *o*-halogenopyridines have yielded three markedly different products with considerable differences not only in structure, but also in chemical composition. *o*-Chloropyridine yielded a double salt comprised of fully deprotonated [Fe(CN)$_6$]$^{4-}$ anions and both pyridinium and oxonium (H$_3$O$^+$) cations (**I**). The hexacyanoferrate anions and oxonium cations form a 3D hydrogen bonded network with each oxonium bridging three hexacyanoferrate anions and each hexacyanoferrate bonding to six oxonium cations. The voids in this network are filled by [**2-Clpy**···H···**py**]$^+$ cations, comprising 2-chloropyridine and pyridine molecules interconnected by N···H···N hydrogen bonds of 2.85(7) Å (Fig. 1; Table 3). The presence of unsubstituted pyridine in the structure was quite surprising, as no pyridine had been added to the reaction mixture. As crystals of **I** have been obtained only after several weeks, it is probable that **2-Clpy** partially decomposed in the presence of hexacyanoferric acid over the prolonged period of time, thus forming the pyridine which eventually yielded crystals of **I**. The chlorine atoms of the [**2-Clpy**···H···**py**]$^+$ cations do not form halogen bonds with any surrounding potential acceptors, rather, the chlorine atom participates only in very long type I[79] Cl1···Cl1 contacts of 3.63(3) Å.

Unlike **2-Clpy**, **2-Brpy** yielded a crystalline product **II** within several hours. This has been shown to comprise a quasi-cubic 3D network of hydrogen bonded H$_3$[Fe(CN)$_6$]$^-$ anions (each anion acting as a donor and an acceptor of three hydrogen bonds with six neighbouring anions) with protonated and neutral **2-Brpy** filling the cavities of the network. There is a considerable excess of **2-Brpy** with respect to the expected stoichiometry – while only one protonated **2-Brpy** is needed to offset the charge of each anion, the actual ratio of **2-Brpy** and anions is 8 : 3. Half of the **2-Brpy** molecules form N11···H10···N10 hydrogen bonded [**2-Brpy**···H···**2-Brpy**]$^+$ two-molecular cations, analogous to the [**2-Clpy**···H···**py**]$^+$ cations in **I**. To each of these cations another molecule of **2-Brpy** is bonded *via* a C–H···N hydrogen bond contact (Fig. 2). The remaining **2-Brpy** molecules are

Table 1 Used pyridines with corresponding pK_a values and molar volumes

Pyridine	pK_a (pyridine)	V_m (pyridine)/cm^3 mol^{-1}
2-Clpy	0.49	94.6
2-Brpy	0.90	95.4
2-Ipy	1.82	106.3
3-Clpy	2.84	95.1
3-Brpy	2.84	96.3
3-Ipy	3.25	97.6
4-Ipy	4.06	97.6

Published on 09 November 2020. Downloaded by University of Zagreb on 10/21/2021 3:52:05 PM.

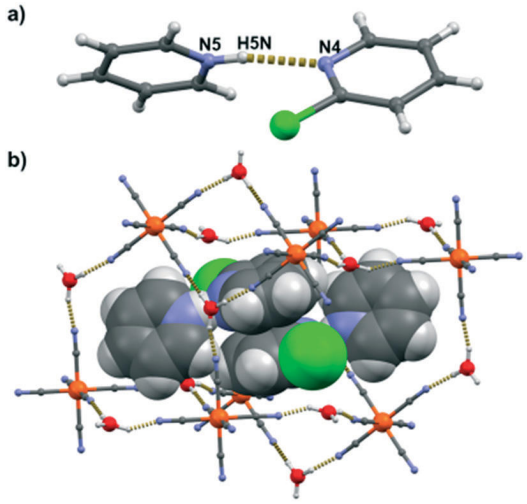

Fig. 1 Crystal structure of **I**: a) hydrogen bonded two-molecular [**2-Clpy**···H···**py**]$^+$ cations; b) a pair of [**2-Clpy**···H···**py**]$^+$ occupying a void in the $(H_3O^+)_2$ $[Fe(CN)_6]^{4-}$ hydrogen bonded network.

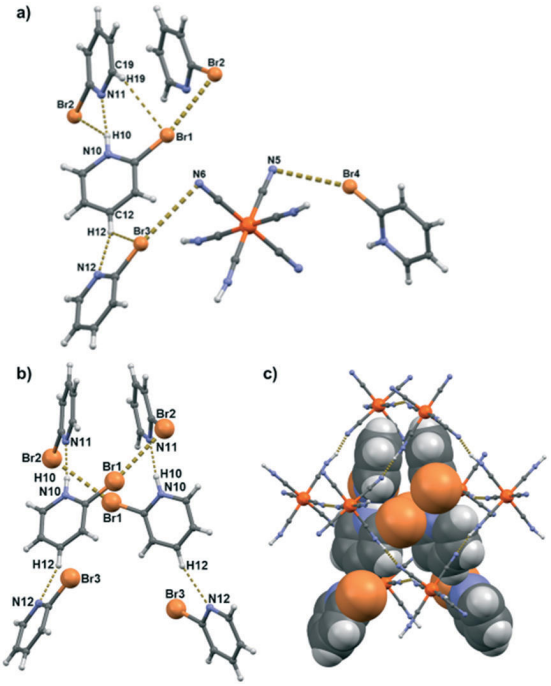

Fig. 2 Crystal structure of **II**: a) halogen and hydrogen bonding between neutral **2-Brpy** molecules, 2-**Brpy**H$^+$ cations and $H_3[Fe(CN)_6]^{2-}$ anions; b) halogen and hydrogen bonded [(**2-Brpy**)$_4$(**2-BrpyH**)$_2$]$^{2+}$ hexamers; c) [(**2-Brpy**)$_4$(**2-BrpyH**)$_2$]$^{2+}$ hexamers filling the voids in the type **b** hydrogen bonded $H_3[Fe(CN)_6]^-$ network.

severely disordered with one half of the symmetrically equivalent molecules protonated. Unlike in **I**, there are multiple halogen bonding contacts (albeit relatively long) in **II**, both the protonated and neutral **2-Brpy** molecules acting as halogen bond donors to neighbouring cyanide groups (Br4···N5 of 3.566(13) Å and Br3···N6 of 3.640(12) Å) as well as type II interhalogen contacts (Br1···Br2 of 3.55(3) Å) which interconnect pairs of [**2-Brpy**···H···**2-Brpy**]$^+$ cations, leading to the formation of [(**2-Brpy**)$_4$(**2-BrpyH**)$_2$]$^{2+}$ hexamers positioned about the C_2 symmetry axis.

Using an even stronger halogen bond donor – **2-Ipy** – yielded **III** in which the presence of the halogen bond is even more pronounced (Fig. 3a) and b)). Here the structure is layered, with 2D networks of hydrogen bonded $H_2[Fe(CN)_6]^{2-}$ anions, each anion additionally binding two **2-Ipy**H$^+$ cations in the axial positions. This places the iodine of the cation in the correct position to form a bifurcated halogen bonding contact with two cyanide ligands of the neighbouring anion. The bifurcated bond is quite asymmetric, similar to the bifurcated halogen bonds noted in cocrystals of neutral halogen bond donors with *ortho*-hydroxymethoxybenzenes.[80,81] Even though

Table 3 Halogen and hydrogen bond lengths and angles in the prepared compounds

Product	Bond (D–X···A or D–H···A)	d(X···A)/d(D–H···A) (Å)	α(D–X···A)/α(D–H···A) (°)
I	N5···H5N···N4	2.85(7)	168.8
I	C4–Cl1···Cl1	3.63(3)	143.9(2)
II	N11···H10···N10	2.720(18)	169.4
II	C12–H12···N12	3.31(2)	156.5
II	C25–Br4···N5	3.566(13)	153.7(4)
II	C20–Br3···N6	3.640(12)	157.1(5)
II	C10–Br1···Br2	3.55(3)	153.7(5)
III	C4–I1···N1	3.81(4)	152.3(1)
III	C4–I1···N2	3.60(4)	128.9(1)
IV	N7–H7N···N5	3.60(4)	167.1
IV	N8–H8N···O1	3.60(4)	171.9
IV	O1–H1···N1	3.60(4)	171.4(3)
V	C5–Br1···N1	3.16(3)	173.9(9)
V	N4–H4N···N1	2.69(3)	157.5
VI	C5–I1···N1	3.12(4)	174.3(1)
VI	N4–H4N···N1	2.71(5)	155.0
VII	N4–H4N···N1	2.77(4)	150.4
VII	O1–H1···N1	2.90(5)	127.8
VII	C6–I1···N2	3.19(3)	158.8(1)
VII	C6–I1···C2	3.55(3)	176.6(1)

 This journal is © The Royal Society of Chemistry 2020

Published on 09 November 2020. Downloaded by University of Zagreb on 10/21/2021 3:52:05 PM.

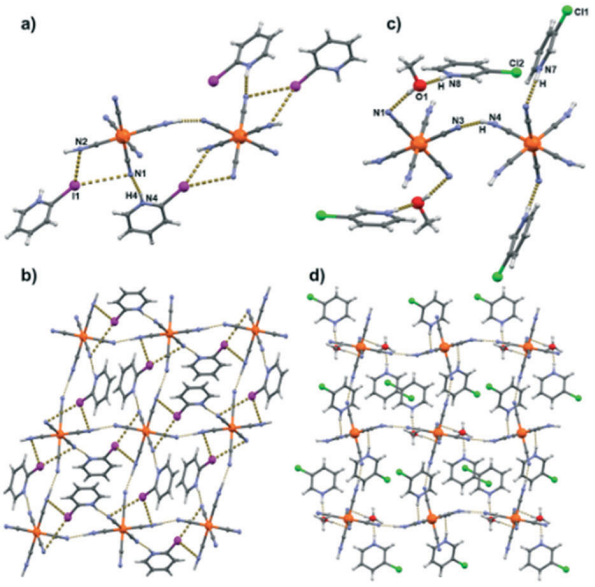

Fig. 3 Crystal structures of III and IV: a) halogen and hydrogen bonding of the anions and cations in III; b) the hydrogen bonded network of $H_2[Fe(CN)_6]^{2-}$ anions with halogen and hydrogen bonded **2-IpyH**$^+$ in III; c) hydrogen bonding of the anions, cations and solvent molecules in IV; d) the hydrogen bonded network of $H_2[Fe(CN)_6]^{2-}$ anions hydrogen bonded **3-ClpyH**$^+$ and MeOH in IV.

these halogen bonds are quite long and (expectedly) weak, the resulting effect is a slight distortion of the hydrogen bonded network of $H_2[Fe(CN)_6]^{2-}$ anions, the mean planes of the anions (defined by the cyanide groups participating in hydrogen bonds between anions) are twisted out of the mean plane of the network (at a dihedral angle of *ca.* 29°) and the network itself is not rectangular. Both these structural features also make the hydrogen bonds forming the anionic 2D network less linear.

Using *m*-halogenopyridine instead of the *o*-halogenopyridine decreases the steric hindrance to formation of halogen bonds, and could expectedly render formation of halogen bonds between cations and anions easier. In particularly, in case of structures where the anions form hydrogen bonded 2D networks (such as in **III**), the cations might act as bridges between the networks. **3-Clpy** has yielded a concomitant mixture of two phases, of which only one could be obtained in the form of single crystals suitable for X-ray diffraction experiments. This was **IV**, which indeed did comprise 2D hydrogen bonded networks of $H_2[Fe(CN)_6]^{2-}$ anions similar to that in **III** (Fig. 3c) and d)). There are two anions independent by symmetry, one of which acts as a hydrogen bond acceptor to a pair of cations, and the other to two methanol molecules which in turn bind a cation each, leading to the overall stoichiometry of (**3-ClpyH**)$_2$H$_2$[Fe(CN)$_6$]MeOH. However, of the two independent **3-ClpyH**$^+$ cations, neither chlorine atom participates in any intermolecular contacts.

3-Brpy and **3-Ipy** have yielded a pair of isostructural hydrates, **V** and **VI**. As in the **3-Clpy** derivative **IV**, the structure also comprised $H_2[Fe(CN)_6]^{2-}$ anions, however here they were not directly connected into 2D hydrogen bonded networks. Instead, water molecules have been interposed between the anions, with a pair of water molecules bridging two $H_2[Fe(CN)_6]^{2-}$ anions, each water molecule acting as an acceptor of a N–H···O and a donor of an O–H···N hydrogen bond.[82] This has lead to hydrogen bonded chains, with the remaining water hydrogen binding orthogonally to a cyanide group of an anion from the neighbouring chain, interconnecting the chains into a 2D hydrogen bonded network (Fig. 4a).

Unlike the **3-ClpyH**$^+$ in **IV**, here the cations do form halogen bonds with surrounding anions – in both **V** and **VI**, these halogen bonds are approximately orthogonal to the cyano group (CN···Br angle of *ca.* 100° in **V** and CN···I angle of *ca.* 101° in **VI**). However, they do not interconnect the hydrogen bonded layers, but rather provide additional interconnection within the layers: each cation binds to two anions from neighbouring chains (to one *via* an N–H···N hydrogen bond and the other *via* a C–X···N halogen bond; Fig. 4b) and c).

The choice of the halogenopyridine has also a significant effect on the halogen bond length, with the I1···N1 contact in **VI** being shorter (3.12(4) Å) than the corresponding Br1···N1 contact in **V** (3.15(3) Å), in spite of the larger atomic radius of iodine (which in turn corresponds to significantly larger shortening with respect to the sum of the van der Waals radii of I1···N1–11.6% – than that of Br1···N1–7.2%). The difference in the halogen bond strength also slightly affects the hydrogen bond between the cation and the anion, with the N4–H4N···N1 hydrogen bond longer (2.71(4) Å) in **VI** than the one in **V** (2.69(3) Å).

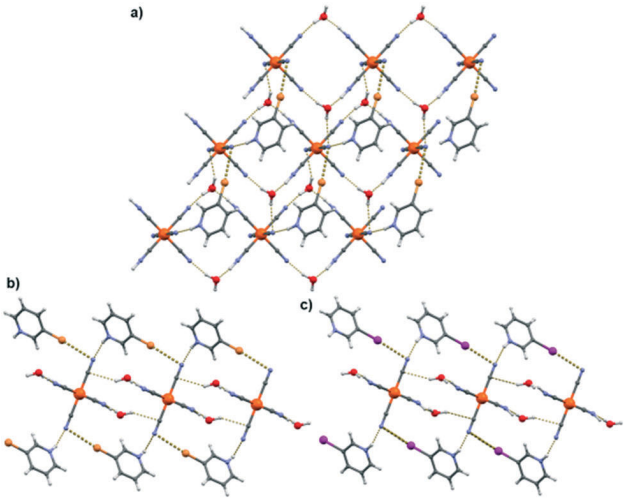

Fig. 4 Crystal structures of V and VI: a) the hydrogen bonded network of $H_2[Fe(CN)_6]^{2-}$ anions and water molecules with halogen and hydrogen bonded **3-BrpyH**$^+$ cations in V (identical as **3-IrpyH**$^+$ cations in VI); b) bridging between hydrogen bonded chains through halogen and hydrogen bonded **3-BrpyH**$^+$ cations in V; c) bridging between hydrogen bonded chains through halogen and hydrogen bonded **3-IpyH**$^+$ cations in VI.

Published on 09 November 2020. Downloaded by University of Zagreb on 10/21/2021 3:52:05 PM.

When **4-Ipy** was used as the base, a methanol solvate **VII** was obtained (Fig. 5). Similarly to **III** and **IV**, the structure comprises 2D hydrogen bonded networks of $H_2[Fe(CN)_6]^{2-}$ anions. The cyanide ligands not involved in hydrogen bonding of the anions act as acceptors of a pair of hydrogen bonds: N4–H4N···N1 of 2.77(4) Å with a protonated **4-Ipy** molecule and O1–H1···N1 of 2.90(4) Å with a solvent methanol molecule. Here, the iodine atom of the **4-IpyH**$^+$ cation participates in a halogen bonding contact with a cyanide ligand belonging to a neighbouring hydrogen bonded anion network. The halogen bond is approximately orthogonal to the cyanide group (CN···I angle of *ca.* 98°), with I1···N2 contact considerably shorter (3.19(3) Å *vs.* 3.55(3) Å), but less linear than the I1···C2 contact (C–I···N2 angle of 158.8(1) *vs.* C–I···C2 angle of 176.6(1)). This makes **VII** the only structure in which the hydrogen bonded anionic networks are bridged by halogen bonds to form a 3D structure.

General discussion

The obtained seven solids display considerably more structural variability than one might expect solely on consideration of the similarity of the reactant pyridines. There are however some regularities worth considering. The seven obtained hexacyanoferrate networks can be classified into four types (Fig. 6). Three structures (**III**, **IV** and **VII**) comprise generally the most common motif of simple 2D networks of hydrogen bonded $H_2[Fe(CN)_6]^{2-}$ anions (denoted **a** in Fig. 6). The second type (denoted **c** in Fig. 6) are the hydrogen bonded 2D networks comprising $H_2[Fe(CN)_6]^{2-}$ anions and water molecules present in **V** and **VI**. The remaining two structures exhibit 3D networks derived from the corresponding 2D networks: a pseudo-cubic network of $H_3[Fe(CN)_6]^-$ anions in **II** (**b** in Fig. 6), and a 3D network of $[Fe(CN)_6]^{4-}$ anions and oxonium cations in **I** (**d** in Fig. 6).

The largest structural diversity has been achieved among the *o*-halogenopyridine derivatives, where the three halogenopyridines yielded products not only of three distinct structural types (Table 2), but also of different stoichiometries. Among these is **II**, which is the only structure found to contain $H_3[Fe(CN)_6]^-$ anions. The 3D network **b** is obtained from the 2D network **a** by additional protonation of each anion which makes it both a donor and an acceptor of three hydrogen bonds. The high degree of protonation of the hexacyanoferrate in this structure may be brought into connection with the fact it was derived from one of the least basic pyridines used (pK_a(**2-Brpy**) = 0.90). However, this obviously cannot be the only reason, as an even weaker base (*o*-chloropyridine, pK_a(**2-Clpy**) = 0.49) yielded a structure comprising of $[Fe(CN)_6]^{4-}$ anions H_3O^+ in ratio 1 : 2 (corresponding to only two protons per anion). The deciding factor therefore seems to be the potential of the constituents

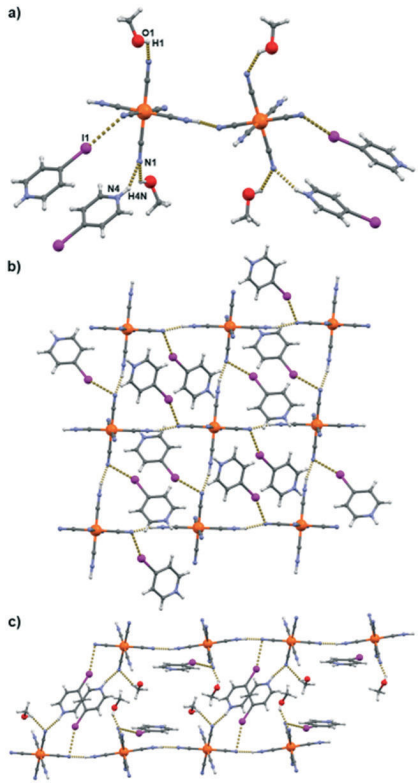

Fig. 5 Crystal structure of **VII**: a) halogen and hydrogen bonding of the anions, cations and solvent molecules; b) the hydrogen bonded network of $H_2[Fe(CN)_6]^{2-}$ anions with halogen and hydrogen bonded **4-IpyH**$^+$ cations; c) hydrogen bonded anionic hexacyanoferrate networks bridged by halogen bonds to form a 3D structure.

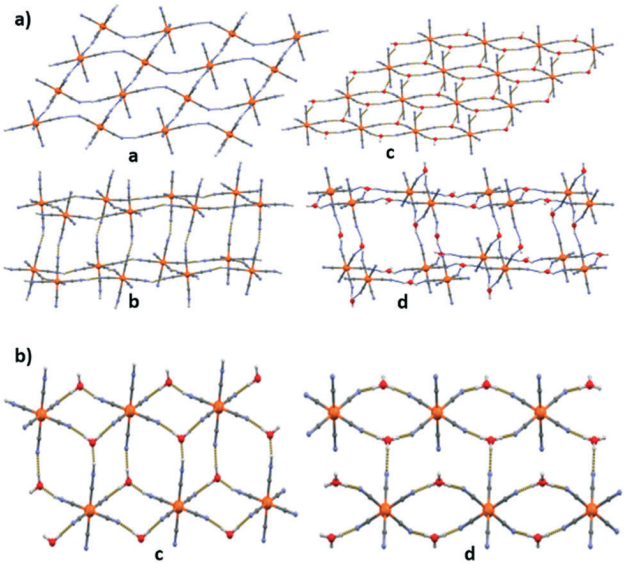

Fig. 6 a) Types of hydrogen bonded networks. Type **a**: a 2D network of hydrogen bonded $H_2[Fe(CN)_6]^{2-}$ anions, (in structures of **III**, **IV** and **VII**); type **b**: quasi-cubic 3D network of hydrogen bonded $H_3[Fe(CN)_6]^-$ anions (in **II**); type **c**: 2D networks of hydrogen bonded $H_2[Fe(CN)_6]^{2-}$ anions with bridging water molecules (**V** and **VI**); type **d**: 3D network of $[Fe(CN)_6]^{4-}$ anions bridged by H_3O^+ cations (**I**); b) comparison of hydrogen bonding patterns in type **c** hexacyanoferrate network (**V**) and in type **d** hexacyanoferrate network (in **I**). The oxonium hydrogen atoms in **d** not involved in hydrogen bonding with the neighbouring hexacyanoferrate anions bind to anions in another layer.

This journal is © The Royal Society of Chemistry 2020

Published on 09 November 2020. Downloaded by University of Zagreb on 10/21/2021 3:52:05 PM.

to form clusters of cations and neutral molecules to effectively fill the voids of hydrogen bonded (anionic) networks. Although the hydrogen bonds responsible for the formation of the networks are the strongest intermolecular interactions in both cases, the formation of a given network is not independent of the 'guest' clusters present within the network. On the one hand, the 'guest' clusters are sufficiently flexible to conform to the surrounding network, while, on the other, the network itself will form so as to accommodate the 'guest' clusters. The most significant difference between **2-Clpy** and **2-Brpy** is in their halogen bonding potential. Indeed, both protonated and neutral **2-Brpy** molecules in **II** do form halogen bonds including the Br···Br contacts responsible for formation of the $[(\mathbf{2\text{-}Brpy})_4(\mathbf{2\text{-}BrpyH})_2]^{2+}$ hexamers which fit the voids of the type **b** hexacyanoferrate network, as well as those interconnecting these hexamers with the network. The inability of **2-Clpy** to form halogen bonds prevents it from forming similar molecular clusters, and therefore the structure of **I** is markedly different from that of **II**. An additional argument for this is the fact that **2-Brpy** formed **II** almost instantly in reaction with $H_4[Fe(CN)_6]$ (indicating relatively low solubility of the product). **2-Clpy**, instead of forming an equivalent compound, yielded **I** only after a long period of time – sufficient for some of **2-Clpy** to decompose into pyridine and form an entirely different type of cationic clusters (discrete $[\mathbf{2\text{-}Clpy}\cdots H\cdots\mathbf{py}]^+$ cations), which could efficiently fill the voids of an entirely different 3D hydrogen bonded network.

The 3D network **d** (in **I**) is closely related to the layered network **c** present in **V** and **VI**. The difference between the 2D layers in **V** and **VI**, as compared to the 3D network in **I**, is that in the 2D layers the hydrogen bonds between the chains interconnect each chain only with two neighbours (leading to a 2D network) while in the network **d** each chain is interconnected through the bridging oxonium cations with four neighbours, leading to a 3D network (Fig. 6b). Also, the hydrogen bonds interconnecting the chains into the 3D structure in **I** are O–H···N hydrogen bond similar in length and angle to those within a chain, whereas in **V** and **VI** the hydrogen bonds between the chains are substantially weaker O–H···π bonds with the donor hydroxyl group orthogonal to the acceptor cyanide. This again seems to indicate the effect of the halogen bonding ability of the counterion – in **V** and **VI** the cations bind to the anion network by bridging anions from neighbouring chains through hydrogen and halogen bonds, so that each anion is an acceptor of a pair of N–H···N hydrogen bonds and C–X···N halogen bonds. The combined hydrogen and halogen bonding of the cations on either side of the 2D network thus isolates one network from its neighbours and prevents formation of a 3D network such as in **I**. This is also inferred by the structure of **III** – the only *o*-halogenopyridine derivative to form a 2D hydrogen bonded network of $H_2[Fe(CN)_6]^{2-}$ anions. Using the strongest halogen bond donor, both halogen and hydrogen bonding of the cation to the hydrogen bonded anionic layer is achieved, again insulating the layer form its neighbours and preventing the formation of a 3D structure (in spite of the low basicity of **2-Ipy**, which could be expected to favour the more protonated $H_3[Fe(CN)_6]^-$ and therefore a 2D network similar to that in **II**).

The appearance of the type **c** hydrogen bonded 2D networks, with water molecules interpolated between the $H_2[Fe(CN)_6]^{2-}$ anions, in the *m*-halogenopyridine series, could also be brought into connection with the halogen bonding proclivities of $\mathbf{3\text{-}BrpyH}^+$ and $\mathbf{3\text{-}IpyH}^+$. In both cases the protonated pyridine bridges cyano groups of neighbouring $H_2[Fe(CN)_6]^{2-}$ anions, similarly as the protonated **2-Ipy** does in the structure of **III**. Unlike in **III**, however, where the contact atoms on the cation (the N–H hydrogen and the iodine) are in the *ortho* position leading to simple 2D networks of hydrogen bonded $H_2[Fe(CN)_6]^{2-}$ anions (type **a**), in **V** and **VI** the contact atoms of the cation are in the *meta* position relative to one another. The result is an extension of the hydrogen bonded network by interpolation of water molecules between the anions, leading to an extension of the distances between the anions (8.39 and 8.48 Å in **V**; 8.41 and 8.56 Å in **VI**, as opposed to 8.20 Å in **III**). This effect of the bridging *m*-halogenopyridinium on the hydrogen bonded network is also corroborated by the structures of **IV** (where $\mathbf{3\text{-}ClpyH}^+$ forms no halogen bonds at all) and **VII** (where the $\mathbf{4\text{-}IpyH}^+$ cations form halogen and hydrogen bonds with anions from different layers) which both exhibit type **a** hydrogen bonded anion networks. The effect of $\mathbf{3\text{-}BrpyH}^+$ and $\mathbf{3\text{-}IpyH}^+$ cations is therefore similar to that of (larger) cations which form multipole hydrogen bonds with anions of the same anionic network (*e.g.* 4,4′-bipyridinium dication), which have also been found to cause intercalation of water molecules in the anionic network.[9]

Experimental

Materials and synthesis

Halogenopyridines were purchased from Acros Organics (2-chloropyridine, 2-bromopyridine, 2-iodopyridine, 3-chloropyridine), Apollo Scientific (3-bromopyridine, 4-iodopyridine) and Manchester Scientific (3-iodopyridine). The solvents were purchased from Sigma-Aldrich Company and potassium hexacyanoferrate(II) trihydrate was purchased from Kemika. All of the reagents and solvents were used as received.

Hexacyanoferrous(II) acid was prepared as described in the literature.[83] 4.2 g of potassium hexacyanoferrate(II) trihydrate was dissolved in 35 mL of water, then acidified with 10 mL of concentrated hydrochloric acid. After cooling to about 0 °C, 7 mL of diethyl ether was added to the mixture to precipitate the acid. The precipitate was dissolved in 5 mL of methanol and precipitated with another portion of diethyl ether (7 mL). Yield: 1.4 g, 65.2%.

Compound I. Diluted aqueous (3 mL) solution of hexacyanoferrous(II) acid (110 mg, 0.51 mmol) was added to the methanolic (5 mL) solution of **2-Clpy** (150 μL, 1.59

Published on 09 November 2020. Downloaded by University of Zagreb on 10/21/2021 3:52:05 PM.

mmol). After one week, **I** was isolated as several yellow-green crystals.

Compound II. Diluted aqueous (3 mL) solution of hexacyanoferrous(II) acid (110 mg, 0.51 mmol) was added dropwise to the methanolic (5 mL) solution of **2-Brpy** (250 μL, 2.62 mmol). After one day, **II** was isolated as green crystals. Yield: 258 mg, 27.3%.

Compound III. Diluted aqueous (2 mL) solution of hexacyanoferrous(II) acid (110 mg, 0.51 mmol) was added dropwise to the methanolic (5 mL) solution of **2-Ipy** (150 μL, 1.41 mmol). After one day, **III** was isolated as yellow crystals. Yield: 200 mg, 62.8%.

Compound IV. Diluted methanolic (2 mL) solution of hexacyanoferrous(II) acid (110 mg, 0.51 mmol) was added dropwise to the methanolic (5 mL) solution of **3-Clpy** (150 μL, 1.58 mmol). After 6 hours, **IV** was isolated as mixture of yellow crystals and orange powder. Yield: 187 mg.

Compound V. Diluted aqueous (2 mL) solution of hexacyanoferrous(II) acid (110 mg, 0.51 mmol) was added dropwise to the methanolic (5 mL) solution of **3-Brpy** (150 μL, 1.56 mmol). After one day, **V** was isolated as green crystals. Yield: 167 mg, 57.6%.

Compound VI. Diluted ethanolic (4 mL) solution of hexacyanoferrous(II) acid (110 mg, 0.51 mmol) was added dropwise to the ethanolic (2 mL) solution of **3-Ipy** (250 mg, 1.22 mmol). After one day, **VI** was isolated as green crystals. Yield: 217 mg, 64.3%.

Compound VII. Diluted methanolic (3 mL) solution of hexacyanoferrous(II) acid (110 mg, 0.51 mmol) was added dropwise to the methanolic (6 mL) solution of **4-Ipy** (250 mg, 1.22 mmol) and refrigerated at approximately 4 °C. After two weeks, **VII** was isolated as several orange crystals.

X-ray diffraction measurements

Single crystal X-ray diffraction experiments were performed using an Oxford Diffraction Xcalibur Kappa CCD X-ray diffractometer with graphite-monochromated MoKα (λ = 0.71073 Å) radiation. The data sets were collected using the ω-scan mode over the 2θ—range up to 54°. Programs CrysAlis CCD and CrysAlis RED were employed for data collection, cell refinement, and data reduction.[84,85] The structures were solved by direct methods and refined using the SHELXS (version 2013, Göttingen, Germany) and SHELXL programs (version 2013, Göttingen, Germany), respectively.[86,87] The structural refinement was performed on F^2 using all data. The hydrogen atoms were placed in calculated positions and treated as riding on their parent atoms [C–H = 0.93 Å and U_{iso}(H) = 1.2 U_{eq}(C); C–H = 0.97 Å and U_{iso}(H) = 1.2 U_{eq}(C)]. All calculations were performed using the WinGX crystallographic suite of programs.[88] The figures were prepared using Mercury (version 4.3.1).[89] Crystallographic data of the prepared compounds are shown in Table S1 in ESI.†

Powder X-ray diffraction (XRPD) experiments on the samples were performed on a PHILIPS PW 1840 X-ray diffractometer (Philips Analytical, Almelo, The Netherlands) with CuKα_1 (1.54056 Å) radiation at 40 mA and 40 kV. The scattered intensities were measured with a scintillation counter. The angular range was from 5° to 45° (2θ) with a continuous step size of 0.02° and measuring a time of 0.5 s per step. Data collection was performed using the program package Philips X'Pert (version 1.3e),[90] and analysed in X'Pert HighScore plus (version 2.2).[91] Comparisons of the measured and calculated diffractograms for cocrystals are shown in Fig. S8–S14 in the ESI.†

Thermal analysis

Thermogravimetric (TG) and differential scanning calorimetry (DSC) measurements were performed on a Mettler-Toledo TGA/DSC 3+ module. Samples were placed in 70 μL alumina crucibles and heated from 25 to 600 °C, at a rate of 10 °C min^{-1} under nitrogen flow of 50 mL min^{-1}.

Data collection and analysis were performed using the program package STARe software (version 15.00)[92] TG and DSC thermograms of the prepared compounds are shown in Fig. S15–S18 in ESI.†

Conclusion

The considerable variability in compositions and structures of the obtained products makes the proposed control of the crystal structures of hexacyanoferrates through halogen bonding seem somewhat dubious.

As chloropyridines were not found to participate in halogen bonding, the differences in structures (and compositions) between the chloropyridine derivatives and structures derived from bromo- and iodopyridines could be ascribed to the effects of halogen bonding. In the (sterically unfavourable) *o*-halogenopyridine series only the strongest halogen bond donor – *o*-iodopyridine – formed a complex with the expected C–X$\cdots$N$_{cyano}$ halogen bonds, while in the *m*-halogenopyridine series, where the halogenopyridinium donor geometry is more favourable, only the weakest donor (*m*-chloropyridine) formed a structure without a halogen bond between the cations and the hexacyanoferrate anions. The two stronger halogen bond donors not only formed isostructural **V** and **VI** in which halogen bonding was present, but have also shown that the selection of the halogen bond donor (stronger iodine *vs.* weaker bromine) can indeed (although only in some cases) be used for fine-tuning the geometry of hexacyanoferrate hydrogen bonded networks.

Conflicts of interest

There are no conflicts to declare.

Acknowledgements

This research was supported by the Croatian Science Foundation under the project IP-2019-04-1868.

 This journal is © The Royal Society of Chemistry 2020

Published on 09 November 2020. Downloaded by University of Zagreb on 10/21/2021 3:52:05 PM.

Notes and references

1 C. D. Wessells, R. A. Huggins and Y. Cui, *Nat. Commun.*, 2011, **2**, 550.
2 Y. Lu, L. Wang, J. Cheng and J. B. Goodenough, *Chem. Commun.*, 2012, **48**, 6544–6546.
3 P. Nie, L. Shen, H. Luo, B. Ding, G. Xu, J. Wang and X. Zhang, *J. Mater. Chem. A*, 2014, **2**, 5852–5857.
4 M. Pasta, C. D. Wessells, N. Liu, J. Nelson, M. T. McDowell, R. A. Huggins, M. F. Toney and Y. Cui, *Nat. Commun.*, 2014, **5**, 3007.
5 H.-W. Lee, R. Y. Wang, M. Pasta, S. W. Lee, N. Liu and Y. Cui, *Nat. Commun.*, 2014, **5**, 5280.
6 Y. You, X.-L. Wu, Y.-X. Yin and Y.-G. Guo, *Energy Environ. Sci.*, 2014, **7**, 1643–1647.
7 P. Canepa, G. S. Gautam, D. C. Hannah, R. Malik, M. Liu, K. G. Gallagher, K. A. Persson and G. Ceder, *Chem. Rev.*, 2017, **117**, 4287–4341.
8 S. Ferlay, T. Mallah, R. Ouahes, P. Veillet and M. Verdaguer, *Nature*, 1995, **378**, 701–703.
9 M. Ohba, H. Ōkawa, N. Fukita and Y. Hashimoto, *J. Am. Chem. Soc.*, 1997, **119**, 1011–1019.
10 M. Ohba, N. Usuki, N. Fukita and H. Ōkawa, *Angew. Chem., Int. Ed.*, 1999, **38**, 1795–1798.
11 M. Verdaguer, A. Bleuzen, V. Marvaud, J. Vaissermann, M. Seuleiman, C. Desplanches, A. Scuiller, C. Train, R. Garde, G. Gelly, C. Lomenech, I. Rosenman, P. Veillet, C. Cartier and F. Villain, *Coord. Chem. Rev.*, 1999, **190–192**, 1023–1047.
12 M. Ohba and H. Ōkawa, *Coord. Chem. Rev.*, 2000, **198**, 313–328.
13 C.-M. Liu, S. Gao, H.-Z. Kou, D.-Q. Zhang, H.-L. Sun and D.-B. Zhu, *Cryst. Growth Des.*, 2006, **6**, 94–98.
14 X.-Y. Wang, C. Avendaño and K. R. Dunbar, *Chem. Soc. Rev.*, 2011, **40**, 3213–3238.
15 E. Coronado and G. M. Espallargas, *Chem. Soc. Rev.*, 2013, **42**, 1525–1539.
16 O. Sato, T. Iyoda, A. Fujishima and K. Hashimoto, *Science*, 1996, **272**, 704–705.
17 S. Ohkoshi, Y. Einaga, A. Fujishima and K. Hashimoto, *J. Electroanal. Chem.*, 1999, **473**, 245–249.
18 Y. Zhang, D. Li, R. Clerac, M. Kalisz, C. Mathoniére and S. M. Holmes, *Angew. Chem., Int. Ed.*, 2010, **49**, 3752–3756.
19 Y.-Z. Zhang, P. Ferko, D. Siretanu, R. Ababei, N. P. Rath, M. J. Shaw, R. Clerac, C. Mathoniére and S. M. Holmes, *J. Am. Chem. Soc.*, 2014, **136**, 16854–16864.
20 L.-Z. Cai, Q.-S. Chen, C.-J. Zhang, P.-X. Li, M.-S. Wang and G.-C. Guo, *J. Am. Chem. Soc.*, 2015, **137**, 10882–10885.
21 J. Kuyper and G. Boxhoorn, *J. Catal.*, 1987, **105**, 163–174.
22 J. Balmaseda, E. Reguera, J. Rodríguez-Hernandez, L. Reguera and M. Autie, *Microporous Mesoporous Mater.*, 2006, **96**, 222–236.
23 D. Maspoch, D. Ruiz-Molina and J. Veciana, *Chem. Soc. Rev.*, 2007, **36**, 770–818.
24 V. Nigrovic, *Phys. Med. Biol.*, 1965, **10**, 81–91.
25 H. H. Kamerbeek, A. G. Rauws, M. ten Ham and A. N. P. van Heijst, *Acta Med. Scand.*, 1971, **189**, 321–324.
26 D. Parajuli, A. Takahashi, H. Noguchi, A. Kitajima, H. Tanaka, M. Takasaki, K. Yoshino and T. Kawamoto, *Chem. Eng. J.*, 2016, **283**, 322–1328.
27 S. S. Kaye and J. R. Long, *J. Am. Chem. Soc.*, 2005, **127**, 6506–6507.
28 L. J. Murray, M. Dincă and J. R. Long, *Chem. Soc. Rev.*, 2009, **38**, 1294–1314.
29 M. P. Suh, H. J. Park, T. K. Prasad and D.-W. Lim, *Chem. Rev.*, 2012, **112**, 782–835.
30 A. Takahashi, H. Tanaka, D. Parajuli, T. Nakamura, K. Minami, Y. Sugiyama, Y. Hakuta, S. Ohkoshi and T. Kawamoto, *J. Am. Chem. Soc.*, 2016, **138**, 6376–6379.
31 M. Ohba, N. Usuki, N. Fukita and H. Ōkawa, *Inorg. Chem.*, 1998, **37**, 3349–3354.
32 A. Yuan, J. Zou, B. Li, Z. Zha, C. Duan, Y. Liu, Z. Xu and S. Keizer, *Chem. Commun.*, 2000, 1297–1298.
33 J. Larionova, R. Clérac, B. Donnadieu, S. Willemin and C. Guérin, *Cryst. Growth Des.*, 2003, **3**, 267–272.
34 C. J. Shorrock, H. Jong, R. J. Batchelor and D. B. Leznoff, *Inorg. Chem.*, 2003, **42**, 3917–3924.
35 R. Koner, M. Nayak, G. Ferguson, J. N. Low, C. Glidewell, P. Misra and S. Mohanta, *CrystEngComm*, 2005, **7**, 129–132.
36 B. Sieklucka, R. Podgajny, P. Przychodzen and T. Korzeniak, *Coord. Chem. Rev.*, 2005, **249**, 2203–2221.
37 P. Przychodzen, T. Korzeniak, R. Podgajny and B. Sieklucka, *Coord. Chem. Rev.*, 2006, **250**, 2234–2260.
38 W.-T. Chen, M.-S. Wang, L.-Z. Cai, G. Xu, T. Akitsu, M. Akita-Tanaka, G.-C. Guo and J.-S. Huang, *Cryst. Growth Des.*, 2006, **6**, 1738–1741.
39 Z.-X. Wang, P. Zhang, X.-F. Shen, Y. Song, X.-Z. You and K. Hashimoto, *Cryst. Growth Des.*, 2006, **6**, 2457–2462.
40 M. J. Katz, H. Kaluarachchi, R. J. Batchelor, G. Schatte and D. B. Leznoff, *Cryst. Growth Des.*, 2007, **7**, 1946–1948.
41 J.-R. Li, W.-T. Chen, M.-L. Tong, G.-C. Guo, Y. Tao, Q. Yu, W.-C. Song and X.-H. Bu, *Cryst. Growth Des.*, 2008, **8**, 2780–2792.
42 A.-H. Yuan, R.-Q. Lu, H. Zhou, Y.-Y. Chen and Y.-Z. Li, *CrystEngComm*, 2010, **12**, 1382–1384.
43 R. Mittal, M. Zbiri, H. Schober, S. N. Achary, A. K. Tyagi and S. L. Chaplot, *J. Phys.: Condens. Matter*, 2012, **24**, 505404.
44 B. Nowicka, T. Korzeniak, O. Stefańczyk, D. Pinkowicz, S. Chorązy, R. Podgajny and B. Sieklucka, *Coord. Chem. Rev.*, 2012, **256**, 1946–1971.
45 S. Ferlay, P. Dechambenoit, N. Kyritsakas and M. W. Hosseini, *Dalton Trans.*, 2013, **42**, 11661–11671; J. A. Hill, A. L. Thompson and A. L. Goodwin, *J. Am. Chem. Soc.*, 2016, **138**, 5886–5896.
46 S. Ferlay, P. Dechambenoit, N. Kyritsakas and M. W. Hosseini, *Dalton Trans.*, 2013, **42**, 11661–11671.
47 S. Ferlay, V. Bulach, O. Felix, M. W. Hosseini, J. M. Planiex and N. Kyritsakas, *CrystEngComm*, 2002, **4**, 447–453.
48 M. W. Hosseini, *Coord. Chem. Rev.*, 2003, **240**, 157–166.
49 M. W. Hosseini, *Acc. Chem. Res.*, 2005, **38**, 313–323.
50 P. Dechambenoit, S. Ferlay and M. W. Hosseini, *Cryst. Growth Des.*, 2005, **5**, 2310–2312.

Published on 09 November 2020. Downloaded by University of Zagreb on 10/21/2021 3:52:05 PM.

51 P. Dechambenoit, S. Ferlay, M. W. Hosseini, J.-M. Planeix and N. Kyritsakas, *New J. Chem.*, 2006, **30**, 1403–1410.
52 P. Dechambenoit, S. Ferlay, M. W. Hosseini and N. Kyritsakas, *Chem. Commun.*, 2007, 4626–4628.
53 P. Dechambenoit, S. Ferlay, N. Kyritsakas and M. W. Hosseini, *J. Am. Chem. Soc.*, 2008, **130**, 17106–17113.
54 P. Dechambenoit, S. Ferlay, B. Donnio, D. Guillon and M. W. Hosseini, *Chem. Commun.*, 2011, **47**, 734–736.
55 P. Dechambenoit, S. Ferlay, N. Kyritsakas and M. W. Hosseini, *CrystEngComm*, 2011, **13**, 1922–1930.
56 A. Hazra, K. L. Gurunatha and T. K. Maji, *Cryst. Growth Des.*, 2013, **13**, 4824–4836.
57 I. Cvrtila and V. Stilinović, *Cryst. Growth Des.*, 2017, **17**(12), 6793–6800.
58 R. Tanaka, A. Okazawa, N. Kojima and N. Matsushita, *Org. Lett.*, 2018, **47**, 697–699.
59 S. I. Gorelsky, A. B. I. Lyukhin, P. V. Kholin, V. Y. Kotov, B. V. Lokshin and N. V. Sapoletova, *Inorg. Chim. Acta*, 2007, **360**, 2573–2582.
60 P. Xydias, S. Lymperopoulou, V. Dokorou, M. Manos and J. C. Plakatouras, *Polyhedron*, 2019, **157**, 341–357.
61 C. R. Groom, I. J. Bruno, M. P. Lightfoot and S. C. Ward, *Acta Crystallogr., Sect. B: Struct. Sci., Cryst. Eng. Mater.*, 2016, **72**, 171.
62 G. Cavallo, P. Metrangolo, R. Milani, T. Pilati, A. Priimagi, G. Resnati and G. Terraneo, *Chem. Rev.*, 2016, **116**, 2478–2601.
63 V. Stilinović, G. Horvat, T. Hrenar, V. Nemec and D. Cinčić, *Chem. – Eur. J.*, 2017, **23**, 5244–5257.
64 R. W. Troff, T. Makelä, F. Topić, A. Valkonen, K. Raatikainen and K. Rissanen, *Eur. J. Org. Chem.*, 2013, **2013**, 1617–1637.
65 C. B. Aakeroy, M. Baldrighi, J. Desper, P. Metrangolo and G. Resnati, *Chem. – Eur. J.*, 2013, **19**, 16240–16247.
66 C. B. Aakeröy, T. K. Wijethunga, M. A. Haj, J. Desper and C. Moore, *CrystEngComm*, 2014, **16**, 7218–7225.
67 K. Lisac, F. Topić, M. Arhangelskis, S. Cepić, P. A. Julien, C. W. Nickels, A. J. Morris, T. Friščić and D. Cinčić, *Nat. Commun.*, 2019, **10**, 61.
68 L. Fotović and V. Stilinović, *CrystEngComm*, 2020, **22**, 4039–4046.
69 V. Nemec, L. Fotović, T. Vitasović and D. Cinčić, *CrystEngComm*, 2019, **21**, 3251–3255.
70 S. Derossi, L. Brammer, C. A. Hunter and M. D. Ward, *Inorg. Chem.*, 2009, **48**, 1666–1677.
71 J. E. Ormond-Prout, P. Smart and L. Brammer, *Cryst. Growth Des.*, 2012, **12**, 205–216.
72 G. M. Espallargas, F. Zordan, L. A. Marín, H. Adams, K. Shankland, J. van de Streek and L. Brammer, *Chem. – Eur. J.*, 2009, **15**, 7554–7568.
73 F. Zordan, S. L. Purver, H. Adamsa and L. Brammer, *CrystEngComm*, 2005, **7**, 350–354.
74 F. F. Awwadi, D. Taher, S. F. Haddad and M. M. Turnbull, *Cryst. Growth Des.*, 2014, **14**, 1961–1971.
75 I. D. Gorokh, S. A. Adonin, A. S. Novikov, A. N. Usoltsev, P. E. Plyusnin, I. V. Korolkov, M. N. Sokolov and V. P. Fedin, *Polyhedron*, 2019, **166**, 137–140.
76 R. D. Willett, F. Awwadi, R. Butcher, S. Haddad and B. Twamley, *Cryst. Growth Des.*, 2003, **3**(3), 301–311.
77 F. Zordan, G. Mínguez Espallargas and L. Brammer, *CrystEngComm*, 2006, **8**, 425–431.
78 G. Mínguez Espallargasa, L. Brammer and P. Sherwood, *Angew. Chem., Int. Ed.*, 2006, **45**, 435–440.
79 P. Metrangolo and G. Resnati, *IUCrJ*, 2014, **1**, 5–7.
80 M. Zbačnik, M. Pajski, V. Stilinović, M. Vitković and D. Cinčić, *CrystEngComm*, 2017, **19**, 5576–5582.
81 A. Carletta, M. Zbačnik, M. Vitković, N. Tumanov, V. Stilinović, J. Wouters and D. Cinčić, *CrystEngComm*, 2018, **20**, 5332–5339.
82 The proton positions have been assigned according to the maxima in the electron difference map, which seem to indicate that in **I** proton transfer along the N···H···O hydrogen bond had occurred (leading to fully deprotonated $[Fe(CN)_6]^{4-}$ anions hydrogen bonded to oxonium cations), while in **V** and **VI** it has not (the structures comprising $H_2[Fe(CN)_6]^{2-}$ anions and water molecules). Such difference seems somewhat counterintuitive, as the bonding network in **I** as well as **V** and **VI** is almost identical. Taking into consideration pK_a values of hexacyanoferric(II) acid (pK_{a3} = 2.2 ± 0.2; pK_{a4} = 4.17 ± 0.02; M. T. Beck, *Pure & Appl. Chem.* 1987, **59**, 1703–1720), $H_2[Fe(CN)_6]^{2-}$ anions should be expected more likely to be present (as are $H[Fe(CN)_6]^{3-}$) than $[Fe(CN)_6]^{4-}$. It is possible therefore that there is some proton disorder (only partial proton transfer along the N···H···O hydrogen bond) in **I**.
83 G. Brauer, *Handbook of Preparative Inorganic Chemistry*, Academic Press, New York, 2nd edn, 1963, vol. 1, p. 1509.
84 CrysAlis CCD, *V171.34, Oxford Diffraction 2003*, Oxford Diffraction Ltd., Abingdon, UK, 2003.
85 CrysAlis RED, *V171.34, Oxford Diffraction 2003*, Oxford Diffraction Ltd., Abingdon, UK, 2003.
86 G. M. Sheldrick, *Acta Crystallogr., Sect. A: Found. Crystallogr.*, 2008, **64**, 112–122.
87 G. M. Sheldrick, *Acta Crystallogr., Sect. A: Found. Adv.*, 2015, **71**, 3–8.
88 L. J. Farrugia, *J. Appl. Crystallogr.*, 1999, **32**, 837.
89 C. F. Macrae, I. J. Bruno, J. A. Chisholm, P. R. Edgington, P. McCabe, E. Pidcock, L. Rodriguez-Monge, R. Taylor, J. van de Streek and P. A. Wood, *J. Appl. Crystallogr.*, 2008, **41**, 466–470.
90 *Philips X'Pert Data Collector 1.3e; Philips X'Pert Graphics & Identify 1.3e; Philips X'Pert Plus 1.0*, Philips Analytical B.V., Lelyweg, The Netherlands, 1999.
91 T. Degen, M. Sadki, E. Bron, U. König and G. Nénert, The highScore suite, *Powder Diffr.*, 2014, **29**, S13–S18.
92 *STARe Software, v.15.00*, Mettler Toledo, Greifensee, Switzerland, 2016.

 This journal is © The Royal Society of Chemistry 2020

§ 3. RASPRAVA

3.1. Kationi kao donori halogenske veze

Kao kationski donori halogenske veze do sada su proučavane dvije skupine spojeva: halogenirani primarni aromatski amini[62–65] i halogenirani *N*-heterocikli i njihovi derivati.[66–97] Halogenirani *N*-heterocikli (halogenpiridini i halogenimidazoli) logičan su izbor za sintezu kationskih donora halogenske veze zato što se lako se mogu prevesti u katione bilo *N*-protoniranjem bilo *N*-alkiliranjem, a osim toga zbog svoje rigidne strukture pružaju mogućnost predvidljivosti i ugađanja geometrije halogenskih veza u kojima sudjeluju.

Tijekom zadnjih 20-ak godina protonirani i metilirani halogenpiridini proučavaju se kao donori halogenske veze u sustavima gdje stvaraju veze s organskim (npr. saharinat[66] i bromanilat[67]) i anorganskim anionima (halogenidi,[68–73] halogenmetalati,[74–84] cijanometalati,[85–87] itd.). Kemijske vrste koje sadrže jodpiridinijeve ogranke uspješno se koriste pri dizajnu anionskih receptora[88–92] i kao katalizatori pri ekstrakciji halogenidnih aniona.[93] U $Ni(dmit)_2$ (dmit = 1,3-ditiol-2-tion-4,5-ditiolat) solima, koje se proučavaju kao supramolekulski vodiči, *N*-alkilirani halogenpiridinijevi kationi koriste se kao protuioni upravo zbog njihove mogućnosti ostvarivanja višestrukih vodikovih i halogenskih veza što se koristi kako bi se ugodila vodljiva i magnetska svojstva ovih materijala.[94–97]

Iako postoji mnoštvo literaturnih zapisa o proučavanju i upotrebi halogenpiridinijevih kationa, prije početka istraživanja u okviru ove disertacije nisu postojala sustavna istraživanja koja bi evaluirala njihov potencijal kao donora halogenske veze te ih usporedila s klasičnim neutralnim donorima kao što su razni halogenirani perfluorirani ugljikovodici.

Upravo zbog gorenavedenog u okviru ove disertacije istraživane su halogenidne soli halogenpiridinijevih kationa kao kombinacija najjednostavnijih kationskih donora i anionskih akceptora halogenske veze što je polučilo 4 publikacije u kojima je evaluiran njihov potencijal i svojstva kao donora halogenske veze i uspoređen s klasičnim neutralnim donorima.

3.2. *N*-protonirani halogenpiridinijevi kationi kao donori halogenske i vodikove veze u jodpiridinijevim halogenidima

Kako u zadnje vrijeme u području supramolekulske kemije i kristalnog inženjerstva, uz brojna istraživanja vodikove veze, raste interes i za proučavanjem halogenske veze tako se i halogenidni anioni sve više proučavaju kao akceptori halogenske veze. Usporede li se afiniteti halogenidnih aniona prema sudjelovanju u vodikovoj odnosno halogenskoj vezi, može se uočiti da u slučaju vodikove veze afinitet pada s porastom veličine aniona ($F^- > Cl^- > Br^- > I^-$) dok u slučaju halogenske veze u literaturi postoji mnogo primjera ostavrenih halogenskih veza s jodidnim anionom kao akceptorom, dok su s fluoridnim anionom vrlo rijetke (Slika 2).[a] Navedeno upućuje na to da se afinitet halogenidnih aniona za halogensku vezu mijenja obrnuto ($I^- > Br^- > Cl^- > F^-$) što je u skladu s principom tvrdih i mekih kiselina i baza (*eng*. hard and soft acid and base – HSAB)[89,98,99] – σ-šupljina donornog atoma halogena je *meka* Lewisova kiselina pa će preferirati vezanje *najmekše* baze među halogenidima – jodidnog aniona.[36,100,101]

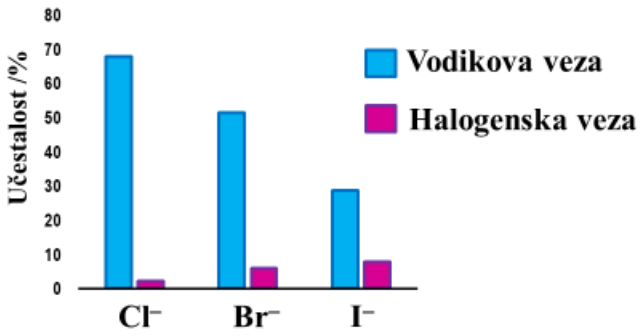

Slika 2. Učestalost sudjelovanja halogenidnih aniona u halogenskim i vodikovim vezama prema podacima iz kristalografske baze *The Cambridge Structural Database* (CSD).

[a] Pretragom baze CSD[107] na temelju motiva kokristala halogenidnih soli s perfluoriranim jodbenzenima nađeno je 50 kristalnih struktura s jodidima, 30 s bromidima, 27 s kloridima i 0 s fluoridima.

S druge pak strane postoje istraživanja u kojima je pokazano da se energije halogenskih veza s halogenidnim anionima mijenjaju na isti način kao i energije vodikovih veza, odnosno da energija veza pada s porastom veličine halogenida ($F^- > Cl^- > Br^- > I^-$).[102,103] Mogući razlog za pojavu ovakva dva oprečna trenda je međusobna kompeticija halogena i vodika za vezanje halogenidnih aniona. Jones i suradnici odredili su strukture 4-halogenpiridinijevih halogenida (4-klorpridinijevog klorida, 4-brompiridinijevog bromida i 4-jodpiridinijevog jodida) u kojima s porastom veličine halogenidnog aniona vodikove veze postaju relativno duže, dok halogenske veze postaju relativno kraće.[72] Berryman i suradnici odredili su konstante vezanja (u smjesi CD_3NO_2 i $CDCl_3$) halogenida na (izostrukturne) anionske receptore koji u jednom slučaju vežu halogenidni anion halogenskom vezom, a u drugom vodikovom vezom. Ustanovili su da receptor koji je donor halogenske veze preferira veće halogene, dok receptor koji je donor vodikove veze preferira manje halogene.[90] Isti trend uočili su García i suradnici prilikom izučavanja hidrata *N*,*N*-bis(4-jodbenzil)-4,4-bipiridinijevih halogenida u kojima su halogenske veze bile relativno kraće s bromidom kao akceptorom, dok su vodikove veze bile relativno kraće s kloridnim anionom.[104] Najnoviju sistematičnu studiju objavili su Bryce i suradnici koji su kombinacijom difrakcijskih i NMR ekperimenata izučili 2- i 3-(jodetinil)-piridinijeve halogenide u kojima su (jodetinil)-piridinijevi kationi istovremeno donori i vodikove i halogenske veze.[105]

S obzirom da postoji relativno malo literaturnih zapisa o proučavanju suodnosa i kompeticije vodikove i halogenske veze pri vezanju halogenidnih aniona u sklopu ove disertacije provedeno je istraživanje na još jednostavnijem sustavu – jodpiridinijevim halogenidima. Ovo istraživanje objavljeno je u redu **I**.

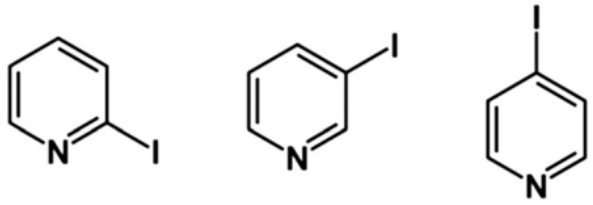

Shema 1. Jodpiridini korišteni za sintezu halogenidnih soli.

Kristalizacijskim eksperimentima tri monojodpiridina uspješno je priređeno svih 9 jednostavnih (1 : 1) jodpiridinijevih halogenida (klorida, bromida i jodida) u čijim se strukturama kationi i

anioni povezuju halogenskim vezama C–I···X⁻ i vodikovim vezama N–H···X⁻. Prostorni raspored kationa i aniona u strukturama priređenih soli prvenstveno ovisi o geometriji jodpiridinijevog kationa, preciznije o kutu između kovalentnih veza kojima su na kation vezani donor halogenske (C–I) i vodikove veze (N–H).

U slučaju *o*-jodpiridina, sve tri halogenidne soli u svojim strukturama sadrže lance sastavljene od alternirajućih kationa i aniona povezanih halogenskim vezama C–I···X⁻ i vodikovim vezama N–H···X⁻. (Slika 3) Lanci se dalje povezuju kontaktima C–H···Cl⁻ i C–H···I u slojeve u slučaju *o*-jodpiridinijevog klorida, odnosno kontaktima C–H···X⁻ u trodimenzijske mreže u slučaju bromida i jodida. Halogenske veze C–I···X⁻ u *o*-jodpiridinijevim halogenidima kraće su od sume van der Waalsovih radijusa oko 17% i gotovo linearne s vrijednostima kuteva oko 175°. U slučaju vodikovih veza N–H···X⁻ uočen je očekivani blagi pad u relativnom skraćenju istih od oko 11% s kloridnim anionom prema 8% s jodidnim anionom. Osim što su relativna skraćenja za vodikovu vezu manja nego za halogensku, i kutevi φ(N–H···X⁻) su manje linerani također opadajući od 173° u slučaju klorida prema 165° u slučaju jodida.

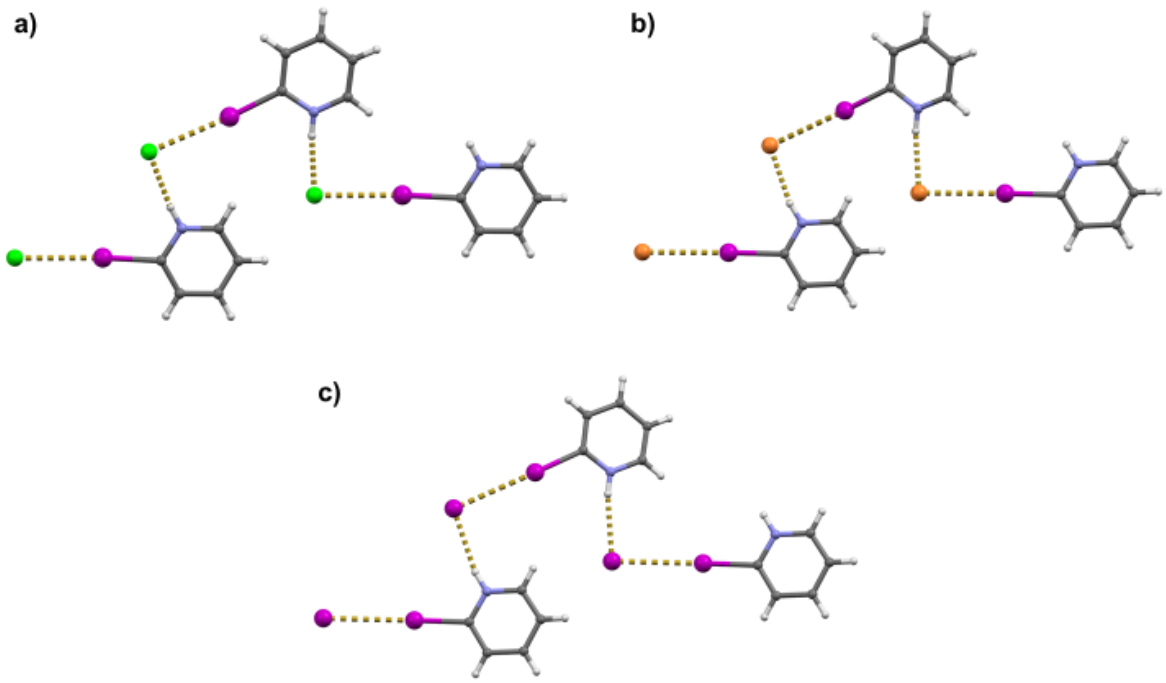

Slika 3. Kationi i anioni povezani halogenskim i vodikovim vezama u lance u strukturi: a) **2-IPy**HCl; b) **2-IPy**HBr; c) **2-IPy**HI.

Prilikom sinteze halogenidnih soli *m*-jodpiridina dobiveni su izostrukturni bromid i jodid koji u strukturi sadrže centrosimetrične cikličke tetramere kationa i aniona povezanih halogenskim vezama C–I···X^- (Slika 4). Halogenske veze opet su poprilično kratke i linearne (≈ 15,5% kraće su od sume van der Waalsovih radijusa, φ(C–I···X^-) kutevi ≈ 175°), dok su vodikove veze N–H···X^- duže i savijenije nego u slučaju *o*-jodpiridinijevih halogenida (≈ 6% kraće su od sume van der Waalsovih radijusa, kutevi φ(N–H···X^-) ≈ 145°) što je vrlo lijep pokazatelj kako su geometrije vodikovih veza punu fleksibilnije od geometrije halogenskih veza. U strukturi *m*-jodpiridinijevog klorida kationi i anioni nisu povezani u tetramere nego u lance slične onima u strukturama *o*-jodpiridinijevih halogenida. Od ostalih *m*-jodpiridinijevih halogenida također se razlikuju i po geometriji halogenskih i vodikovih veza; halogenska veza C–I···Cl^- je savijenija (φ(C–I···Cl^-) kutevi ≈ 172°), a vodikova veza N–H···Cl^- linearnija (φ(N–H···Cl^-) ≈ 145°). Zanimljivo je da se sinteza *m*-jodpiridinijevog klorida morala provoditi u apsolutno bezvodnim uvjetima jer se u protivnom dobivao hidrat željene soli vrlo sličan literaturno poznatom etanolnom solvatu iste soli.

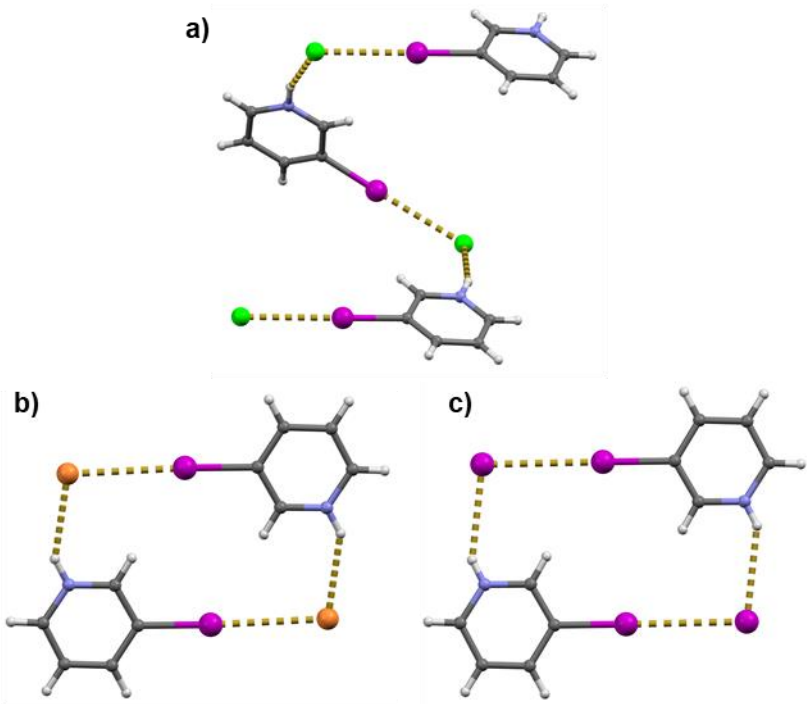

Slika 4. a) Kationi i anioni povezani halogenskim i vodikovim vezama u lance u strukturi **3-IPy**HCl; Kationi i anioni povezani halogenskim i vodikovim vezama u tetramere u strukturi b) **3-IPy**HBr and c) **3-IPy**HI.

Kao što je očekivano, sve tri halogenidne soli priređene iz *p*-jodpiridina sadže lance alternirajućih kationa i aniona povezanih vodikovim i halogenskim vezama (Slika 5). U slučaju klorida i bromida lanci su poprilično ravni s kutom I···X⁻···H (kut između halogenske veze C–I···X⁻ i vodikove veze N–H···X⁻) od oko 160°, dok su u slučaju jodidne soli lanci savijeniji sa značajno nižom vrijednosti istog kuta (φ(I···X⁻···H) ≈ 126°). S druge pak strane, halogenske veze C–I···X⁻ u slučaju klorida i bromida su puno savijenije (≈ 167° u slučaju klorida i 170° u slučaju bromida), dok je veza C–I···I⁻ gotovo linearna (φ(C–I···I⁻) ≈ 176°).

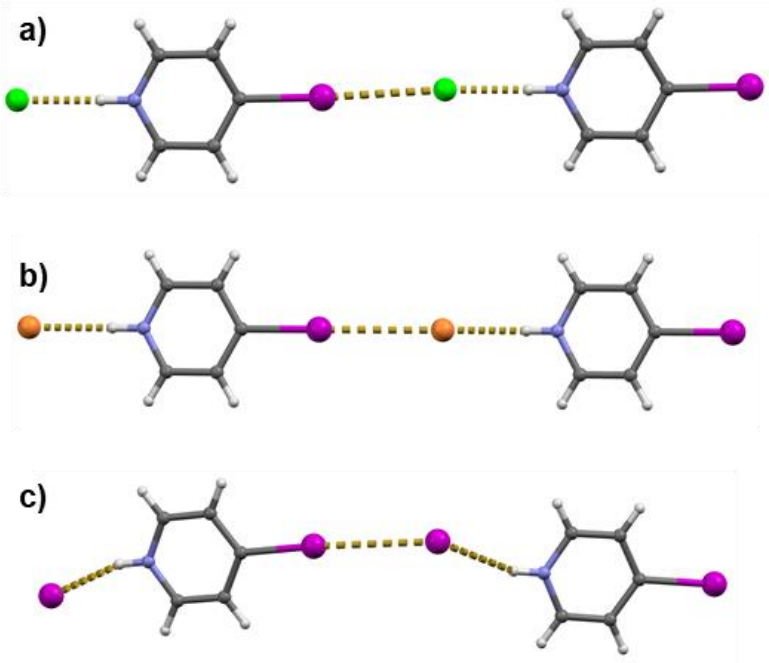

Slika 5. Kationi i anioni povezani halogenskim i vodikovim vezama u lance u strukturi: a) **4-IPy**HCl; b) **4-IPy**HBr; c) **4-IPy**HI.

Uz opisane bezvodne soli, uspješno su izolirana dva hidrata te jedna dvosol – *o*-jodpiridinijev klorid jodid. Iako neočekivani nusprodukt, ova dvosol prvi je objavljeni primjer soli koja sadrži donor i vodikove i halogenske veze te dva različita halogenidna aniona. U ovoj vrlo zanimljivoj strukturi *o*-jodpiridinijevi kationi povezuju se naizmjenično s jodidnim i kloridnim anionima u centrosimetrične oktamere. Kationi se povezuju s jodidnim anionima isključivo halogenskim

vezama C–I···I^-, dok se s kloridnim anionima povezuju isključivo vodikovim vezama N–H···Cl^- (Slika 6). Anioni su također akceptori kontakata C–H···X^- kojima se oktameri povezuju u slojeve.

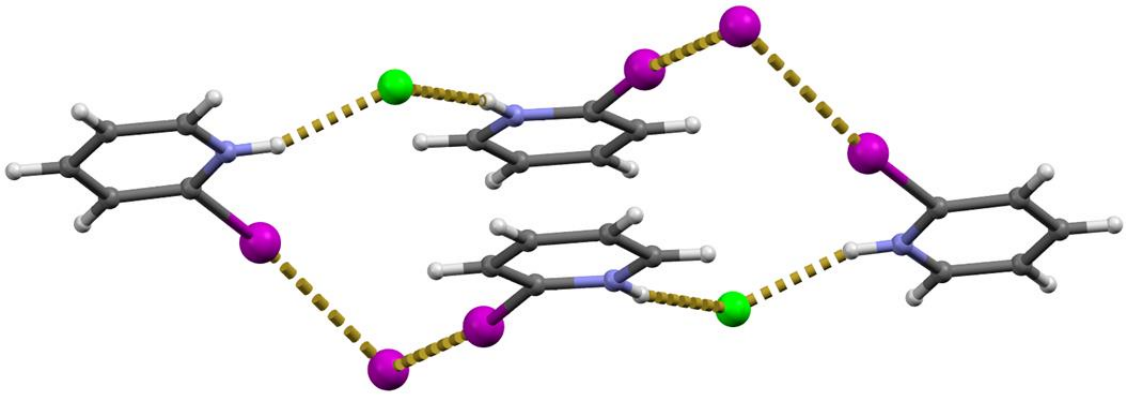

Slika 6. Kationi i anioni povezani halogenskim i vodikovim vezama u oktamere u strukturi (**2-IPy**H)$_2$ClI dvosoli.

Usporedbom vodikovih i halogenskih veza u svih 9 struktura jodpiridinijevih halogenida utvrđeno je da su vodikove veze relativno kraće od halogenskih veza (u odnosu na sumu vdW radijusa atoma donora i akceptora). Srednje vrijednosti relativnih skraćenja vodikovih veza smanjuju se s porastom radijusa halogenidnog aniona (akceptora): 72% u slučaju klorida, 76% u slučaju bromida i 80% u slučaju jodida. Iako se u slučaju halogenskih veza s halogenidima srednje vrijednosti relativnih skraćenja (≈ 84,5%) ne mijenjaju s promjenom halogenida kao akceptora, čini se da ipak postoji trend da, kada se u strukturama kationi i anioni povezuju relativno kraćim vodikovim vezama, da se ujedno povezuju i relativno kraćim halogenskim vezama. Štoviše, u slučaju *o*-jodpiridinijevih halogenida, graf međusobnog odnosa relativnih duljina vodikovih i halogenskih veza je gotovo linearan pri čemu se vrijednosti relativnih duljina za obje interakcije povećavaju s povećanjem radijusa halogenidnog aniona (Slika 7).

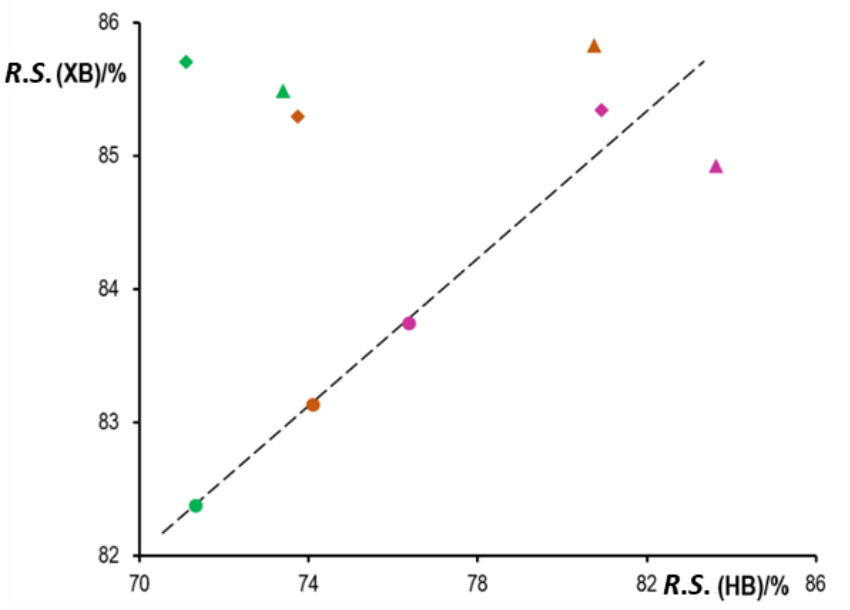

Slika 7. Relativna skraćenja halogenskih (***R.S.***(XB)) i vodikovih (***R.S.***(HB)) veza u jodpiridinijevim halogenidima. Krugovi označavaju **2-IPy**, trokuti **3-IPy** i rombovi **4-IPy**, pri čemu su zelenim simbolima označeni kloridi, smeđima bromidi, a ljubičastima jodidi.

Iz navedenoga se čini da halogenska veza također slijedi isti opći trend kao i vodikova veza: relativne duljine obaju interakcija povećavaju se s veličinom halogenidnog aniona kao akceptora. Međutim, na vodikovu vezu više utječe veličina halogenida (akceptora) nego na halogensku vezu; u seriji *o*-jodpiridina relativna duljina vodikove veze povećava se za oko 5% od klorida do jodida, dok se halogenska veza povećava za samo oko 1%. S druge strane, na halogensku vezu (koja je relativno slaba u proučavanom nizu soli) više utječe kristalno pakiranje.

Zanimljivo je usporediti ovaj rezultat sa zaključcima nedavne studije kompeticije halogenske i vodikove veze u različitim otapalima.[106] Ova studija je pokazala da je dobivanje spojeva povezanih halogenskom vezom povoljnije u otapalima veće polarnosti jer je vodikova veza osjetljivija na utjecaj otapala zbog jače solvatacije donora vodikove veze u usporedbi s donorima halogenske veze. Isti učinak ima i manji halogen (s većom gustoćom naboja); manji halogenid (Cl^-) sudjelovati će u jačim i halogenskim i vodikovim vezama od većeg halogenida (npr. I^-).

U slučaju moguće kompeticije između donora vodikove i halogenske veze za ostvarivanje supramolekulskih interakcija s halogenidima kao akceptorima, lakši halogenidi (klorid, a posebno fluorid) prvenstveno stvarati će vodikove veze, dok će teži halogenidi (bromid, a posebno jodid) preferirati sudjelovanje u halogenskim vezama, što je i vjerojatan razlog za razliku u osjetljivosti halogenskih i vodikovih veza na promjenu halogenidnog aniona kao akceptora. Ovo je potvrđeno strukturom dvosoli u kojoj se kationi s kloridnim anionom povezuju isključivo vodikovim vezama, a s jodidnim anionom isključivo halogenskim vezama.

Kako bi se navedeno testiralo na široj osnovi napravljena je analiza struktura pohranjenih u kristalografskoj bazi podataka CSD[107]. Analizirane su strukutre koje sadrže halogenidni anion (klorid, bromid ili jodid), barem jedan jaki donor vodikove veze (skupina O−H ili N−H) i kovalentno vezan jod (C−I ili N−I) kao donor halogenske veze. Prva uočljiva razlika je u udjelu struktura u kojima je jedna od konkurentskih interakcija odsutna – dok je halogenska veza bila odsutna u oko 20% slučajeva za svaki halogenid (23% za klorid, 20% za bromid i 22% za jodid), vodikova veza je izostala u samo 17% klorida, 27% bromida te čak 58% jodida. Ovaj trend se slaže s tvrdnjom da je halogenska veza manje ovisna o halogenidu nego vodikova veza.

Kada se za sva tri halogenida grafički prikaže pojavnost struktura s različitim brojem halogenskih i vodikovih veza koje ostvaruju u istima (Slika 8), može se vidjeti da je opća raspodjela broja veza za klorid i bromid prilično slična, dok je u slučaju jodida kao akceptora ta distribucija nešto drugačija. U sva tri slučaja postoji velik broj struktura u kojima je halogenid akceptor jedne halogenske i jedne vodikove veze. U slučaju pojave višestrukih halogenskih i vodikovih veza opet se uočava gore spomenuti trend: mala je promjena u učestalosti pojavljivanja više (dvije ili više) halogenskih veza (29% za klorid, 33% za bromid i 50% za jodid), dok se učestalost većeg broja vodikovih veza dramatično smanjuje od klorida (55%) preko bromida (43%) do jodida (12%).

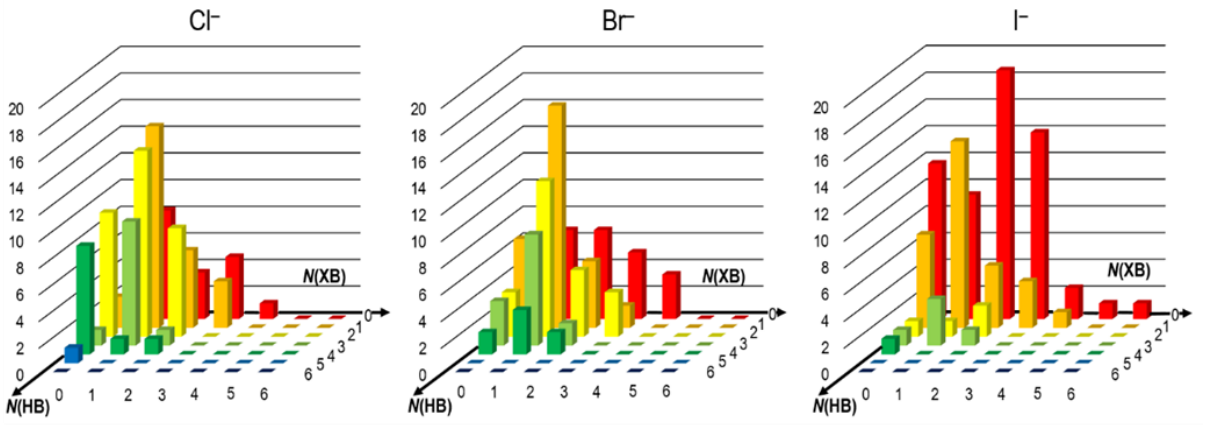

Slika 8. Pojavnost (u %) broja vodikovih (*N*(HB)) i halogenskih (*N*(XB)) veza s halogenidnim anionima u kristalnim strukturama gdje postoje donori i vodikovih veza (O−H ili N−H skupina) i halogenskih veze (C−I) prema podacima iz baze CSD.

Kao što se može vidjeti na Slici 8, sva tri halogenida prvenstveno tvore mali broj jakih vodikovih i/ili halogenskih veza, pri čemu ukupan broj interakcija rijetko prelazi četiri. S obzirom da navedeno ukazuje na vrlo niske koordinacijske brojeve, za očekivati je da halogenidi također sudjeluju u drugim interakcijama, prvenstveno slabim vodikovim vezama C−H···X^-. Stoga je provedeno i detaljnije istraživanje međuodnosa halogenskih veza C−I···X^- i sveprisutnih vodikovih veza C−H···X^-. Kada se uzmu u obzir i vodikove veze C−H···X^-, ukupni prosječni koordinacijski broj (zbroj halogenskih, jakih vodikovih i slabih vodikovih veza) je 6, dok se većinom javljaju koordinacijski brojevi od 5 do 8 (s iznenađujuće velikim brojem struktura koje sadrže oktakoordinirani klorid, slika 9). Kloridni anion uglavnom stvara do dvije halogenske veze, a ostatak su jake i slabe vodikove veze. Postoje i strukture u kojima kloridni anion djeluje kao akceptor 3 ili 4 halogenske veze. Osim dviju iznimaka, u tim strukturama nema jakih vodikovih veza N−H···Cl^- i O−H···Cl^-. Bromidni anion, kao i kloridni, uglavnom stvara do dvije halogenske veze. U strukturama u kojima je bromidni anion akceptor više od dvije halogenske veze C−I···Br^-, nastaju samo slabe vodikove veze C−H···Br^-. Jodidni anion većinom tvori jednu halogensku vezu C−I···I^- s istodobnim vodikovim vezama. Također postoji značajan broj struktura u kojima je jodidni anion akceptor dvije ili tri halogenske veze C−I···I^-, te nekoliko primjera struktura u kojima se formira četiri, pet ili čak šest halogenskih veza C−I···I^- uz istovremene vodikove veze C−H···I^-.

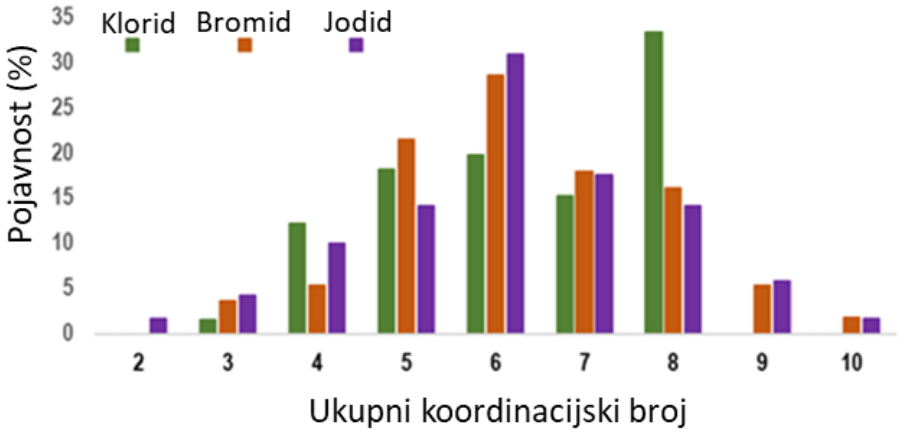

Slika 9. Pojavnost totalnih koordinacijskih brojeva (kao akceptora halogenskih, jakih i slabih vodikovih veza) halogenidnih aniona u kristalnim strukturama prema podacima iz baze CSD.

Sve u svemu, ovi rezultati u skladu su s očekivanjima temeljenim na dosad provedenim računalnim studijama i studijama u otopini koje pokazuju da afinitet prema halogenskoj vezi opada s veličinom halogenidnog aniona kao akceptora, isto kao i u slučaju vodikove veze. S druge pak strane, čini se da je efekt mnogo izraženiji u slučaju vodikove nego u slučaju halogenske veze, pri čemu se relativna duljina potonje povećava za samo oko 1% od klorida do jodida. Ova razlika između halogenske i vodikove veze s halogenidima u čvrstom stanju u skladu je s prethodno opisanim učinkom otapala na stvaranje vodikove i halogenske veze. Manji halogenidi (tj. oni s većom gustoćom naboja) su akceptori jačih halogenskih, ali i jačih vodikovih veza od većih halogenida. Međutim, razlika u jakosti vodikovih veza biti će znatna, dok će razlika u jakosti halogenskih veza biti mala ili čak zanemariva. Iako su halogenske veze s većim halogenidima slabije, iz analize baze CSD jasno se vidi da će se halogenske veze u puno većem broju slučajeva ostvariti s većim halogenidom, a još jasnije u strukturi dvosoli (**2-IPy**H)$_2$ClI. U kontekstu ciljane priprave krutina, lakši halogenidi se bolje otapaju u protičnim otapalima (zbog jačih vodikovih veza) i manja je vjerojatnost da će dati produkte povezane halogenskom vezom (objašnjavajući prevlast soli i kokristala u kojima se ostvaruju halogenske veze s jodidima nad onima u kojima se ostvaruju halogenske veze s bromidima i kloridima i općenito odsutnost struktura u kojima postoji halogenska veza s fluoridima), kao i pojava solvata ((**3-IPy**HCl)$_2$ · H$_2$O i (3-IPyHCl)$_4$ · EtOH[64]). Pojava solvata može se izbjeći korištenjem aprotičnih otapala (u ovom slučaju CH_2Cl_2 za sintezu bezvodnog **3-IPy**HCl).

3.3. Utjecaj položaja i naravi halogena halogenpiridinijevih kationa na ostvarivanje i geometriju halogenskih veza u halogenpiridinijevim jodidima

S obzirom da je u prethodnom radu (**I**) pokazano da u halogenidnim solima protoniranih halogenpiridina uz jake vodikove veze mogu istovremeno postojati i halogenske veze s halogenidnim anionima,[70] u znanstvenom radu **II** nastavlja se istraživanje halogenpiridinijevih kationa kao donora halogenske veze. U radu **II** opisana je studija potencijala i ograničenja halogenpiridinijevih kationa kao donora halogenske veze. U tu svrhu odabrani su monohalogenirani derivati piridina (*ortho*-, *meta*- i *para*-; klor, brom i jod) kao neutralne molekule, ali i *N*-protonirani i *N*-metilirani kationi.[108]

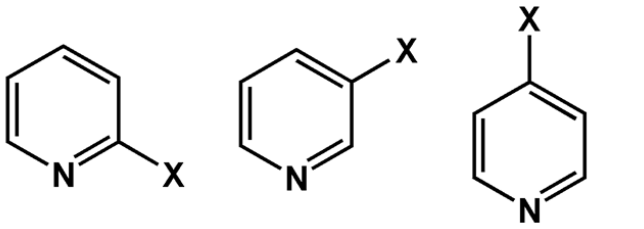

2-ClPy: X = Cl	**3-ClPy: X = Cl**	**4-ClPy: X = Cl**
2-BrPy: X = Br	**3-BrPy: X = Br**	**4-BrPy: X = Br**
2-IPy: X = I	**3-IPy: X = I**	**4-IPy: X = I**

Shema 2. Halogenpiridini korišteni za izučavanje utjecaja položaja i naravi halogena halogenpiridinijevih kationa na ostvarivanje i geometriju halogenskih veza u halogenpiridinijevim jodidima.

Kako bi se utvrdilo postoji li statistički značajan trend povećanja vjerojatnosti ostvarivanja halogenskih veza s dodatkom pozitivnog naboja halogenpiridinskom prstenu prvo je provedena analiza struktura (koje sadrže halogeni atom vezan na aromatski prsten *N*-heterocikla) pohranjenih u bazi podataka CSD. Od ukupno 3112 struktura koje su zadovoljavale gorenavedene uvijete, većina su neutralne molekule, a 655 kationi izvedeni iz njih. Od toga 524 strukture sadrže *N*-protonirane katione, a samo 131 struktura sadrži *N*-alkilirane katione. Za neutralne halogenheterocikle pronađeno je da je u oko 33% struktura atom halogena u bliskom kontaktu (kraćem od sume odgovarajućih van der Waalsovih radijusa) s potencijalnim

akceptorom halogenskih veza (bilo atomima dušika ili kisika, odnosno halogenidnim anionom), što ukazuje na prisutnost halogenske veze. Očekivano, halogenske veze najrjeđe se javljaju u strukturama s klorheterociklima (27%), zatim s bromheterociklima nešto češće (39%) i na kraju u strukturama koje sadrže jodheterocikle halogenska veza javlja se s najvećom učestalošću (70%). Dodavanje pozitivnog naboja (protoniranjem ili alkiliranjem heterocikličkog dušikovog atoma) dovodi do definitivnog povećanja učestalosti ostvarivanja halogenskih veza koje se povećalo na: 56% za katione izvedene iz klorheterocikala, 82% za katione izvedene iz bromheterocikla i 89% za katione izvedene jodheterocikla. U slučaju kada se ista analiza provede samo na strukturama koje sadrže monohalogenpiridine, uočeno povećanje incidencije halogenskih veza pri dodavanju pozitivnog naboja na halogenpiridinski prsten postaje još izraženije. U slučaju klorpiridina poveća se sa svega oko 7% na značajnih 51%, u slučaju brompiridina s 8% na čak 87% i na kraju s oko 40% na 90% u slučaju jodpiridina. Povećanje je nešto veće za *o*-halogenpiridine (s 8% na 79%) nego za *m*-halogenpiridine (s 4% na 70%) što je očekivano kako zbog blizine atoma halogena protoniranom/alkiliranom atomu dušika, tako i zbog rezonantnog učinka. Sveukupno, rezultati analize baze CSD pokazuju da su atomi halogena na neutralnom piridinskom prstenu prilično loši donori halogenskih veza (osim joda), ali kada je piridinski prsten pozitivno nabijen, učestalost sudjelovanja atoma halogena u halogenskoj vezi drastično se povećava.

U svrhu detaljnijeg istraživanja halogenskih veza halogenpiridinijevih kationa odabrane su jodidne soli. Jodidni anion logičan je izbor jer je utvrđeno da najpouzdanije formira halogenske veze među halogenidima,[70] a osim toga je jednostavan sferni anion što omogućava izbjegavanje steričkih i drugih problema koji mogu zakomplicirati cjelokupnu sliku supramolekulskih interakcija u kristalu. Strukture (protoniranih) halogenpiridinijevih jodida opisane su u radu Twamleyja[71] i suradnika te u prethodnom radu u sklopu ove disertacije,[70] dok su *N*-metilirani halogenpiridinijevi jodidi sintetizirani i strukturno karakterizirani u okviru ove studije.[108] Uz usporedno proučavanje geometrije halogenskih veza u strukturama dviju serija kristalnih čvrstih tvari (*N*-protoniranih i *N*-metiliranih halogenpiridinijevih jodida), napravljene su i kvantno-kemijski izračuni kako bi se detaljnije istražili i objasnili temeljni razlozi uočenog ponašanja halogenpiridinijevih kationa u riješenim strukturama.

Iako nažalost nije bilo moguće izolirati i riješiti strukture dva člana *N*-metilirane serije (izvedena od *o*-brompiridina i *p*-brompiridina), kristalne strukture preostalih sedam spojeva dovoljne su da istaknu značajne razlike od trendova uočenih u seriji protoniranih

halogenpiridinijevih jodida. Iako u strukturama *N*-metiliranih halogenpiridinijevih jodida postoje usmjerene i poprilično kratke halogenske veze, odsutnost usmjeravajućeg utjecaja vodikove veze dovodi do znatno manjih strukturnih sličnosti unutar *N*-metiliranih soli *o*-, *m*- i *p*-halogenpiridina nego što je to slučaj u seriji *N*-protoniranih soli.

Najveće razlike među analognim jodidima, [**2-ClPy**Me]I i [**2-IPy**Me]I. U strukturi [**2-IPy**Me]I ionski parovi *o*-jodpiridinijevih kationa i jodidnih aniona povezuju se halogenskim vezama C–I···I⁻, a dalje se ionski parovi međusobno povezuju vodikovim vezama C–H··· I⁻ u spiralne lance (slika 2. b). Suprotno tome, struktura [**2-ClPy**Me]I je složena mreža sastavljena preko kontakata C–Cl···I⁻ i C–H···I⁻ s četiri *o*-klorpiridinijeva kationa i četiri jodidna aniona u asimetričnoj jedinici (Slika 10). Oni ne tvore jednostavne ionske parove povezane halogenskom vezom kao što je slučaj u [**2-IPy**Me]I – samo dva aniona i tri kationa formiraju halogenske veze (dva kationa se vežu na isti jodid), dok se preostali kation i anioni povezuju vodikovim vezama C–H···I⁻.

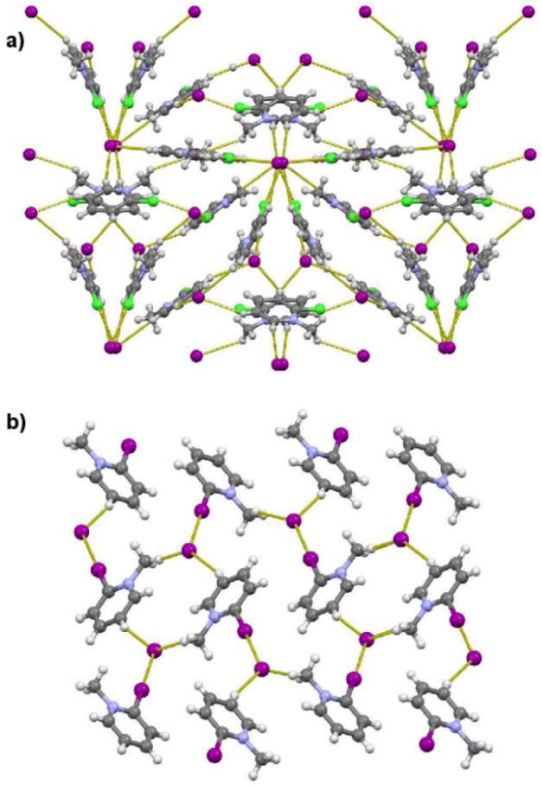

Slika 10. Halogenske veze i kratki kontakti C–H···I⁻ u kristalnim strukturama *N*-metiliranih-2-halogenpiridinijevih jodida: a) trodimenzijska mreža u [**2-ClPy**Me]I (pogled duž kristalografske osi *c*) i b) dvodimenzijska mreža u [**2-IPy**Me]I (pogled duž kristalografske osi *a*). (Duljine halogenskih veza navedene su u tablici 1.)

U strukturama jodida dobivenih iz *m*-supstituiranih piridina ([**3-IPy**Me]I, [**3-BrPy**Me] i [**3-ClPy**Me]I) halogenpiridinijevi kationi i jodidni anioni povezani su u lance halogenskim vezama C−X···I⁻ i vodikovim vezama C−H···I⁻. Iako nisu izostrukturni (razlikuju se po simetriji prostorne grupe), [**3-BrPy**Me]I i [**3-IPy**Me]I su prilično slični u prostornom rasporedu kationa i aniona. U obje strukture lanci su povezani u slojeve dodatnim kontaktima C−H···I⁻ (slika 11. b, c). Halogenske veze C−I···I⁻ i C−Br···I⁻ kraće su od odgovarajuće sume van der Waalsovih radijusa za oko 11%, odnosno 5%. U [**3-ClPy**Me]I lanci ionskih parova također su međusobno povezani u slojeve putem vodikovih veza C−H···I⁻ (Slika 11), međutim slojevi koji se ovdje formiraju nisu ravni nego valoviti. Iako duži (oko 1%) od sume odgovarajućih van der Waalsovih radijusa, kontakt C−Cl···X⁻ i dalje ima značajan utjecaj na strukturni raspored,[109] kao što je slučaj u strukturi [**3-ClPy**Me]I.

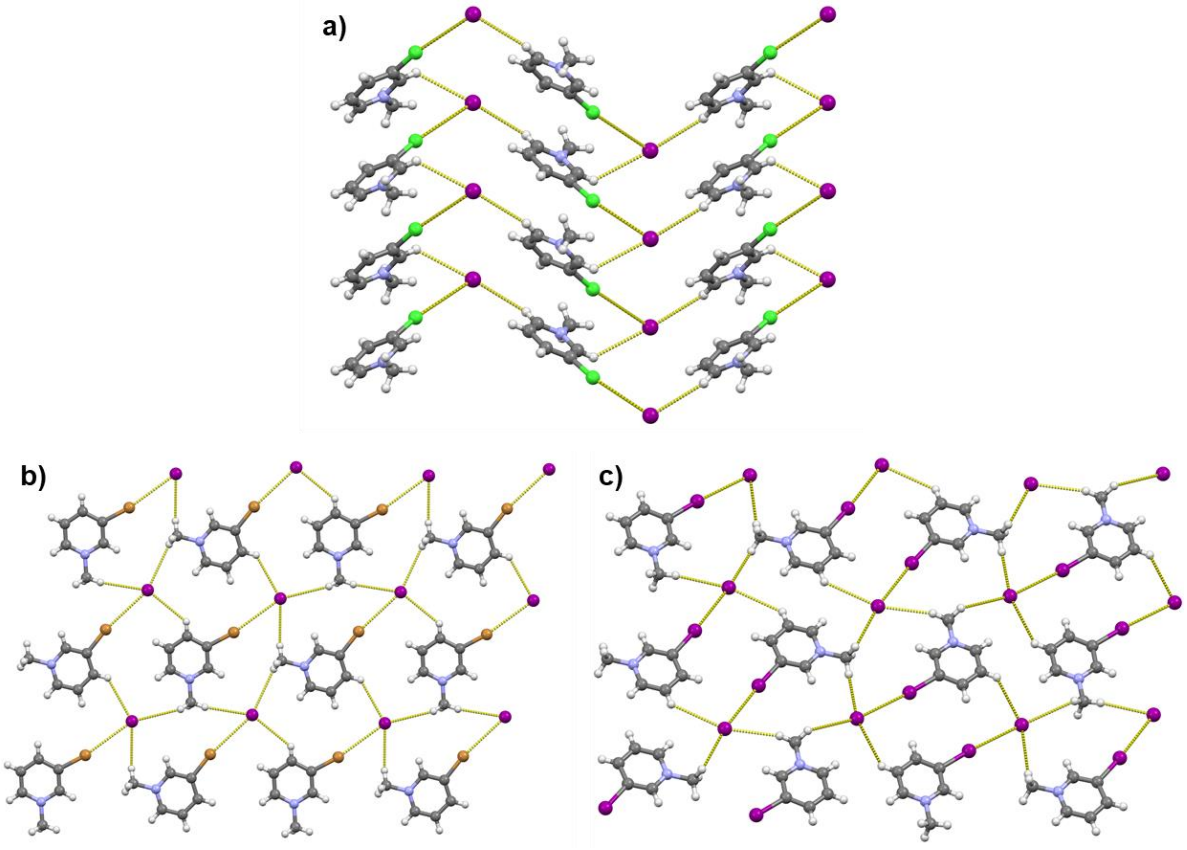

Slika 11. Kationi i anioni povezani halogenskim i vodikovim vezama u 2D mreže u strukturama *N*-metiliranih-3-halogenpiridinijevih jodida: a) [**3-ClPy**Me]I (pogled duž kristalografske osi *a*); b) [**3-BrPy**Me]I (pogled duž kristalografske osi *c*); c) [**3-IPy**Me]I (pogled duž kristalografske osi *a*). Duljine halogenskih veza navedene su u tablici 1.

U slučaju struktura izvedenih iz *p*-supstituiranih piridina, [**4-IPy**Me]I i [**4-ClPy**Me]I, kationi i anioni povezani su halogenskim vezama C−X···I⁻ i vodikovim vezama C−H···I⁻ u centrosimetrične cikličke tetramere ([**4-XPy**Me]I)$_2$ (Slika 12). U obje strukture kontakti C−X···I⁻ su kraći od sume van der Waalsovih radijusa (oko 10% i 4%) i prilično linearni (φ(C−X···I⁻) ≈ 170°). U vodikovim vezama C−H···I⁻ u oba slučaja sudjeluju ekvivalentni atomi vodika (*ortho* u odnosu na metilirani dušik), ali je prostorni raspored tetramera povezanih vodikovim vezama C−H···I⁻ sasvim drugačiji. U slučaju [**4-IPy**Me]I vodikova veza je gotovo linearna (φ(C−H···I⁻) ≈ 178°) što uzrokuje da su dva piridinijeva prstena unutar tetramera gotovo savršeno koplanarna (ravnine aromatskih prstenova kationa posmaknute su za samo 0,12 Å). Suprotno tome, u [**4-ClPy**Me]I kut C−H···I⁻ je znatno niži (oko 152°), a ravnine aromatskih prstenova piridinijevih kationa su posmaknute za 2,18 Å.

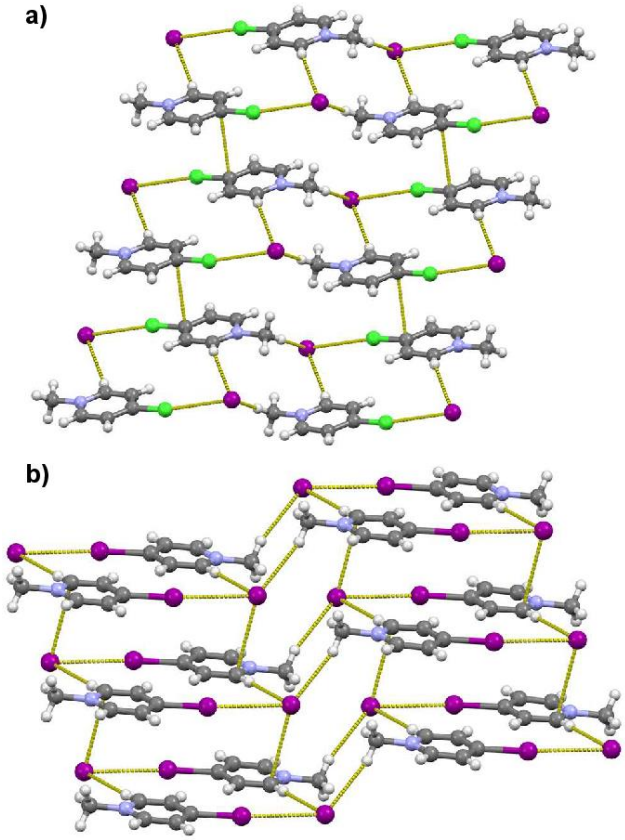

Slika 12. Kationi i anioni povezani halogenskim i vodikovim vezama u tetramere u strukturama *N*-metiliranih-4-halogenpiridinijevih jodida povezanih vodikovim vezama C−H···I⁻ i: a) kontaktima π-π u [**4-ClPy**Me]I; b) kontaktima anion-π u [**4-IPy**Me]I. Duljine halogenskih veza navedene su u tablici 1.

Duljine halogenskih veza koje tvore *N*-metilirani jodpiridinijevi kationi u većini su struktura usporedive s onima koje tvore njihovi protonirani analozi, a razlike između relativnih skraćenja bilo koja dva analoga općenito su manje od 0,5% (Tablica 1). Međutim, postoji značajna razlika između protoniranih i metiliranih klorpiridinijevih jodida, pri čemu je kontakt C−Cl···I⁻ u [**4-ClPy**Me]I 3,8% kraći, a u [**4-ClPy**H]I 0,1% duži od sume odgovarajućih van der Waalsovih radijusa što ukazuje da prisutnost jake vodikove veze N−H···I⁻ ima jači utjecaj na produljenje (slabije) halogenske veze C−Cl···I⁻, dok je njezin učinak na (jaču) halogensku vezu C−I···I⁻ zanemariv.

Tablica 1. Pregled halogenskih veza u jodidima protoniranih i *N*-metiliranih halogenpiridinijevih kationa pri sobnoj temperaturi.

Protonirani halogenpiridinijevi jodidi	***d*(XB) / Å**	***R.S.** (XB) / %**	***N*-metilirani halogenpiridinijevi jodidi**	***d*(XB) / Å**	***R.S.* (XB) / %**
[**2-ClPy**H]I	**3,768**	**–0,1**	[**2-ClPy**Me]I**	**3,496**	**6,3**
				3,509	**5,9**
				3,511	**5,9**
[**2-BrPy**H]I	**3,575**	**5,9**	/	/	/
[**2-IPy**H]I	**3,467**	**12,4**	[**2-IPy**Me]I	**3,459**	**12,7**
[**3-ClPy**H]I	**3,739**	**–0,2**	[**3-ClPy**Me]I	**3,774**	**–1,2**
[**3-BrPy**H]I	**3,589**	**6,3**	[**3-BrPy**Me]I	**3,637**	**5,0**
[**3-IPy**H]I	**3,516**	**11,2**	[**3-IPy**Me]I	**3,538**	**10,7**
[**4-ClPy**H]I	**3,733**	**–0,1**	[**4-ClPy**Me]I	**3,587**	**3,8**
[**4-BrPy**H]I	**3,648**	**4,8**	/	/	/
[**4-IPy**H]I	**3,532**	**10,8**	[**4-IPy**Me]I	**3,552**	**10,3**

[*] *R.S.* (XB)% = 100[1 − (*d*(X···I⁻) / (*r*(X) + *r*(I⁻))]; *r*(X) i *r*(I⁻) su van der Waalsovi radijusi odgovarajućih iona i atoma.

[**] Mjereno pri 170 K.

U usporedbi s halogenskim vezama između "klasičnih" (neutralnih) donora halogenskih veza i jodidnog aniona kao akceptora, može se vidjeti da postoji vrlo mala razlika u duljini halogenskih veza između halogenskih veza formiranih s jodpiridinijevim kationima i neutralnim perfluoriranim jodbenzenom kao donorima halogenskih veza. Prvi tvore halogenske veze koje su u prosjeku 11,4% kraće od sume odgovarajućih van der Waalsovih radijusa, dok druge tvore halogenske veze koje su u prosjeku 9,9% kraće od sume van der Waalsovih radijusa (na temelju 19 kristalnih struktura kokristali jodida s neutralnim perfluoriranim jodbenzenima određenih na sobnoj temperaturi deponiranih u bazi CSD). U usporedbi s još jačim neutralnim donorom halogenske veze kao što je *N*-jodsukcinimid, jodpiridinijevi kationi su očigledno manje pouzdani donori halogenske veze (u jedinoj do sada objavljenoj kristalnoj strukturi kokristala *N*-jodsukcinimida i jodidnog aniona, halogenska veza je oko 21% kraća od sume odgovarajućih van der Waalsovih radijusa[110]).

Također je ustanovljeno da neutralni donori halogenske veze (fluorirani halogenbenzeni, halogenalkini i halogenimidi) stvaraju kraće veze s atomima dušika kao akceptorima u usporedbi s kationima izvedenim iz halogenheterocikala. U slučaju kada je kisik akceptor halogenske veze, duljine halogenskih veza koje formiraju brom- i jod-heterociklički kationi poprimaju približno iste srednje vrijednosti duljina halogenskih veza koje stvaraju perfluorirani halogenbenzeni. Kao što je ranije spomenuto, halogenske veze C−I···I$^-$ u protoniranim i *N*-metiliranim jodpiridinijevim jodidima pokazuju najveće relativno skraćivanje (*R.S.*(XB)) u odnosu na sumu odgovarajućih van der Waalsovih radijusa (općenito dvostruko veće nego za halogenske veze C−Br···I$^-$). U usporedbi s vodikovim vezama prisutnim u sve tri strukture protoniranih kationa, C−I···I$^-$ halogenske veze imaju nešto manje vrijednosti *R.S.* od vodikovih veza N−H···I$^-$ (19,3% za N−H···I$^-$ u [**2-IPy**H]I, 11,5% u [**3-IPy**H]I i 14,5% u [**4-IPy**H]I), osim u [**3-IPy**H]I, gdje su praktički ekvivalentni. Kao što se i očekivalo, aromatski atomi vodika u [**3-IPy**Me]I i [**4-IPy**Me]I ostvaruju vodikove veze C−H···I$^-$ kraće od sume odgovarajućih van der Waalsovih radijusa. U metiliranoj seriji dodatne vodikove veze povezuju katione s jodidnim anionima preko vodikovih atoma metilne skupine. Zanimljivo je da u [**4-IPy**Me]I jodidni anion također sudjeluje u bliskom kontaktu s aromatskim ugljikovim atomom [**4-IPy**Me]$^+$ kationa. Ovaj kontakt anion···π (s odgovarajućom vrijednosti *R.S.*(XB) od oko 1%)[111,112] stoga se može klasificirati kao tetrelna interakcija π-šupljine atoma ugljika (pozitivne regije okomite u odnosu na ravninu prstena) i jodidnog aniona. Slični kontakti anion···π također su pronađeni u kristalnim strukturama nekoliko *N*-alkil-3-halogenpiridinijevih halogenida.[113]

Može se vidjeti da, iako su u svim proučavanim strukturama prisutne halogenske veze, samo među *N*-metil-3-brompiridinijevim i *N*-metil-3-jodpiridinijevim jodidima halogenska veza jest dominantna interakcija. Kationi ne stupaju u interakcije s jodidima samo putem atoma halogena (i grupe N–H u protoniranim analozima), već i ostvarivanjem prilično kratke vodikove veze C–H···I^-, pa čak i C···I^- tetrelne π interakcije. Štoviše, čini se da su u klorpiridinijevim jodidima ove 'slabe' interakcije dominantne. Mogući razlozi ovog fenomena mogu se razjasniti analizom elektrostatskog potencijala (*V*) protoniranih i *N*-metiliranih piridinijevih kationa. I protoniranje i *N*-metiliranje halogenpiridina očekivano dovode do povećanja *V* σ-šupljine atoma halogena (V_{max}(X)). To je najizraženije kod *o*-halogenpiridina gdje se V_{max}(X) povećava za oko 400–420 kJ mol^{-1} e^{-1}, dok se u *m*- i *p*-halogenpiridinima povećava za oko 320–350 kJ mol^{-1} e^{-1}. Protoniranje dovodi do nešto većeg porasta V_{max}(X) (10–20 kJ mol^{-1} e^{-1}) na atomu halogena od metilranja, što je očekivano budući da u protoniranim piridinijevim kationima ima manje atoma na koje se raspoređuje pozitivan naboj. Uz povećanje V_{max}(X), uvođenje pozitivnog naboja u halogenpiridinski prsten također dovodi do promjene u polarizaciji atoma halogena. Prikladna mjera za polarizaciju atoma halogena jest razlika između V_{max}(X) i V_{min}(X) – elektrostatski potencijal atoma halogena u području okomitom na σ-šupljinu. Općenito je utvrđeno da na razliku V_{max}(X) – V_{min}(X) (Δ*V*(X)), položaj atoma halogena nema značajan utjecaj. U neutralnim halogenpiridinima ona u prosjeku iznosi 80±2 kJ mol^{-1} e^{-1} za klor, 122±2 kJ mol^{-1} e^{-1} za brom i 151±3 kJ mol^{-1} e^{-1} za jod. S druge pak strane, u kationima su i V_{max}(X) i V_{min}(X) znatno pozitivniji. Na Δ*V*(X) položaj atoma halogena opet gotovo da nema utjecaj, isto kao ni način uvođenja pozitivnog naboja (protoniranjem ili *N*-metiliranjem), nego prvenstveno ovisi o atomu halogena. Ako se usporede vrijednosti Δ*V*(X) na neutralnim halogenpiridinima s onima u kationima, može se vidjeti da je u slučaju sva tri klorpiridinijeva kationa vrijednost Δ*V*(X) smanjena u prosjeku na 59±4 kJ mol^{-1} e^{-1}, za brompiridinijeve katione ostaje gotovo nepromijenjena (122±7 kJ mol^{-1} e^{-1}), dok se za jodpiridinijeve katione Δ*V*(X) poveća na 164±6 kJ mol^{-1} e^{-1}. Stoga se može reći da se uvođenjem pozitinog naboja u piridinski prsten polarizacija klora smanjuje, polarizacija atoma broma se bitno ne mijenja, dok jod postaje više polariziran kada je piridin protoniran ili metiliran.

Očekuje se da bi dramatično povećanje V_{max}(X) također trebalo dovesti do jednako dramatičnog povećanja potencijala halogenpiridinijevih kationa kao donora halogenih veza. Međutim, iako prema podacima iz baze CSD evidentno postoji povećanje incidencije halogenskih veza u strukturama koje sadrže halogenpiridinijeve katione (u usporedbi sa

strukturama koje sadrže neutralne halogenpiridine), to povećanje nije tako dramatično u slučaju klorpiridinijevih kationa. Vrijednost V_{max}(X) na atomu halogena znatno je veća (390-435 kJ mol^{-1} e^{-1}) nego na neutralnim donorima (npr. 175 kJ mol^{-1} e^{-1} u 1,4-diodotetrafluorbenzenu) koji unatoč tome imaju puno veću incidenciju stvaranja halogenskih veza s potencijalnim akceptorima prisutnim u kristalnim strukturama. Najvjerojatniji razlog tome je raspodjela pozitivnog naboja na halogenpiridinijevom kationu. Dodavanje protona ili metilne skupine na piridinski dušik ne utječe samo na atom halogena – pozitivni naboj je raspoređen na cijeli kation. Kako bi se testiralo kako to utječe na sklonost halogenpiridinijevih kationa k ostvarivanju halogenskih veza, uspoređene su vrijednosti V_{max}(X) s vrijednostima V ostatka molekule neutralnih halogenpiridina i halogenpiridinijevih kationa. Ako se usporedi V_{max}(X) s srednjom vrijednosti V na drugim nevodikovim atomima na neutralnim molekulama halogenpiridina (tj. njihovim odgovarajućim π-šupljinama okomitim na ravninu prstena), može se vidjeti da je σ-šupljina na atomu halogena u svim slučajevima najpozitivnije područje. To se drastično mijenja dodavanjem pozitivnog naboja na piridinski prsten. Dodani naboj se raspoređuje po cijelom piridinskom prstenu što dovodi do povećanja V svih atoma kationa (najizraženije atoma dušika i susjednih atoma ugljika i vodika). Kao rezultat toga, σ-šupljina atoma halogena ne odgovara nužno najpozitivnijoj regiji na kationu. Doista, samo u slučaju jodpiridina i *o*-brompiridina vrijednost V_{max}(X) je veća od srednje vrijednosti V atoma dušika i ugljika u piridinskom prstenu. Međutim, čak i u tim strukturama V na π-šupljinama atoma dušika i ugljika je značajan, a u strukturi [**4-IPy**Me]I dovodi do pojave kratkog kontakta jodid···ugljik koji odgovara interakciji anion···π, pri čemu je vrijednost V π-šupljine atoma ugljika (V_{max}(C) = 436 kJ mol^{-1} e^{-1}) samo nešto niža od one σ-šupljine atoma joda ($\boldsymbol{V}_{max}$(X) = 456 kJ mol^{-1} e^{-1}).

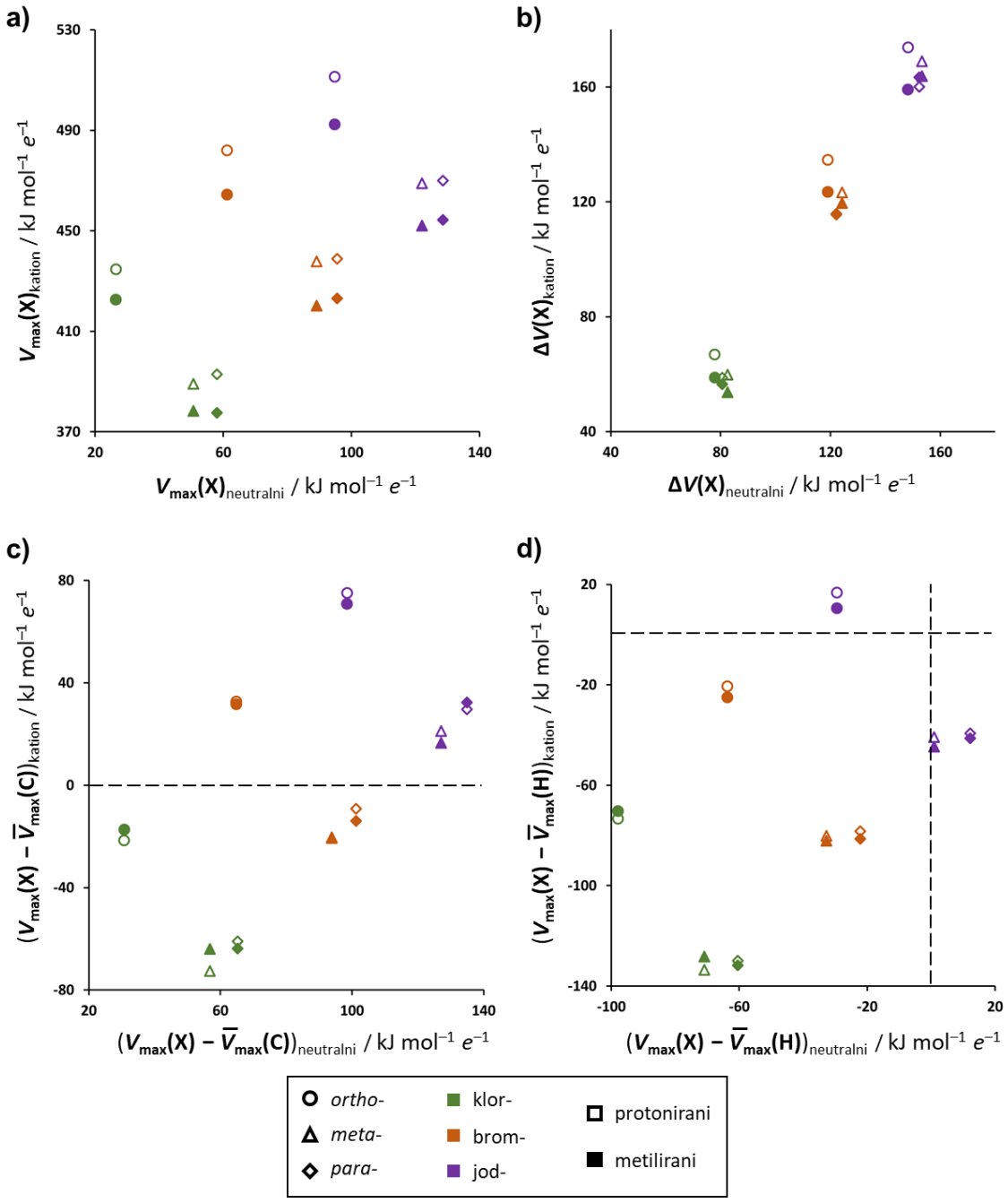

Slika 13. Promjene elektrostatskog potencijala na halogenpiridinima uslijed protonacije i *N*-alkilacije: a) prikaz odnosa V_{max}(X) halogenpiridinijevih kationa *vs* neutralnih halogenpiridina; b) prikaz razlike između V_{max}(X) i V_{min}(X) (ΔV(X)) na kationima *vs* neutralnim halogenpiridinima; c) prikaz razlike između V_{max}(X) i srednje vrijednosti *V* ugljikovih i dušikovog atoma piridinskog prstena (V_{max}(C)) na kationima *vs* neutralnim halogenpiridinima; d) prikaz razlike između V_{max}(X) i srednje vrijednosti *V* vodikovih atoma piridinskog prstena na kationima *vs* neutralnim halogenpiridinima. U c) i d) isprekidane linije prikazuju gdje su vrijednosti varijabli jednake nuli.

U svim kristalnim strukturama *N*-metil-halogenpiridinijevih jodida najprisutniji kontakti su vodikove veze C–H···I$^-$. Ako se usporedi V_{max}(X) sa srednjom vrijednosti *V* vodikovih atoma piridinskog prstena (V_{max}(H)), u neutralnim halogenpiridinima srednja vrijednost V_{max}(H) pozitivnija je od σ-šupljine halogena (V_{max}(X)) osim u *m*- i *p*-jodpiridinima. Kod kationa V_{max}(H) svih atoma vodika značajno se povećava tako da gotovo svi vodikovi atomi piridinskog prstena u *m*- i *p*-jodpiridinijevim kationima postaju pozitivniji od V_{max}(I). Međutim, u oba *o*-jodpiridinijeva kationa vrijednost V_{max}(I) se značajno poveća pri čemu postaje pozitivnija od vrijednosti V_{max}(H) vodikovih atoma piridinskog prstena, s izuzetkom atoma vodika u *ortho* položaju u odnosu na piridinijev dušik. Naravno, u slučaju svih protoniranih halogenpiridinijevih kationa, vodik koji se nalazi na atomu dušika je daleko najpozitivniji atom kationa (V_{max}(H) u rasponu od oko 665–690 kJ mol^{-1} e^{-1}, što prelazi V_{max}(X) za oko 150–310 kJ mol^{-1} e^{-1}, ovisno o kationu). Stoga je očito da će u slučaju protoniranih halogenpiridinijevih kationa vodikova veza koju formira skupina N–H uvijek biti dominantna interakcija, dok se u *N*-metiliranim kationima očekuje kompeticija između skupine C–H kao donora vodikove veze i skupine C–X kao donora halogenske veze, čak i u slučaju jodpiridinijevih kationa.

Izračunate energije vezanja molekule piridina (akceptora neutralne halogene veze) na *N*-metilirane halogenpiridine korelirane su s vrijednostima V_{max}(X). Dobivene energije interakcija prilično su značajne: oko 34–40 kJ mol^{-1} za klorpiridinij, 43–51 kJ mol^{-1} za brompiridinij i 57–68 kJ mol^{-1} za jodpiridinijeve katione. Iako apsolutne vrijednosti dobivenih energija mogu biti pomalo nepouzdane, ipak ukazuju da energije vezivanja slijede isti opći trend kao i vrijednosti V_{max}(X) unutar svakog niza izomera – *meta*- i *para*- izomeri sudjeluju u vezama vrlo sličnih energija, dok *ortho* izomer tvori vezu koja je 6-10 kJ mol^{-1} jača. Doista, energije veze za klorpiridinijeve i brompiridinijeve katione gotovo linearno su ovisne o vrijednostima V_{max}(X) za slobodne katione ($R^2 = 0{,}96$), dok su energije veze za jodpiridinijeve katione nešto veće: iako je V_{max}(Br) u slučaju **2-BrPy**Me$^+$ kationa za oko 40 kJ mol^{-1} e^{-1} veći od V_{max}(I) na kationima **3-IPy**Me$^+$ i **4-IPy**Me$^+$, energija Br···N halogenske veze (koju stvara s molekulom piridina) je za oko 6-7 kJ mol^{-1} manja od energija I···N halogenskih veza koje formiraju **3-IPy**Me$^+$ ili **4-IPy**Me$^+$ (Slika 14). Navedeno upućuje na zaključak da su Cl···N i Br···N halogenske veze (koje stvaraju halogenpiridinijevi kationi) prvenstveno elektrostatske prirode, dok kod I···N halogenskih veza postoji značajan udio prijenosa naboja. Prilično visoke energije veze za sve proučavane slučajeve pokazuju da svi halogenpiridinijevi kationi stvaraju prilično jake halogenske veze što je u suprotnosti s činjenicom da klorpiridinijevi kationi vrlo rijetko

sudjeluju u halogenskim vezama. Međutim, kako je pozitivni naboj raspoređen na cijelu molekulu, što dovodi do pojave brojnih lokalnih maksimuma V_{max}(X), halogenska veza nastala sa σ-šupljinom klorpiridinijevog kationa nije nužno najpovoljnija interakcija između kationa i molekule piridina. S druge strane, činjenica da klorpiridinijevi kationi sudjeluju u halogenskim vezama u gotovo 50% kristalnih struktura (deponiranih u bazi CSD) jasno pokazuje da se ponašanje atoma klora kao donora halogenske veze ne može objasniti samo s vrijednosti V_{max}(X). Značajnu ulogu moraju imati i drugi doprinosi kao što je veličina atoma halogena što olakšava pristup Lewisovoj bazi.

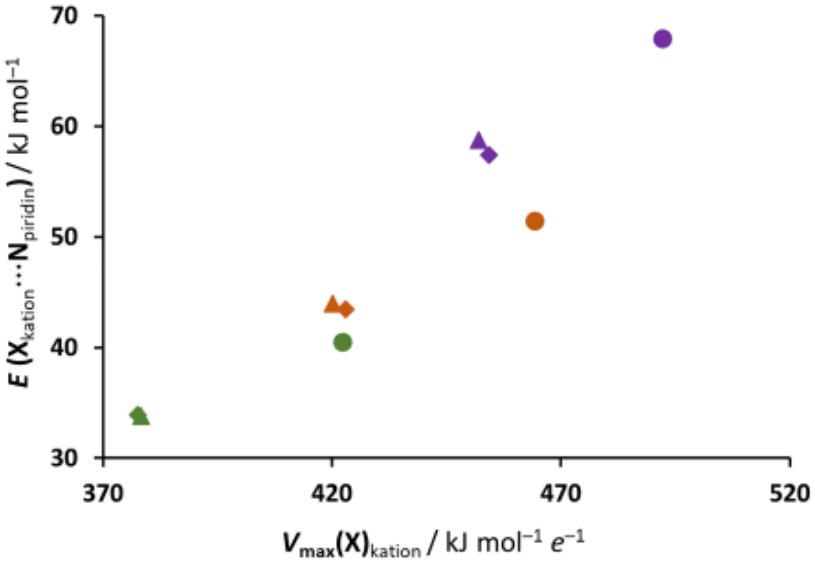

Slika 14. Ovisnost V_{max}(X) vrijednosti *N*-metiliranih halogenpiridina i energija halogenskih veza između (neutralne) molekule piridina i *N*-metiliranih halogenpiridinijevih kationa.

3.4. Utjecaj duljine *N*-supstituiranog ugljikovodičnog lanca i raspodjele naboja kationa na ostvarivanje halogenske veze u *N*-alkilhalogenpiridinijevim halogenidima

Ranije u sklopu ove disertacije (u istraživanjima objavljenim u znanstvenim radovima **I** i **II)** pokazano je kako *N*-protoniranje i *N*-metiliranje halogenpiridina (posebno jodpiridina) značajno povećava V_{max}(X) čineći ih pritom dobrim donorima halogenskih veza. To je također vidljivo i iz strukturnih podataka koji pokazuju da jodpiridinijevi kationi imaju tendenciju stvaranja prilično kratkih halogenskih veza s anionskim akceptorima halogenskih veza kao što su halogenidni anioni.[108] Stoga je u radu **III** sitetizirana serija *N*-etil-3-halogenpiridinijevih (klor, brom i jod) jodida kako bi se ispitalo ima li povećanje duljine alkilnog lanca (*N*-supstituiranog na halogenpiridinijev kation) učinak na sposobnost ostvarivanja halogenske veze s halogenidnim anionima. Sintetizirane soli uspoređene su s *N*-metiliranim analozima. Osim toga, pokušana je sinteza halogenpiridinijevih kationa koji sadrže dva 3-jodpiridinijeva prstena razdvojena alifatskom poveznicom (propil (**Prop**) i but-2-enil (**Buen**)). Ovakvi dikationi bili bi potencijalni ditopični kationski donori halogenskih veza (Shema 1).

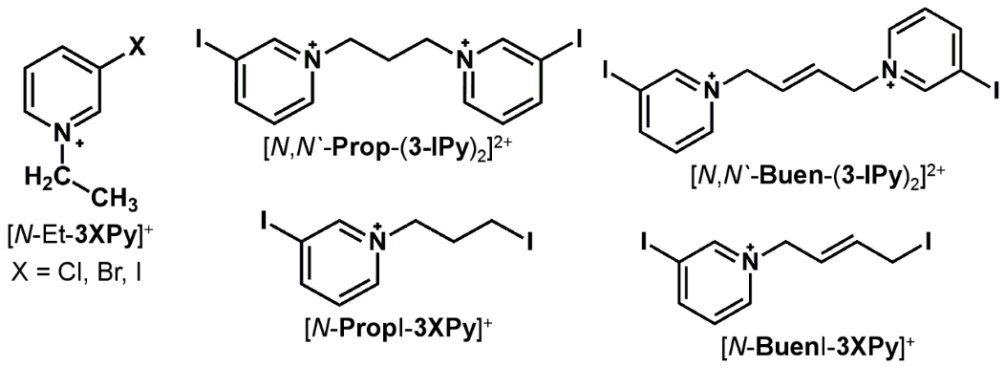

Shema 3. Kationski donori halogenske veze korišteni za proučavanje utjecaja duljine *N*-supstituiranog ugljikovodičnog lanca i raspodjele naboja kationa na ostvarivanje halogenske veze u *N*-alkilhalogenpiridinijevim halogenidima.

Sva tri *m*-halogenpiridina (klor, brom i jod) uspješno su *N*-etilirana korištenjem EtI pri čemu su dobivene odgovarajuće jodidne soli. Kristalna struktura [*N*-Et-**3-ClPy**]I sadrži centrosimetrične cikličke tetramere [*N*-Et-**3-ClPy**]$_2$I$_2$ u kojima su kationi [*N*-Et-**3-ClPy**]$^+$ i jodidni anioni

međusobno povezani vodikovim vezama C–H···I$^-$ (d(C···I) = 3,901 Å i 3,876 Å) (Slika 15a). Tetrameri su povezani u slojeve preko vodikovih veza C–H···I$^-$ (d(C···I) = 3,866 Å), a slojevi se zatim slažu jedan na drugi. Atomi klora ne sudjeluju ni u kakvim značajnim supramolekularnim interakcijama. Analizom V mapiranog na Hirshfeldovu plohu (Slika 15b) utvrđeno je da je V na Hirshfeldovoj plohi u području σ-šupljine (V_{max}(X) = 294 kJ mol^{-1} e^{-1}) manje pozitivan od srednje vrijednosti V klorpiridinjevog kationa (389 kJ mol^{-1} e^{-1}). S druge strane, vrijednosti V_{max}(H) na Hirshfeldovoj plohi u blizini atoma vodika (koji sudjeluju u supramolekularnim interakcijama) odgovaraju najpozitivnijim područjima kationa [*N*-Et-**3-ClPy**]$^+$ (V_{max}(H) = 601 kJ mol^{-1} e^{-1}).

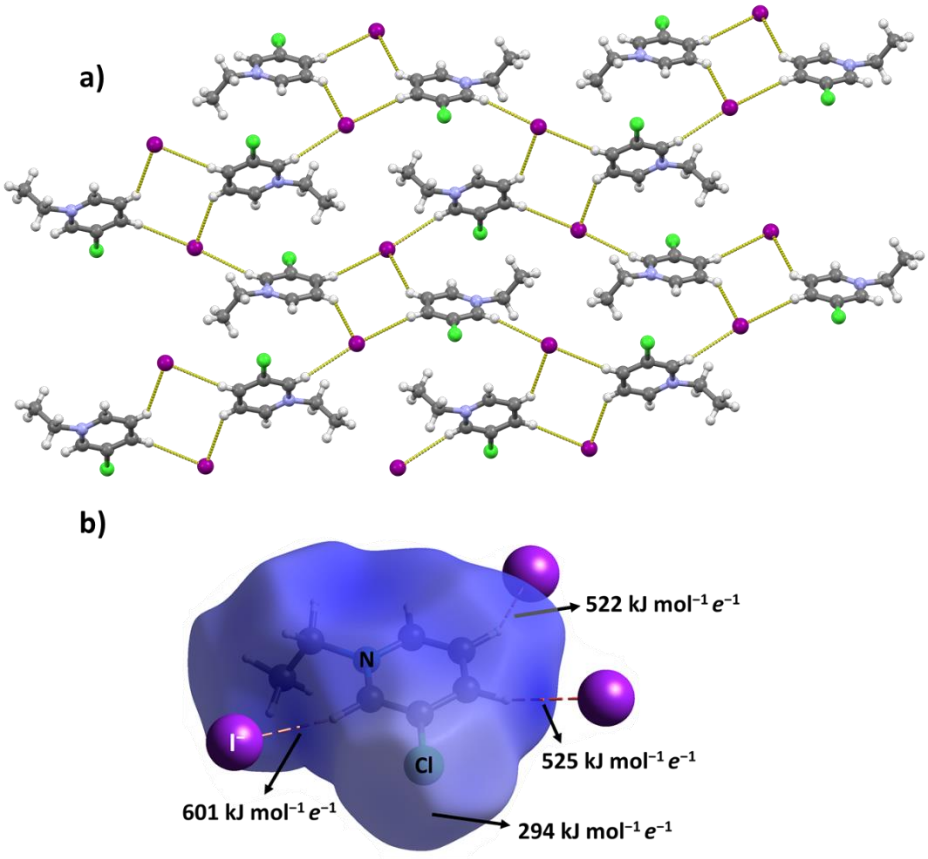

Slika 15. a) Slojevi [*N*-Et-**3-ClPy**]$^+$ kationa i jodidnih aniona povezanih C–H···I$^-$ vodikovim vezama u strukturi [*N*-Et-**3-ClPy**]I; b) Hirshfeldova ploha [*N*-Et-**3-ClPy**]$^+$ kationa s mapiranim V (izračinatim na razini teorije B3LYP-DGDZVP) i kontaktni jodidni anioni u strukturi [*N*-Et-**3-ClPy**]I.

Supstitucija klora na piridinskom prstenu s bromom dovodi do značajne razlike u strukturnom rasporedu kationa i aniona. Glavna razlika je prisutnost halogenske veze C−Br···I⁻ kraće za oko 6% od sume odgovarajućih van der Waalsovih radijusa. Jedan metilenski atom vodika etilne skupine sudjeluje u vodikovoj vezi C−H···I⁻ s jodidnim anionom. Ova kombinacija halogenskih i vodikovih veza povezuje brompiridinijeve katione i jodidne anione u spiralne lance koji se protežu duž kristalografske osi *b*. Jodidni anioni također sudjeluju u kontaktima anion-π s kationima iz susjednih lanaca, što dovodi do stvaranja slojeva okomitih na os *c* (Slika 16).

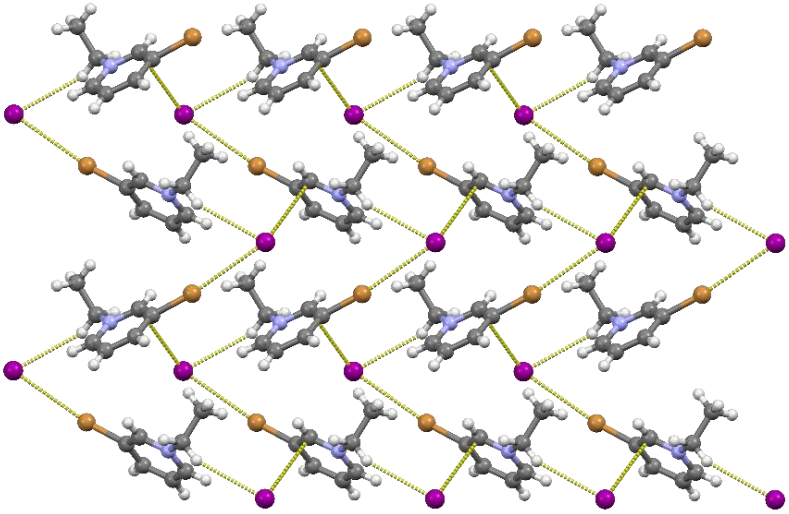

Slika 16. Kationi [*N*-Et-**3-BrPy**]$^+$ i jodidni anioni povezani u slojeve halogenskim vezama C−Br···I⁻, vodikovim vezama C−H···I⁻ i kontaktima anion-π u strukturi [*N*-Et-**3-BrPy**]I.

U strukturi [*N*-Et-**3-IPy**]I kationi i anioni također su povezani u lance (duž kristalografske osi *b*) halogenskim vezama C−I···I⁻ kraćim za oko 12% od zbroja odgovarajućih van der Waalsovih radijusa i vodikovim vezama C−H···I⁻. Lanci su međusobno povezani u slojeve vodikovim vezama C−H···I⁻ u kojima je donor jedan od metilnih vodikovih atoma (Slika 17).

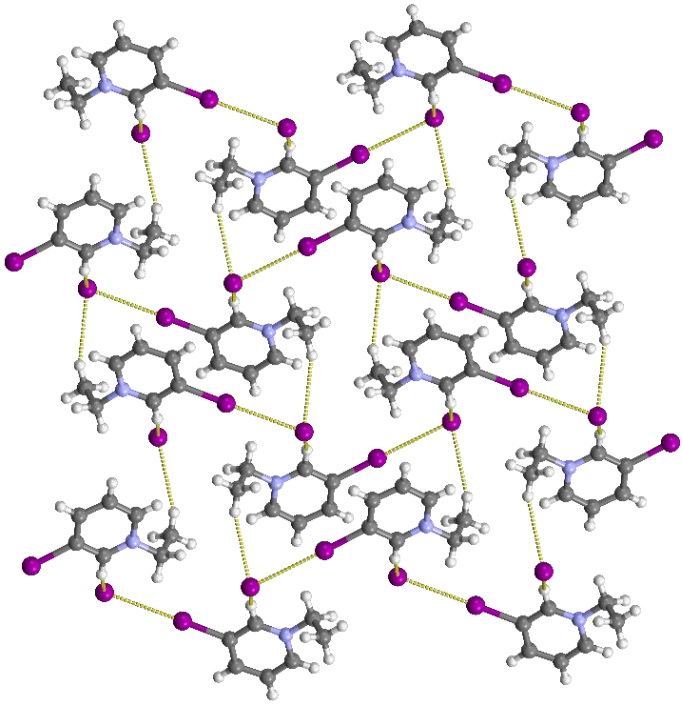

Slika 17. Kationi [*N*-Et-**3-IPy**]$^+$ i jodidni anioni povezani u slojeve halogenskim vezama C–I···I$^-$ i vodikovim vezama C–H···I$^-$ u strukturi [*N*-Et-**3-IPy**]I.

Duljina halogenih veza također se odražava na termička svojstva jodidnih soli *N*-etiliranih 3-halogenpiridina. Analizom rezultata termičke analize ustanovljeno je da sva tri spoja imaju dobro definirana tališta nakon čega slijede istovremeni raspad i isparavanje. Temperature pri kojima se soli tale rastu od 110 °C za [*N*-Et-**3-ClPy**]I preko 116 °C za [*N*-Et-**3-BrPy**]I te do konačnih 127 °C za [*N*-Et-**3-IPy**]I pokazujući jasno povećanje tališta s veličinom atoma donora halogene veze, odnosno jakosti halogenske veze C–X···I$^-$. Ako se usporede halogenske veze u *N*-etiliranim 3-halogenpiridinijevim jodidima s onima u *N*-metiliranim 3-halogenpiridinijevim jodidima, može se vidjeti da u oba niza kationa izvedenih iz 3-brompiridina i 3-jodpiridina postoje halogenske veze C–X···I$^-$. Suprotno tome, u *N*-etil-3-klorpiridinijevom jodidu kationi ne sudjeluju u halogenskoj vezi, dok u *N*-metil-3-klorpiridinijevom jodidu neki od simetrijski neovisnih kationa sudjeluju u halogenskim vezama C–Cl···I$^-$ s jodidnim anionom koje su dulje od sume odgovarajućih van der Waalsovih radijusa. Usporedbom duljine halogenskih veza u dva niza jodida vidi se da su halogenske veze C–Br···I$^-$ i C–I···I$^-$ kraće u *N*-etiliranim solima od onih u *N*-metiliranim solima (Tablica 2). Vrijednosti ***V*** mapiranih na Hirshfeldovim plohama kationa slične su kod 3-brompiridinijevih kationa, dok u slučaju 3-jodpiridinijevih kationa, *N*-

metilirani ima nešto manju vrijednost $\boldsymbol{V}_{max}$(X) od *N*-etiliranog kationa. Sve u svemu, nema značajne razlike u halogenskim vezama između *N*-etiliranih i *N*-metiliranih halogenpiridinijevih kationa s jodidnim anionima.

Tablica 2. Pregled duljina halogenskih veza C−X···I$^-$ (*d*(XB)), relativnih skraćenja (*R.S.* (XB)) i odgovarajućih vrijednosti *V* u području σ-šupljine (V_{max}(X)) u *N*-etiliranim and *N*-metiliranim 3-halogenpiridinima.

	***N*-etilirani**			***N*-metilirani**		
	***d*(XB) / Å**	***R.S.* (XB) / %**	V_{max}**(X) / kJ mol^{-1} *e*$^{-1}$**	***d*(XB) / Å**	***R.S.* (XB)**	V_{max}**(X) / kJ mol^{-1} *e*$^{-1}$**
3-ClPy	/	/	294	3,776	–1,2	381
3-BrPy	3,611	5,7	449	3,637	5,0	452
3-IPy	3,473	12,3	570	3,538	10,7	554

U svrhu proširivanja niza *N*-etiliranih jodpiridinijevih soli, pokušana je sintetiza i *N*-etil-4-jodpiridinijevog jodida iz 4-jodpiridina i etil-jodida. Unatoč brojnim pokušajima sinteze, nije izoliran željeni produkt nego mala količina (dva monokristala) čvrstog produkta koji je identificiran kao 4-jodpiridinijev hemihidrojodid ((**4-IPy**)$_2$HI). Vjerojatno je nastao reakcijom **4-IPy** i tragovima jodovodične kiseline nastale hidrolizom etil-jodida s vodom apsorbiranom iz zraka tijekom vremena. Iako se u strukturi (**4-IPy**)$_2$HI položaj vodikovog atoma vezanog na piridinski dušikov atom nije mogao utvrditi iz diferentne mape elektrnoske gustoće, iz udaljenosti N···N (*d*(N···N) = 3,202(8) Å) vidljivo je da je par **4-IPy** molekula međusobno povezan vodikovom vezom što jasno ukazuje na da je atom vodika smješten između atomâ dušika, odnosno da je par **4-IPy** molekula međusobno povezan (vjerojatno simetričnom) vodikovom vezom N···H···N potpomognutom nabojem u [(4-IPy)$_2$H]$^+$ kompleks. Jodidni anion sudjeluje u dvije halogenske veze C−I···I$^-$ s dva susjedna [(4-IPy)$_2$H]$^+$ kompleksa. Ova kombinacija vodikovih i halogenskih veza tvori supramolekulske lance koji su međusobno povezani u parove vodikovim vezama C−H···I$^-$ (Slika 18). Zanimljivo je primijetiti da ova struktura, slično kao i ranije opisana strukura dvosoli, predstavlja izvrsnu ilustraciju principa HSAB[98,99] – atom joda [(**4-IPy**)$_2$H]$^+$ kompleksa najmekša je Lewisova kiselina i stoga se preferencijalno veže s najmekšom Lewisovom bazom – jodidnim anionom. Suprotno tome, proton je najtvrđa Lewisova kiselina i stoga se preferencijalno veže s najtvrđom dostupnom Lewisovom bazom – piridinskim atomom dušika.

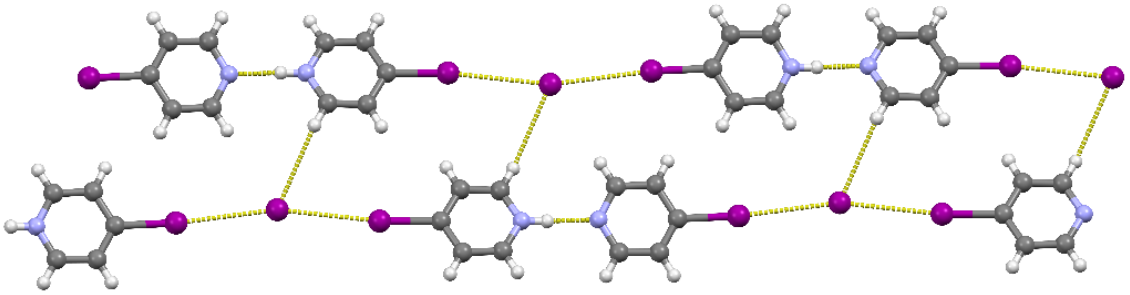

Slika 18. Kompleksi $[(\mathbf{4\text{-}IPy})_2H]^+$ i jodidni anioni povezani halogenskim vezama C−I···I⁻ i vodikovim vezama C−H···I⁻ u dvosturkim lancima u strukturi $[(\mathbf{4\text{-}IPy})_2H]I$.

Također je pokušano sintetiziranje ditopičnih kationskih donora halogenske veze povezivanjem para jodiranih piridinskih prstenova s različitim ugljikovodičnim poveznicama koji bi se ponašali slično kao $[(\mathbf{4\text{-}IPy})_2H]^+$ kompleks u strukutri 4-jodpirinijevog hemihidrojodida. U tu svrhu odabran je **3-IPy** (koji se pokazao pouzdanijim supstratom za *N*-alkilaciju od **4-IPy**) kao piridin te propilenski i (*E*)-buta-2-enilenski lanci kao poveznice piridinskih prstenova. Ove poveznice odabrane su jer se očekivalo da će sinteza s potonjim rezultirati linearnim ditopičnim donorom (zbog ograničene rotacije oko C−C dvostruke veze), dok bi prvi rezultirao savijenim kationom (s obzirom da je poveznica ugljikovodični lanac neparnim brojem ugljikovih atoma). Reakcija **3-IPy** s 1,3-dijodpropanom u omjeru 2:1, za koju se očekivalo da će dati savijeni dikation, nije dala željeni produkt. Umjesto toga dobiven je *N*-(3-jodpropan)-3-jodpiridinijev jodid ([*N*-I**Prop**-**3-IPy**]I) koji kristalizira u centrosimetričnoj prostornoj grupi $P2_1/c$ s dva kristalografski neovisna ionska para u asimetričnoj jedinici. Ova struktura se sastoji od lanaca naizmjeničnih kationa i aniona povezanih halogenskim vezama C−I···I⁻ (Slika 19a). Unatoč činjenici da je samo jedan atom joda 1,3-dijodpropana supstituiran s **3-IPy**, dobiveni kationi ipak su se ponašali kao ditopični donori halogenske veze. Oba kationa vežu dva jodidna aniona, jedan preko halogenske veze C−I···I⁻ s atomom joda piridinskog prstena, a drugi halogenskom vezom C−I···I⁻ s atomom joda alkilnog lanca. Halogenske veze koje uključuju piridinski atom joda kao donora halogenske veze su oko 10% i 12% kraći od sume odgovarajućih van der Waalsovih radijusa. S druge pak strane, jedna od dvije halogenske veze koje uključuju alkilni atom joda kao donor halogenske veze je tek oko 2% kraća, dok je druga čak oko 2% dulja od sume odgovarajućih van der Waalsovih radijusa. Susjedni lanci su dalje međusobno povezani mrežom C−H···I⁻ i C−H···I kontakata u trodimenzijsku strukturu (Slika 19b).

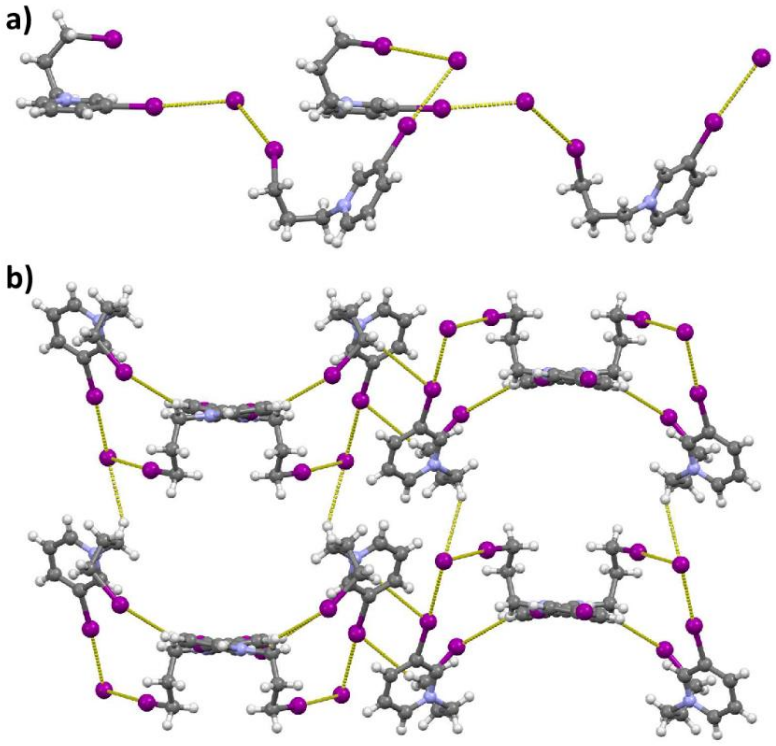

Slika 19. a) Lanci [*N*-I**Prop**-**3-IPy**]$^+$ kationa i jodidnih aniona povezanih halogenskim vezama C–I···I$^-$ u strukturi [*N*-I**Prop**-**3-IPy**]I; b) Susjedni lanci dalje se povezuju kontaktima C–H···I$^-$ i C–H···I u trodimenzijsku strukturu.

Za razliku od 1,3-dijodpropana, (*E*)-1,4-dibrombuta-2-en reagirao je s **3-IPy** u očekivanom omjeru 1:2 pri čemu je dobivema bromidna sol [*N*,*N*`-**Buen**-(**3-IPy**)$_2$]$^{2+}$ kationa (Slika 20a). Ova sol također kristalizira u centrosimetričnoj prostornoj grupi $P2_1/c$ s kationom na centru inverzije. Kation veže dva bromidna aniona halogenskim vezama C–I···Br$^-$. Uz ovu halogensku vezu, bromidni anion sudjeluje i u vodikovim vezama C–H···Br$^-$ s aromatskim i metilenskim atomima vodika četiri susjedna kationa (Slika 20b).

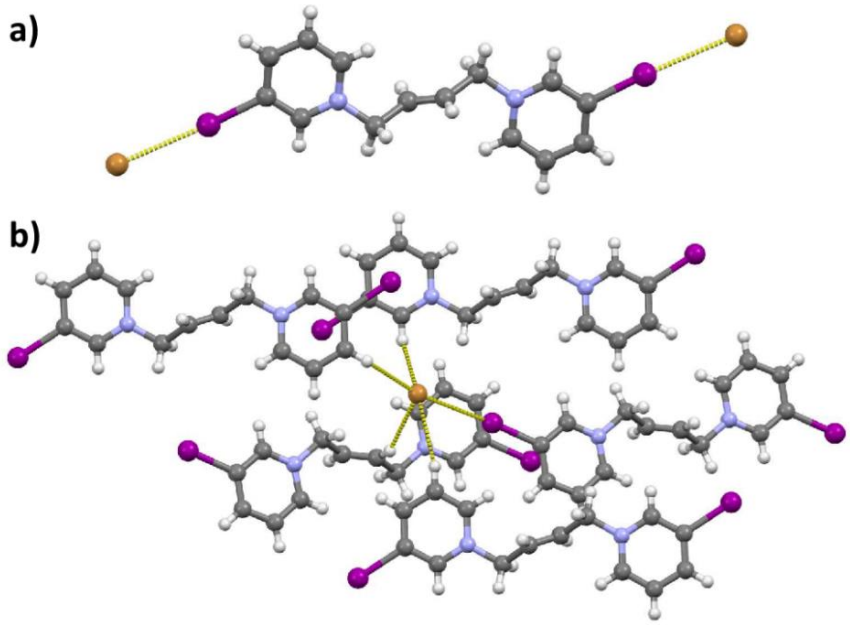

Slika 20. a) U strukturi [*N*,*N*`-**Buen**-(**3-IPy**)$_2$]Br$_2$ jedan kation [*N*,*N*`-**Buen**-(**3-IPy**)$_2$]$^{2+}$ povezan je s dva bromidna aniona halogenskim vezama C−I···Br$^-$; b) Bromidni anion povezan je sa susjednim kationima u tri dimenzije vodikovim vezama C−H···Br$^-$ i halogenskim vezama C−I···Br$^-$.

Kako bismo mogli bolje usporediti [*N*,*N*`-**Buen**-(**3-IPy**)$_2$]$^{2+}$ kation s drugim donorima halogenske veze obuhvaćenim ovom studijom (koji su dobiveni kao jodidne soli), pokušana je priprava njegove jodidne soli ionskom izmjenom. Nažalost, uslijed postupka ionske izmjene kation se raspada te je umjesto očekivanog produkta, dobiven [*N*-I**Buen**-(**3-IPy**)]I, jodidna sol monokationa ekvivalentnog gore opisanom [*N*-I**Prop**-**3-IPy**]$^+$ kationu. Za razliku od [*N*-I**Prop**-**3-IPy**]I, u [*N*-I**Buen**-(**3-IPy**)]I, kation nije ditopični donor halogenske veze. U ovoj strukturi samo piridinski atomi joda sudjeluju u halogenskim vezama C−I···I$^-$ s jodidnim anionima. Halogenske veze C−I···I$^-$ su oko 14% i 10% kraće od sume odgovarajućih van der Waalsovih radijusa. Ta dva (simetrijski neovisna) ionska para povezana su u tetramere vodikovim vezama C−H···I$^-$ preko metilenskih i aromatskih atoma vodika (*ortho* prema piridinskom dušiku). Tetrameri su povezani u lance vodikovim vezama C−H···I$^-$ u kojima sudjeluju atomi vodika u *meta* položaju prema piridinskom atomu dušika (Slika 21).

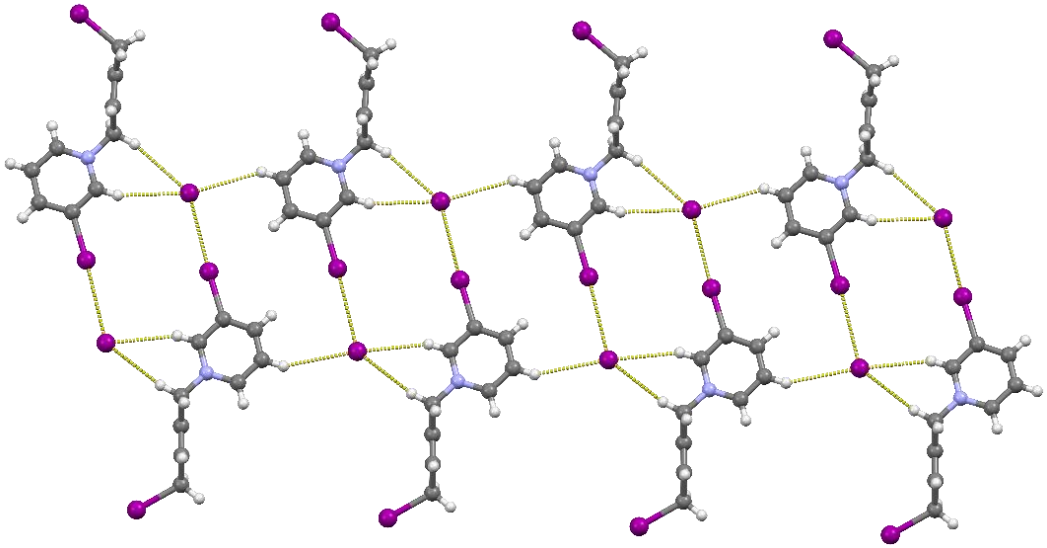

Slika 21. a) U strukturi [*N*-I**Buen**-(**3-IPy**)]I jodidni anioni i kationi [*N*-I**Buen**-(**3-IPy**)]$^+$ povezani su halogenskim vezama C−I···I$^-$ i vodikovim vezama C−H···I$^-$ u cikličke tetramere [*N*- I**Buen**-(**3-IPy**)]$_2$I$_2$ koji se dalje povezuju u lance vodikovim vezama C−H···I$^-$.

Izostajanje halogenskih veza s alkilnim atomima joda kationa [*N*-I**Buen**-(**3-IPy**)]$^+$ kao donorima halogenske veze, može se objasniti analizom raspodjele *V* mapiranog na Hirshfeldove plohe kationa (Slika 22a). Pozitivni naboj uglavnom je lokaliziran oko piridinskog atoma dušika i njemu susjednih atoma (ugljika i vodika) te se širi na piridinski prsten, ali ne i na alkilni lanac. Kao rezultat toga, $\boldsymbol{V}_{max}$(I) znatno je niži u u slučaju kada je atom jod vezan na alifatski lanac nego kada je vezan na piridinski prsten. Posljedično tome, alifatski atom joda puno je slabiji donor halogenske veze. To se također može vidjeti iz usporedbe duljine halogenskih veza C−I···I$^-$ koje uključuju piridinski atom joda i alifatski atom joda kao donor halogenske veze u [*N*-I**Prop-3-IPy**]I. Halogenske veze koje uključuju atome joda vezane na piridinski prsten (V_{max}(X) od 559 kJ mol^{-1} e^{-1} i 536 kJ mol^{-1} e^{-1}) kraće su 10-14% od sume odgovarajućih van der Waalsovih radijusa, dok su one koje uključuju jod vezan na alifatski lanac u jednom slučaju (V_{max}(X) od 391 kJ mol^{-1} e^{-1}) nešto kraće, a u drugom (V_{max}(X) od 310 kJ mol^{-1} e^{-1}) čak i duži od sume odgovarajućih van der Waalsovih radijusa (Slika 22b).

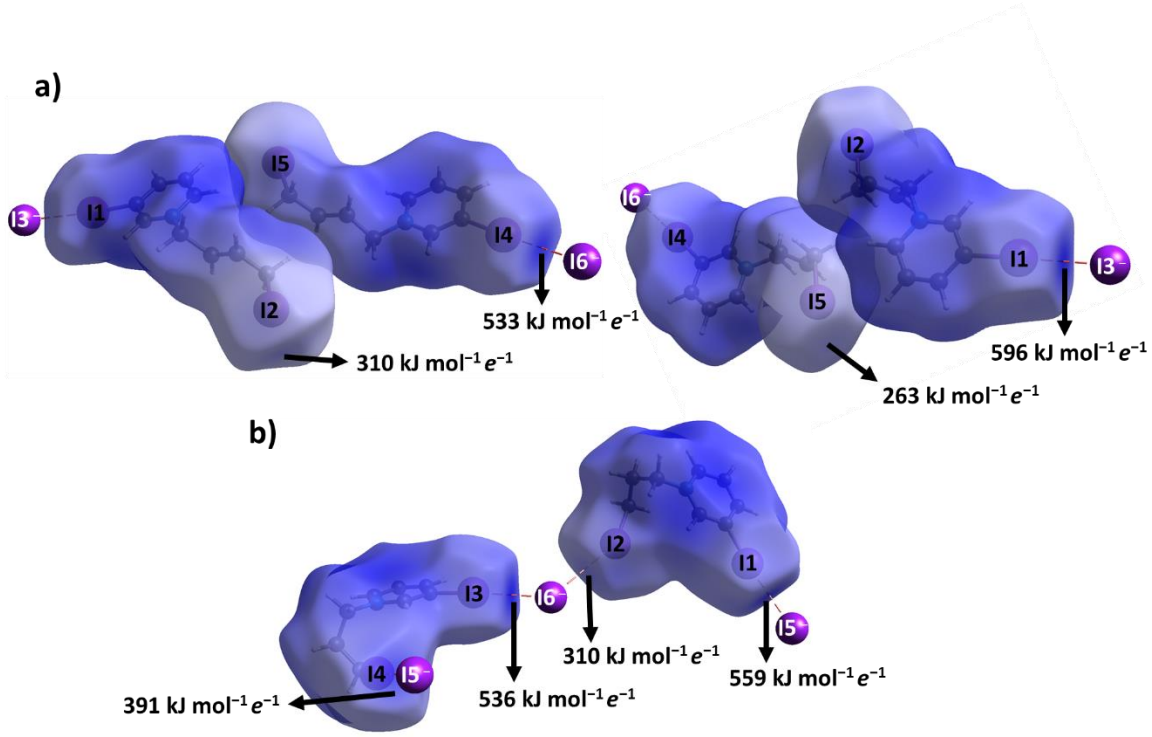

Slika 22. Hirshfeldove plohe s mapiranim *V* (izračinatim na razini teorije B3LYP-DGDZVP) za: a) kation [*N*-I**Buen**-(**3-IPy**)]$^+$ i b) kation [*N*-I**Prop**-(**3-IPy**)]$^+$.

Ako usporedimo halogenske veze C_{py}–I···I$^-$ u [*N*-I**Prop**-**3-IPy**]I i [*N*-I**Buen**-(**3-IPy**)]I, možemo vidjeti da kation [*N*-I**Buen**-(**3-IPy**)]$^+$ stvara nešto kraće halogenske veze s jodidnim anionima od kationa [*N*-I**Prop**-(**3-IPy**)]$^+$. Nadalje, iako su halogenske veze C_{py}–I···I$^-$ u [*N*-I**Prop**-**3-IPy**]I nešto duže od analogne halogenske veze u [*N*-Et-**3-IPy**]I, čini se da postoji trend da što je duži ugljikovodični lanac *N*-supstituiran na jodpiridinski prsten to su kraće halogenske veze C_{py}–I···I$^-$ u *N*-alkil-3-jodpiridinijevim jodidima (Slika 23). Vrijednosti *V* koje odgovaraju σ-šupljini joda (V_{max}(I)) na piridinijevom prstenu (mapirane na Hirshfeldove plohe ova četiri kationa) također prate isti trend, odnosno najpozitivnija σ-šupljina joda je u slučaju kationa [*N*-I**Buen**-(**3-IPy**)]$^+$, dok je najmanje pozitivna u slučaju kationa [*N*-Me-**3-IPy**]$^+$.

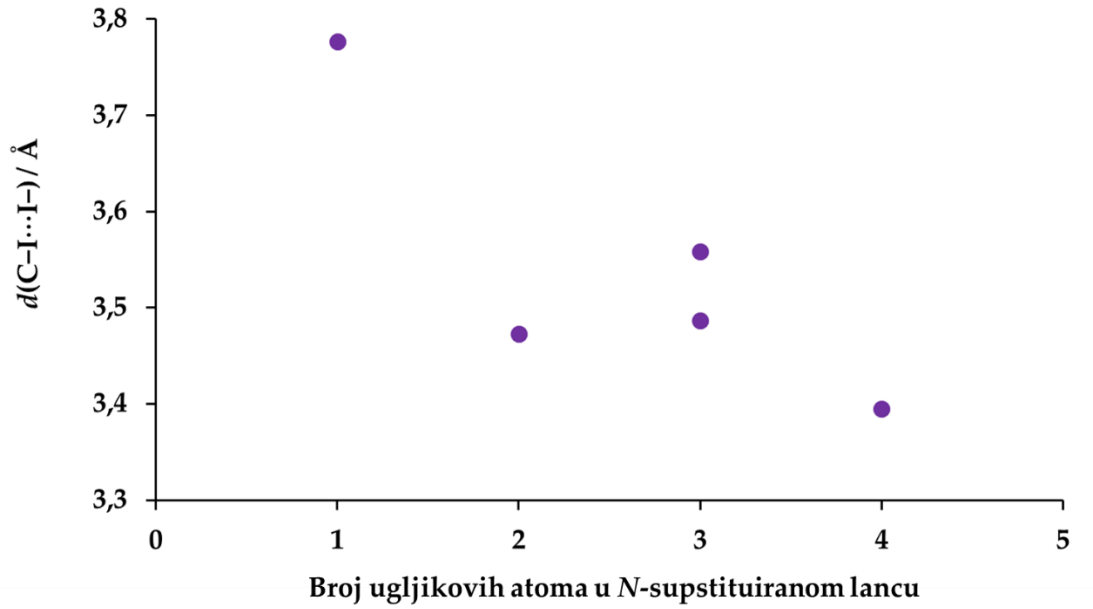

Slika 23. Ovisnost broja atoma ugljika *N*-supstituiranog alkilnog lanca *N*-alkil-3-iodpyridinijevih kationa i duljine halogenskih veza C–I···I⁻.

3.5. *N*-(4-halogenbenzil)-3-halogenpiridinijevi kationi – asimetrični ditopični donori halogenske veze

Istraživanjima objavljenim u znanstvenim radovima **I**, **II** i **III** pokazano je kako su *N*-protonirani i *N*-alkilirani halogenpiridini dobri donori halogenskih veza, pri čemu rezultati objavljeni u radu **III** pokazuju da su i asimetrični halogenpiridinijevi monokationi dobar sustav za izučavanje kationskih donora halogenske veze. Stoga je u ovom radu[b] priređena, te strukturno i termički izučena serija *N*-(4-halogenbenzil)-3-halogenpiridinijevih halogenida. Odabrani kationi potencijalni su donori dviju neekvivalentnih halogenskih veza – jedne s donornim atomom halogena vezanim na piridinski prsten (na kojem se očekuje lokalizacija većine pozitivnog naboja), i druge s donornim atomom halogena na benzilnom *N*-supstituentu.[114]

Kationi su pripravljeni reakcijom *meta*-halogenpiridina (Cl, Br i I) s (4-halogenbenzil) bromidima (Br i I) što je dalo niz od šest bromidnih soli *N*-(4-halogenbenzil)-3-halogenpiridinijevih kationa. Jodidi i kloridi pripravljeni su iz bromida ionskom izmjenom potencijalno dajući ukupno 18 spojeva koji se razlikuju samo po jednom ili više atoma halogena (Shema 3). Radi jednostavnosti, oni će se u cijelom tekstu označavati kao $X^1X^2X^3$, gdje je X^1 halogeni supstituent na benzilnom prstenu, X^2 supstituent na piridinskom prstenu, a X^3 halogenidni anion.

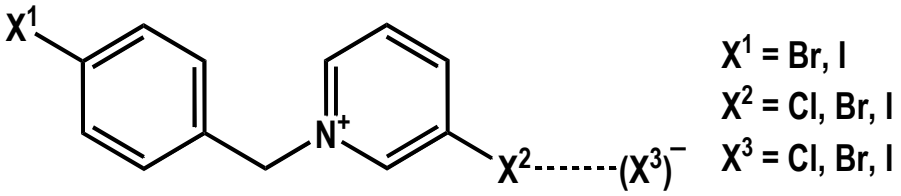

Shema 4. Opća formula ionskog para *N*-(4-halogenbenzil)-3-halogenpiridinijevih kationa i halogenidnog aniona povezanih halogenskom vezom. Na shemi su naznačene oznake tri različita atoma halogena koje se koriste dalje u tekstu.

[b] Ovaj znanstveni rad nalazi se u poglavlju Dodatak jer je prihvaćen za objavljivanje nakon odobrenja molbe za pisanje ove disertacije po skandinavskom modelu.

Svi bromidi i jodidi kristaliziraju kao jednostavne 1:1 soli bez kristalizacijskih molekula otapala. U slučaju kloridâ, međutim, utvrđeno je da ishod sinteze ovisi o halogenom supstituentu na piridinskom prstenu. Dva kationa izvedena iz 3-jodpiridina tako su dala jednostavne kloridne soli ekvivalentne jodidima i bromidima, za razliku od kationa izvedenih iz 3-brompiridina kada kloridi kristaliziraju kao hidrati ($IBrCl \cdot H_2O$ i $BrBrCl \cdot 1{,}5H_2O$). Dvije kloridne soli kationa dobivenih iz 3-klorpiridina nisu izolirane. Tako je od osamnaest mogućih kombinacija $X^1X^2X^3$ dobiveno ukupno 16 – 14 jednostavnih soli i dva hidrata.

Kako bi se procijenio potencijal atoma halogena na ovim kationima za stvaranje halogenskih veza, provedeni su DFT izračuni elektrostatskih potencijala kationa u vakuumu. Rezultati su pokazali da halogeni supstituenti na piridinskom prstenu u svim slučajevima imaju pozitivnije vrijednosti $V_{max}(X)$ u području σ-šupljina (V_{max}) od benzilnog supstituenta: za atom halogena vezan na piridinski prsten, vrijednosti $V_{max}(X^2)$ opadaju od joda (oko 435 kJ mol $^{-1}$ e^{-1}) preko broma (oko 400 kJ mol^{-1} e^{-1}) do klora (oko 360 kJ mol^{-1} e^{-1}) dok je u slučaju halogenih atoma na benzilnom supstituentu $V_{max}(X^1)$ oko 320 kJ mol^{-1} e^{-1} za jod i oko 290 kJ mol^{-1} e^{-1} za brom (Slika 24).

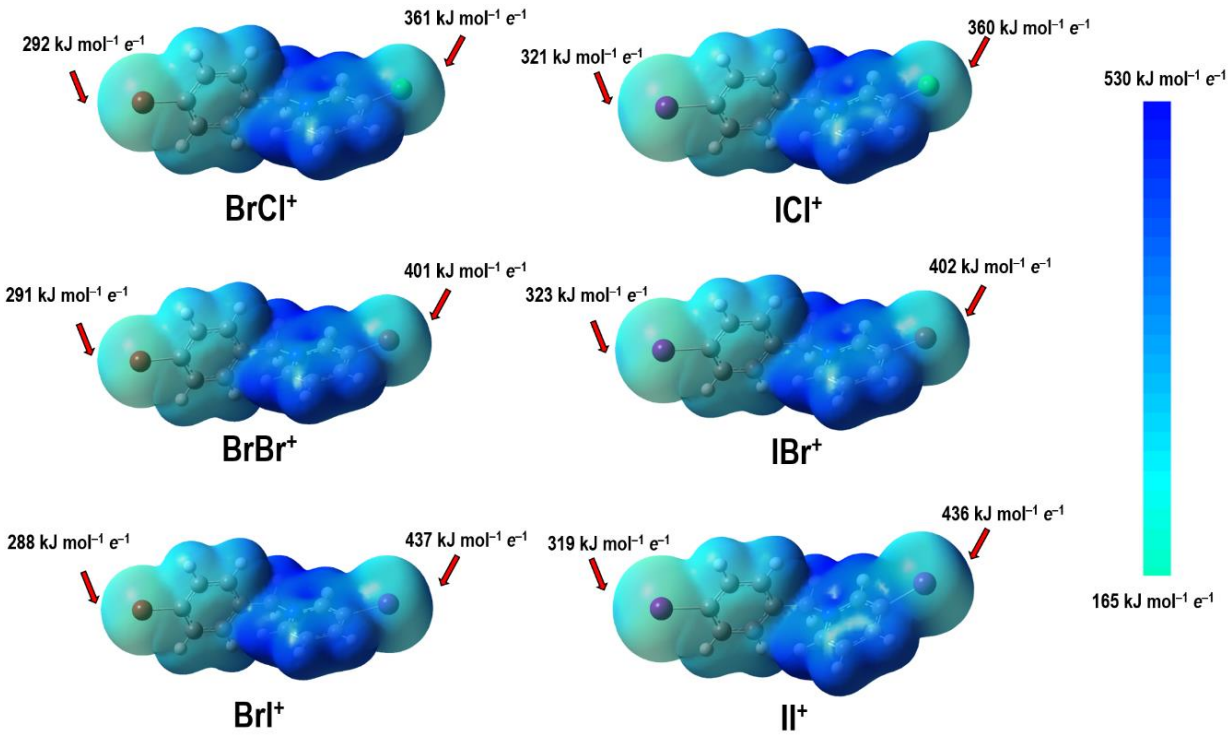

Slika 24. *V* mapiran na 0.002 *e* Å^{-3} izoplohu elektornske gustoće za šest kationa proučavanih u ovom radu s prikazanim vrijednostima V_{max} σ-šupljina za $\mathbf{X^1}$ i $\mathbf{X^2}$ atome halogena.

Stoga je očito da se od atoma halogena na piridinskom prstenu očekuje da formiraju jače halogenske veze, koje će posljedično tome imati dominantan doprinos u određivanju svojstava materijala. Navedeno je ilustrirano sintezom klorida − kako je od tri halogenidna aniona klorid najbolji akceptor vodikove veze, samo najjači donori halogenskih veza (jodpiridinijevi kationi) mogu u potpunosti zamijeniti molekule vode koje solvatiraju kloridne anione u otopini. Slabiji donori halogenskih veza (brompiridinijevi kationi) mogu zamijeniti samo dio vode u otapalu pritom dajući hidrate u kojima je klorid istovremeno akceptor halogenskih i vodikovih veza. Međutim, kada su prisutni samo najslabiji donori halogenih veza (klorpiridinijevi kationi), klorid ostaje potpuno hidratiziran čineći sol iznimno topljivom (i vjerojatno higroskopnom), što objašnjava neuspjeh izoliranja kloridnih soli kationa izvedenih iz 3-klorpiridina kao čvrstih produkata. Od 14 bezvodnih soli, 11 pripada jednoj izostrukturnoj seriji (tip I), a preostale tri drugoj (tip II). Prvi izostrukturni niz obuhvaća jodide svih 6 kationa i 5 bromida, dok drugi obuhvaća dva klorida i preostali bromid (IIBr). Kristalne strukture obje serije sadrže lance u kojima su kationi i anioni međusobno povezanim halogenskim vezama (Slika 25); svaki anion akceptor je dviju halogenskih veza, jedne halogenske veze $X^2\cdots(X^3)^-$ s atomom halogena piridinskog prstena, i druge halogenske veze $X^1\cdots(X^3)^-$ s atomom halogena benzilnog supstituenta. Uz dvije halogenske veze, halogenidni anion također je akceptor nekoliko slabih vodikovih veza $C{-}H\cdots(X^3)^-$ s kationima koji pripadaju susjednim lancima. Ove interakcije međusobno povezuju lance u tri dimenzije.

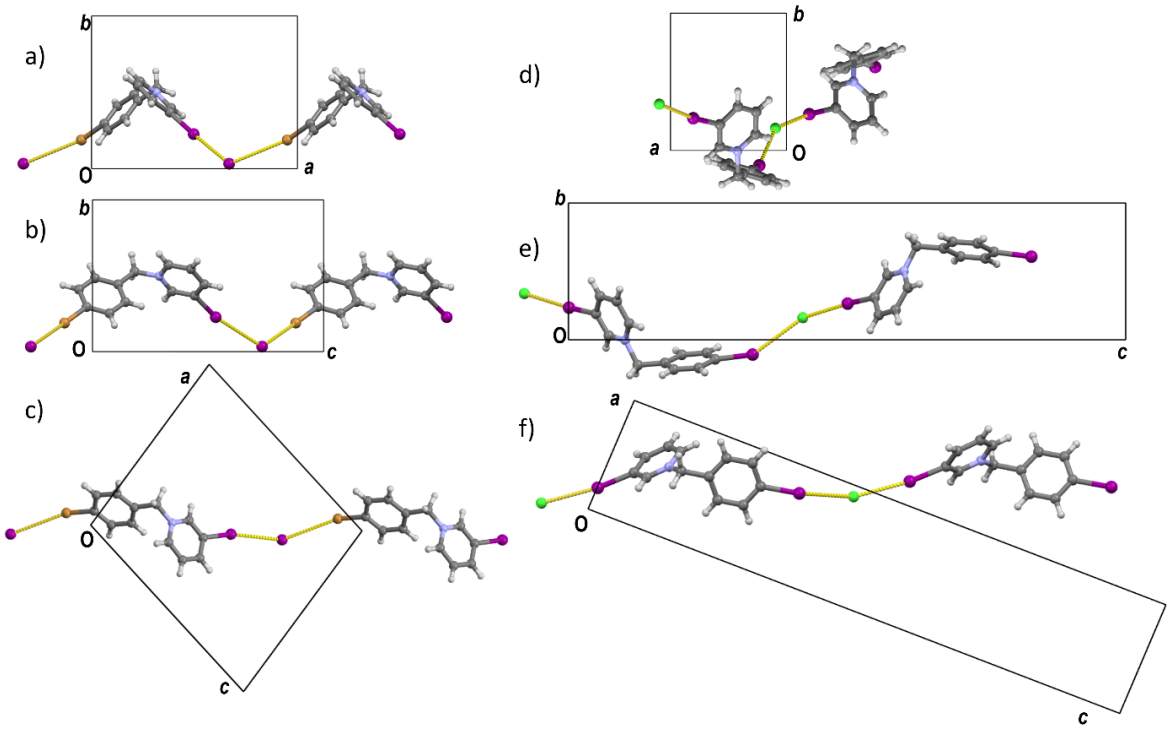

Slika 25. Položaj lanaca kationa i aniona povezanih halogenskom vezom u odnosu na jediničnu ćeliju kod struktura tipa I (u **BrII**; a), b) i c)) i kod struktura tipa II (u **IICl**; d), e) i f)). Pogled duž: a), d) kristalografske osi *c* ; b), e) kristalografske osi *a*; c), f) kristalografske osi *b*.

Kako bi se kvantificirala sličnost struktura 11 izosturkturnih soli tipa I, izračunali smo indekse sličnosti jediničnih ćelija:

$$\pi_{AB} = \left| (a_A+b_A+c_A)/(a_B+b_B+c_B)-1 \right|,$$

(gdje su a_A, b_A i c_A parametri jedinične ćelije strukture soli A, a a_B , b_B i c_B parametri jedinične ćelije strukture soli B) za svaki par struktura.

Uz indekse sličnosti jediničnih ćelija izračunati su i izostrukturnosni indeksi:

$$I_s(A,B)= \left| [\Sigma(\Delta R_{AB})^2/n]^{1/2} - 1 \right| \times 100\%$$

(gdje je ΔR_{AB} modul razlike radij-vektora ekvivalentnih atoma u strukturama A i B, a n broj uspoređivanih atoma), također za svaki par struktura.[115–119] Za izračun I_s, u obzir su uzeti svi atomi (osim vodika) jedinične ćelije (n = 56). Vrijednosti π_{AB} i I_s(A,B) za 11 kristala koji pripadaju strukturnom tipu I prikazane su u Tablici 3.

Tablica 3. Indeksi sličnosti jedinićnih ćelija (π_{AB}) i izostrukturnosni indeksi (I_s(A,B)) za 11 kristala koji pripadaju strukturnom tipu I. Za izračun I_s, u obzir su uzeti svi atomi (osim vodika) jedinične ćelije (n = 56).

Indeksi sličnosti ćelija (π·100)	Izostrukturnosni indeksi (I_s)										
	III	**BrII**	**BrBrI**	**IBrI**	**BrClI**	**BrIBr**	**IClI**	**IBrBr**	**BrBrBr**	**BrClBr**	**IClBr**
III		88.6	83.6	82.2	73.2	72.4	71.2	68.9	68.2	61.4	59.6
BrII	1.1		80.9	75.0	69.1	78.3	64.5	67.5	70.4	61.7	57.4
BrBrI	2.0	0.9		90.3	87.3	70.4	82.1	76.1	76.4	73.7	69.9
IBrI	0.9	0.2	1.1		87.2	64.9	88.0	75.5	72.3	71.3	70.8
BrClI	2.5	1.4	0.5	1.6		60.0	90.4	71.4	70.1	72.9	70.3
BrIBr	2.9	1.8	0.9	2.0	0.4		56.0	73.4	78.7	66.2	61.5
IClI	1.3	0.2	0.7	0.4	1.2	1.6		71.6	67.3	71.3	72.1
IBrBr	2.7	1.7	0.7	1.9	0.3	0.9	1.4		89.9	86.8	87.1
BrBrBr	4.0	2.9	2.0	3.1	1.5	1.1	2.7	1.3		87.0	80.9
BrClBr	4.6	3.5	2.6	3.7	2.1	1.9	3.3	1.9	0.6		89.7
IClBr	3.3	2.3	1.4	2.5	0.9	0.5	2.1	0.6	0.6	1.3	

Supstitucija Cl/Br/I dovodi do vrlo značajnih razlika u svojstvima soli kao donora, odnosno akceptora halogenske veze. U strukturama *N*-(4-halogenbenzil)-3-halogenpiridinijevih halogenida kationi i anioni međusobno su povezani u lance dvjema neekvivalentnim halogenskim vezama, čija bi jačina trebala rasti s povećanjem radijusa X^1 i X^2 (II^+ je očekivano najbolji donor) i sa smanjenjem radijusa X^3 (s Cl^- kao najboljim akceptorom). U slučaju halogenske veze koja uključuje piridinski atom halogena kao donor ($X^2\cdots(X^3)^-$), postoji gotovo savršeno linearna korelacija (R^2 = 0,996) između relativnih duljina halogenskih veza (d_{rel} = $d(X\cdots(X^3)^-)$ / [$r_{vdW}(X)$ + $r_{cryst}((X^3)^-)$]) i kuteva halogenskih veza. Oba geometrijska parametra prvenstveno ovise o X^2 (kutovi rastu od oko 156° za X^2 = Cl, preko oko 161° za X^2 = Br do oko 166° za X^2 = I, a relativne duljine od oko 96% za X^2 = Cl, preko oko 90% za X^2 = Br do oko 85% za X^2 = I). Promjena akceptora ima mnogo manji utjecaj na kut halogenske veze, veze koje uključuju bromid kao akceptor su nešto više savijene od onih koje uključuju jodid. (Slika

26a). Priroda X^1, s druge strane, gotovo da nema utjecaja ni na duljinu ni na kut halogenske veze $C–X^2\cdots(X^3)^-$, osim u seriji X^1ClX^3, gdje BrClI i BrClBr tvore nešto kraće i linearnije halogenske veze $X^2\cdots(X^3)^-$ od njihovih odgovarajućih 4-jodbenzilnih analoga (IClI i IClBr).

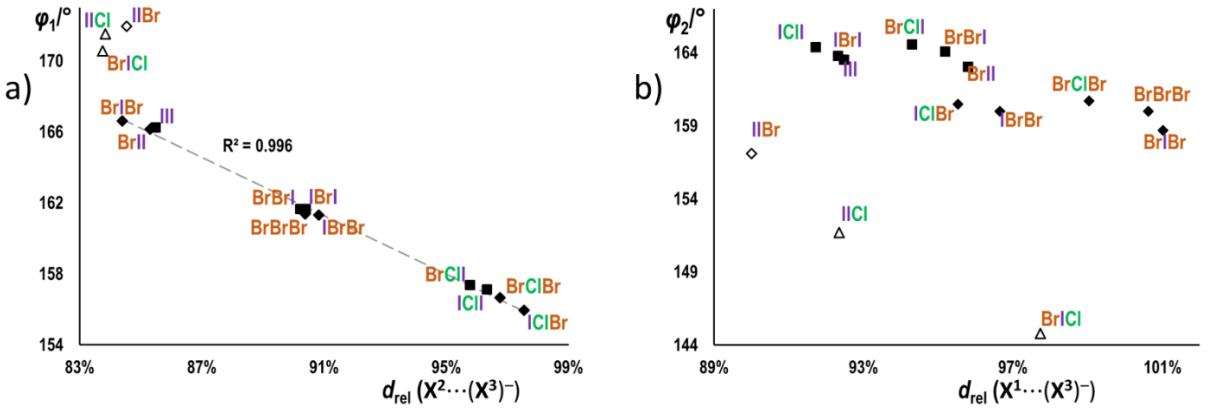

Slika 26. Korelacija relativnih duljina halogenskih veza (d_{rel} = $d(\mathbf{X}\cdots(\mathbf{X^3})^-)/[r_{vdW}(\mathbf{X})$ + $r_{cryst}((\mathbf{X^3})^-)$ kuteva halogenskih veza (φ) za halogenske veze s donornim atomom vezanim na: a) piridinski prsten ($C2–\mathbf{X^2}\cdots(\mathbf{X^3})^-$) i b) benzilni prsten ($C2–\mathbf{X^1}\cdots(\mathbf{X^3})^-$). Strukture tipa I prikazane su kao puni simboli, a strukture tipa II kao prazni simboli crnih rubova.

Halogenske veze koje uključuju benzilni atom halogena ($X^1\cdots(X^3)^-$) linearnije su (kutovi halogenskih veza kreću se u rasponu od oko 159°–165°), ali relativno duže (d_{rel} u rasponu od 92–101%). Međuovisnost veznih kutova u odnosu na relativne duljine slijedi isti opći trend kao u slučaju halogenske veze $X^2\cdots(X^3)^-$, premda sa znatno većim raspršenjem točaka na grafu (Slika 26b) i izraženijom ovisnošću o X^3 i X^2. Strukture s halogenom koji je jači donor halogenske veze (X^1 = I) općenito su relativno kraće i linearnije veze od onih s (X^1 = Br). Suprotno tome, strukture s jačim akceptorom (X^3 = Br) općenito su duže i manje linearne od onih s X^3 = I. Također postoji značajna ovisnost parametara halogenske veze $X^1\cdots(X^3)^-$ o X^2 – unutar svake skupine struktura koje se razlikuju samo po X^2, relativna duljina raste, a kut se smanjuje u nizu X^2 = Cl < Br < I. Sva ova opažanja, kao i (gotovo) savršena linearnost dijagrama $d_{rel}(X^2\cdots(X^3)^-)/\varphi_1$, ukazuju da je halogenska veza $X^2\cdots(X^3)^-$ dominantna interakcija u ovim kristalnim strukturama. Iz toga proizlazi da su strukturne razlike unutar niza struktura tipa II prvenstveno diktirane halogenskom vezom $X^2\cdots(X^3)^-$, dok se geometrije halogenskih veza $X^1\cdots(X^3)^-$ prilagođavaju promjenama kristalnog pakiranja s obzirom na razlike u halogenskim vezama $X^2\cdots(X^3)^-$. Tako su halogenske veze $X^2\cdots(X^3)^-$ s jačim akceptorom (bromidom) obično

kraće i linearnije od onih s jodidom, ali su $X^1\cdots(X^3)^-$ duže i manje linearne, jer unutar $X^2\cdots(X^3))^-\cdots X^1$ skupine jači akceptor (bromid) više privlači jači donor (X^2) čime se produljuje i deformira halogenska veza $X^1\cdots(X^3)^-$. Također, promjena X^2 utječe na geometriju halogenske veze $X1\cdots(X3)^-$ koja postaje nepovoljnija kako jačina donora halogenskih veza $X^2\cdots(X^3)^-$ raste, dok je halogenska veza $X^2\cdots(X^3)^-$ općenito neovisna o X^1. Ova dominacija halogenske veze $X^2\cdots(X^3)^-$ također je u skladu s izračunatim vrijednostima $V_{max}(X)$ koje su u svim slučajevima veće za halogen vezan na piridinski prsten nego za halogen vezan na benzilni prsten (Slika 24). Međutim, treba napomenuti da je razlika u V_{max} za X^2 = Cl i X^1 = I relativno mala (oko 12%), što ukazuje da bi u slučaju kationa izvedenog iz klorpiridina halogenska veza $I_{benzil}\cdots(X^3)^-$ mogla donekle konkurirati halogenskoj vezi $Cl_{piridin}\cdots(X^3)^-$. Čini se da to doista i jest slučaj budući da u seriji X^1ClX^3 parametri halogenske veze $Cl_{piridin}\cdots(X^3)^-$ očito više ovise o prirodi X^1, budući da su nešto duži i manje linearni kada je X^1 = I, nego kada je X^1 = Br (u svakom paru s identičnim X^3).

S obzirom na njegovu veličinu, izostrukturni niz struktura tipa I idealan je sustav na kojem se može istražiti postoji li jasan i mjerljiv učinak malih promjena u halogenskoj vezi na termička svojstva soli koje pripadaju tipu I. Kako je unutar izostrukturnog niza jedina značajna razlika u donorima i akceptorima halogenskih veza, može se očekivati da će razlike u energijama halogenskih veza u različitim kristalima biti dominantan uzrok razlika u njihovim termičkim svojstvima. Termička analiza (TG i DSC) soli tipa I pokazala je da 9 od 11 ovih soli kontinuirano gubi masu (vidljivo u TG-u) u temperaturnom rasponu od 170 do 200 °C bez prethodnih termičkih promjena. DSC krivulje općenito pokazuju dva endotermna signala koji vjerojatno odgovaraju gotovo istovremenom taljenju i isparavanju. U slučaju dva spoja (III i BrIBr) DSC krivulja je složenija, s dodatnim signalima na nižim temperaturama i također nešto nižim temperaturama taljenja/isparavanja (163 °C odnosno 169 °C). Budući da se njihovo toplinsko ponašanje očito razlikuje od ostalih članova serije, isključeni su iz daljnje analize podataka. Postoji jasna linearna korelacija između $E(X^2\cdots X^3)$ i entalpija isparavanja unutar struktura tipa I (Slika 27a), što je posebno vidljivo kada se uspoređuju strukture koje se razlikuju samo po X^2 (za BrII–BrBrI–BrClI niz, R^2 = 0,997). Razlike u entalpijama isparavanja između spojeva koji se razlikuju samo u X^2 općenito su slične odgovarajućim razlikama u $E(X^2\cdots X^3)$. Što se tiče slabije halogenske veze ($X^1\cdots(X^3)^-$), ne postoji jasna korelacija između entalpija isparavanja i izračunatih energija interakcije plinske faze $E(X^1\cdots X^3)$. Međutim, priroda X1 također neznatno utječe na entalpiju isparavanja. Budući da unutar svakog para struktura

BrX2X3 / IX^2X^3 analog IX^2X^3 ima veću entalpiju isparavanja (za 3,5-12,5 kJ mol^{-1}), jasno je da postoji mjerljiv doprinos halogenske veza $X^1\cdots(X^3)^-$ ukupnoj energiji pakiranja. Na entalpiju isparavanja također značajno utječe priroda halogenida (tj. akceptora halogenskih veza) – dok slijede isti trend s obzirom na $E(X^2\cdots X^3)$, bromidi sustavno imaju veće entalpije isparavanja od jodida. S obzirom da se to ne može objasniti razlikom u halogenskim vezama, najvjerojatniji uzrok ove razlike u entalpijama isparavanja između jodida i bromida leži u razlici između energija vodikovih veza $C{-}H\cdots X^-$. U svim strukturama anion, zajedno s halogenskim vezama unutar lanca, također tvori vodikove veze $C{-}H\cdots X^-$ s kationima iz susjednih lanaca. Kako je bromid jači akceptor vodikove veze od jodida, potrebno je više energije da bi se prekinule vodikove veze $C{-}H\cdots Br^-$, što naposlijetku dovodi do viših ukupnih vrijednosti entalpija isparavanja. Za razliku od entalpija isparavanja kojima jasno dominira doprinos halogenskih veza $X^2\cdots(X^3)^-$, temperature pri kojima započinje taljenje/isparavanje ne mijenjaju se u nekim očitim trendom (Slika 27b). Za jače halogenske veze $X^2\cdots(X^3)^-$ (s X^2 = Br, I), početne temperature očekivano rastu s $E(X^2\cdots X^3)$, opet s jodbenzilnim derivatima na nešto višim temperature pri kojima započinje taljenje/isparavanje od njihovih brombenzilnih analoga (za 6–7,5 °C). Međutim, u slučaju slabijih halogenskih veza $X^2\cdots(X^3)^-$ (s X^1 = Cl) trend je suprotan – temperature pri kojima počinje taljenje/isparavanje opadaju s $E(X^2\cdots X^3)$. Razlike u temperaturama pri kojima započinje taljenje/isparavanje unutar parova BrX^2X^3 / IX^2X^3 također su veće (za 7,5–17,5 °C). Potonje opažanje je u skladu s većim doprinosom halogenske veze $X^1\cdots(X^3)^-$ ukupnoj energiji pakiranja (zbog smanjenog doprinosa halogenske veze $X^2\cdots(X^3)^-$ zbog relativno nižeg $\boldsymbol{V}_{max}$(Cl) – vidi rasprava iznad). Međutim, nešto je teže objasniti povećanje početnih temperatura sa smanjenjem $E(X^2\cdots X^3)$ među derivatima klorpiridina. Kako se entalpije isparavanja pravilno mijenjaju s $E(X^2\cdots X^3)$, najvjerojatniji razlog različitog trenda u temperaturama početka taljenja/isparavanja je drugačiji trend entropije rešetke. Može se očekivati da je unutar serije X^1ClX^3 entropija rešetke viša (zbog manjih ograničenja gibanja u slabije povezanim strukturama), te da raste sa smanjenjem $E(X^2\cdots X^3)$. Kako entropija rešetke raste, promjena entropije nakon taljenja/isparavanja se smanjuje, što bi moglo uzrokovati povećanje temperature faznog prijelaza. Međutim, budući da su u skladu s navedenom razlikom samo četiri mjerenja, ne može se isključiti mogućnost da je riječ o prividnom trendu koji je artefakt nasumične distribucije.

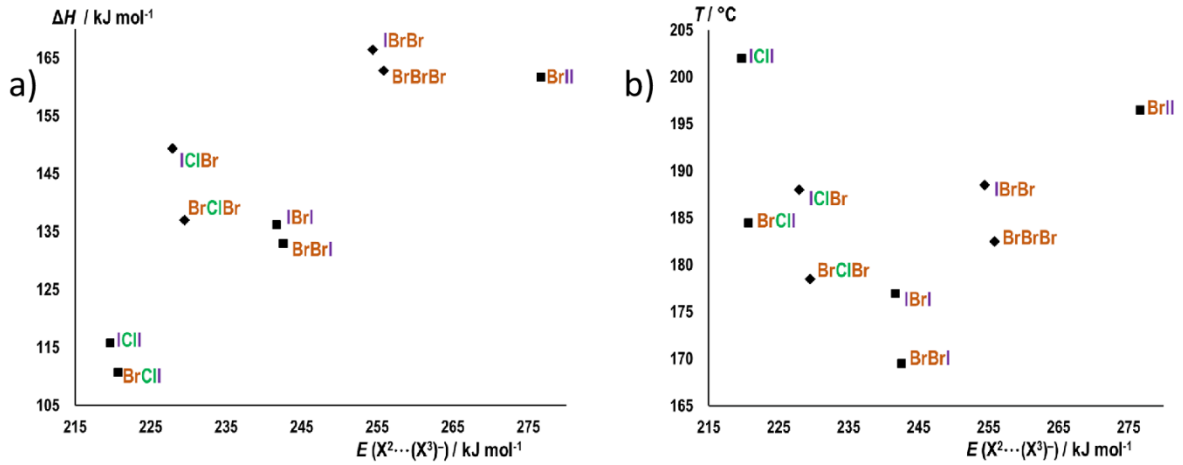

Slika 27. Korelacija računatih energija $\mathbf{X^2}\cdots(\mathbf{X^3})^-$ halogenskih veza (računate *in vacuo* za geometrije pronađene u kristalnim strukturama, $E(\mathbf{X^2}\cdots(\mathbf{X^3})^-)$) i: a) entalpije isparavanja ($\Delta \boldsymbol{H}$), b) temperature pri kojima započinje taljenje/isparavanje (T) za strukture tipa I. Strukture jodidnih soli prikazane su kao kvadrati, a bromidnih soli kao rombovi.

3.6. Primjena halogenpiridinijevih kationa u kristalnom inženjerstvu – halogenpiridinijevi heksacijanoferati

Analozi Berlinskog modrila intenzivno se proučavaju tijekom posljednjih desetljeća jer se pokazalo da imaju brojne potencijalne primjene kao elektrodni materijali,[120–126] molekulski magneti,[127–133] fotoosjetljive magnetske krutine,[134–138] molekulska sita,[139–141] protuotrovi za radioaktivne metale[142–144] te kao materijali za skladištenje plinova.[145–148] Većina strategija za dizajniranje takvih materijala temelji se na svojstvu da su policijanometalati (npr. heksacijanoferatni anioni) Lewisove baze te se stoga koriste kao premošćujući ligandi za formiranje koordinacijskih mreža,[149–163] ali i kao akceptori vodikovih veza.[164–172] Nedavno je pokazano da se strategija dizajniranja derivata heksacijanoferata(II) može temeljiti na djelomično protoniranim heksacijanoferatnim(II) anionima koji su ujedno i donori vodikovih veza.[173] To u principu dovodi do formiranja lanaca ili mreža (dvo- i trodimenzijskih) aniona, međusobno povezanih simetričnim vodikovim vezama [Fe−CN···H···NC−Fe].[174–176] Utvrđeno je da su najčešći strukturni motiv dvodimenzijske mreže $H_2[Fe(CN)_6]^{2-}$ aniona u kojima je svaki anion i donor i akceptor po dvije vodikove veze [Fe−CN···H· ··NC−Fe], pri čemu dva preostala cijanidna liganda (ortogonalna u odnosu na mrežu) ostaju raspoloživa za stvaranje vodikovih veza s kationima ili molekulama otapala. Kristalno pakiranje u takvim strukturama prvenstveno je određeno bazičnošću korištene baze, ali i sposobnošću kationa i molekula otapala da tvore vodikove veze. Upravo zbog toga pokazalo se da je ciljana sinteza željenih struktura ili stupnja protoniranosti heksacijanoferatih aniona neizvediva s obzirom da upotreba sličnih Lewisovih baza (sličnog kemijskog sastava i bazičnosti) dovodi do produkata značajno različite strukture i stehiometrije.

Moguća metoda za postizanje višeg stupnja kontrole mogla bi biti korištenje halogenpiridina kao baza. Unutar svake serije halogenpiridina (*o*-, *m*-, *p*-), postoji vrlo mala varijabilnost bilo pK_a vrijednosti, molekulskog volumena ili molekulske geometrije, a jedina značajna varijabla koja se mijenja unutar serije je potencijal halogenpiridina za sudjelovanje u halogenskim vezama. Budući da su policijanometalati Lewisove baze (s neveznim elektronskim parovima na cijanidnim skupinama) očekuje se da su i potencijalni akceptori halogenskih veza što i jest slučaj u heksacijanoferatnim solima *N*-alkiliranih derivata halogenpiridina gdje su heksacijanoferati protuioni halogenpiridinijevim kationima, a ujedno i donori halogenske veze.[85,86] Stoga bi protonirani halogenpiridini također trebali formirati halogenske veze s heksacijanoferatnim anionima pri čemu se očekuje da će nastati strukture koje se sastoje od

mreža djelomično protoniranih heksacijanoferatnih aniona povezanih vodikovim vezama [Fe–CN···H···NC–Fe].

U ovoj studiji, koja je objavljena u radu **IV**, istraženo je može li korištenje (protoniranih) halogenpiridina kao protuiona doista dovesti do višeg stupnja kontrole strukture u odgovarajućim heksacijanoferatnim solima s obzirom da je u radu **I** pokazano da mogu stvarati i vodikove i halogenske veze s anionima. Istraživanje je uključilo *o*- i *m*-halogenpiridine (Cl, Br i I), kao i *p*-jodpiridin, kako bi se utvrdio i učinak položaja i prirode atoma halogena.

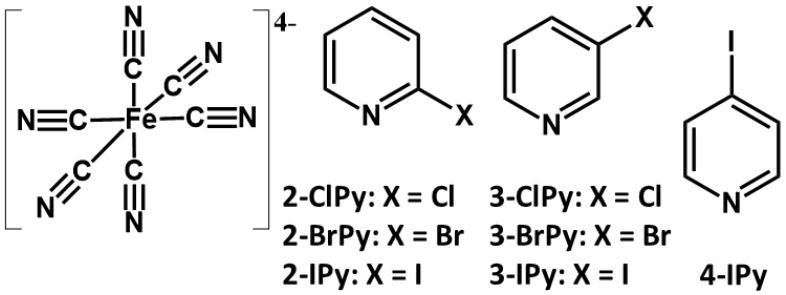

Shema 5. Heksacijanoferatni(II) anion i halogenpiridini korišteni u ovom istraživanju.

Tri *o*-halogenpiridina dala su tri izrazito različite heksacijanoferatne soli sa značajnim razlikama u strukturi, ali i u kemijskom sastavu. *o*-Klorpiridin u reakciji s heksacijanoželjezovom(II) kiselinom dao je dvosol koja se sastoji od potpuno deprotoniranih aniona $[Fe(CN)_6]^{4-}$ te piridinijevih i oksonijevih (H_3O^+) kationa – (**2-ClPy**)$_2$(PyH)$_2$(H_3O)$_2$($[Fe(CN)_6]^{2-}$). Heksacijanoferatni anioni i oksonijevi kationi povezani su u trodimenzijsku mrežu vodikovim vezama pri čemu svaki oksonijev kation premošćuje tri heksacijanoferatna aniona, a svaki heksacijanoferatni anion veže šest oksonijevih kationa. Kanali u ovoj mreži ispunjeni su kationima [**2-ClPy**···H···**Py**]$^+$, koji sadrže molekule 2-klorpiridina i piridina međusobno povezane vodikovim vezama N···H···N (Slika 28). Prisutnost nesupstituiranog piridina u strukturi prilično je iznenađujuća budući da u reakcijsku smjesu nije dodan piridin. Kako su kristali dobiveni tek nakon nekoliko tjedana, vjerojatno je da se **2-ClPy** djelomično razgradio u prisutnosti heksacijanoželjezove(II) kiseline tijekom pri čemu je nastao piridin. Atomi klora kationa [**2-ClPy**···H···**Py**]$^+$ ne stvaraju halogenske veze s okolnim potencijalnim akceptorima, nego vrlo duge interhalogene kontakte (Cl···Cl) tipa I.

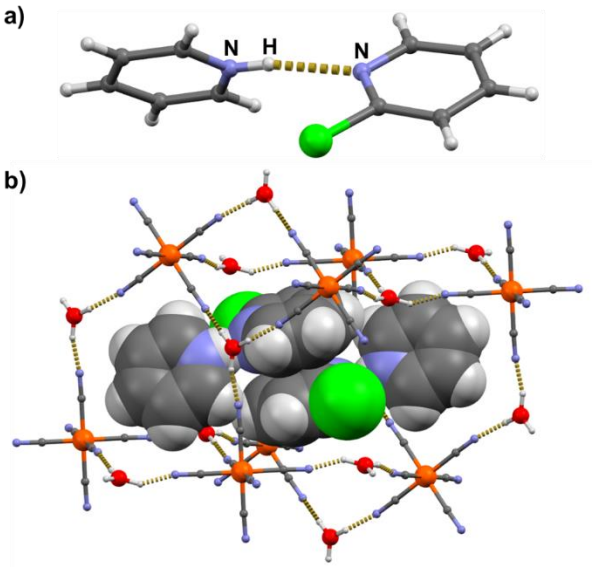

Slika 28. Kristalna struktura soli (**2-ClPy**)$_2$(PyH)$_2$(H$_3$O)$_2$([Fe(CN)$_6$]): a) kationi [**2-ClPy**···H···**Py**]$^+$; b) par kationa [**2-ClPy**···H···**Py**]$^+$ koji ispunjavaju kanale u mreži kationa H$_3$O$^+$ i aniona [Fe(CN)$_6$]$^{4-}$ povezanih vodikovim vezama.

Za razliku od **2-ClPy**, heksacijanoferatna sol **2-BrPy** ((**2-Brpy**)$_5$(**2-BrPy**H)$_3$(H$_3$[Fe(CN)$_6$])$_3$) nastala je unutar nekoliko sati. U strukturi se nalazi kvazi-kubična trodimenzijska mreža aniona H$_3$[Fe(CN)$_6$]$^-$ povezanih vodikovim vezama, a šupljine u mreži popunjavaju protonirane i neutralne molekule **2-BrPy**. Iako je samo jedan protonirani **2-BrPy** potreban kao protuion svakom anionu, stvarni omjer kationa **2-BrPy**H$^+$ i aniona je 8:3. Polovica **2-BrPy** međusobno je povezana vodikovim vezama N···H···N u katione [**2-BrPy**···H···**2-BrPy**]$^+$, analogne kationima [**2-ClPy**···H···**Py**]$^+$ u **I**. Na svaki od ovih kationa vezana je još jedna molekula **2-BrPy** vodikovom vezaom C–H···N (Slika 29). Preostale molekule **2-BrPy** su u neredu, a polovica simetrijski ekvivalentnih molekula je protonirana. U strukturi (**2-ClPy**)$_2$(PyH)$_2$(H$_3$O)$_2$([Fe(CN)$_6$]) postoji više (relativno dugih) halogenskih veza i interhalogenih kontakata tipa II (Br···Br) koji međusobno povezuju parove kationa [**2-BrPy**···H···**2-BrPy**]$^+$ što dovodi do stvaranja heksamera [(**2-BrPy**)$_4$(**2-BrPy**H)$_2$]$^{2+}$.

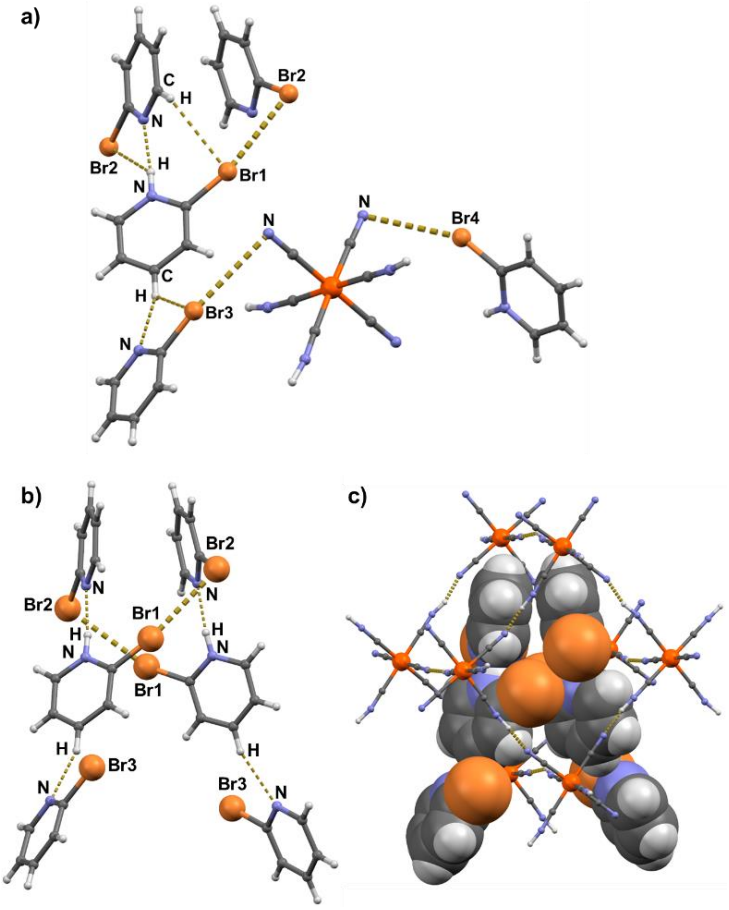

Slika 29. Kristalna struktura soli (**2-Brpy**)$_5$(**2-BrPy**H)$_3$(H$_3$[Fe(CN)$_6$])$_3$: a) molekule **2-BrPy,** kationi 2-**BrPy**H$^+$ i anioni H$_3$[Fe(CN)$_6$]$^{2-}$ povezani halogenskim i vokikovim vezama; b) heksameri [(**2-BrPy**)$_4$(**2-BrPyH**)$_2$]$^{2+}$ povezani halogenskim i vodikovim vezama; c) heksameri [(**2-BrPy**)$_4$(**2-BrPyH**)$_2$]$^{2+}$ ispunjavaju šupljine u anionskoj mreži načinjenoj od aniona H$_3$[Fe(CN)$_6$]$^-$ povezanih vodikovim vezama.

Upotrebom još jačeg donora halogene veze − **2-IPy** − dobivena je sol (**2-IPy**H)$_2$(H$_2$[Fe(CN)$_6$]) u kojoj je prisutnost halogenske veze još izraženija (Slika 30a,b). Ovdje su anioni H$_2$[Fe(CN)$_6$]$^{2-}$ povezani vodikovim vezama u slojeve. Svaki anion vodikovim vezama N···H···N veže dva kationa **2-IPy**H$^+$ u aksijalnim pozicijama što postavlja jod kationa u pogodan položaj da formira bifurkiranu halogensku vezu s dva cijanidna liganda susjednih aniona. Iako su te halogenske veze prilično duge i (očekivano) slabe, rezultiraju laganim izobličenjem slojeva aniona H$_2$[Fe(CN)$_6$]$^{2-}$.

Korištenje *m*-halogenpiridina umjesto *o*-halogenpiridina smanjuje steričke prepreke za sudjelovanje halogenpiridinijevih kationa u halogenim vezama, odnosno olakšavanje stvaranje halogenskih veza između kationa i aniona. Konkretno, u slučaju struktura u kojima anioni tvore slojeve (kao što je u (**2-IPy**H)$_2$(H$_2$[Fe(CN)$_6$])), kationi bi mogli biti mostovi između tih slojeva. **3-ClPy** je u reakciji s heksacijanoželjezovom(II) kiselinom dao sol (**3-ClPy**H)$_2$(MeOH)(H$_2$[Fe(CN)$_6$]$^{2-}$) koja sadrži anion H$_2$[Fe(CN)$_6$]$^{2-}$ povezane vodikovim vezama u slojeve slične onima u (**2-IPy**H)$_2$(H$_2$[Fe(CN)$_6$]) (Slika 30c,d). U strukturi postoje dva simetrijski neovisna aniona koji vodikovim vezama vežu po par kationa, jedan direktno a drugi preko vodikovih veza s hidroksilnim skupinama molekula etanola koje premošćuju između kationa i aniona. Međutim, od dva neovisna kationa **3-ClPy**H$^+$, niti jedan atom klora ne sudjeluje ni u kakvim međumolekulskim kontaktima.

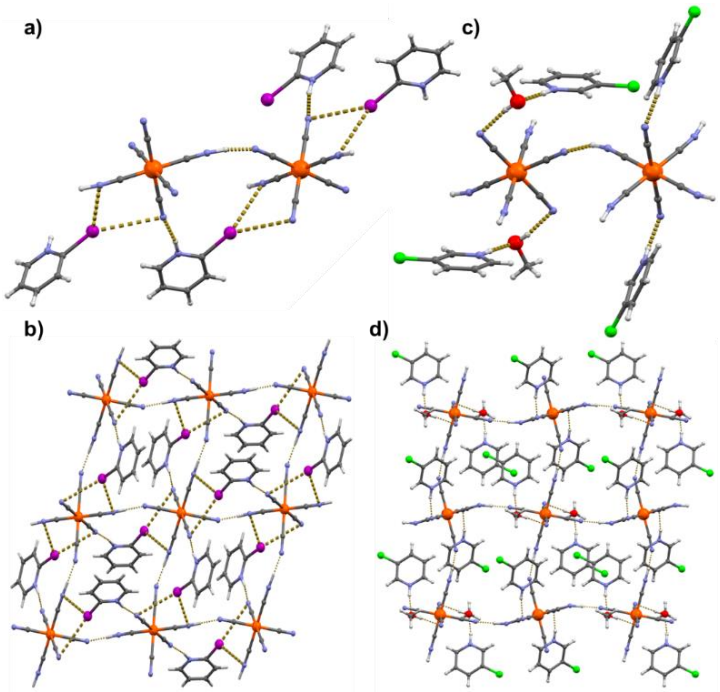

Slika 30. Kristalne strukture soli (**2-IPy**H)$_2$(H$_2$[Fe(CN)$_6$]) i (**3-ClPy**H)$_2$(MeOH)(H$_2$[Fe(CN)$_6$]): a) Kationi i anioni povezani halogenskim i vodikovim vezama (**2-IPy**H)$_2$(H$_2$[Fe(CN)$_6$]); b) Mreža aniona H$_2$[Fe(CN)$_6$]$^{2-}$ povezanih vodikovim vezama na koju su vodikovim i halogenskom vezom vezani kationi **2-IPy**H$^+$ in (**2-IPy**H)$_2$(H$_2$[Fe(CN)$_6$]); c) Kationi **3-ClPy**H$^+$, anioni H$_2$[Fe(CN)$_6$]$^{2-}$ i molekule metanola povezane vodikovim vezama u (**3-ClPy**H)$_2$(H$_2$[Fe(CN)$_6$]); d) Kationi **3-ClPy**H$^+$ i molekule MeOH povezane sa slojevima aniona H$_2$[Fe(CN)$_6$]$^{2-}$ u (**3-ClPy**H)$_2$(H$_2$[Fe(CN)$_6$]).

3-BrPy i **3-IPy** dali su par izostrukturnih hidrata, ((**3-BrPy**H)$_2$(H$_2$O)$_2$(H$_2$[Fe(CN)$_6$]) i (**3-IPy**H)$_2$(H$_2$O)$_2$(H$_2$[Fe(CN)$_6$])) koji u strukturama također (kao i (**3-ClPy**H)$_2$(MeOH)(H$_2$[Fe(CN)$_6$])) sadrže anione H$_2$[Fe(CN)$_6$]$^{2-}$. Međutim, ovdje oni nisu izravno povezani u slojeve nego se između aniona nalaze molekule vode koje premošćuju dva aniona H$_2$[Fe(CN)$_6$]$^{2-}$, pri čemu svaka molekula vode djeluje kao akceptor N–H···O i donor O–H···N vodikovih veza (slika 4a). Za razliku od kationa **3-ClPy**H$^+$ u (**3-ClPy**H)$_2$(MeOH)(H$_2$[Fe(CN)$_6$]), ovdje kationi stvaraju halogenske veze C–X···N s okolnim anionima. Međutim, oni međusobno ne povezuju slojeve, već dodatno povezuju anione unutar slojeva: svaki se kation veže na dva aniona (Slika 31). Izbor halogenpiridina u ovim strukturama ima značajan utjecaj na duljinu halogenskih veza pri čemu je kontakt I···N relativno kraći 11,6%, a kontakt Br···N 7,2% (u odnosu na sumu odgovarajućih van der Waalsovih radijusa). Razlika u jačini halogenske veze također neznatno utječe na vodikovu vezu između kationa i aniona, pri čemu je N–H···N vodikova veza duža u (**3-IPy**H)$_2$(H$_2$O)$_2$(H$_2$[Fe(CN)$_6$]) od one u (**3-BrPy**H)$_2$(H$_2$O)$_2$(H$_2$[Fe(CN)$_6$]).

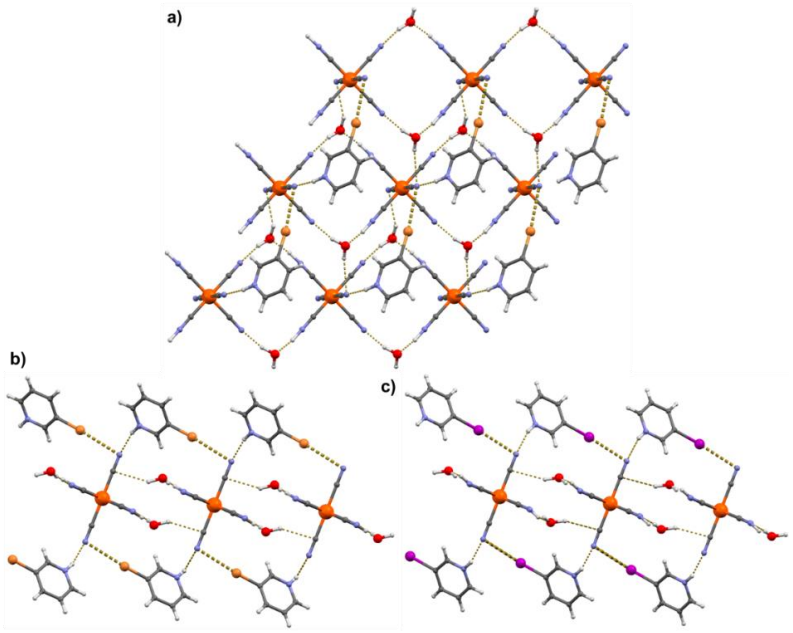

Slika 31. Kristalne strukture soli (**3-BrPy**H)$_2$(H$_2$O)$_2$(H$_2$[Fe(CN)$_6$]) i (**3-IPy**H)$_2$(H$_2$O)$_2$(H$_2$[Fe(CN)$_6$]): a) Mreža aniona H$_2$[Fe(CN)$_6$]$^{2-}$ i molekula vode s vodikovim i halogenskim vezama povezanim kationima **3-BrPy**H$^+$ u (**3-BrPy**H)$_2$(H$_2$O)$_2$(H$_2$[Fe(CN)$_6$]) (identično kao kationi **3-IPy**H$^+$ u (**3-IPy**H)$_2$(H$_2$O)$_2$(H$_2$[Fe(CN)$_6$])); b) Halogenskim i vodikovim vezama kationi **3-BrPy**H$^+$ premošćuju anionske lance u (**3-**

BrPyH)$_2$(H$_2$O)$_2$(H$_2$[Fe(CN)$_6$]); c) Halogenskim i vodikovim vezama kationi **3-IPy**H$^+$ premošćuju anionske lance u (**3-IPy**H)$_2$(H$_2$O)$_2$(H$_2$[Fe(CN)$_6$])**.**

Kada je **4-IPy** korišten kao baza, dobiven je metanolni solvat (**4-IPy**H)$_2$(MeOH)(H$_2$[Fe(CN)$_6$]) (Slika 32). Slično kao kod (**2-IPy**H)$_2$(H$_2$[Fe(CN)$_6$]) i (**3-ClPy**H)$_2$(MeOH)(H$_2$[Fe(CN)$_6$]), struktura se sastoji od aniona H$_2$[Fe(CN)$_6$]$^{2-}$ povezanih vodikovim vezama u slojeve. Cijanidni ligandi, koji nisu uključeni u vodikove veze između aniona, akceptori su vodikove veze N–H···N s kationom **4-IPyH**$^+$ i vodikove veze O–H···N s molekulom metanola (otapala). Ovdje atom joda kationa **4-IPy**H$^+$ sudjeluje u halogenskoj vezi s cijanidnim ligandom koji pripada susjednom anionskom sloju što (**4-IPy**H)$_2$(MeOH)(H$_2$[Fe(CN)$_6$]) čini jedinom strukturom u kojoj su slojevi heksacijanoferatnih aniona (povezanih vodikovim vezama) premošteni halogenskim vezama C–I···N pri čemu nastaje trodimenzijska mreža.

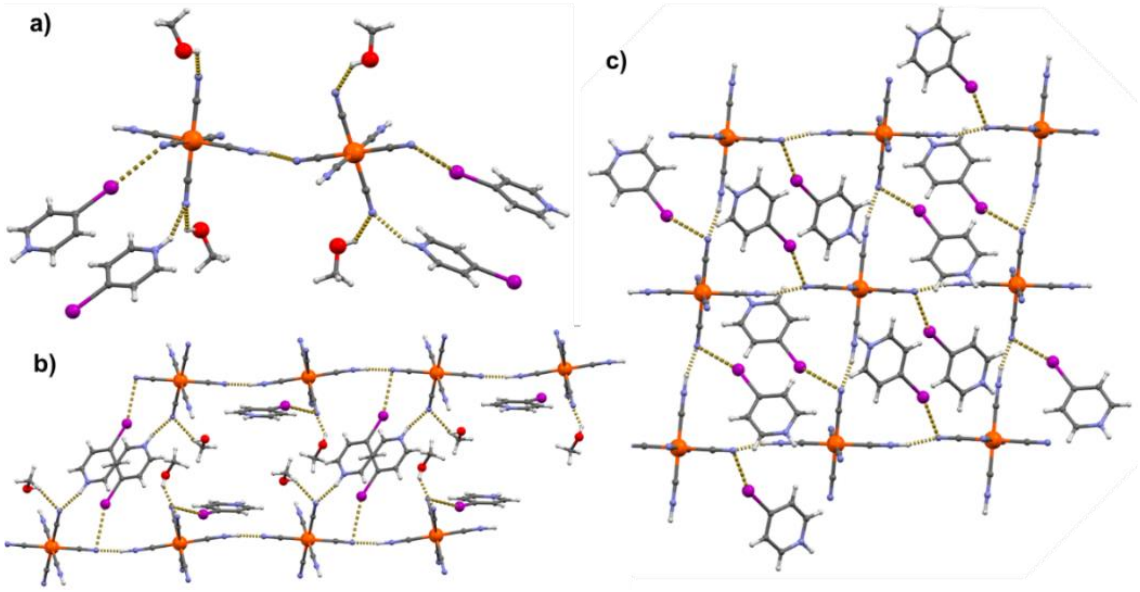

Slika 32. Kristalna struktura soli (**4-IPy**H)$_2$(MeOH)(H$_2$[Fe(CN)$_6$]): a) Halogenskim i vodikovim vezama povezani kationi **4-IPy**H$^+$, anioni H$_2$[Fe(CN)$_6$]$^{2-}$ i molekule metanola; b) Mreža aniona H$_2$[Fe(CN)$_6$]$^{2-}$ na koju se halogenskim i vodikovim vezama vežu kationi **4-IPy**H$^+$; c) Slojevi aniona H$_2$[Fe(CN)$_6$]$^{2-}$ povezanih vodikovim vezama koji su premošteni halogenskim vezama s kationima u trodimenzijsku struktru.

Sedam dobivenih soli pokazuje znatno veću strukturnu varijabilnost nego što se očekivalo samo s obzirom na sličnost korištenih halogenpiridina. Međutim, postoje neke pravilnosti koje su vrijedne razmatranja. Heksacijanoferatne mreže koje se nalaze u strukturama može se razvrstati u četiri tipa (slika 33.). U tri strukture (**2-IPy**H)$_2$(H$_2$[Fe(CN)$_6$]), (**3-ClPy**H)$_2$(MeOH)(H$_2$[Fe(CN)$_6$]i (**4-IPy**H)$_2$(MeOH)(H$_2$[Fe(CN)$_6$])) nalazi se općenito najčešći motiv jednostavnih dvodimenzijskih mreža aniona H$_2$[Fe(CN)$_6$]$^{2-}$ povezanih vodikovim vezama (označeno s c na slici 33). Drugi tip (označen *c* na slici 33) su dvodimenzijske mreže u kojima su vodikovim vezama povezani anioni H$_2$[Fe(CN)$_6$]$^{2-}$ i molekule vode prisutne u (**3-BrPy**H)$_2$(H$_2$O)$_2$(H$_2$[Fe(CN)$_6$]) i (**3-IPy**H)$_2$(H$_2$O)$_2$(H$_2$[Fe(CN)$_6$]). Preostale dvije strukture sadrže trodimenzijske mreže izvedene iz odgovarajućih dvodimenzijskih mreža: pseudokubičnu mrežu aniona H$_3$[Fe(CN)$_6$]$^-$ u II (b na slici 33) i trodimenzijsku mrežu aniona [Fe(CN)$_6$]$^{4-}$ i oksonijevih kationa u (**2-ClPy**)$_2$(PyH)$_2$(H$_3$O)$_2$([Fe(CN)$_6$]) (d na slici 33). Najveća strukturna raznolikost postignuta je među derivatima *o*-halogenpiridina gdje su tri halogenpiridina dala produkte koji sadrže različite strukturne tipove heksacijanoferatnih mreža, ali i različite stehiometrije. Među njima se nalazi jedina struktura koja sadrži anione H$_3$[Fe(CN)$_6$]$^-$ (struktura (**2-BrPy**)$_5$(**2-BrPy**H)$_3$(H$_3$[Fe(CN)$_6$])$_3$). Trodimenzijska mreža tipa b dobiva se iz dvodimenzijske mreže a dodatnim protoniranjem svakog aniona čime on postaje donor i akceptor tri vodikove veze. Visok stupanj protonacije heksacijanoferata u ovoj strukturi može se dovesti u vezu s činjenicom da je ova sol dobivena s jednim od najmanje bazičnih među korištenim piridinima (pK_a(**2-BrPy**) = 0,90). Međutim, to očito ne može biti jedini razlog s obzirom da je još slabija baza (*o*-kloropiridin, pK_a(**2-ClPy**) = 0,49) dala strukturu koja se sastoji od aniona [Fe(CN)$_6$]$^{4-}$ i kationa H$_3$O$^+$ u omjeru 1:2. Izgleda da je odlučujući čimbenik u određivanju strukturnog tipa anionskih mreža ipak potencijal koformera da tvore komplekse kationa i neutralnih molekula kako bi se što učinkovitije popunile praznine mreža. Iako su vodikove veze (odgovorne za formiranje mreža) najjače međumolekulske interakcije u oba slučaja, formiranje mreže svakako ovisi o 'gostujućim' supramolekulski povezanim kationima unutar mreže. S jedne strane, halogenpiridinijevi kationi dovoljno su fleksibilni da se prilagode okolnoj mreži, dok će se s druge strane, mreža formirati tako da adekvatno prihvati kationske komplekse. Najznačajnija razlika između **2-ClPy** i **2-BrPy** je u njihovom potencijalu za stvaranje halogenskih veza što je i slučaj u strukturama (**2-ClPy**)$_2$(PyH)$_2$(H$_3$O)$_2$([Fe(CN)$_6$]) i (**2-Brpy**)$_5$(**2-BrPy**H)$_3$(H$_3$[Fe(CN)$_6$])$_3$.

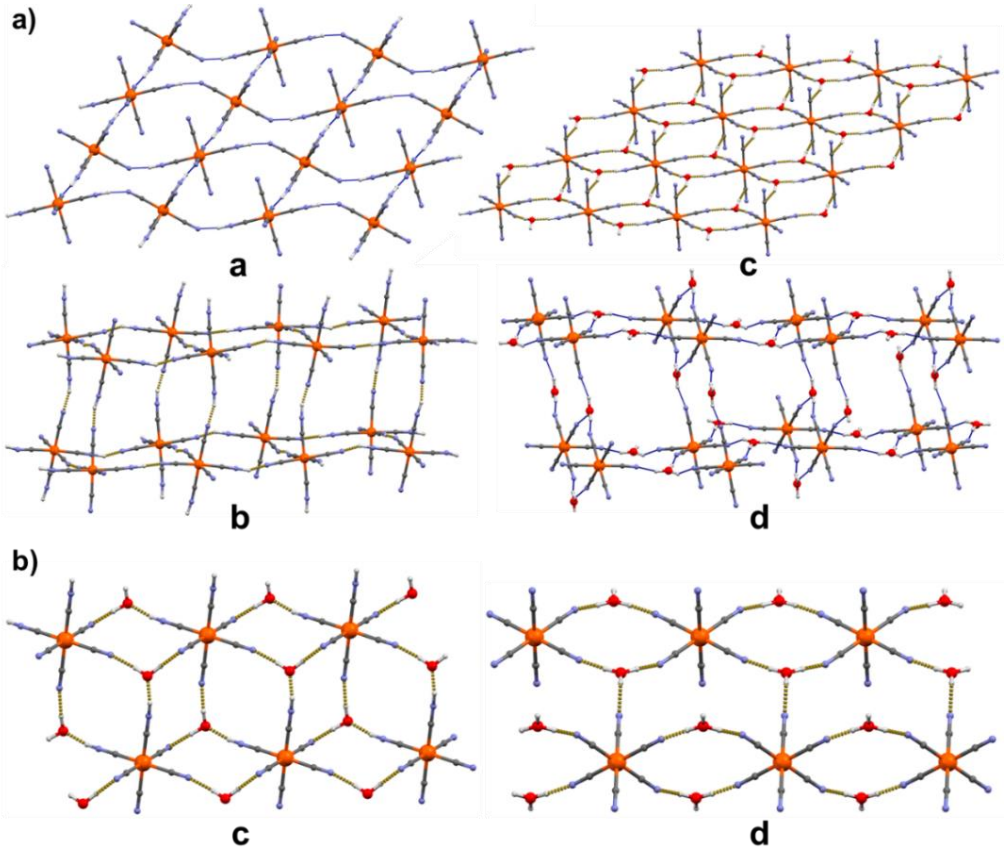

Slika 33. a) Tipovi aninoskih mreža. Tip **a**: slojevi aniona $H_2[Fe(CN)_6]^{2-}$ povezanih vodikovim vezama, (u strukturama (**2-IPy**H)$_2$(H_2[Fe(CN)$_6$]) i (**3-ClPy**H)$_2$(MeOH)(H_2[Fe(CN)$_6$]) i (**4-IPy**H)$_2$(MeOH)(H_2[Fe(CN)$_6$])); Tip **b**: kvazi-kubična trodimenzijskih mreža aniona $H_3[Fe(CN)_6]^-$ povazanih vodikovim vezama (u (**2-Brpy**)$_5$(**2-BrPy**H)$_3$(H_3[Fe(CN)$_6$])$_3$); Tip **c**: 2D mreža sastavljena od aniona $H_2[Fe(CN)_6]^{2-}$ premoštenih molekulama vode (u (**3-BrPy**H)$_2$(H_2O)$_2$(H_2[Fe(CN)$_6$]) i (**3-IPy**H)$_2$(H_2O)$_2$(H_2[Fe(CN)$_6$])); Tip **d**: trodimenzijska mreža sastavljena od aniona $[Fe(CN)_6]^{4-}$ premoštenih kationima H_3O^+ (u (**2-ClPy**)$_2$(PyH)$_2$(H_3O)$_2$([Fe(CN)$_6$])); b) Usporedba vodikovih veza u heksacijanoferatnim mrežama tipa **c** (u (**3-BrPy**H)$_2$(H_2O)$_2$(H_2[Fe(CN)$_6$])) i tipa **d** (u (**2-ClPy**)$_2$(PyH)$_2$(H_3O)$_2$([Fe(CN)$_6$])).

U strukturi (**2-Brpy**)$_5$(**2-BrPy**H)$_3$(H_3[Fe(CN)$_6$])$_3$ i protonirane i neutralne **2-BrPy** molekule stvaraju halogenske veze uključujući kontakte Br···Br s jedne strane odgovorne za stvaranje heksamera [(**2-BrPy**)$_4$(**2-BrPy**H)$_2$]$^{2+}$ koji ispunjavaju praznine heksacijanoferatnih mreža tipa b, a s druge strane za povezivanje heksamera s anionskom mrežom. Odustnost halogenskih veza s **2-ClPy** prepreka je formiranju analognih heksamera. Osim toga, **2-BrPy** formira (**2-Brpy**)$_5$(**2-**

BrPyH)$_3$(H$_3$[Fe(CN)$_6$])$_3$ gotovo trenutno u reakciji s H$_4$[Fe(CN)$_6$] (što ukazuje na relativno nisku topljivost produkata), dok je **2-ClPy** umjesto formiranja ekvivalentnog spoja, dao dvosol **2-ClPy**)$_2$(PyH)$_2$(H$_3$O)$_2$([Fe(CN)$_6$]) tek nakon dugog vremenskog perioda pri čemu se dio **2-ClPy** stigao razgraditi na piridin. Posljedično tome formira i potpuno drugačiji tip kationskih kompleksâ (diskretni kationi [**2-ClPy**···H···Py]$^+$) koji učinkovito popunjavaju praznine u potpuno drugačijim trodimenzijskim mrežama heksacijanoferatnih aniona. Trodimenzijska mreža tipa d (u **2-ClPy**)$_2$(PyH)$_2$(H$_3$O)$_2$([Fe(CN)$_6$])) vrlo je slična slojevitoj mreži tipa c prisutnoj u (**3-BrPy**H)$_2$(H$_2$O)$_2$(H$_2$[Fe(CN)$_6$]) i (**3-IPy**H)$_2$(H$_2$O)$_2$(H$_2$[Fe(CN)$_6$]). Razlika između slojeva u (**3-BrPy**H)$_2$(H$_2$O)$_2$(H$_2$[Fe(CN)$_6$]) i (**3-IPy**H)$_2$(H$_2$O)$_2$(H$_2$[Fe(CN)$_6$]), u usporedbi s mrežom u **2-ClPy**)$_2$(PyH)$_2$(H$_3$O)$_2$([Fe(CN)$_6$]), je u tome što u slojevima vodikove veze između lanaca međusobno povezuju svaki lanac samo s dva susjeda (što vodi do dvodimenzijske mreže) dok je u mreži tipa d svaki lanac međusobno povezan oksonijevim kationima s četiri susjeda što dovodi do nastajanja trodimenzijske mreže (slika 6b). Također, vodikove veze koje međusobno povezuju lance u trodimenzijsku strukturu u **2-ClPy**)$_2$(PyH)$_2$(H$_3$O)$_2$([Fe(CN)$_6$]) su vodikove veze O–H···N slične po duljini i kutu onima unutar lanca, dok su u strukturama (**3-BrPy**H)$_2$(H$_2$O)$_2$(H$_2$[Fe(CN)$_6$]) i (**3-IPy**H)$_2$(H$_2$O)$_2$(H$_2$[Fe(CN)$_6$]) interakcije OH···π između lanaca znatno slabije. Čini se da to opet ukazuje na sposobnost protuiona da stvara halogenske veze – u (**3-BrPy**H)$_2$(H$_2$O)$_2$(H$_2$[Fe(CN)$_6$]) i (**3-IPy**H)$_2$(H$_2$O)$_2$(H$_2$[Fe(CN)$_6$]) kationi se vežu na anionsku mrežu premošćujući susjedne lanace kombinacijom vodikovih i halogenskih veza pri čemu je svaki anion akceptor para vodikovih veza N–H···N i jedne halogenske veze C–X···N što sprječava stvaranje trodimenzijske mreže kao što je slučaj u strukturi (**2-ClPy**)$_2$(PyH)$_2$(H$_3$O)$_2$([Fe(CN)$_6$]). Korištenjem najjačeg donora halogenske veze nastaju i halogenske i vodikove veze između kationa slojeva anionskih mreža, ponovno izolirajući sloj od susjednih čime se sprječava stvaranje trodimenzijske strukture.

Pojava tipa c anionskih dvodimenzijskih mreža, s premošćujućim molekulama vode između aniona H$_2$[Fe(CN)$_6$]$^{2-}$, u nizu *m*-halogenpiridina također se može dovesti u vezu sa sposobnosti **3-BrPy**H$^+$ i **3-IPy**H$^+$ da sudjeluju u halogenskim vezama. U oba slučaja protonirani piridin premošćuje cijano skupine susjednih H$_2$[Fe(CN)$_6$]$^{2-}$ aniona, slično kao što to čini protonirani **2-IPy** u strukturi (**2-IPy**H)$_2$(H$_2$[Fe(CN)$_6$]). Međutim, za razliku od (**2-IPy**H)$_2$(H$_2$[Fe(CN)$_6$]), gdje su kontaktni atomi na kationu (N–H vodik i jod) u *ortho* položaju (što dovodi do jednostavnih 2D mreža aniona H$_2$[Fe(CN)$_6$]$^{2-}$ povezanih vodikovim vezama – tip a), u (**3-BrPy**H)$_2$(H$_2$O)$_2$(H$_2$[Fe(CN)$_6$]) i (**3-IPy**H)$_2$(H$_2$O)$_2$(H$_2$[Fe(CN)$_6$]) kontaktni atomi kationa (N–H

vodik i halogen) su u *meta* položaju jedan prema drugome. Rezultat je proširenje mreže vodikovim vezama s molekulama vode između aniona. Ovaj učinak premošćivanja *m*-halogenpiridinijevih kationa na anionske mreže heksacijanoferatnih aniona također je potkrijepljen strukturama (**3-ClPy**H)$_2$(MeOH)(H$_2$[Fe(CN)$_6$]) (gdje **3-ClPy**H$^+$ uopće ne tvori halogenske veze) i (**4-IPy**H)$_2$(MeOH)(H$_2$[Fe(CN)$_6$]) (gdje kationi **4-IPy**H$^+$ formiraju halogenske i vodikove veze s anionima iz susjednih slojeva) koji oba sadrže anionske mreže tipa a. Utjecaj kationa **3-BrPy**H$^+$ i **3-IPy**H$^+$ je stoga sličan utjecaju (većih) kationa koji tvore višestruke vodikove veze s anionima iste anionske mreže (npr. 4,4'-bipiridinijev dikation), za koje je također ustanovljeno da uzrokuju umetanje molekula vode u anionske mreže heksacijanoferatnih aniona.

Zbog velike varijabilnosti sastava i strukturnog rasporeda kationa i aniona u dobivenim solima izgleda da je predložena kontrola strukture heksacijanoferatnih mreža halogenskim vezama upitna. S obzirom da klorpiridinijevi kationi ne sudjeluju u halogenskim vezama, razlike u strukturama (i sastavima) između heksacijanoferatnih soli klorpiridina brom- i jodpiridina mogu se pripisati nastalim halogenskim vezama. U (sterički nepovoljnom) nizu *o*-halogenpiridina samo je najjači donor halogenskih veza – *o*-jodpiridin formirao kompleks u kojem postoje očekivane C–X$\cdots$N$_{cijano}$ halogenske veze. S druge strane, u nizu *m*-halogenpiridina, (kod kojih je geometrija donora povoljnija) samo najslabiji donor halogenske veze (*m*-klorpiridin) nije formirao halogenske veze s heksacijanoferatnim anionima. Dva jača donora halogenskih veza (*m*-brompiridin i *m*-jodpiridin) ne samo da su formirali izostrukturne soli (**3-BrPy**H)$_2$(H$_2$O)$_2$(H$_2$[Fe(CN)$_6$]) i (**3-IPy**H)$_2$(H$_2$O)$_2$(H$_2$[Fe(CN)$_6$]) u kojima su prisutne C–X$\cdots$N$_{cijano}$ halogenske veze, već su i pokazali da se odabir donora halogenih veza (jači jod naspram slabijeg broma) doista može (iako samo u nekim slučajevima) koristi se za ugađanje geometrije heksacijanoferatnih mreža.

§ 4. ZAKLJUČAK

Ovo istraživanje halogenpiridinijevih kationa kao donora halogenske veze temelji se na 4 znanstvena rada od kojih svaki donosi vrijedne rezultate i zaključke za istraživanje halogenskih veza. Istraživanja objavljena u radovima **I**, **II**, **III**, **IV** međusobno se nadovezuju jedno na drugo, a dobiveni rezultati se nadopunjuju i omogućuju postizanje širih zaključaka o halogenpiridinijevim kationima kao donorima halogenske veze. U cjelovitom istraživanju ukupno je pripravljeno te strukturno, termički i spektroskopski okarakterizirano 49 novih soli protoniranih i *N*-alkiliranih halogenpiridina (**2-ClPy**, **2-BrPy**, **2-IPy**, **3-ClPy**, **3-BrPy**, **3-IPy**, **4-ClPy** i **4-IPy**) koje su objavljene u okviru pet publikacija. Ustanovljeno je da je uvođenje različitih (alifatskih) supstituenata na piridinski dušikov atom halogenpiridina (osobito *meta* izomera) pouzdana metoda za sintezu cijele klase kationskih donora halogenske veze.

Analizom kristalnih struktura jodpiridinijevih halogenida utvrđeno je da afinitet prema halogenskoj vezi opada s veličinom halogenidnog aniona kao akceptora, odnosno slijedi isti trend kao i u slučaju vodikove veze. Međutim, afinitet u slučaju vodikove veze mijenja se puno više nego u slučaju halogenske veze. Relativna duljina potonje povećava za samo oko 1% od klorida do jodida što dovodi do zaključka da će razlika u jakosti vodikovih veza biti znatna, dok će razlika u jakosti halogenskih veza biti mala ili čak zanemariva. Sve u svemu, iako su halogenske veze s većim halogenidima slabije, iz statističke analize podataka dobivenih pretragom baze CSD i kristalne strukture dvosoli (**2-IPy**H)$_2$ClI jasno se vidi da će atomi halogena preferirati ostvarivanje halogenske veze s većim halogenidom kao akceptorom. Stoga se može zaključiti da unatoč tome što je među halogenidima jodid najslabiji akceptor halogenske veze, činjenica da je još slabiji donor vodikove veze, čini ga najpouzdanijim građevnim blokom (od svih halogenidnih aniona) za sintezu struktura povezanih halogenskom vezom.

Dalje je analizom raspodjele naboja na halogenpiridinijevim kationima utvrđeno da i protoniranje i *N*-metiliranje halogenpiridina dovode do značajnog povećanja elektrostatskog potencijala σ-šupljine halogena (V_{max}(X)), ali i da σ-šupljina halogena općenito nije najpozitivniji dio površine kationa. Čak i među jodpiridinijevim kationima, samo u onima koji su izvedeni iz **2-IPy**, V_{max}(I) pozitivniji je od potencijala većine vodikovih atoma, što dovodi do toga da oni tvore najkraće halogenske veze C–I···I$^-$ među protoniranim i metiliranim

halogenpiridinijevim jodidima. Također je utvrđeno da u čak 90% slučajeva (struktura deponiranih u bazi CSD) jod- ili brompiridinijevi kationi tvore halogenske veze pa je vjerojatno da je niža vrijednost V_{max}(X) kompenzirana veličinom atoma halogena što s jedne strane omogućava jednostavniji i bliži pristup Lewisovoj bazi (s manje steričkih smetnji pri prilasku Lewisove baze σ-šupljini atoma halogena nego atoma vodika piridinskog prstena), a s druge strane veća je i potencijalna kontaktna površina između kontaktnih atoma. To, međutim, ne isključuje uspostavljanje kompetitivnih interakcija, što i jest slučaj u opisanim strukturama jodida u kojima postoje brojni kratki kontakti C–H···I^- i interakcije anion···π između kationâ i jodidnih aniona. Međutim, iako dodavanje pozitivnog naboja na halogenpiridinski prsten tvori brojna potencijalna vezna mjesta za Lewisove baze, u brompiridinijevim, a posebno jodpiridinijevim kationima, vjerojatno je da će doći do supramolekulskih kontakata akceptora halogenske veze i atoma halogena halogenpiridinijevog kationa. To čini halogenpiridinijeve katione (jodpiridinijeve posebno) prilično pouzdanim donorima halogenskih veza, te na taj način opravdava njihovu upotrebu u dizajnu i sintezi supramolekulskih struktura povezanih halogenskom vezom.

Usporedbom halogenskih veza u strukturama *N*-alkil-3-jodpiridinijevih jodida utvđeno je da postoji trend da što je duži ugljikovodični lanac supstiturian na dušikov atom jodpiridinskog prstena to su kraće halogenske veze C_{py}–I···I^-. Halogenidne soli većih *N*-alkiliranih halogenpiridinijevih kationa (*N*-(4-halogenbenzil)-3-halogenpiridinijevih halogenida) pokazale su se izvrsnim sustavom za proučavanje izostrukturne izmjene halogena, a pri tome i utjecaja razlika u halogenskoj vezi kako na kristalnu strukturu tako i na svojstva ovih materijala. Ustanovljeno je da u ovim solima dominantna interakcija (koja se ostvaruje s atomom halogena vezanim na piridinski prsten) ostvaruje optimalnu geometriju, dok se geometrija druge (slabije) halogenske veze prilagođava dominantnoj. Dominantna halogenska veza je također glavni uzrok razlika u entalpijama isparavanja unutar izostrukture serije soli tipa I. S obzirom da slabija halogenska veza ima primjetan učinak kako na strukturu tako i na svojstva ovih soli, može se zaključiti da je međudjelovanje obje halogenske veze odgovorno za strukturne značajke i svojstva *N*-(4-halogenbenzil)-3-halogenpiridinijevih halogenida. Doista, činjenica da tako velik broj kombinacija kationa/aniona (11) poprima istu strukturu posljedica je, s jedne strane, postojanja snažno usmjerenih interakcija koje osiguravaju istu supramolekulsku topologiju (lanci), a s druge strane dovoljnim stupnjem fleksibilnosti u slučaju slabije

halogenske veze koja se može prilagoditi kako bi kompenzirala promjene veličine atoma, ali i duljinu i kut jače halogenske veze.

Iz struktura halogenpiridinijevih heksacijanoferata(II) jasno se vidi da halogenpiridinijevi kationi mogu tvoriti soli s heksacijanoferatnim anionima pri čemu se s istima povezuju halogenskim vezama te bi se u budućnosti slični kationi mogli koristi za ugađanje geometrije heksacijanoferatnih mreža.

Ovim istraživanjem pokazano je da se *N*-alkiliranjem (i *N*-protoniranjem) jodpiridina mogu sintetizirati kationi koji su pouzdani i stabilni kationski donori halogenskih veza. Također je otvoren put prema sintezi piridinijevih dikationa koji su potencijalno još bolji i pozudaniji donori halogenskih veza upravo zbog većeg ukupnog naboja, a samim time i veće vrijednosti V_{max}(X). S obzirom da su u okviru ovog istraživanja proučavane soli halogenpiridina s halogenidnim anionima (i heksacijanoferatnim anionima) u budućnosti bi trebalo prirediti i analizirati soli s drugim anionima, ali i kokristale u kojima bi se mogle ostvariti halogenske veze između kationa i neutralnih molekula kao akceptora halogenske veze. Istraživanja soli halogenpiridinijevih (di)kationa s većim organskim i anorganskim anionima (u prvom redu cijanometalatima i (poli)oksometalatima) su u tijeku.

§ 5. POPIS OZNAKÂ, KRATICÂ I SIMBOLÂ

kratica	naziv	**kratica**	naziv
Buen	but-2-enilna grupa	**Δ*H***	promjena entalpije
CSD	Cambridge Structural Database	TG	termogravimetrija
d_{rel}	relativna duljina	φ	kut veze
DSC	razlikovna pretražna kalorimetrija	π_{AB}	indeksi sličnosti jediničnih ćelija
E	energija interakcije	**2-ClPy**	2-klorpiridin
Et	etilna grupa	**2-BrPy**	2-brompiridin
$\boldsymbol{I}_s$	izostrukturnosni indeksi	**2-IPy**	2-jodpiridin
KPC	koeficijent kristalnog pakiranja	**3-ClPy**	3-klorpiridin
Me	metilna grupa	**3-BrPy**	3-brompiridin
Prop	propilna grupa	**3-IPy**	3-jodpiridin
R.S.	relativno skraćenje	**4-ClPy**	4-klorpiridin
V_{max}	maksimum elektrostatskog potencijala	**4-BrPy**	4-brompiridin
V_{min}	minimum elektrostatskog potencijala	**4-IPy**	4-jodpiridin

§ 6. LITERATURNI IZVORI

1. J.J. Colin, *Ann. Chim.* **91** (1814) 252–272.
2. F. Guthrie, *J. Chem. Soc.* **16** (1863) 239–244.
3. T. Bjorvatten, O. Hassel, A.I. Virtanen, K. Motzfeldt, O. Theander, H. Flood, *Acta Chem. Scand.* **16** (1962) 249–255.
4. T. Bjorvatten, O. Hassel, O. Buchardt, G.E. Olsen, C. Pedersen, J. Toft, *Acta Chem. Scand.* **15** (1961) 1429–1436.
5. O. Hassel, C. Rømming, T. Tufte, W.G. Terry, B. Sjöberg, J. Toft, *Acta Chem. Scand.* **15** (1961) 967–974.
6. O. Hassel, H. Hope, N.A. Sörensen, H. Dam, B. Sjöberg, J. Toft, *Acta Chem. Scand.* **15** (1961) 407–416.
7. T. Bjorvatten, O. Hassel, M. Ojamäe, B. Högberg, P. Kneip, H. Palmstierna, *Acta Chem. Scand.* **13** (1959) 1261–1262.
8. O. Hassel, C. Rømming, J.G. Ormerod, E. Stenhagen, B. Thorell, *Acta Chem. Scand.* **10** (1956) 696–698.
9. G. Eia, O. Hassel, R.B. Jensen, E. Stenhagen, B. Thorell, *Acta Chem. Scand.* **10** (1956) 139–141.
10. O. Hassel, J. Hvoslef, K. Taugbøl, H. Theorell, B. Thorell, *Acta Chem. Scand.* **10** (1956) 138–139.
11. O. Hassel, J. Hvoslef, E.H. Vihovde, N.A. Sörensen, *Acta Chem. Scand.* **8** (1954) 873–873.
12. A.C. Legon, *Chem. - A Eur. J.* **4** (1998) 1890–1897.
13. A.C. Legon, *Angew. Chemie Int. Ed.* **38** (1999) 2686–2714.
14. E. Corradi, S.V. Meille, M.T. Messina, P. Metrangolo, G. Resnati, *Tetrahedron Lett.* **40** (1999) 7519–7523.
15. V. Amico, S.V. Meille, E. Corradi, M.T. Messina, G. Resnati, *J. Am. Chem. Soc.* **120** (1998) 8261–8262.
16. M.T. Messina, P. Metrangolo, W. Panzeri, E. Ragg, G. Resnati, *Tetrahedron Lett.* **39** (1998) 9069–9072.
17. P. Metrangolo, G. Resnati, *Chem. - A Eur. J.* **7** (2001) 2511–2519.
18. A. Lunghi, P. Cardillo, T. Messina, P. Metrangolo, W. Panzeri, G. Resnati, *J. Fluor. Chem.* **91** (1998) 191–194.
19. G. Gilli, F. Bellucci, V. Ferretti, V. Bertolasi, *J. Am. Chem. Soc.* **111** (1989) 1023–1028.

20. M.C. Etter, *Acc. Chem. Res.* **23** (1990) 120–126.
21. P. Metrangolo, H. Neukirch, T. Pilati, G. Resnati, *Acc. Chem. Res.* **38** (2005) 386–395.
22. G.R. Desiraju, P.S. Ho, L. Kloo, A.C. Legon, R. Marquardt, P. Metrangolo, P. Politzer, et al., *Pure Appl. Chem.* **85** (2013) 1711–1713.
23. T. Clark, M. Hennemann, J.S. Murray, P. Politzer, *J. Mol. Model.* **13** (2007) 291–296.
24. P. Politzer, J.S. Murray, T. Clark, *Phys. Chem. Chem. Phys.* **15** (2013) 11178.
25. P. Politzer, J.S. Murray, T. Clark, G. Resnati, *Phys. Chem. Chem. Phys.* **19** (2017) 32166–32178.
26. P. Politzer, J.S. Murray, T. Clark, *Phys. Chem. Chem. Phys.* **12** (2010) 7748–7757.
27. P. Politzer, J.S. Murray, *Crystals.* **7** (2017).
28. V. Stilinović, G. Horvat, T. Hrenar, V. Nemec, D. Cinčić, *Chem. - A Eur. J.* **23** (2017) 5244–5257.
29. K.E. Riley, J.S. Murray, J. Fanfrlík, J. Řezáč, R.J. Solá, M.C. Concha, F.M. Ramos, et al., *J. Mol. Model.* **17** (2011) 3309–3318.
30. G. Cavallo, P. Metrangolo, R. Milani, T. Pilati, A. Priimagi, G. Resnati, G. Terraneo, *Chem. Rev.* **116** (2016) 2478–2601.
31. C.B. Aakeröy, T.K. Wijethunga, J. Desper, *J. Mol. Struct.* **1072** (2014) 20–27.
32. M. Kolář, J. Hostaš, P. Hobza, *Phys. Chem. Chem. Phys.* **16** (2014) 9987–9996.
33. V. Oliveira, E. Kraka, D. Cremer, *Phys. Chem. Chem. Phys.* **18** (2016) 33031–33046.
34. R.W. Troff, T. Mäkelä, F. Topić, A. Valkonen, K. Raatikainen, K. Rissanen, *European J. Org. Chem.* **2013** (2013) 1617–1637.
35. L.C. Roper, C. Präsang, V.N. Kozhevnikov, A.C. Whitwood, P.B. Karadakov, D.W. Bruce, *Cryst. Growth Des.* **10** (2010) 3710–3720.
36. N. Bedeković, V. Stilinović, T. Friščić, D. Cinčić, *New J. Chem.* **42** (2018) 10584–10591.
37. V. Nemec, K. Lisac, N. Bedeković, L. Fotović, V. Stilinović, D. Cinčić, *CrystEngComm.* **23** (2021) 3063–3083.
38. E. Uran, L. Fotović, N. Bedeković, V. Stilinović, D. Cinčić, *Crystals.* **11** (2021) 529–540.
39. X.H. Ding, Y.Z. Chang, C.J. Ou, J.Y. Lin, L.H. Xie, W. Huang, *Natl. Sci. Rev.* **7** (2020) 1906–1932.
40. V. Nemec, L. Fotović, T. Vitasović, D. Cinčić, *CrystEngComm*. **21** (2019) 3251–3255.
41. A. Farina, S.V. Meille, M.T. Messina, P. Metrangolo, G. Resnati, G. Vecchio, *Angew. Chemie - Int. Ed.* **38** (1999) 2433–2436.
42. P. Metrangolo, F. Meyer, T. Pilati, G. Resnati, G. Terraneo, *Angew. Chemie - Int. Ed.* **47** (2008) 6114–6127.
43. K. Raatikainen, K. Rissanen, *CrystEngComm.* **11** (2009) 750–752.

44. S.T. Nguyen, T.L. Ellington, K.E. Allen, J.D. Gorden, A.L. Rheingold, G.S. Tschumper, N.I. Hammer, et al., *Cryst. Growth Des.* **18** (2018) 3244–3254.
45. S. V. Rosokha, E.A. Loboda, *J. Phys. Chem. A.* **119** (2015) 3833–3842.
46. C.I. Nwachukwu, Z.R. Kehoe, N.P. Bowling, E.D. Speetzen, E. Bosch, *New J. Chem.* **42** (2018) 10615–10622.
47. S. V. Baykov, S.I. Filimonov, A. V. Rozhkov, A.S. Novikov, I. V. Ananyev, D.M. Ivanov, V.Y. Kukushkin, *Cryst. Growth Des.* **20** (2020) 995–1008.
48. C.B. Aakeröy, M. Baldrighi, J. Desper, P. Metrangolo, G. Resnati, *Chem. - A Eur. J.* **19** (2013) 16240–16247.
49. D.E. Barry, C.S. Hawes, S. Blasco, T. Gunnlaugsson, *Cryst. Growth Des.* **16** (2016) 5194–5205.
50. S.T. Nguyen, A.L. Rheingold, G.S. Tschumper, D.L. Watkins, *Cryst. Growth Des.* **16** (2016) 6648–6653.
51. M. Baldrighi, D. Bartesaghi, G. Cavallo, M.R. Chierotti, R. Gobetto, P. Metrangolo, T. Pilati, et al., *CrystEngComm.* **16** (2014) 5897–5904.
52. K. Raatikainen, K. Rissanen, *CrystEngComm.* **13** (2011) 6972–6977.
53. K. Raatikainen, K. Rissanen, *Chem. Sci.* **3** (2012) 1235–1239.
54. O. Makhotkina, J. Lieffrig, O. Jeannin, M. Fourmigué, E. Aubert, E. Espinosa, *Cryst. Growth Des.* **15** (2015) 3464–3473.
55. R. Puttreddy, O. Jurček, S. Bhowmik, T. Mäkelä, K. Rissanen, *Chem. Commun.* **52** (2016) 2338–2341.
56. R. Puttreddy, J.M. Rautiainen, T. Mäkelä, K. Rissanen, *Angew. Chemie - Int. Ed.* **58** (2019) 18610–18618.
57. J. Mavračić, D. Cinčić, B. Kaitner, *CrystEngComm.* **18** (2016) 3343–3346.
58. D. Dolenc, B. Modec, *New J. Chem.* **33** (2009) 2344–2349.
59. M. Eraković, D. Cinčić, K. Molčanov, V. Stilinović, *Angew. Chemie - Int. Ed.* **58** (2019) 15702–15706.
60. M. Eraković, V. Nemec, T. Lež, I. Porupski, V. Stilinović, D. Cinčić, *Cryst. Growth Des.* **18** (2018) 1182–1190.
61. J. Pelletier, J.J. Caventou, *Ann. Chim.* **10** (1819) 142–177.
62. M. Oszajca, Ľ. Smrčok, H. Pálková, W. Łasocha, *J. Mol. Struct.* **1021** (2012) 70–75.
63. R.J. Attrell, C.M. Widdifield, I. Korobkov, D.L. Bryce, *Cryst. Growth Des.* **12** (2012) 1641–1653.
64. K. Raatikainen, M. Cametti, K. Rissanen, *Beilstein J. Org. Chem.* **6** (2010) 4.
65. K. Kubo, K. Takahashi, S. Nakagawa, K.I. Sakai, S.I. Noro, T. Akutagawa, T. Nakamura,

Cryst. Growth Des. **21** (2021) 2340–2347.

66. E. Aubert, E. Espinosa, I. Nicolas, O. Jeannin, M. Fourmigué, *Faraday Discuss.* **203** (2017) 389–406.
67. L.H. Thomas, M.S. Adam, A. O'Neill, C.C. Wilson, *Acta Crystallogr. Sect. C Cryst. Struct. Commun.* **69** (2013) 1279–1288.
68. D.A. Decato, A.M.S. Riel, J.H. May, V.S. Bryantsev, O.B. Berryman, *Angew. Chemie*. **133** (2021) 3729–3736.
69. T.A. Logothetis, F. Meyer, P. Metrangolo, T. Pilati, G. Resnati, *New J. Chem.* **28** (2004) 760–763.
70. L. Fotović, V. Stilinović, *CrystEngComm*. **22** (2020) 4039–4046.
71. F.F. Awwadi, R.D. Willett, K.A. Peterson, B. Twamley, *J. Phys. Chem. A.* **111** (2007) 2319–2328.
72. M. Freytag, P.G. Jones, B. Ahrens, A.K. Fischer, *New J. Chem.* **23** (1999) 1137–1139.
73. G.M. Espallargas, F. Zordan, L.A. Marín, H. Adams, K. Shankland, J. De Van Streek, L. Brammer, *Chem. - A Eur. J.* **15** (2009) 7554–7568.
74. F.F. Awwadi, R.D. Willett, B. Twamley, *Cryst. Growth Des.* **7** (2007) 624–632.
75. R.D. Willett, F. Awwadi, R. Butcher, S. Haddad, B. Twamley, *Cryst. Growth Des.* **3** (2003) 301–311.
76. D. Bulfield, S.M. Huber, *Chem. - A Eur. J.* **22** (2016) 14434–14450.
77. L. Brammer, G.M. Espallargas, H. Adams, *CrystEngComm*. **5** (2003) 343–345.
78. G. Mínguez Espallargas, L. Brammer, P. Sherwood, *Angew. Chemie - Int. Ed.* **45** (2006) 435–440.
79. F. Zordan, L. Brammer, *Acta Crystallogr. Sect. B Struct. Sci.* **60** (2004) 512–519.
80. F. Zordan, S.L. Purver, H. Adams, L. Brammer, *CrystEngComm*. **7** (2005) 350–354.
81. I.J. Vitorica-Yrezabal, R.A. Sullivan, S.L. Purver, C. Curfs, C.C. Tang, L. Brammer, *CrystEngComm.* **13** (2011) 3189–3196.
82. F. Zordan, L. Brammer, P. Sherwood, *J. Am. Chem. Soc.* **127** (2005) 5979–5989.
83. J. Wolf, F. Huber, N. Erochok, F. Heinen, V. Guérin, C.Y. Legault, S.F. Kirsch, et al., *Angew. Chemie - Int. Ed.* **59** (2020) 16496–16500.
84. R.L. Sutar, E. Engelage, R. Stoll, S.M. Huber, *Angew. Chemie - Int. Ed.* **59** (2020) 6806–6810.
85. S. Derossi, L. Brammer, C.A. Hunter, M.D. Ward, *Inorg. Chem.* **48** (2009) 1666–1677.
86. J.E. Ormond-Prout, P. Smart, L. Brammer, *Cryst. Growth Des.* **12** (2012) 205–216.
87. N. Jakupec, L. Fotović, V. Stilinović, *CrystEngComm*. **22** (2020) 8142–8150.
88. V. Amendola, G. Bergamaschi, M. Boiocchi, N. Fusco, M.V. La Rocca, L. Linati, E. Lo Presti, et al., *RSC Adv.* **6** (2016) 67540–67549.

89. A.M.S. Riel, M.J. Jessop, D.A. Decato, C.J. Massena, V.R. Nascimento, O.B. Berryman, *Acta Crystallogr. Sect. B Struct. Sci. Cryst. Eng. Mater.* **73** (2017) 203–209.
90. A.M.S. Riel, D.A. Decato, J. Sun, C.J. Massena, M.J. Jessop, O.B. Berryman, *Chem. Sci.* **9** (2018) 5828–5836.
91. É.M. Foyle, N.G. White, *CrystEngComm*. **22** (2020) 2526–2536.
92. J.A. Lohrman, C.L. Deng, T.A. Shear, L.N. Zakharov, M.M. Haley, D.W. Johnson, *Chem. Commun.* **55** (2019) 1919–1922.
93. S.H. Jungbauer, S.M. Huber, *J. Am. Chem. Soc.* **137** (2015) 12110–12120.
94. Y. Kosaka, H.M. Yamamoto, A. Nakao, M. Tamura, R. Kato, *J. Am. Chem. Soc.* **129** (2007) 3054–3055.
95. T. Kusamoto, H.M. Yamamoto, N. Tajima, Y. Oshima, S. Yamashita, R. Kato, *Inorg. Chem.* **51** (2012) 11645–11654.
96. Y. Kosaka, H.M. Yamamoto, A. Tajima, A. Nakao, H. Cui, R. Kato, *CrystEngComm*. **15** (2013) 3200–3211.
97. X. Ren, Q. Meng, Y. Song, C. Lu, C. Hu, X. Chen, *Inorg. Chem.* **41** (2002) 5686–5692.
98. P.K. Chattaraj, H. Lee, R.G. Parr, *J. Am. Chem. Soc.* **113** (1991) 1855–1856.
99. R.G. Parr, P.K. Chattaraj, *J. Am. Chem. Soc.* **113** (1991) 1854–1855.
100. M. Freytag, P.G. Jones, *Zeitschrift Fur Naturforsch. - Sect. B J. Chem. Sci.* **56** (2001) 889–896.
101. P.G. Jones, V. Lozano, *Acta Crystallogr. Sect. E Struct. Reports Online*. **59** (2003) o632–o634.
102. Q. Jin Shen, W. Jun Jin, *Phys. Chem. Chem. Phys.* **13** (2011) 13721.
103. H. Wang, X.R. Zhao, W.J. Jin, *Phys. Chem. Chem. Phys.* **15** (2013) 4320–4328.
104. M.D. Garci, V. Blanco, C. Platas-Iglesias, C. Peinador, J.M. Quintela, *Cryst. Growth Des.* **9** (2009) 5009–5013.
105. P.M.J. Szell, G. Cavallo, G. Terraneo, P. Metrangolo, B. Gabidullin, D.L. Bryce, *Chem. - A Eur. J.* **24** (2018) 11364–11376.
106. C.C. Robertson, J.S. Wright, E.J. Carrington, R.N. Perutz, C.A. Hunter, L. Brammer, *Chem. Sci.* **8** (2017) 5392–5398.
107. C.R. Groom, I.J. Bruno, M.P. Lightfoot, S.C. Ward, *Acta Crystallogr. Sect. B Struct. Sci. Cryst. Eng. Mater.* **72** (2016) 171–179.
108. L. Fotović, N. Bedeković, V. Stilinović, *Cryst. Growth Des.* **21** (2021) 6889–6901.
109. L. Posavec, V. Nemec, V. Stilinović, D. Cinčić, *Cryst. Growth Des.* **21** (2021) 6044–6050.
110. M. Ghassemzadeh, K. Dehnicke, H. Goesmann, D. Fenske, *Zeitschrift Fur Naturforsch. - Sect. B J. Chem. Sci.* **49** (1994) 602–608.
111. M. Mascal, A. Armstrong, M.D. Bartberger, *J. Am. Chem. Soc.* **124** (2002) 6274–6276.
112. D. Quiñonero, C. Garau, C. Rotger, A. Frontera, P. Ballester, A. Costa, P.M. Deyà, *Angew.*

Chemie. **114** (2002) 3539–3542.

113. L. Fotović, V. Stilinović, *Crystals*. **11** (2021) 1240–1256.
114. L. Fotović, N. Bedeković, V. Stilinović, *Cryst. Growth Des.* (2022) acs.cgd.1c01285.
115. A. Kálmán, L. Párkányi, G. Argay, *Acta Crystallogr. Sect. B Struct. Sci.* **49** (1993) 1039–1049.
116. A. Kálmán, *Acta Crystallogr. Sect. B Struct. Sci.* **61** (2005) 536–547.
117. L. Fábián, A. Kálmán, *Acta Crystallogr. Sect. B Struct. Sci.* **55** (1999) 1099–1108.
118. P. Bombicz, *Crystallogr. Rev.* **23** (2017) 118–151.
119. P. Bombicz, N. V. May, D. Fegyverneki, A. Saranchimeg, L. Bereczki, *CrystEngComm*. **22** (2020) 7193–7203.
120. C.D. Wessells, R.A. Huggins, Y. Cui, *Nat. Commun.* **2** (2011) 550.
121. Y. Lu, L. Wang, J. Cheng, J.B. Goodenough, *Chem. Commun.* **48** (2012) 6544–6546.
122. P. Nie, L. Shen, H. Luo, B. Ding, G. Xu, J. Wang, X. Zhang, *J. Mater. Chem. A.* **2** (2014) 5852–5857.
123. M. Pasta, C.D. Wessells, N. Liu, J. Nelson, M.T. McDowell, R.A. Huggins, M.F. Toney, et al., *Nat. Commun.* **5** (2014) 3007.
124. H.-W. Lee, R.Y. Wang, M. Pasta, S. Woo Lee, N. Liu, Y. Cui, *Nat. Commun.* **5** (2014) 5280.
125. Y. You, X.-L. Wu, Y.-X. Yin, Y.-G. Guo, *Energy Environ. Sci.* **7** (2014) 1643–1647.
126. P. Canepa, G. Sai Gautam, D.C. Hannah, R. Malik, M. Liu, K.G. Gallagher, K.A. Persson, et al., *Chem. Rev.* **117** (2017) 4287–4341.
127. S. Ferlay, T. Mallah, R. Ouahès, P. Veillet, M. Verdaguer, *Nature*. **378** (1995) 701–703.
128. M. Ohba, H. Ōkawa, N. Fukita, Y. Hashimoto, *J. Am. Chem. Soc.* **119** (1997) 1011–1019.
129. M. Ohba, N. Usuki, N. Fukita, H. Ōkawa, *Angew. Chemie Int. Ed.* **38** (1999) 1795–1798.
130. M. Verdaguer, A. Bleuzen, V. Marvaud, J. Vaissermann, M. Seuleiman, C. Desplanches, A. Scuiller, et al., *Coord. Chem. Rev.* **190**–**192** (1999) 1023–1047.
131. M. Ohba, H. Ōkawa, *Coord. Chem. Rev.* **198** (2000) 313–328.
132. C.-M. Liu, S. Gao, H.-Z. Kou, D.-Q. Zhang, H.-L. Sun, D.-B. Zhu, *Cryst. Growth Des.* **6** (2006) 94–98.
133. X.-Y. Wang, C. Avendaño, K.R. Dunbar, *Chem. Soc. Rev.* **40** (2011) 3213–3238.
134. O. Sato, T. Iyoda, A. Fujishima, K. Hashimoto, *Science (80-.).* **272** (1996) 704–705.
135. S. Ohkoshi, Y. Einaga, A. Fujishima, K. Hashimoto, *J. Electroanal. Chem.* **473** (1999) 245–249.
136. Y. Zhang, D. Li, R. Clérac, M. Kalisz, C. Mathonière, S.M. Holmes, *Angew. Chemie*. **122** (2010) 3840–3844.
137. Y.-Z. Zhang, P. Ferko, D. Siretanu, R. Ababei, N.P. Rath, M.J. Shaw, R. Clérac, et al., *J. Am. Chem. Soc.* **136** (2014) 16854–16864.

138. L.-Z. Cai, Q.-S. Chen, C.-J. Zhang, P.-X. Li, M.-S. Wang, G.-C. Guo, *J. Am. Chem. Soc.* **137** (2015) 10882–10885.
139. J. Kuyper, *J. Catal.* **105** (1987) 163–174.
140. J. Balmaseda, E. Reguera, J. Rodríguez-Hernández, L. Reguera, M. Autie, *Microporous Mesoporous Mater.* **96** (2006) 222–236.
141. D. Maspoch, D. Ruiz-Molina, J. Veciana, *Chem. Soc. Rev.* **36** (2007) 770–818.
142. V. Nigrovic, *Phys. Med. Biol.* **10** (1965) 81–91.
143. H.H. Kamerbeek, A.G. Rauws, M. Ham, A.N.P. Heijst, *Acta Med. Scand.* **189** (2009) 321–324.
144. D. Parajuli, A. Takahashi, H. Noguchi, A. Kitajima, H. Tanaka, M. Takasaki, K. Yoshino, et al., *Chem. Eng. J.* **283** (2016) 1322–1328.
145. S.S. Kaye, J.R. Long, *J. Am. Chem. Soc.* **127** (2005) 6506–6507.
146. L.J. Murray, M. Dincă, J.R. Long, *Chem. Soc. Rev.* **38** (2009) 1294–1314.
147. M.P. Suh, H.J. Park, T.K. Prasad, D.-W. Lim, *Chem. Rev.* **112** (2012) 782–835.
148. A. Takahashi, H. Tanaka, D. Parajuli, T. Nakamura, K. Minami, Y. Sugiyama, Y. Hakuta, et al., *J. Am. Chem. Soc.* **138** (2016) 6376–6379.
149. M. Ohba, N. Usuki, N. Fukita, H. Ōkawa, *Inorg. Chem.* **37** (1998) 3349–3354.
150. A. Yuan, B. Li, Z. Zha, C. Duan, Y. Liu, Z. Xu, J. Zou, et al., *Chem. Commun.* (2000) 1297–1298.
151. J.-R. Li, W.-T. Chen, M.-L. Tong, G.-C. Guo, Y. Tao, Q. Yu, W.-C. Song, et al., *Cryst. Growth Des.* **8** (2008) 2780–2792.
152. A.-H. Yuan, R.-Q. Lu, H. Zhou, Y.-Y. Chen, Y.-Z. Li, *CrystEngComm.* **12** (2010) 1382–1384.
153. R. Mittal, M. Zbiri, H. Schober, S.N. Achary, A.K. Tyagi, S.L. Chaplot, *J. Phys. Condens. Matter*. **24** (2012) 505404.
154. B. Nowicka, T. Korzeniak, O. Stefańczyk, D. Pinkowicz, S. Chorąży, R. Podgajny, B. Sieklucka, *Coord. Chem. Rev.* **256** (2012) 1946–1971.
155. S. Ferlay, P. Dechambenoit, N. Kyritsakas, M.W. Hosseini, *Dalt. Trans.* **42** (2013) 11661–11671.
156. J. Larionova, R. Clérac, B. Donnadieu, S. Willemin, C. Guérin, *Cryst. Growth Des.* **3** (2003) 267–272.
157. C.J. Shorrock, H. Jong, R.J. Batchelor, D.B. Leznoff, *Inorg. Chem.* **42** (2003) 3917–3924.
158. R. Koner, M. Nayak, G. FergusonPermanent address: Departme, J.N. Low, C. Glidewell, P. Misra, S. Mohanta, *CrystEngComm.* **7** (2005) 129.
159. B. Sieklucka, R. Podgajny, P. Przychodzeń, T. Korzeniak, *Coord. Chem. Rev.* **249** (2005) 2203–2221.
160. P. Przychodzen, T. Korzeniak, R. Podgajny, B. Sieklucka, *Coord. Chem. Rev.* **250** (2006)

2234–2260.

161. W.-T. Chen, M.-S. Wang, L.-Z. Cai, G. Xu, T. Akitsu, M. Akita-Tanaka, Guo, et al., *Cryst. Growth Des.* **6** (2006) 1738–1741.
162. Z.-X. Wang, P. Zhang, X.-F. Shen, Y. Song, X.-Z. You, K. Hashimoto, *Cryst. Growth Des.* **6** (2006) 2457–2462.
163. M.J. Katz, H. Kaluarachchi, R.J. Batchelor, G. Schatte, D.B. Leznoff, *Cryst. Growth Des.* **7** (2007) 1946–1948.
164. S. Ferlay, V. Bulach, O. Félix, M.W. Hosseini, J.-M. Planeix, N. Kyritsakas, *CrystEngComm.* **4** (2002) 447–453.
165. M.W. Hosseini, *Coord. Chem. Rev.* **240** (2003) 157–166.
166. M.W. Hosseini, *Acc. Chem. Res.* **38** (2005) 313–323.
167. P. Dechambenoit, S. Ferlay, M.W. Hosseini, J.-M. Planeix, N. Kyritsakas, *New J. Chem.* **30** (2006) 1403–1410.
168. P. Dechambenoit, S. Ferlay, M.W. Hosseini, N. Kyritsakas, *Chem. Commun.* (2007) 4626–4628.
169. P. Dechambenoit, S. Ferlay, N. Kyritsakas, M.W. Hosseini, *J. Am. Chem. Soc.* **130** (2008) 17106–17113.
170. P. Dechambenoit, S. Ferlay, B. Donnio, D. Guillon, M.W. Hosseini, *Chem. Commun.* **47** (2011) 734–736.
171. P. Dechambenoit, S. Ferlay, N. Kyritsakas, M.W. Hosseini, *CrystEngComm*. **13** (2011) 1922–1930.
172. A. Hazra, K.L. Gurunatha, T.K. Maji, *Cryst. Growth Des.* **13** (2013) 4824–4836.
173. I. Cvrtila, V. Stilinović, *Cryst. Growth Des.* **17** (2017) 6793–6800.
174. R. Tanaka, A. Okazawa, N. Kojima, N. Matsushita, *Chem. Lett.* **47** (2018) 697–699.
175. S.I. Gorelsky, A.B. Ilyukhin, P. V. Kholin, V.Y. Kotov, B. V. Lokshin, N. V. Sapoletova, *Inorganica Chim. Acta*. **360** (2007) 2573–2582.
176. P. Xydias, S. Lymperopoulou, V. Dokorou, M. Manos, J.C. Plakatouras, *Polyhedron*. **157** (2019) 341–357.

§ 7. DODATAK

Znanstveni rad:

Isostructural halogen exchange and halogen bond – the case of *N*-(4-halogenobenzyl)-3-halogenopyridinium halogenides

L. Fotović, N. Bedeković i V. Stilinović,
Cryst. Growth Des. **22** (2022) 1333–1344.

Rad je reproduciran uz dozvolu Američkog kemijskog društva.*

*Reprinted with permission from *Cryst. Growth Des.* **2021**. Copyright 2021 American Chemical Society.

CRYSTAL GROWTH & DESIGN

pubs.acs.org/crystal

Article

Isostructural Halogen Exchange and Halogen Bonds: The Case of *N*-(4-Halogenobenzyl)-3-halogenopyridinium Halogenides

Luka Fotović, Nikola Bedeković, and Vladimir Stilinović*

Cite This: https://doi.org/10.1021/acs.cgd.1c01285

Read Online

ACCESS | Metrics & More | Article Recommendations | Supporting Information

ABSTRACT: Six *N*-(4-halogenobenzyl)-3-halogenopyridinium cations were prepared by reacting *meta*-halogenopyridines (Cl, Br, and I) with (4-halogenobenzyl) bromides (Br and I) and were isolated as bromide salts, which were further used to obtain iodides and chlorides. Sixteen compounds (out of 18 possible cation/anion combinations) were obtained; two crystallized as hydrates and 14 as solvent free salts, 11 of which belonged to one isostructural series and 3 to another. All crystal structures comprise halogen-bonded chains, with the anion as an acceptor of two halogen bonds, with the pyridine and the benzyl halogen substituents of two neighboring cations. The halogen bonds with the pyridine halogen show a linear correlation between the relative halogen bond length and angle, which primarily depend on the donor halogen. The parameters of the other halogen bonds vary with all three halogens, indicating that the former halogen bond is the dominant interaction. This is also in accord with the calculated electrostatic potential in the σ-holes of the halogens and the thermal properties of the solids. The second isostructural group comprises combinations of the best halogen bond donors and acceptors, and features a more favorable halogen bond geometry of the dominant halogen bond, reaffirming its significance as the main factor in determining the structure.

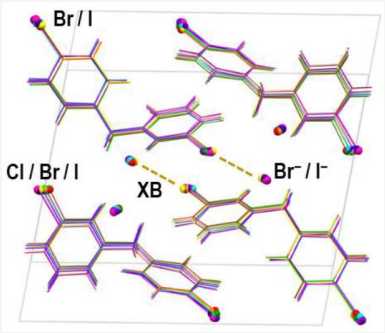

Downloaded via UNIV OF ZAGREB on January 20, 2022 at 14:10:38 (UTC).
See https://pubs.acs.org/sharingguidelines for options on how to legitimately share published articles.

INTRODUCTION

The goal of crystal engineering is the deliberate design of crystals with planned structures and predictable physical and chemical properties.[1−6] In attempting to achieve this, one must take into account both the geometric properties of the constituent molecules, as well as their proclivity to participate in intermolecular interactions. The intricate interplay of these two effects is perhaps best illustrated by two phenomena: the ability of one substance to crystallize in more the one crystal structure—polymorphism[7−11]—and the occurrence of different substances adopting very similar (or almost identical) crystal structures—isostructurality.[12−16] Of these two phenomena, isostructurality is particularly useful for the study of minute differences in crystal structures and properties, as in isostructural materials the majority of various contributions of the overall crystal packing can be taken to be equivalent, leaving the differences between the constituent molecules as the main cause of any variability between the structures and the properties within an isostructural series.[17−25]

One field of solid state of supramolecular chemistry which has particularly benefited from the study of isostructural systems is the study of the halogen-bonded materials.[26−34] The reason for this is that replacing one halogen atom with another in a molecule generally has only a minute effect on molecular geometry. It was already noted by Kitaigorodsky in his seminal *Organic Crystallochemistry*[35] that replacing one halogen atom with its neighbor in the group (Cl/Br or Br/I) will in roughly 50% of cases lead to isostructural materials. As the halogen bond energy greatly increases with the donor atom size,[36] in such isostructural crystals (providing the halogen atom does act as a halogen bond donor), the only significant difference between the two crystals will be the strength of the halogen bond. Furthermore, as the only significant difference between two such isostructural crystals lies in the halogen bond strength, all differences in physical and chemical properties are also mainly due to the difference in halogen bond energies. This has been employed for experimental observations of the effect of the halogen bond on the macroscopic properties of isostructural halogen-bonded materials, as well as fine-tuning of their properties.[37,38] Unfortunately, this approach does have its limitations: while isomorphous dual exchange Cl/Br and Br/I is a fairly common phenomenon,[17−19] triple isomorphous exchange Cl/Br/I is quite rare. To the best of our knowledge, there have been to date only eight published systems with triple isomorphous exchange[30,32,39−44] involving halogen which acts as a halogen bond donor.

The tunability of halogen bond strength within a set of isostructural crystals can be increased if the acceptor atom can also be replaced without changing the overall structure of the crystal. One method for systematic application of this principle

Received: November 3, 2021
Revised: December 7, 2021

ACS Publications

© XXXX The Authors. Published by American Chemical Society

is using halogen atoms not only as donors but also as halogen bond acceptors. This can be achieved in several ways; halogen atoms can act as halogen bond acceptors either of part of the neutral molecule (type II XB) or as halogenide anions (in their "free" form or coordinated as ligands to metal centers). The latter approach was very successfully employed by the Brammer group for the study of the hierarchy of intermolecular interactions in 3-halogenopyridinium tetrahalogenometalates, demonstrating that the structure type is dependent on both the hydrogen and the halogen bond strength.[37] Also, halogenopyridinium halogenides were shown to be extremely prone to isostructurality: among both the *ortho*- and *para*-halogenopyridinium halogenides (halogen = Cl, Br, I), there are groups of six isostructural salts, while among *meta*-halogenopyridinium halogenides there are two groups of four.[45−48]

In the present work, we are describing the design, preparation, and study of a series of *N*-(4-halogenobenzyl)-3-halogenopyridinium halogenides. The cation was selected as a potential donor of two inequivalent halogen bonds—one through the halogen on the pyridine ring (on which the majority of the charge is expectedly located) and the other through the halogen on the *N*-benzyl substituent. Using a halogenide counterion as a halogen-bond acceptor gives a total of three halogen atoms (two on the cation and one of the anion) which can be interchanged in order to investigate in which cases the exchange of the halogen will induce a change in the structure and when it will yield an isostructural solid. Additionally, as we are using a relatively large cation (comprising two rings), the exchange of halogen substituents will only lead to small differences in the overall molecular volume, which should lead to a higher probability of obtaining isostructural crystals.[49] This would enable us to study in more detail how halogen bond affects the structures and properties of the crystals.

RESULTS AND DISCUSSION

The cations were prepared by reacting *meta*-halogenopyridines (Cl, Br, and I) with (4-halogenobenzyl) bromides (Br and I), which yielded a series of six bromide salts of *N*-(4-halogenobenzyl)-3-halogenopyridinium cations. Iodides and chlorides were prepared from the bromides by ion exchange, giving an overall potential of 18 compounds which differ only in one or more halogen atoms (Scheme 1). For the sake of simplicity, these will be referred throughout the text as $\mathbf{X^1X^2X^3}$, where $\mathbf{X^1}$ is the halogen substituent on the benzyl ring, $\mathbf{X^2}$ the substituent on the pyridine ring, and $\mathbf{X^3}$ the halogenide anion.

Scheme 1. Halogen-Bonded Cation−Anion Pair with Annotation of the Three Halogen Atoms

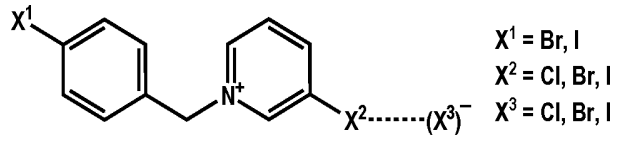

All the bromides and iodides crystallized as simple 1:1 salts with no inclusion of solvent molecules. In the case of chlorides, however, the outcome of the synthesis was found to depend on the halogen substituent on the pyridine ring. The two cations derived from 3-iodopyridine thus yielded simple chloride salts equivalent to the iodides and the bromides. When bromine replaced the iodine atom on the pyridine ring, the chlorides crystallized as hydrates (**IBrCl**·H_2O and **BrBrCl**·1.5H_2O), while the two chlorides of the cations derived from 3-chloropyridine could not be isolated. Thus, out of the 18 possible $\mathbf{X^1X^2X^3}$ combinations, a total of 16 were obtained: 14 as simple salts, and two as hydrates.

In order to evaluate the potential of the halogen atoms on the cations for formation of halogen bonds, we performed DFT computations of the electrostatic potential (ESP) of the cations *in vacuo*. These have shown that the halogen substituent on the pyridine ring in all cases has a more positive σ-hole ESP (V_{max}) than the benzyl substituent: for the halogen on the pyridine ring, $V_{max}(\mathbf{X^2})$ decreases from iodine (ca. 435 kJ mol^{-1} e^{-1}) over bromine (ca. 400 kJ mol^{-1} e^{-1}) to chlorine (ca. 360 kJ mol^{-1} e^{-1}), whereas for the benzyl halogenides $V_{max}(\mathbf{X^1})$ is ca. 320 kJ mol^{-1} e^{-1} for iodine and ca. 290 kJ mol^{-1} e^{-1} for bromine (Figure 1). It is therefore evident that the pyridine halogen atom is expected to form stronger halogen bonds, which will therefore (expectedly) be the dominant contribution in determining the properties of the materials. Indeed, this seems to be illustrated by the synthesis of the chlorides. As chloride is the best hydrogen bond acceptor of the three anions, only the strongest halogen bond donors (iodopyridinium cations) can entirely replace the water molecules which solvate the chloride in solution. Weaker halogen bond donors (bromopyridinium cations) do replace some of the solvent water, giving hydrates in which the chloride is an acceptor of a halogen bond and several HO−H···Cl^- hydrogen bonds. However, when only the weakest halogen bond donors (chloropyridinium cations) are present, the chloride remains entirely hydrated, rendering the salt extremely soluble (and probably hygroscopic and deliquescent), which explains our failure to obtain solid products.

Out of the 14 anhydrous salts, 11 belong to one isostructural series (type I) and the remaining three to another (type II). The first isostructural series comprises the iodide salts of all six cations and five bromides, while the second comprises the two chlorides and the remaining bromide (**IIBr**). The crystal structures of both series contain halogen-bonded chains, with cations and anions interconnected by halogen bonds (Figure 2, Figure S35 in the Supporting Information); each anion is an acceptor of two halogen bonds, one with the pyridine halogen atom ($\mathbf{X^2}\cdots(\mathbf{X^3})^-$), and one with the benzyl halogen atom ($\mathbf{X^1}\cdots(\mathbf{X^3})^-$). Along with the two halogen bonds, the halogenide anion is also an acceptor of several weak C−H···$(\mathbf{X^3})^-$ hydrogen bonding contacts with cations belonging to neighboring halogen-bonded chains (see Table S3 in the Supporting Information). These interactions interconnect the halogen-bonded chains into a 3D structure.

Isostructurality within the Type I Structures. In order to quantify the similarity of the 11 structures belonging to type I, we have calculated the unit cell similarity indices:

$$\pi_{AB} = |(a_A + b_A + c_A)/(a_B + b_B + c_B) - 1|$$

where a_A, b_A, and c_A are orthogonalized cell parameters for structure A, and a_B, b_B and c_B are orthogonalized cell parameters for structure B, as well as the isostructurality indices:

$$I_s(A, B) = \left|\left[\sum (\Delta R_{AB})^2/n\right]^{1/2} - 1\right| \times 100\%$$

where ΔR_{AB} is the difference of distances of atomic coordinates of equivalent atoms in structures A and B, and n is the number

https://doi.org/10.1021/acs.cgd.1c01285
Cryst. Growth Des. XXXX, XXX, XXX−XXX

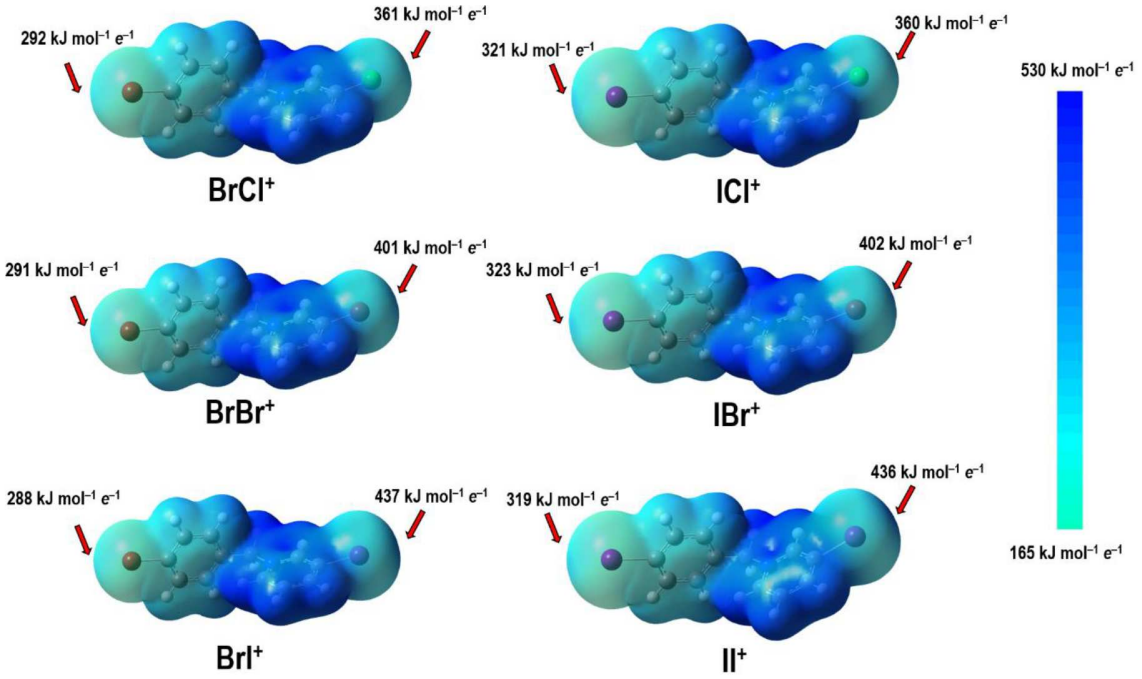

Figure 1. Electrostatic potential plotted on a 0.002 e Å^{-3} electron density isosurface for the six cations covered by this study, with values of ESP on the halogen σ-holes (V_{max}) for $\mathbf{X^1}$ and $\mathbf{X^2}$.

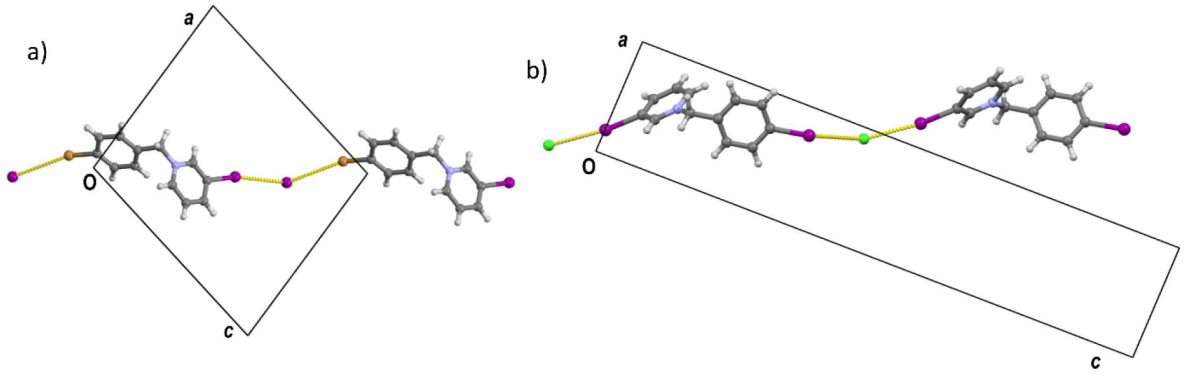

Figure 2. Halogen-bonded chains within the unit cell in (a) type I structures (in **BrII**) and (b) type II structures (in **IICl**). Both structures viewed along the crystallographic b axis.

of atoms in the section of the structure which is being compared for each pair of the structures.[13] For computation of I_s, all non-hydrogen atoms in the unit cell were taken into account (n = 56). The values of π_{AB} and I_s(A,B) for the 11 crystals belonging to the structural type I are given in Table 1.

Expectedly, the most similar structures (with I_s values above 85%) are generally those where only a single Cl/Br or Br/I substitution has occurred, although there are two highly isostructural pairs which differ in two halogen atoms (**IBrI**/**BrClI** with I_s of 87.2% and **IBrBr**/**BrClBr** with I_s of 86.8%). It should be noted that the structures are generally less sensitive to replacement of the halogen atoms of the cation (all of the above-mentioned pairs differ only in $\mathbf{X^1}$ or/and in $\mathbf{X^2}$) than the anion. This is most probably due to the larger differences in the radii of the halogenide anions. On the other hand, while the same observations generally hold for overall cell similarities, some of the isostructural pairs with the most similar cells do differ in the anion (**BrIBr**/**BrClI** with π = 0.004 and **IClBr**/**BrClI** with π = 0.009). Also, some pairs with the lowest π_{AB} feature Cl/I exchange (the above-mentioned **BrIBr**/**BrClI**, **IClI**/**BrII** with π = 0.002 and **IClBr**/**BrIBr** with π = 0.005). It is interesting to note that the Cl/I exchange with the least effect on cell similarity occurs only in $\mathbf{X^2}$ and is always in conjunction with a second (Br/I) exchange so that the large increase in the size of $\mathbf{X^2}$ is apparently somewhat compensated by a decrease in $\mathbf{X^1}$ or $\mathbf{X^3}$ and consequently does not significantly affect the overall unit cell dimensions (although it does lead to an overall change in atom positions, as evidenced by lower corresponding isostructurality indices: I_s(**BrIBr**/**BrClI**) = 60.0%; I_s(**IClI**/**BrII**) = 64.5% and I_s(**IClBr**/**BrIBr**) = 61.5%).

Generally, unit cell parameters within the type I series change fairly little—there is only ca. 4% difference between the maximum and minimum a and c lengths, ca. 7.5% between the maximum and minimum b lengths, and mere 1% between the maximum and minimum β angles. All the unit cell parameters

https://doi.org/10.1021/acs.cgd.1c01285
Cryst. Growth Des. XXXX, XXX, XXX−XXX

Table 1. Unit Cell Similarity (π_{AB}) and Isostructurality Indices (I_s(A,B)) for the 11 Crystals Belonging to Structural Type I[a]

Cell similarity indices (π·100) \ Isostructurality indices (I_s)	III	BrII	BrBrI	IBrI	BrClI	BrIBr	IClI	IBrBr	BrBrBr	BrClBr	IClBr
III		88.6	83.6	82.2	73.2	72.4	71.2	68.9	68.2	61.4	59.6
BrII	1.1		80.9	75.0	69.1	78.3	64.5	67.5	70.4	61.7	57.4
BrBrI	2.0	0.9		90.3	87.3	70.4	82.1	76.1	76.4	73.7	69.9
IBrI	0.9	0.2	1.1		87.2	64.9	88.0	75.5	72.3	71.3	70.8
BrClI	2.5	1.4	0.5	1.6		60.0	90.4	71.4	70.1	72.9	70.3
BrIBr	2.9	1.8	0.9	2.0	0.4		56.0	73.4	78.7	66.2	61.5
IClI	1.3	0.2	0.7	0.4	1.2	1.6		71.6	67.3	71.3	72.1
IBrBr	2.7	1.7	0.7	1.9	0.3	0.9	1.4		89.9	86.8	87.1
BrBrBr	4.0	2.9	2.0	3.1	1.5	1.1	2.7	1.3		87.0	80.9
BrClBr	4.6	3.5	2.6	3.7	2.1	1.9	3.3	1.9	0.6		89.7
IClBr	3.3	2.3	1.4	2.5	0.9	0.5	2.1	0.6	0.6	1.3	

[a]The isostructurality indices have been computed taking into account all non-hydrogen atoms in the unit cell (n = 56).

Scheme 2. Definition of the Parameters Describing the Halogen-Bonded Chains in Type I and Type II Structures

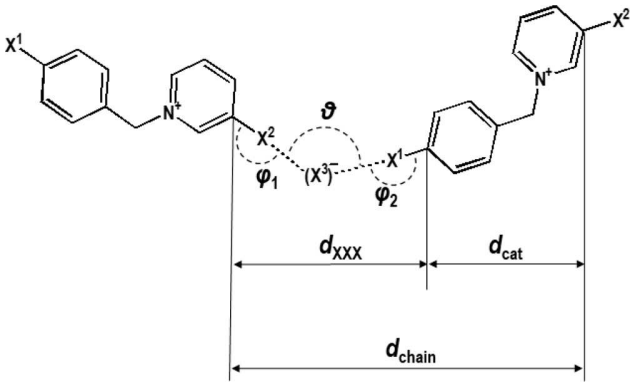

are somewhat affected by the nature of all three halogens. The unit cell vector lengths (a, b, and c) generally increase with the size of all three halogens, while β generally increases with $\mathbf{X^2}$ and decreases with $\mathbf{X^1}$ and $\mathbf{X^3}$. However, apart from the cell angle which appears to be affected by all three halogens to a more-or-less equal measure, a, b, and c cell parameters depend more on some of the halogens. Thus, a is mostly affected by $\mathbf{X^1}$ and to a lesser extent by $\mathbf{X^2}$ and $\mathbf{X^3}$, with bromides more sensitive to the changes of $\mathbf{X^1}$ than the iodides. Conversely, c is primarily dependent on $\mathbf{X^3}$ and to a smaller degree on $\mathbf{X^1}$; among the bromides, c is almost entirely independent of $\mathbf{X^2}$, but among the iodides, c slightly increases with the size of $\mathbf{X^2}$. The change of $\mathbf{X^2}$ has by far the largest effect on the length of b, as well as on the unit cell angle (Figure 3).

As the halogen-bonded chains in type I structures extend along the <101> direction (Figure 2c), the increase in a and c cell parameters, as well as the decrease of β, all correspond to an increase in the overall length of the period of the chain (total length of a cation−anion unit, d_{chain}, which in type I structures corresponds to the lattice period in the <101> direction, $d(101) = [a^2 + c^2 + 2ac \cos \beta]^{1/2}$; Scheme 2). Therefore, the increase of a and c with the size of all three halogens is to be expected, as the increase of the radius of either of the halogens is bound to lead to longer chains. However, the increase of β with the increase of the size (and halogen-bond donor strength) of $\mathbf{X^2}$, implies an effect of the halogen bond, rather than simply the radius of the halogen atom on the unit cell.

There is quite a significant difference in halogen bond donor and -acceptor properties when Cl/Br/I substitution occurs. Cations and anions are interconnected into chains by two inequivalent halogen bonds, the strength of which should increase with the increase of $\mathbf{X^1}$ and $\mathbf{X^2}$, ($\mathbf{II^+}$ being the expectedly best donor) and with the decrease of $\mathbf{X^3}$ (with Cl^- as the best acceptor). In the case of the halogen bond involving the pyridine halogen ($\mathbf{X^2}\cdots(\mathbf{X^3})^-$), there is an almost perfectly linear correlation (R^2 = 0.996) between the relative halogen bond length ($d_{rel} = d(\mathbf{X}\cdots(\mathbf{X^3})^-)/[r_{vdW}(\mathbf{X}) + r_p((\mathbf{X^3})^-)]$ (where is r_p the Pauling ionic radius[50])) and the halogen bond angle. Both primarily depend on $\mathbf{X^2}$ (angles increasing from ca. 156° for $\mathbf{X^2}$ = Cl, over ca. 161° for $\mathbf{X^2}$ = Br to ca. 166° for $\mathbf{X^2}$ = I, and the relative lengths from ca. 96% for $\mathbf{X^2}$ = Cl, over ca. 90% for $\mathbf{X^2}$ = Br to ca. 85% for $\mathbf{X^2}$ = I). The nature of the acceptor has much less effect on the halogen bond angle, the bonds involving bromide as an acceptor being slightly more contracted than those involving iodide (Figure 4a). The nature of $\mathbf{X^1}$ on the other hand has very little effect on either the length or the angle of the $\mathbf{X^2}\cdots(\mathbf{X^3})^-$ halogen bond, except in the $\mathbf{X^1ClX^3}$ series, where **BrClI** and **BrClBr** form somewhat

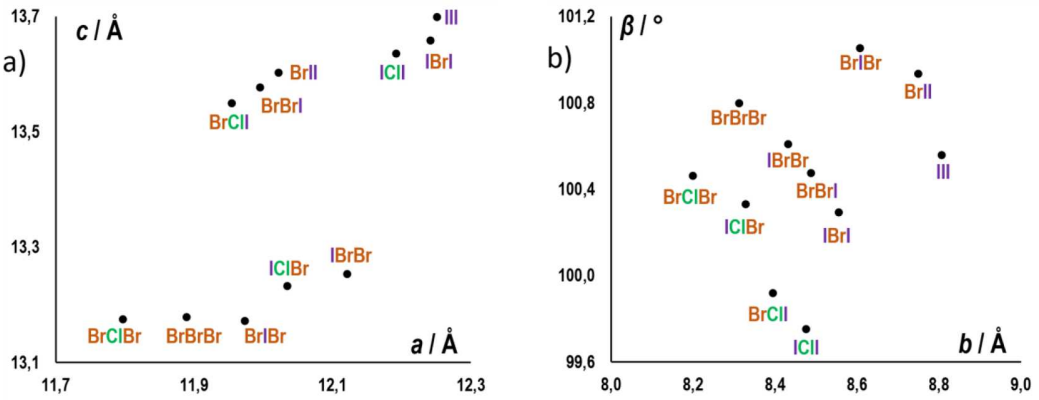

Figure 3. Unit cell parameters of type I structures (a) c vs a plot, (b) β vs b plot.

https://doi.org/10.1021/acs.cgd.1c01285
Cryst. Growth Des. XXXX, XXX, XXX−XXX

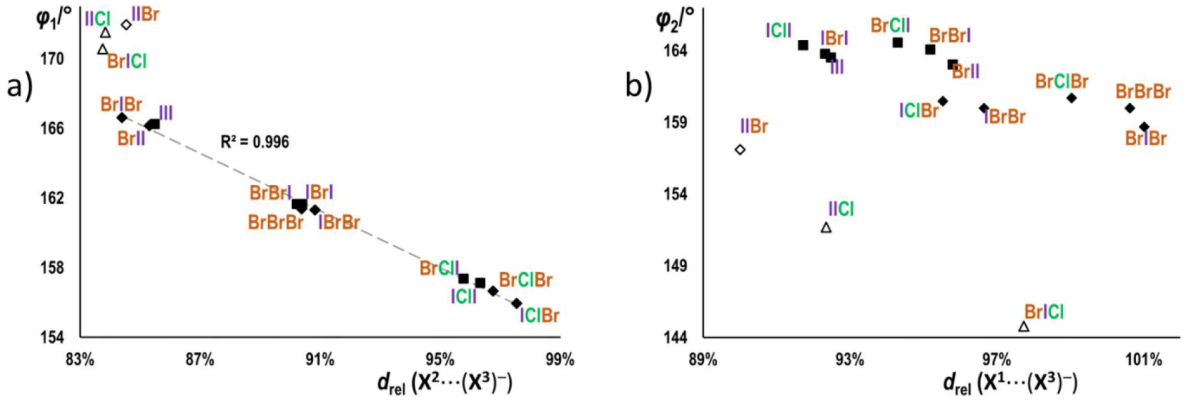

Figure 4. Correlation between the relative halogen bond length ($d_{rel} = d(X\cdots(X^3)^-)/[r_{vdW}(X) + r_p((X^3)^-)$ and the halogen bond angle (φ) for the (a) halogen bond with the donor atom on the pyridine ring (C2−$X^2\cdots(X^3)^-$) and (b) on the benzyl ring (C2−$X^1\cdots(X^3)^-$). Type I structures are represented by black circles, and type II structures are represented with white circles with a black border.

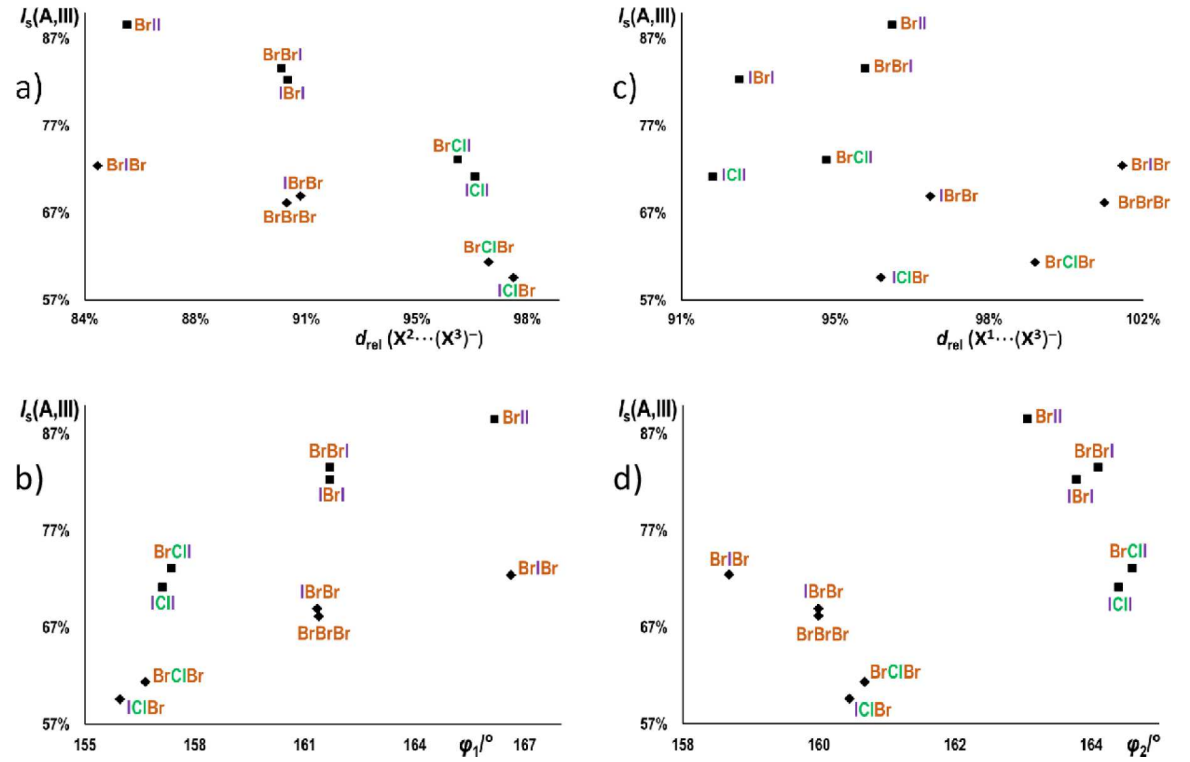

Figure 5. Correlations between the halogen bond parameters and the isostructurality index with respect to **III** (I_s(A,**III**), A ≠ **III**)) for structures of the type I series with (a) relative length of the $X^2\cdots X^3$ halogen bond, $d_{rel}(X^2\cdots X^3)$ plot; (b) angle of the $X^2\cdots X^3$ halogen bond, φ_1 plot; (c) relative length of the $X^1\cdots X^3$ halogen bond, $d_{rel}(X^1\cdots X^3)$, (d) angle of the $X^1\cdots X^3$ halogen bond, φ_2. Structures of iodide salts are represented by squares and bromide salts as rhombi.

shorter and more linear $X^2\cdots(X^3)^-$ bonds than their respective 4-iodobenzyl analogues (**ICII** and **ICIBr**).

The halogen bonds involving the benzyl halogen ($X^1\cdots(X^3)^-$) tend to be somewhat more linear (halogen bond angles mostly in the ca. 159−165° range) but relatively longer (d_{rel} = in the 92−101% range). The interdependence of the bond angles versus relative lengths follows the same general trend as in the case of the $X^2\cdots(X^3)^-$ bond, albeit with a considerably larger scatter of the data points (Figure 4b) and dependence on X^3 and X^2. The structures with the stronger donor atom (X^1 = I) generally exhibit relatively shorter and more linear bonds than those with (X^1 = Br). Conversely, the structures with the stronger acceptor (X^3 = Br) are generally longer and less linear than those with X^3 = I. There is also a significant dependence of the $X^1\cdots(X^3)^-$ halogen-bond parameters on X^2—within each group of structures which differ only in X^2, the relative length increases, and the angle decreases, in the order X^2 = Cl < Br < I.

All of these observations, as well as the (almost) perfect linearity of the $d_{rel}(X^2\cdots X^3)/\varphi_1$ plot, indicate that the $X^2\cdots(X^3)^-$ halogen bond is the dominant interaction in the crystal structure—the structural differences within the type I series of structures are primarily dictated by the $X^2\cdots(X^3)^-$ halogen bond, while the geometry of the $X^1\cdots(X^3)^-$ halogen bond is modified so that the crystal packing may better accommodate the difference in the $X^2\cdots(X^3)^-$ halogen bond. Thus, $X^2\cdots(X^3)^-$

https://doi.org/10.1021/acs.cgd.1c01285
Cryst. Growth Des. XXXX, XXX, XXX−XXX

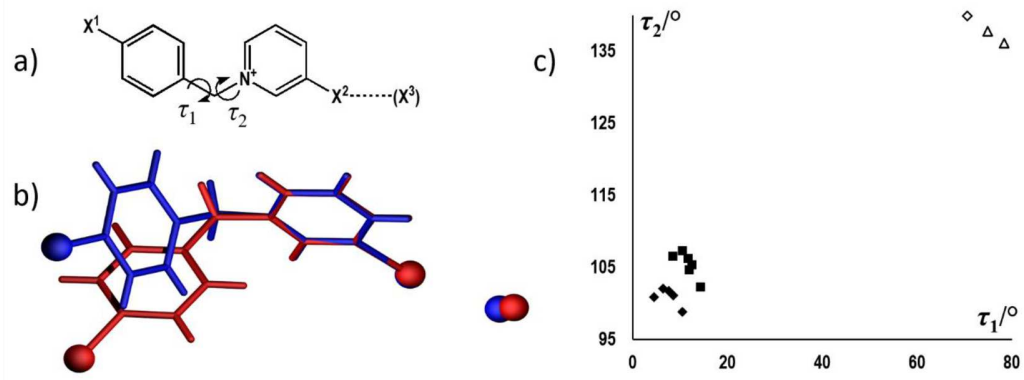

Figure 6. Comparison of conformations of cations in type I and type II structures: (a) τ_1 and τ_2 torsion angles, (b) overlay of a cation−anion pair (pyridine ring defined as the anchor) in a type I structure (**BrIBr**, red) and a type II structure (**IIBr**, blue), (c) scatterplot of τ_1 and τ_2 torsion angles for type I (black) and type II structures (white with black border). Structures of iodide salts are represented by squares, bromide salts as rhombi, and chloride as triangles.

halogen bonds with the stronger acceptor anion (bromide) tend to be shorter and more linear than those with the iodide, but $\mathbf{X^1}\cdots(\mathbf{X^3})^-$ bonds are longer and less linear since within a $\mathbf{X^2}\cdots(\mathbf{X^3})^-\cdots\mathbf{X^1}$ group the stronger acceptor (bromide) is more drawn to the stronger donor ($\mathbf{X^2}$), thus elongating and deforming the $\mathbf{X^1}\cdots(\mathbf{X^3})^-$ halogen bond. Also, the change of $\mathbf{X^2}$ affects the geometry of $\mathbf{X^1}\cdots(\mathbf{X^3})^-$ so that the geometry of the $\mathbf{X^1}\cdots(\mathbf{X^3})^-$ halogen bond becomes less favorable as the strength of the halogen bond donor of the $\mathbf{X^2}\cdots(\mathbf{X^3})^-$ halogen bond increases, while the $\mathbf{X^2}\cdots(\mathbf{X^3})^-$ halogen bond is generally independent of $\mathbf{X^1}$.

This dominance of the $\mathbf{X^2}\cdots(\mathbf{X^3})^-$ halogen bond is also in accord with the calculated electrostatic potential in the σ-holes of the halogens (V_{max}(X)) which are in all cases higher for the halogen bonded on the pyridine ring than on the halogen on the benzyl ring (Figure 1). It should be noted, however, that the difference in V_{max} for $\mathbf{X^2}$ = Cl and $\mathbf{X^1}$ = I is relatively small (ca. 12%), which indicates that in the case of chloropyridine derivatives the competition between the benzyl-I$\cdots(\mathbf{X^3})^-$ halogen bond might be able to somewhat compete with the pyridine-Cl$\cdots(\mathbf{X^3})^-$ halogen bond. This indeed does seem to be the case, seeing that in the $\mathbf{X^1ClX^3}$ series, the pyridine-Cl$\cdots(\mathbf{X^3})^-$ bond parameters are apparently more dependent on the nature of $\mathbf{X^1}$, being somewhat longer and less linear when $\mathbf{X^1}$ = I, as opposed to $\mathbf{X^1}$ = Br (in each pair with identical $\mathbf{X^3}$).

Seeing that the $\mathbf{X^2}\cdots(\mathbf{X^3})^-$ halogen bond has been demonstrated as the dominant interaction in the type I isostructural series, the obvious question which arises is whether, and in what manner, is the isostructurality within the series dependent on this halogen bond. As a unique descriptor for each structure within the isostructural series, we have decided to use the similarity between a given structure and an arbitrarily selected standard "structure". As the standard, we have selected **III**. This is because we have calculated the I_s with respect to the entire contents of the unit cell, and, consequently, I_s for any pair of structures depends on the difference of the unit cell sizes, and therefore a structure with one of the extreme cell volumes (**BrClBr** with the smallest, or **III** with the largest cell volume) is a logical choice as the standard for comparison.

The correlations between the halogen bond parameters and the isostructurality index with respect to **III** (I_s(A,**III**) for structures of the type I series (A ≠ **III**)) are given in Figure 5. It was noted earlier that the structures are more affected by the exchange of $\mathbf{X^3}$ than either $\mathbf{X^1}$ or $\mathbf{X^2}$. This is once more demonstrated by the plots of I_s(A,**III**) vs the halogen bond lengths and angles, which show that the dominant determinator of the similarity of the structures is not the halogen bond geometry, but rather the anion, with the iodides more similar to **III** than the bromides. However, there is a definite correlation between the I_s(A,**III**) and both relative length and the angle of the (stronger) $\mathbf{X^2}\cdots(\mathbf{X^3})^-$ halogen bond: within both the iodide and the bromide series, there is an increase in I_s(A,**III**) as the halogen bond becomes more linear and a decrease as it becomes longer. As the $\mathbf{X^2}\cdots(\mathbf{X^3})^-$ halogen bond in **III** is (relatively) shorterst and most linear within the type I structures ($d_{rel}(\mathbf{X^2}\cdots\mathbf{X^3})$ = 85.49%; φ_1 = 166.25°), it follows that an increase in similarity of the halogen bond parameters should lead to an increase in the overall similarity of the crystal structures. Conversely, there is no discernible correlation between the I_s(A,**III**) and the relative length of the (weaker) $\mathbf{X^1}\cdots(\mathbf{X^3})^-$ halogen bond—the plot of I_s(A,**III**) versus $d_{rel}(\mathbf{X^1}\cdots\mathbf{X^3})$ reveals only the general trends of I_s(A,**III**) rising with the sizes of all three halogens. However, the angle of the $\mathbf{X^2}\cdots(\mathbf{X^3})^-$ halogen bond does show a definite correlation with the I_s(A,**III**)—again the same general trend among the iodides and the bromides—of reduction of the similarity of structures as compared to **III** with the increase of φ_2. As **III** has one of the smallest φ_2 angles in the series (φ_2(**III**) = 163.52°), the decrease of similarity to **III** with the increase of φ_2 is to be expected. On the other hand, as all the bromides have lower φ_2 angles than **III**, the increasing similarity in values of φ_2 is *reducing* the overall similarity of the crystal structures. However, the increase of φ_2 follows the decrease in the $\mathbf{X^2}\cdots(\mathbf{X^3})^-$ halogen bond strength (notice that in both iodides and bromides it increases with the reduction of $\mathbf{X^2}$: $\mathbf{X^1IX^3}$ < $\mathbf{X^1BrX^3}$ < $\mathbf{X^1ClX^3}$). It can therefore be concluded that the structural similarity within the type I is primarily determined by the anion and the $\mathbf{X^2}\cdots(\mathbf{X^3})^-$ halogen bond, the observed correlation between I_s(A,**III**) and φ_2 being one of the consequences thereof.

Type II Structures. The two chloride salts which did not crystallize as hydrates (**IICl** and **BrICl**), as well as one of the bromides (**IIBr**), form a second isostructural series (type II). Type II structures are somewhat less closely packed than the type I structures (average KPC 68.9 for type I and 66.9 for type II). They also comprise halogen-bonded chains; however, there are significant differences as compared with Type I

https://doi.org/10.1021/acs.cgd.1c01285
Cryst. Growth Des. XXXX, XXX, XXX−XXX

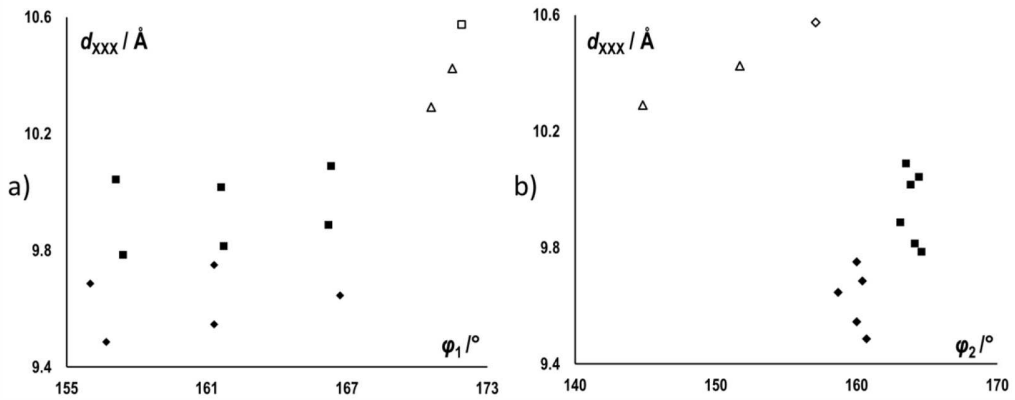

Figure 7. Parameters describing the halogen-bonded chains in type I (black) and type II structures (white with black border): length of the fragment of the halogen-bonded chain which contains both halogen bonds (d_{XXX}) vs (a) angle of the $\mathbf{X^2}\cdots(\mathbf{X^3})^-$ halogen bond (φ_1) and (b) *s* angle of the $\mathbf{X^1}\cdots(\mathbf{X^3})^-$ halogen bond (φ_2). Structures of iodide salts are represented by squares, bromide salts as rhombi, and chloride as triangles.

structures. One of the differences is the conformation of the cation (Figure 6a,b), which is best described by the two torsion angles about the two single bonds: τ_1 (C12−C7−C6−N1) and τ_2 (C1−N1−C6−C7): while in type I structures τ_1 is generally quite small (in the range 5−12°), in type II structures it increases to above 70°. The values of τ_2 also increase from 98° to 108° in type I structures (where τ_2 is somewhat dependent on the counterion, being under 102.1° in all bromides and above 102.2° in all iodides) to 136−140° (Figure 6c). This increase in the torsion angles leads to an increase of the overall length of the hydrocarbon skeleton of the cation (d_{cat}, measured as the distance between the two halogenated carbon atoms (C2 and C10) on the same cation, see Scheme 2) from ca. 9.5 Å to 10.1 Å in type I to ca. 10.3 to 10.6 Å in type II.

The most obvious difference in the halogen-bonded chains in type II structures, as compared to type I, is in the angle between the two halogen bonding contacts formed by the anion (ϑ, see Figure S36 in the Supporting Information), which in type I always remains within the range of ca. 123.8−126.4°, while in type II it takes up values between ca. 150.8 and 153.2° (Figure 7). As ϑ increases, so does the length of the fragment of the halogen-bonded chain which contains both halogen bonds (d_{XXX}, measured as the distance between the two halogenated carbon atoms (C2 and C10′) on neighboring cations forming halogen bonds with the same anion see Figure S36 in the Supporting Information). Interestingly, although both d_{cat} and d_{XXX} are considerably longer in type II structures, the overall length of a unit of the halogen-bonded chain (d_{chain}) differs relatively little between the two types (Figure S36 in the Supporting Information)—bromides of type I and II differ by ca. 0.8 Å in d_{XXX} and ca. 0.4 in d_{cat}, while the difference in d_{chain} is only ca. 0.5 Å (much less than $d_{XXX} + d_{cat}$). This is because the increase in d_{XXX} and d_{cat} in type II structures is compensated for by changes in halogen bond geometries. The halogen bond involving the pyridine halogen donor ($\mathbf{X^2}\cdots(\mathbf{X^3})^-$) in type II structures is both shorter and more linear (Figure 3a) than in type I structures. On the other hand, the halogen bond involving the benzyl halogen donor ($\mathbf{X^1}\cdots(\mathbf{X^3})^-$) is generally shorter, but also less linear in type II structures, leading to an overall decrease in the C10$\cdots(\mathbf{X^3})^-$ distance (Figure 3b).

The differences between the halogen bonds in the two structural types indicate the probable cause for the existence of the two types. The main discriminator between the two structural types is the halogen bond, primarily, the dominant $\mathbf{X^2}\cdots(\mathbf{X^3})^-$ halogen bond. The increased ϑ in type II structures allows for a closer approach of the donor ($\mathbf{X^2}$) to the acceptor ($(\mathbf{X^3})^-$) and therefore a more favorable geometry leading to a higher bond energy. Importantly, type II is achieved by the combination of the strongest halogen bond donors (iodopyridinium derivatives) and the strongest acceptors (chloride anions). The bromide anion also forms a type II structure with one iodopyridinium donor (**IIBr**) but not the other (**BrIBr** crystallizes as type I), indicating that the benzyl halogen (and therefore the $\mathbf{X^1}\cdots(\mathbf{X^3})^-$ halogen bond) is also a factor in discriminating between the two types of structure. This principle is illustrated in Figure 8 where the distribution of

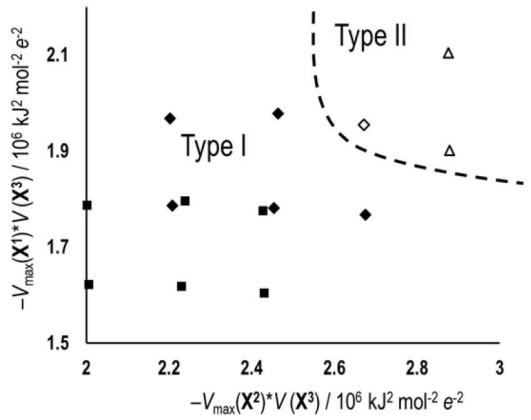

Figure 8. Distribution of the two isostructural series on a plot of the products of the electrostatic potentials of weaker cation donor and halogenide anion acceptor ($V_{max}(\mathbf{X^1})*V(\mathbf{X^3})$) vs products of the electrostatic potentials of stronger cation donor and halogenide anion acceptor ($V_{max}(\mathbf{X^2})*V(\mathbf{X^3})$).

the two types is shown on a plot of the products of the electrostatic potentials of cation donors and halogenide anion acceptors (being a convenient measure for the relative potential for halogen bonding in a given donor/acceptor pair within a closely related group).

Another convenient descriptor of the halogen bond strength is the *in vacuo* interaction energy of the ion pairs with the $\mathbf{X^2}\cdots(\mathbf{X^3})^-$ (or $\mathbf{X^1}\cdots(\mathbf{X^3})^-$) contacts with geometries as found in the crystals ($E(\mathbf{X^2}\cdots\mathbf{X^3})$ viz. $E(\mathbf{X^1}\cdots\mathbf{X^3})$). While these energies are

https://doi.org/10.1021/acs.cgd.1c01285
Cryst. Growth Des. XXXX, XXX, XXX−XXX

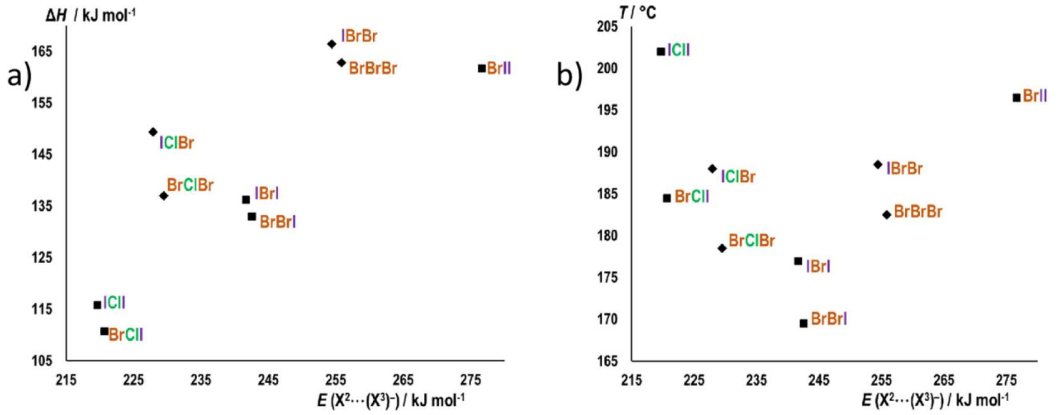

Figure 9. Correlation between the computed $X^2\cdots(X^3)^-$ interaction energies of ion pairs (computed *in vacuo* for geometries as found in the crystals, $E(X^2\cdots(X^3)^-)$) and (a) the evaporation enthalpies (ΔH), (b) onset temperatures (T) of the melting/evaporation within the type I structures. Structures of iodide salts are represented by squares and bromide salts as rhombi.

by no means realistic estimates of the energies of the corresponding contacts in the solid state, they are indicative of the general trends these energies should follow. When these are calculated for the $X^2\cdots(X^3)^-$ contacts for all 14 structures, they show that $X^2\cdots(X^3)^-$ contacts in geometries corresponding to type II correspond to higher interaction energies than those of type I geometries (Figure S37 in the Supporting Information). This once more suggests that the energy gain due to the more favorable geometry of the $X^2\cdots(X^3)^-$ halogen bond is the main driving force for the formation of type II structures.

Thermal Properties of Type I Structures. The size of the type I isostructural series has prompted us to investigate whether there is a clear and measurable effect of the halogen bond on the thermal properties of the type I solids. As within the isostructural series the only significant difference is in the halogen bond donors and acceptors, it can be expected that the differences in the halogen bond energies in various crystals will be the dominant cause of differences in their thermal properties. In order to investigate this, we have performed thermal analysis (TG and DSC) for the compounds which have crystallized with type I structures. These have shown that nine of these salts undergo evaporation in the temperature range from 170 to 200 °C without previous thermal events. The evaporation is characterized by a continuous loss of the entire mass of the sample in the TG, with the DSC curves generally exhibiting two endothermic signals (probably corresponding to almost simultaneous melting and evaporation) which are to a larger or lesser degree coalesced into one (Figures S17−S31 in the Supporting Information). In the case of two compounds (**III** and **BrIBr**), the DSC curve is more complex, with additional signals at lower temperatures and also somewhat lower temperatures of the melting/evaporation event (163 and 169 °C, respectively). As their thermal behavior is obviously different from that of the remaining members of the series, they have been excluded from the further analysis of the data.

There is a clear linear correlation between the $E(X^2\cdots X^3)$ and the evaporation enthalpies within the type I structures (Figure 9a), which is particularly evident when comparing structures which differ only in X^2 (for the **BrII**−**BrBrI**−**BrClI** series, R^2 = 0.997). The differences in evaporation enthalpies between compounds which differ only in X^2 are generally similar to the corresponding differences in $E(X^2\cdots X^3)$ (Table S4 in the Supporting Information). As for the weaker, $X^1\cdots(X^3)^-$ halogen bond, there is no apparent correlation between the enthalpies and the gas phase interaction energy $E(X^1\cdots X^3)$ (Figure S32 in the Supporting Information). However, the nature of X^1 also slightly affects the evaporation enthalpy, as within each BrX^2X^3/IX^2X^3 pair of structures, the IX^2X^3 analogue has higher evaporation enthalpy (by 3.5−12.5 kJ mol^{-1}), indicating the contribution of the $X^1\cdots(X^3)^-$ bond to the total packing energy.

The evaporation enthalpy is also significantly affected by the nature of the halogenide (i.e., halogen bond acceptor)—while following the same trend with respect to $E(X^2\cdots X^3)$, the bromides systematically have higher evaporation enthalpies than the iodides. This cannot be accounted for by a difference in halogen bonding. Rather, the most likely cause for this difference between the iodides and the bromides lies in the difference between the C−H···X^- hydrogen bond energies for iodide and bromide. In all structures, the anion, along with the halogen bonds within a halogen-bonded chain, also forms C−H···X^- hydrogen bonds with cations from neighboring chains. As bromide is a stronger hydrogen bond acceptor than the iodide, more energy is required in order to sever the C−H···Br^- hydrogen bonds upon evaporation, leading to higher overall enthalpies.

Unlike the evaporation enthalpies which are clearly dominated by the contribution of the $X^2\cdots(X^3)^-$ halogen bonds, the onset temperatures of the melting/evaporation show a somewhat more complex behavior (Figure 9b). For stronger $X^2\cdots(X^3)^-$ halogen bonds (with X^2 = Br, I), the onset temperatures expectedly increase with the $E(X^2\cdots X^3)$, again with iodobenzyl derivatives at somewhat higher onset temperatures than their bromobenzyl analogues (by 6−7.5 °C). However, in the case of weaker $X^2\cdots(X^3)^-$ halogen bonds (with X^1 = Cl), the trend is apparently the opposite—onset temperatures decrease with $E(X^2\cdots X^3)$. The differences in the onset temperatures within the BrX^2X^3/IX^2X^3 pairs are also higher (by 7.5−17.5 °C). The latter observation is in line with the larger contribution of the $X^1\cdots(X^3)^-$ halogen bond to the overall packing energy (due to the reduced contribution of $X^2\cdots(X^3)^-$ halogen bond because of relatively lower V_{max}(Cl)—see discussion above). The increase of the onset temperatures with the decrease of $E(X^2\cdots X^3)$ among the chloropyridine derivatives is however somewhat more difficult to account for. As the evaporation enthalpies change regularly

https://doi.org/10.1021/acs.cgd.1c01285
Cryst. Growth Des. XXXX, XXX, XXX−XXX

with $E(\mathbf{X}^2\cdots\mathbf{X}^3)$, the most probable reason for the different trend in melting/evaporation onset temperatures is a different trend in the lattice entropies. It can be expected that within the $\mathbf{X}^1\mathbf{ClX}^3$ series the lattice entropy is higher (due to less constricted thermal motion in less strongly bonded structures), increasing with decreasing $E(\mathbf{X}^2\cdots\mathbf{X}^3)$. As the lattice entropy increases, the entropy change upon melting/evaporation decreases, which can be expected to cause an increase in the phase transition temperature. However, as only four data points are involved, one cannot exclude the possibility that the apparent trend is merely an artifact of a random distribution.

CONCLUSION

N-(4-Halogenobenzyl)-3-halogenopyridinium halogenides have proven to be an excellent platform for the study of isostructural halogen exchange, as they fall within two series of isostructural solids. The larger series (type I) comprises 11 structures and allows for an in-depth study of the effect of halogen exchange (and therefore differences in the halogen bonding) on the crystal structure and properties. The halogenide anion acts as an acceptor of two inequivalent halogen bonds with neighboring cations. Of these, the one formed by the halogen on the pyridine ring (which exhibits a more positive σ-hole potential than the halogen on the benzyl ring, even in the case of chloropyridine derivatives) is dominant—it adopts the optimal geometry (within the given structure type), while the other halogen bond distorts in order to accommodate it. This halogen bond is also the reason for the appearance of the second structural type, which allows it to adopt an even more favorable geometry. Also, it is the main cause of the differences in evaporation enthalpies within the type I structures. However, the halogen bond involving the benzyl ring halogen as the donor also has a noticeable effect, both on the structure (within the **IIBr**/**BrIBr** pair the nature of this donor is the discriminating factor of the structural type) and on the properties (within each $\mathbf{BrX}^2\mathbf{X}^3/\mathbf{IX}^2\mathbf{X}^3$ pair of structures, the $\mathbf{IX}^2\mathbf{X}^3$ analogue has higher evaporation enthalpy). It can therefore be concluded that although one halogen bond is clearly dominant, the interplay of both is responsible for the structural features of *N*-(4-halogenobenzyl)-3-halogenopyridinium halogenides. Indeed, it can be hypothesized that the fact that such a large number of cation/anion combinations (11) adopt essentially the same structure (type I) is due, on the one hand, to the existence of strongly directing interactions which ensure the same supramolecular topology (chains), and on the other to a sufficient degree of flexibility in the weaker halogen bond (and somewhat in the cation structure), which can adapt in order to compensate for the changes in the atom size and (stronger) halogen bond length and angle.

EXPERIMENTAL SECTION

Synthesis. All solvents (acetone, dichloromethane, ethanol), acids (hydrochloric and hydroiodic), and the ion-exchange resin (Dowex 21K chloride form, 16-30 mesh) were purchased from Sigma-Aldrich Company. 3-Chloropyridine, 3-bromopyridine, and (4-bromobenzyl) bromide were purchased from Acros Organics, while 3-iodopyridine (4-iodobenzyl) bromide was from Apollo Scientific. All the solvents and reagents were used as received.

N-(4-Halogenobenzyl)-3-halogenopyridinium bromides were prepared by dissolving equimolar amounts (1 mmol) of corresponding 3-halogenopyridine and (4-halogenobenzyl) bromide in hot acetone (20 mL) whereupon the solutions were left to cool and evaporate.

Iodide and chloride salts of *N*-(4-halogenobenzyl)-3-halogenopyridinium cations were synthesized by ion exchange. *N*-(4-Halogenobenzyl)-3-halogenopyridinium hydroxides were prepared by passing the solutions of *N*-(4-halogenobenzyl)-3-halogenopyridinium bromides in deionized water (c = 0.1 mol L^{-1}) through the anion exchange column. The ion-exchange resin was regenerated with a 50 mL aqueous solution of sodium hydroxide (c = 1 mol L^{-1}). Obtained solutions of *N*-(4-halogenobenzyl)-3-halogenopyridinium hydroxides were neutralized with hydroiodic acid (c = 1 mol L^{-1}). Hydroiodic acid was added dropwise in the obtained solution until neutralization. The same procedure was used to prepare the chloride salts using hydrochloric acid instead of hydroiodic acid.

Single crystals (suitable for single crystal X-ray diffraction experiment) of *N*-(4-halogenobenzyl)-3-halogenopyridinium bromides and iodides were obtained directly from synthesis. In the case of chlorides, single crystals were obtained by recrystallizing the obtained solid product from a mixture of dry ethanol and dry acetone.

X-ray Diffraction Measurements. All single-crystal X-ray diffraction experiments were performed using an Oxford Diffraction XtaLAB Synergy, Dualflex, HyPix X-ray four-circle diffractometer with mirror-monochromated MoKα (λ = 0.71073 Å) radiation. The data sets were collected using the ω-scan mode over the 2θ range up to 60°. Programs CrysAlis PRO CCD and CrysAlis PRO RED were employed for data collection, cell refinement, and data reduction.[51,52] The structures were solved by SHELXT[53] or by direct methods using the SHELXS and refined using SHELXL programs.[54] The structural refinement was performed on F^2 using all data. The hydrogen atoms were placed in calculated positions and treated as riding on their parent atoms (C−H = 0.95 Å and U_{iso}(H) = 1.2 U_{eq}(C) for aromatic hydrogen atoms; C−H = 0.99 Å and U_{iso}(H) = 1.2 U_{eq}(C) for methylene hydrogen atoms). In the case of both hydrates, the water hydrogen bonding atoms were located in the electron difference map. All calculations were performed using the WinGX[55] or Olex2 1.3-ac4[56] crystallographic suite of programs. A summary of data pertinent to X-ray crystallographic experiments is provided in Table S1 (see Supporting Information). Further details are available from the Cambridge Crystallographic Centre (CCDC 2118712−2118727 contain crystallographic data for this paper). Molecular structures of compounds and their packing diagrams were prepared using Mercury.[57]

Thermal Analysis. Differential scanning calorimetry (DSC) and thermogravimetric (TG) measurements were performed simultaneously on a Mettler Toledo TGA/DSC 3+ module. Samples were placed in alumina crucibles (40 μL) and heated 25 to 300 °C, at a heating rate of 10 °C min^{-1} under nitrogen flow of 50 mL min^{-1}.

Data collection and analysis were performed using the program package STARe Software (Version 15.00, Mettler Toledo, Greifensee, Switzerland).[58] TG and DSC thermograms of the prepared compounds are shown in Figures S11−S15 in Supporting Information.

Computational Details. All calculations were performed using the Gaussian 09 software package.[59] Geometry optimizations of cation molecules for analysis of the molecular electrostatic potential were performed using the b3lyp/dgdzvp level of theory.[60,61] Harmonic frequency calculations were performed on the optimized geometries to ensure the success of each geometry optimization. Single-point energies of the ion pairs *in vacuo* were determined using the M062X/dgdzvp[62] lever of theory on geometries obtained by X-ray crystallography. This combination of the functional and the basis set was shown to reproduce experimental halogen bond energies in the gas phase with good accuracy, which are comparable to energies obtained by using larger and more time-consuming triple-ζ basis sets.[63] Interaction energies between ions were calculated and corrected by basis set superposition errors (BSSE) according to the counterpoise method of Boys and Bernardi.[64,65] The figures were prepared using GaussView.[66]

https://doi.org/10.1021/acs.cgd.1c01285
Cryst. Growth Des. XXXX, XXX, XXX−XXX

■ ASSOCIATED CONTENT

Supporting Information

The Supporting Information is available free of charge at https://pubs.acs.org/doi/10.1021/acs.cgd.1c01285.

Crystallographic data for all compounds; ORTEP representations of the formula units of the prepared compounds; TG and DSC curves; an overview of supramolecular interactions in studied *N*-(4-halogenobenzyl)-3-halogenopyridinium halogenides; calculated ESP products and halogen bond energies; calculated Kitaigorodsky packing coefficient (KPC) and other parameters describing the halogen-bonded chains; measured melting/sublimation point temperatures and enthalpies, correlation between the computed $X^1\cdots(X^3)$−halogen bond energies and (a) the evaporation enthalpies (ΔH), (b) onset temperatures (T) of the melting/evaporation within the type I structures; correlation of *Is* and the unit cell parameters of type I structures: (a) *Is* vs *V* plot, (b) *Is* vs *a* plot, (c) *Is* vs *b* plot, (d) *Is* vs *c* plot, (e) *Is* vs β plot, (f) *Is* vs M_r plot; plot of the distance between the (a) [101] planes and (b) $[\bar{1}\ 0\ \bar{1}]$ planes vs isostructurality indices (*Is*(A, III)) for the 11 crystals belonging to the structural type I; total electron energies and Cartesian coordinates for optimized structures of *N*-(4-halogenobenzyl)-3-halogenopyridinium cations; single-point electron energies and Cartesian coordinates of *N*-(4-halogenobenzyl)-3-halogenopyridinium halogenides (PDF)

Accession Codes

CCDC 2118712−2118727 contain the supplementary crystallographic data for this paper. These data can be obtained free of charge via www.ccdc.cam.ac.uk/data_request/cif, or by emailing data_request@ccdc.cam.ac.uk, or by contacting The Cambridge Crystallographic Data Centre, 12 Union Road, Cambridge CB2 1EZ, UK; fax: +44 1223 336033.

■ AUTHOR INFORMATION

Corresponding Author

Vladimir Stilinović − *Department of Chemistry, Faculty of Science, University of Zagreb, 10000 Zagreb, Croatia;* orcid.org/0000-0002-4383-5898; Email: vstilinovic@chem.pmf.hr

Authors

Luka Fotović − *Department of Chemistry, Faculty of Science, University of Zagreb, 10000 Zagreb, Croatia*

Nikola Bedeković − *Department of Chemistry, Faculty of Science, University of Zagreb, 10000 Zagreb, Croatia*

Complete contact information is available at: https://pubs.acs.org/10.1021/acs.cgd.1c01285

Funding

Croatian Science Foundation, Project IP-2019-04-1868.

Notes

The authors declare no competing financial interest.

■ ACKNOWLEDGMENTS

We are grateful to Prof. Josip Požar for fruitful discussions. We also acknowledge the support of Project CIuK cofinanced by the Croatian Government and the European Union through the European Regional Development Fund-Competitiveness and Cohesion Operational Programme (Grant KK.01.1.1.02.0016).

■ DEDICATION

Dedicated to Dora Bedeković, in honor of her birth.

■ REFERENCES

(1) Desiraju, G. R. *Crystal Engineering. The Design of Organic Solids*; Elsevier: Amsterdam, 1989.

(2) Desiraju, G. R. Crystal Engineering: From Molecule to Crystal. *J. Am. Chem. Soc.* **2013**, *135* (27), 9952−9967.

(3) Aakeröy, C. B.; Champness, N. R.; Janiak, C. Recent Advances in Crystal Engineering. *CrystEngComm* **2010**, *12* (1), 22−43.

(4) Braga, D. Crystal Engineering, Where from? Where To? *Chem. Commun.* **2003**, No. 22, 2751.

(5) Nangia, A. K.; Desiraju, G. R. Crystal Engineering: An Outlook for the Future. *Angew. Chem., Int. Ed.* **2019**, *58* (13), 4100−4107.

(6) Desiraju, G. R. Crystal Engineering: A Holistic View. *Angew. Chem., Int. Ed.* **2007**, *46* (44), 8342−8356.

(7) Bernstein, J. *Polymorphism in Molecular Crystals*; Oxford University Press, 2020. DOI: 10.1093/oso/9780199655441.001.0001.

(8) Bučar, D.-K.; Lancaster, R. W.; Bernstein, J. Disappearing Polymorphs Revisited. *Angew. Chem., Int. Ed.* **2015**, *54* (24), 6972−6993.

(9) Bernstein, J. Pinching Polymorphs. *Nat. Mater.* **2005**, *4* (6), 427−428.

(10) Price, S. The Computational Prediction of Pharmaceutical Crystal Structures and Polymorphism. *Adv. Drug Delivery Rev.* **2004**, *56* (3), 301−319.

(11) Braga, D.; Brammer, L.; Champness, N. R. New Trends in Crystal Engineering. *CrystEngComm* **2005**, *7* (1), 1.

(12) Kálmán, A. Morphotropism: Link between the Isostructurality, Polymorphism and (Stereo)Isomerism of Organic Crystals. *Acta Crystallogr., Sect. B: Struct. Sci.* **2005**, *61* (5), 536−547.

(13) Kálmán, A.; Párkányi, L.; Argay, G. Classification of the Isostructurality of Organic Molecules in the Crystalline State. *Acta Crystallogr., Sect. B: Struct. Sci.* **1993**, *49* (6), 1039−1049.

(14) Fábián, L.; Kálmán, A. Volumetric Measure of Isostructurality. *Acta Crystallogr., Sect. B: Struct. Sci.* **1999**, *55* (6), 1099−1108.

(15) Bombicz, P.; May, N. V.; Fegyverneki, D.; Saranchimeg, A.; Bereczki, L. Methods for Easy Recognition of Isostructurality − Lab Jack-like Crystal Structures of Halogenated 2-Phenylbenzimidazoles. *CrystEngComm* **2020**, *22* (43), 7193−7203.

(16) Bombicz, P. The Way from Isostructurality to Polymorphism. Where Are the Borders? The Role of Supramolecular Interactions and Crystal Symmetries. *Crystallogr. Rev.* **2017**, *23* (2), 118−151.

(17) Grineva, O. V.; Zorkii, P. M. Isostructural and Nonisostructural Compounds in Series of Halogenated Organic Crystal Substances. Structure of Hal-Aggregates. *J. Struct. Chem.* **2001**, *42* (1). 16.

(18) Grineva, O. V.; Zorkii, P. M. Aggregation of Halogen Atoms in Crystalline Isomers. *J. Struct. Chem.* **2002**, *43* (6), 995−1005.

(19) Tella, A. C.; Owalude, S. O.; Omotoso, M. F.; Olatunji, S. J.; Ogunlaja, A. S.; Alimi, L. O.; Popoola, O. K.; Bourne, S. A. Synthesis, Crystal Structures and Luminescence Properties of New Multi-Component Co-Crystals of Isostructural Co(II) and Zn(II) Complexes. *J. Mol. Struct.* **2018**, *1157*, 450−456.

(20) Reddy, C. M.; Kirchner, M. T.; Gundakaram, R. C.; Padmanabhan, K. A.; Desiraju, G. R. Isostructurality, Polymorphism and Mechanical Properties of Some Hexahalogenated Benzenes: The Nature of Halogen···Halogen Interactions. *Chem. - Eur. J.* **2006**, *12* (8), 2222−2234.

(21) Claborn, K.; Kahr, B.; Kaminsky, W. Calculations of Optical Properties of the Tetraphenyl-X Family of Isomorphous Crystals (X = C, Si, Ge, Sn, Pb). *CrystEngComm* **2002**, *4* (46), 252−256.

(22) Chennuru, R.; Muthudoss, P.; Voguri, R. S.; Ramakrishnan, S.; Vishweshwar, P.; Babu, R. R. C.; Mahapatra, S. Iso-Structurality

Induced Solid Phase Transformations: A Case Study with Lenalidomide. *Cryst. Growth Des.* **2017**, *17* (2), 612−628.
(23) Wood, P. A.; Oliveira, M. A.; Zink, A.; Hickey, M. B. Isostructurality in Pharmaceutical Salts: How Often and How Similar? *CrystEngComm* **2012**, *14* (7), 2413.
(24) Krishna, G. R.; Devarapalli, R.; Lal, G.; Reddy, C. M. Mechanically Flexible Organic Crystals Achieved by Introducing Weak Interactions in Structure: Supramolecular Shape Synthons. *J. Am. Chem. Soc.* **2016**, *138* (41), 13561−13567.
(25) Saha, S.; Desiraju, G. R. Crystal Engineering of Hand-Twisted Helical Crystals. *J. Am. Chem. Soc.* **2017**, *139* (5), 1975−1983.
(26) Cinčić, D.; Friščić, T.; Jones, W. Structural Equivalence of Br and i Halogen Bonds: A Route to Isostructural Materials with Controllable Properties. *Chem. Mater.* **2008**, *20* (21), 6623−6626.
(27) Cinčić, D.; Friščić, T.; Jones, W. A Stepwise Mechanism for the Mechanochemical Synthesis of Halogen-Bonded Cocrystal Architectures. *J. Am. Chem. Soc.* **2008**, *130* (24), 7524−7525.
(28) Cinčić, D.; Friščić, T.; Jones, W. A Cocrystallisation-Based Strategy to Construct Isostructural Solids. *New J. Chem.* **2008**, *32* (10), 1776.
(29) Cinčić, D.; Friščić, T.; Jones, W. Structural Equivalence of Br and I Halogen Bonds: A Route to Isostructural Materials with Controllable Properties. *Chem. Mater.* **2008**, *20* (21), 6623−6626.
(30) Buldakov, A. V.; Kinzhalov, M. A.; Kryukova, M. A.; Ivanov, D. M.; Novikov, A. S.; Smirnov, A. S.; Starova, G. L.; Bokach, N. A.; Kukushkin, V. Y. Isomorphous Series of PdII-Containing Halogen-Bond Donors Exhibiting Cl/Br/I Triple Halogen Isostructural Exchange. *Cryst. Growth Des.* **2020**, *20* (3), 1975−1984.
(31) Adonin, S. A.; Bondarenko, M. A.; Novikov, A. S.; Sokolov, M. N. Halogen Bonding in Isostructural Co(II) Complexes with 2-Halopyridines. *Crystals* **2020**, *10* (4). 289.
(32) Dey, A.; Desiraju, G. R. Supramolecular Equivalence of Ethynyl, Chloro, Bromo and Iodo Groups. A Comparison of the Crystal Structures of Some 4-Phenoxyanilines. *CrystEngComm* **2004**, *6* (104), 642.
(33) Abate, A.; Martí-Rujas, J.; Metrangolo, P.; Pilati, T.; Resnati, G.; Terraneo, G. Tetrahedral Oxyanions in Halogen-Bonded Coordination Networks. *Cryst. Growth Des.* **2011**, *11* (9), 4220−4226.
(34) Bennion, J. C.; Vogt, L.; Tuckerman, M. E.; Matzger, A. J. Isostructural Cocrystals of 1,3,5-Trinitrobenzene Assembled by Halogen Bonding. *Cryst. Growth Des.* **2016**, *16* (8), 4688−4693.
(35) Kitaigorodsky, A. I. *Organicheskaya Kristallochimia (in Russian)*; Izdatelstvo akademii nauk SSSR: Moscow, 1955.
(36) Stilinović, V.; Horvat, G.; Hrenar, T.; Nemec, V.; Cinčić, D. Halogen and Hydrogen Bonding between (N-Halogeno)-Succinimides and Pyridine Derivatives in Solution, the Solid State and In Silico. *Chem. - Eur. J.* **2017**, *23* (22), 5244−5257.
(37) Espallargas, G. M.; Zordan, F.; Marín, L. A.; Adams, H.; Shankland, K.; van de Streek, J.; Brammer, L. Rational Modification of the Hierarchy of Intermolecular Interactions in Molecular Crystal Structures by Using Tunable Halogen Bonds. *Chem. - A Eur. J.* **2009**, *15* (31), 7554−7568.
(38) Bombicz, P.; Gruber, T.; Fischer, C.; Weber, E.; Kálmán, A. Fine Tuning of Crystal Architecture by Intermolecular Interactions: Synthon Engineering. *CrystEngComm* **2014**, *16* (18), 3646−3654.
(39) Hutchins, K. M.; Kummer, K. A.; Groeneman, R. H.; Reinheimer, E. W.; Sinnwell, M. A.; Swenson, D. C.; MacGillivray, L. R. Thermal Expansion Properties of Three Isostructural Co-Crystals Composed of Isosteric Components: Interplay between Halogen and Hydrogen Bonds. *CrystEngComm* **2016**, *18* (43), 8354−8357.
(40) Saraswatula, V. G.; Saha, B. K. A Thermal Expansion Investigation of the Melting Point Anomaly in Trihalomesitylenes. *Chem. Commun.* **2015**, *51* (48), 9829−9832.
(41) Saraswatula, V. G.; Saha, B. K. The Effect of Temperature on Interhalogen Interactions in a Series of Isostructural Organic Systems. *New J. Chem.* **2014**, *38* (3), 897−901.
(42) Powell, B. M.; Heal, K. M.; Torrie, B. H. The Temperature Dependence of the Crystal Structures of the Solid Halogens, Bromine and Chlorine. *Mol. Phys.* **1984**, *53* (4), 929−939.
(43) Ibberson, R. M.; Moze, O.; Petrillo, C. High Resolution Neutron Powder Diffraction Studies of the Low Temperature Crystal Structure of Molecular Iodine (I 2). *Mol. Phys.* **1992**, *76* (2), 395−403.
(44) Hursthouse, M. B.; Montis, R.; Tizzard, G. J. Intriguing Relationships and Associations in the Crystal Structures of a Family of Substituted Aspirin Molecules. *CrystEngComm* **2010**, *12* (3), 953−959.
(45) Awwadi, F. F.; Willett, R. D.; Peterson, K. A.; Twamley, B. The Nature of Halogen···halide Synthons: Theoretical and Crystallographic Studies. *J. Phys. Chem. A* **2007**, *111* (12), 2319−2328.
(46) Freytag, M.; Jones, P. G.; Ahrens, B.; Fischer, A. K. Hydrogen Bonding and Halogen-Halogen Interactions in 4-Halopyridinium Halides. *New J. Chem.* **1999**, *23* (12), 1137−1139.
(47) Frey, M.; Jones, P. G. Secondary Bonding Interactions in Some Halopyridinium and Dihalopyridinium Halides. *Zeitschrift fur Naturforsch. - Sect. B, J. Chem. Sci.* **2001**, *56* (9), 889−896.
(48) Fotović, L.; Stilinović, V. Halogenide Anions as Halogen and Hydrogen Bond Acceptors in Iodopyridinium Halogenides. *CrystEngComm* **2020**, *22* (23), 4039−4046.
(49) Nangia, A.; Desiraju, G. R. Supramolecular Structures − Reason and Imagination. *Acta Crystallogr., Sect. A: Found. Crystallogr.* **1998**, *54* (6), 934−944.
(50) Pauling, L. The Sizes of Ions and the Structure of Ionic Crystals. *J. Am. Chem. Soc.* **1927**, *49* (3), 765−790.
(51) *CrysAlis Pro User Manual*; Agilent Technologies Ltd: Yarnton, Oxfordshire, England, 2010.
(52) *CrysAlis Pro CCD*; Agilent Technologies Ltd: Yarnton, Oxfordshire, England, 2014.
(53) Sheldrick, G. M. SHELXT - Integrated Space-Group and Crystal-Structure Determination. *Acta Crystallogr., Sect. A: Found. Adv.* **2015**, *71* (1), 3−8.
(54) Sheldrick, G. M. Crystal Structure Refinement with SHELXL. *Acta Crystallogr., Sect. C: Struct. Chem.* **2015**, *71* (1), 3−8.
(55) Farrugia, L. J. WinGX Suite for Small-Molecule Single-Crystal Crystallography. *J. Appl. Crystallogr.* **1999**, *32* (4), 837−838.
(56) Dolomanov, O. V.; Bourhis, L. J.; Gildea, R. J.; Howard, J. A. K.; Puschmann, H. OLEX2: A Complete Structure Solution, Refinement and Analysis Program. *J. Appl. Crystallogr.* **2009**, *42* (2), 339−341.
(57) Macrae, C. F.; Bruno, I. J.; Chisholm, J. A.; Edgington, P. R.; McCabe, P.; Pidcock, E.; Rodriguez-Monge, L.; Taylor, R.; Van De Streek, J.; Wood, P. A. Mercury CSD 2.0 - New Features for the Visualization and Investigation of Crystal Structures. *J. Appl. Crystallogr.* **2008**, *41* (2), 466−470.
(58) *STARe Software*, v.15.00. Mettler Toledo: Greifensee, Switzerland, 2016.
(59) Frisch, M. J.; Trucks, G. W.; Schlegel, H. B.; Scuseria, G. E.; Robb, M. A.; Cheeseman, J. R.; Scalmani, G.; Barone, V.; Mennucci, B.; Petersson, G. A.; Nakatsuji, H.; Caricato, M.; Li, X.; Hratchian, H. P.; Izmaylov, A. F.; Bloino, J.; Zheng, G.; Sonnenberg, J. L.; Hada, M.; Ehara, M.; Toyota, K.; Fukuda, R.; Hasegawa, J.; Ishida, M.; Nakajima, T.; Honda, Y.; Kitao, O.; Nakai, H.; Vreven, T.; Montgomery, J. A., Jr.; Peralta, J. E.; Ogliaro, F.; Bearpark, M.; Heyd, J. J.; Brothers, E.; Kudin, K. N.; Staroverov, V. N.; Kobayashi, R.; Normand, J.; Raghavachari, K.; Rendell, A.; Burant, J. C.; Iyengar, S. S.; Tomasi, J.; Cossi, M.; Rega, N.; Millam, J. M.; Klene, M.; Knox, J. E.; Cross, J. B.; Bakken, V.; Adamo, C.; Jaramillo, J.; Gomperts, R.; Stratmann, R. E.; Yazyev, O.; Austin, A. J.; Cammi, R.; Pomelli, C.; Ochterski, J. W.; Martin, R. L.; Morokuma, K.; Zakrzewski, V. G.; Voth, G. A.; Salvador, P.; Dannenberg, J. J.; Dapprich, S.; Daniels, A. D.; Farkas, O.; Foresman, J. B.; Ortiz, J. V.; Cioslowski, J.; Fox, D. J. *Gaussian 09*; Gaussian, Inc.: Wallingford, CT, 2016.
(60) Lee, C.; Yang, W.; Parr, R. G. Development of the Colle-Salvetti Correlation-Energy Formula into a Functional of the Electron

https://doi.org/10.1021/acs.cgd.1c01285
Cryst. Growth Des. XXXX, XXX, XXX−XXX

Density. *Phys. Rev. B: Condens. Matter Mater. Phys.* **1988**, *37* (2), 785−789.
(61) Peverati, R.; Truhlar, D. G. An Improved and Broadly Accurate Local Approximation to the Exchange−Correlation Density Functional: The MN12-L Functional for Electronic Structure Calculations in Chemistry and Physics. *Phys. Chem. Chem. Phys.* **2012**, *14* (38), 13171.
(62) Zhao, Y.; Truhlar, D. G. The M06 Suite of Density Functionals for Main Group Thermochemistry, Thermochemical Kinetics, Noncovalent Interactions, Excited States, and Transition Elements: Two New Functionals and Systematic Testing of Four M06-Class Functionals and 12 Other Functionals. *Theor. Chem. Acc.* **2008**, *120* (1−3), 215.
(63) Siiskonen, A.; Priimagi, A. Benchmarking DFT Methods with Small Basis Sets for the Calculation of Halogen-Bond Strengths. *J. Mol. Model.* **2017**, *23* (2), No. 50.
(64) Simon, S.; Duran, M.; Dannenberg, J. J. How Does Basis Set Superposition Error Change the Potential Surfaces for Hydrogen-bonded Dimers? *J. Chem. Phys.* **1996**, *105* (24), 11024−11031.
(65) Boys, S. F.; Bernardi, F. The Calculation of Small Molecular Interactions by the Differences of Separate Total Energies. Some Procedures with Reduced Errors. *Mol. Phys.* **1970**, *19* (4), 553−566.
(66) *GaussView*; Semichem Inc.: Shawnee Mission, KS, 2008.

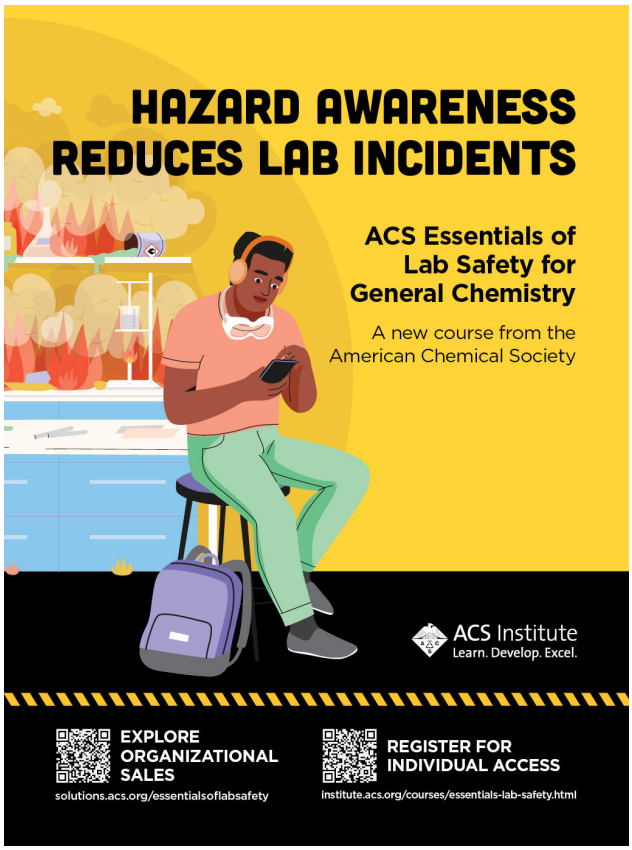

https://doi.org/10.1021/acs.cgd.1c01285
Cryst. Growth Des. XXXX, XXX, XXX−XXX

§ 8. ŽIVOTOPIS

Ime i prezime: Luka Fotović

Datum rođenja: 7. veljače 1995.

Mjesto rođenja: Zagreb, Hrvatska

Adresa stanovanja: Lonjica 321a, 10340 Vrbovec, Hrvatska

Broj telefona: +38591 6029 015

e-mail: lfotovic@chem.pmf.hr

Jezici: Engleski

Obrazovanje:

2013.–2018. Prirodoslovno-matematički fakultet, Biološki odsjek, Zagreb; Sveučilišni Integrirani preddiplomski i diplomski studij kemije i biologije – magistar edukacije biologije i kemije (mag. educ. biol. et chem.)

2018. –; Prirodoslovno-matematički fakultet, Kemijski odsjek, Zagreb; Sveučilišni doktorski studij kemije, anorganska i strukturna kemija

Radno iskustvo:

2018.–; asistent, Zavod za opću i anorgansku kemiju, Kemijski odsjek, Prirodoslovno-matematički fakultet u Zagrebu

Istraživačko iskustvo:

2018.–2019.; istraživač na projektu „Kristalno inženjerstvo višekomponentnih metaloorganskih materijala povezanih halogenskom vezom: ususret supramolekulskom ugađanju strukture i svojstava" (voditelj: doc. dr. sc. Dominik Cinčić; izvor financiranja: Hrvatska zaklada za znanost).

2020.–; istraživač na projektu „Nove građevne jedinke u supramolekulskom dizajnu složenih višekomponentnih molekulskih kristala temeljenih na halogenskim vezama" (voditelj: izv. prof. dr. sc. Dominik Cinčić; izvor financiranja: Hrvatska zaklada za znanost).

Nastavne aktivnosti:

2018.– ; asistent na kolegiju Opća i anorganska kemija (praktikum)

2018.– ; asistent na kolegiju Fizikalna anorganska kemija (seminar)

Neposredni voditelj izrade 2 diplomska rada:

1. Erik Uran, Aromatski diamini kao akceptori halogenske veze (2021.)
2. Nikola Jakupec, Halogenska veza u solima halogenpiridina i heksacijanoželjezove(III) te heksacijanokobaltove(III) kiseline (2021.)

Publikacije:

I. L. Fotović, N. Bedeković, V. Stilinović, Evaluation of Halogenopyridinium Cations as Halogen Bond Donors, *Cryst. Growth Des.* **21** (2021) 6889–6901.

II. L. Fotović, N. Bedeković, V. Stilinović, Isostructural Halogen Exchange and Halogen Bond – The Case of *N*-(4-halogenobenzyl)-3-halogenopyridinium Halogenides, *Cryst. Growth Des.* **22** (2022) 1333–1344.

III. N. Bedeković, L. Fotović, V. Stilinović, D. Cinčić, Conservation of the Hydrogen-bonded Pyridone Homosynthon in Halogen-bonded Cocrystals, *Cryst. Growth Des.* **22** (2022) 987–992.

IV. L. Fotović, V. Stilinović, Halogen Bonding in *N*-Alkyl-3-halogenopyridinium Salts, *Crystals* **11** (2021) 1240-1256.

V. Nemec, K. Lisac, N. Bedeković, L. Fotović, V. Stilinović, D. Cinčić, Crystal engineering strategies towards halogen-bonded metal–organic multi-component solids: salts, cocrystals and salt cocrystals, *CrystEngComm* **23** (2021) 3063-3083.

VI. E. Uran, L. Fotović, N. Bedeković, V. Stilinović, D. Cinčić, The Amine Group as Halogen Bond Acceptor in Cocrystals of Aromatic Diamines and Perfluorinated Iodobenzenes**,** *Crystals* **11** (2021) 529-540.

VII. L. Fotović, V. Stilinović, Halogenide anions as halogen and hydrogen bond acceptors in iodopyridinium halogenides, *CrystEngComm* **22** (2020) 4039-4046.

VIII. N. Jakupec, L. Fotović, V. Stilinović, The effect of halogen bonding on protonated hexacyanoferrate networks in hexacyanoferrates of halogenopyridines, *CrystEngComm* **22** (2020) 8142-8150.

IX. V. Nemec, L. Fotović, T. Vitasović i D. Cinčić, Halogen bonding of the aldehyde oxygen atom in cocrystals of aromatic aldehydes and 1,4-diiodotetrafluorobenzene**,** *CrystEngComm* **21** (2019) 3251-3255.

X. V. Nemec, L. Fotović, T. Friščić i D. Cinčić, A large family of halogen-bonded cocrystals involving metal-organic building blocks with open coordination sites, *Cryst. Growth Des.* **17** (2017) 6169–6173.

Sudjelovanja na skupovima:

1. L. Fotović, V. Stilinović, *N*-(4-halogeno)benzyl-(3-halogeno)pyridinium cations as asymmetric ditopic halogen bond donors, International School of Crystallography, 55th Course: Molecular Crystal Engineering, Ettore Majorana Foundation and Centre for Scientific Culture, Erice, Italija, 2021. (poster)
2. V. Stilinović, L. Fotović, N. Bedeković, halogenated aromatic cations as halogen bond donors, 27th Croatian Meeting of Chemists and Chemical Engineers, Veli Lošinj, Hrvatska, 2021. (pozvano predavanje)
3. N. Bedeković, L. Fotović, V. Stilinović, D. Cinčić, preservation of pyridone homosynthon in halogen-bonded cocrystals, 27th Croatian Meeting of Chemists and Chemical Engineers, Veli Lošinj, Hrvatska, 2021. (poster)
4. L. Fotović, N. Bedeković, V. Stilinović, *N*-(4-halogenobenzyl)-(3-halogeno)pyridinium cations as halogen bond donors, 27th Croatian Meeting of Chemists and Chemical Engineers, Veli Lošinj, Hrvatska, 2021. (poster)
5. E. Uran, L. Fotović, V. Stilinović, D. Cinčić, Salen complexes as halogen bond acceptors, Solid State Science and Research, Zagreb, Hrvatska, 2021. (poster)
6. N. Bedeković, L. Fotović, V. Stilinović, D. Cinčić, Sustainability of the robust pyridone homosyntone in halogen-bonded cocrystals, 3rd Solid State Science and Research, Zagreb, Hrvatska, 2021. (poster)
7. L. Fotović, V. Stilinović, Halogen and hydrogen bonds with halogenide ions – database survey and crystal structure analysis of *o*-, *m*- and *p*-iodopyridinium halogenides, III. simpozij supramolekulske kemije – Supramolecular Chemistry 2019, Zagreb, Hrvatska, 2019. (poster)
8. L. Fotović, V. Nemec, V. Stilinović, D. Cinčić, Kompeticija aldehidne i hidroksilne skupine u ostvarivanju halogenske veze u kokristalima 2-hidroksi-1-naftaldehida i perfluoriranih halogenbenzena, Simpozij studenata doktorskih studija PMF-a, Zagreb, Hrvatska, 2019. (poster)

9. L. Fotović, V. Stilinović, Intermolecular interactions in *o*-, *m*- and *p*-iodopyridinium halogenide salts, 2nd Solid State Science and Research, Zagreb, Hrvatska, 2019. (poster)
10. L. Fotović, V. Stilinović, Synthesis and structure characterization of *N*,*N*'-alkyl-bis(halogenpyridinium) cations as new potential polytopic halogen bond donors, 27th Slovenian – Croatian Crystallographic Meeting, Rogaška Slatina, Slovenija, 2019. (predavanje)
11. V. Nemec, L. Fotović, T. Vitasović, D. Cinčić, The propensity of the carbonyl functional group for halogen bonding in 1, 4-diiodotetrafluorobenzene cocrystals, ChemCYS 2018 Chemistry Conference for Young Scientists, Blankenberge, Belgija, 2018. (predavanje)
12. L. Fotović, V. Nemec, V. Stilinović, D. Cinčić, Sklonost aldehidne skupine sudjelovanju u halogenskoj vezi u kokristalima 2-hidroksi-1-naftaldehida i perfluoriranih halogenbenzena, II. simpozij supramolekulske kemije Supramolecular Chemistry 2018, Zagreb, Hrvatska, 2018. (poster)
13. L. Fotović, V. Nemec, V. Stilinović, D. Cinčić, The halogen bonding proclivity of the aldehyde group in cocrystals of 2-hydroxy-1-naphthaldehyde and perfluorohalogenobenzenes, 7th National Crystallographic Symposium with International Participation, Sofija, Bugarska, 2018. (poster)
14. L. Fotović, V. Nemec, V. Stilinović, D. Cinčić, Influence of experimental conditions on the crystallization of a Schiff base copper(II) complex, 25th Slovenian – Croatian Crystallographic Meeting, Ljubljana, Slovenia, 2017. (poster)
15. L. Fotović, V. Nemec, D. Cinčić, The influence of reaction conditions on the supramolecular outcome of a copper(II) complex synthesis, Solid-State Science & Research, Zagreb, Hrvatska, 2017. (poster)
16. L. Fotović, T. Vitasović, V. Nemec, D. Cinčić, Novel halogen-bonded cocrystals of aromatic aldehydes with 1, 4-diiodotetrafluorobenzenene. Solid-State Science & Research, Zagreb, Hrvatska, 2017. (poster,)
17. L. Fotović, V. Nemec, D. Cinčić, Sinteza adukata kompleksnog spoja bakra(II) s iminom izvedenim iz 2-hidroksi-1-naftaldehida i 4-nitroanilina, 3. Simpozij studenata kemičara, Zagreb, Hrvatska, 2016. (predavanje)

18. L. Fotović, V. Nemec, D. Cinčić, Sinteza porozne supramolekulske mreže nikla(II) metodama starenja i mljevenja, XI. Susret mladih kemijskih inženjera, Zagreb, 2016. (poster)
19. L. Fotović, V. Nemec, D. Cinčić, Adduct formation from a copper(II) complex with an imine ligand by combining mechanochemical and solution synthesis, 24th Croatian-Slovenian Crystallographic Meeting, Bol, Hrvatska, 2016. (predavanje)
20. L. Fotović, V. Nemec, D. Cinčić, Utjecaj reakcijskih uvjeta na supramolekulski ishod sinteze koordinacijskog spoja bakra(II) s iminom izvedenim iz 2-hidroksi-1-naftaldehida, 2. Simpozij studenata kemičara, Zagreb, Hrvatska, 2015. (predavanje)

Sudjelovanja na međunarodnim školama:

1. 55th Course - Molecular Crystal Engineering at the International School of Crystallography, Erice, Italija (2021.)

2. Training School - Mechanochemistry: from supramolecular to covalent bonds – synthesis and structural characterization, Lisabon, Portugal (2021.)

3. 17th BCA/CCG Intensive Teaching School in X-Ray Structure Analysis, Durham, Ujedinjeno Kraljevstvo (2019.)

Ostale aktivnosti:

2017. - organizacija i provedba konferencije Solid State Science and Research

2016. - organizacija i provedba Simpozija studenata kemičara (SiSK)

2013., 2014., 2015., 2016., 2017., 2018., Otvoreni dan Kemijskog odsjeka

2019., Čarolije u kemiji, edukativna predstava Kemijskog odsjeka

Nagrade:

2017. – Posebna Rektorova nagrada za društveno koristan rad u akademskoj i široj zajednici za sudjelovanje u organizaciji znanstvenog skupa *Simpozij studenata kemičara*

Članstva:

Hrvatsko kemijsko društvo (HKD)

Hrvatska kristalografska zajednica (HKZ)

Europska kristalografka zajednica (ECA)